The Receptor Tyrosine Kinase, c-KIT: Its Involvement in Signal Transduction and Biological Response

Sonia Marie Young, B.Sc. (Hons.)

Enrolled in the Department of Medicine, The University of Adelaide.

Research conducted in the Division of Haematology,

Hanson Centre for Cancer Research,

Institute of Medical and Veterinary Science,

Adelaide.

A thesis submitted for the degree of Doctor of Philosophy,

Faculty of Medicine

at The University of Adelaide.

March, 2003

TABLE OF CONTENTS

ABSTRACT

The receptor tyrosine kinase (RTK), c-KIT is involved in normal haemopoiesis and is constitutively active in some haemopoietic malignancies. Objectives of this study were to investigate the mechanisms by which proto-oncogenic and oncogenic forms of c-KIT mediate cellular responses. The overall aim was to aid in the understanding of signal transduction pathways and their relation to biological responses and leukaemic transformation in haemopoietic cells.

In the haemopoietic system, c-KIT is expressed by stem and progenitor cells of bone marrow and tissue mast cells. The receptor and its ligand, stem cell factor (SCF) are involved in normal haemopoietic responses including proliferation, survival, adhesion and migration. Two naturally occurring isoforms of human c-KIT, differing by the insertion or deletion of 12 base pairs encoding a 4 amino acid stretch, GNNK, in the extracellular region displayed significant differences in signalling and cellular responses when expressed in fibroblasts and stimulated with human SCF (huSCF). It was of interest to observe any differences between the function of c-KIT isoforms in a more physiologically relevant cellular environment, specifically factor dependent haemopoietic cells. Factor dependent haemopoietic progenitor cells, FDC-P1 and murine foetal liver cells immortalised with a truncated constitutively active form of the myb transcription factor (MIHC), were retrovirally transduced with cDNA encoding *c-KIT* isoforms and clones expressing physiological levels of the receptor were selected. Regression analysis indicated that huSCF mediated growth was directly related to the surface expression level of c-KIT for both isoforms ($r^2 > 0.9$). Growth in huSCF for cells expressing the GNNK- isoform was at a higher rate as compared to the GNNK+ isoform. Associated with these observations was rapid and transient phosphorylation of the GNNK- isoform as compared to a slower and more sustained response for the GNNK+ isoform. Internalisation and degradation of c-KIT isoforms exhibited similar kinetics to their

phosphorylation profiles. The intensity of phosphorylation and internalisation was also higher for the GNNK- isoform relative to the GNNK+ isoform. In summary, these results confirmed previous observations in NIH-3T3 fibroblasts indicating that differences were intrinsic to the isoforms.

A direct association of phosphoinositide 3-kinase (PI 3-K) with both isoforms of c-KIT was observed when cells were treated with huSCF. This has been reported to be via the autophosphorylation site, Y721. To investigate the role of direct recruitment of PI 3-K, Y721 was mutated to phenylalanine (Y721F). Constructs containing either wild type (WT) or Y721F *c-KIT* in the retroviral vector, pRUFMC1*neo,* were expressed in two haemopoietic progenitor cell models, FDC-P1 and MIHC and clones thereof were selected based on surface expression levels of c-KIT. Mutation of the PI 3-K binding site reduced growth in the presence of huSCF in both cellular models. Separation of parameters involved in cell yield revealed that direct recruitment of PI 3-K was mainly involved in survival, rather than proliferation. Mutation of the PI 3-K binding site did not alter the kinetics of activation and internalisation of c-KIT in response to huSCF. The intensity of peak phosphorylation was decreased 1.7 fold suggesting that it was an important site. In the absence of direct PI 3-K activation, Akt was still activated by huSCF albeit at 50% of the level for WT c-KIT. Phosphorylation of ERK was also reduced in Y721F c-KIT expressing cells. A potential compensatory mechanism identified was Y721 independent activation of PI 3-K as shown by an effect of the PI 3-K inhibitor LY294002 on cellular yield and survival. These results indicated that direct recruitment of PI 3-K to Y721 of c-KIT is important but not solely required for the survival of haemopoietic cells and that alternate recruitment site(s) and/or indirect activation of PI 3-K may play a role.

Oncogenic forms of c-KIT have been identified in certain leukaemias and solid tumours. The amino acid substitution of D816V in c-KIT found in human mast cell leukaemia, systemic mastocytosis and occasional cases of acute myeloid leukaemia (AML)

results in constitutive phosphorylation and activation, which gives rise to factor independent growth and an ability to produce tumours in mice. The mechanism by which the D816V c-KIT mutation mediates its oncogenicity was unknown, therefore the role of the constitutive association of PI 3-K was addressed. MIHC were infected with WT and D816V *c-KIT* constructs with or without the Y721F mutation in pRUFMC1*neo* and their ability to grow in the absence of factor was assessed in liquid culture and semi-solid medium. Cells expressing D816V c-KIT lacking the PI 3-K binding site, Y721F/D816V c-KIT, formed colonies in the absence of exogenous factor, however the number of colonies was significantly lower than D816V c-KIT expressing cells ($p < 0.00001$) despite there being no difference in formation in muGM-CSF ($p > 0.1$). Results from liquid culture confirmed the colony growth indicating that mutation of the PI 3-K binding site reduced but did not abolish factor independent growth. The reduced growth observed in the absence of factor for Y721F/D816V c-KIT as compared to D816V c-KIT expressing cells was primarily due to an effect on survival rather than proliferation. Tumourigenesis studies in syngeneic mice revealed that mutation of the PI 3-K binding site abolished tumour formation induced by subcutaneous injection of MIHC expressing D816V c-KIT. Attempts to further deduce the mechanism involved analysis of the signal transduction pathways activated by D816V and Y721F/D816V c-KIT. In contrast to the response triggered by huSCF acting on WT c-KIT, neither Akt nor ERK were activated by D816V c-KIT maintained in the absence of factor. Therefore the mechanism remains unknown. Overall, these results indicated that direct recruitment of PI 3-K via Y721 was involved in factor independent growth through an effect on survival, however it was not the sole mechanism, whereas in tumourigenicity it was crucial.

STATEMENT

This work contains no material which has been accepted for the award of any other degree or diploma in any university or other tertiary institution and, to the best of my knowledge and belief, contains no material previously published or written by another person, except where due reference has been made in the text.

When accepted for the award of the degree, I consent for this thesis to be available for loan and photocopying.

Sonia Marie Young B.Sc. (Hons.)

March, 2003

ACKNOWLEDGEMENTS

I would like to thank The University of Adelaide for the opportunity to do this PhD and for the Australian Postgraduate Award. I am thankful to the Division of Haematology at the Hanson Centre for Cancer Research for allowing me to perform experimental research in a medical based environment. I am also thankful to The University of Newcastle for the use of their facilities during the writing of this thesis.

Without the support and encouragement many people, this thesis would not have been possible. I am extremely grateful to my supervisor, Professor Leonie Ashman for giving me the opportunity to do this PhD in her laboratory and for her guidance and support. From Leonie I have learnt much regarding research and I am thankful for her input into my scientific career. I thank both the past and present laboratory members for their guidance, patience in answering my endless questions, for their putting up with 'Evil Son' and for making the laboratory an enjoyable place to work. I especially thank Tony Cambareri for his suggestions regarding experimental technique, endless assistance and on a more personal note, for his friendship. I thank Petranel Ferrao for her assistance with cell biology techniques, her never-ending patience and for her friendship. I also wish to acknowledge Ly Nguyen for her help with cell biology, Peter Konstantopoulos (and Tony) for the fun times had at the Western blot factory, Steve Fitter for assistance with molecular biology procedures, Rowan Koina for reading this thesis, Sean Geary for listening and Stuart Read for conversations in the corridors about theses.

I am much indebted to my family for their constant love and support. I thank my father for his enormous patience and practical assistance in helping me with computer programs. My Mother for our chats and the comfort she gave, Paul for his company and helping me with the computer and finally Cleo for the welcome study breaks. I also thank my family and friends for taking an active interest in my research and the encouragement each has offered.

At this point, I wish to acknowledge my grandparents, who are very dear to me. I dedicate this thesis to them for enlightening me about life. I thank them for their love, the wisdom that they have shared and the interesting stories about their life that they have told me.

Lastly, I thank God for His help in unravelling a piece of His puzzle.

'Let us give thanks to the God and Father of our Lord Jesus Christ, the merciful Father, the God from whom all help comes!' 2 Corinthians 1: 3 (Today's English Version).

PUBLICATIONS

RuJu Chian, **Sonia Young**, Alla Danilkovitch-Miagkova, Lars Rönnstrand, Edward Leonard, Petranel Ferrao, Leonie Ashman and Diana Linnekin. (2001). Phosphatidylinositol 3 kinase mediates transformation of hematopoietic cells by the V816 c-Kit mutant. *Blood* **98:** 1365–1373.

(Both RuJu Chian and Sonia Young made equal contributions to this work.)

CONFERENCE PRESENTATIONS

11th Lorne Cancer Conference

Lorne, Victoria, 11 - 14th February 1999

Mechanism of c-KIT mediated adhesion in haemopoietic cells.

Sonia Young, Steve Fitter and Leonie Ashman.

Australian Society of Medical Research (South Australia Division) Annual Scientific Meeting

Adelaide, South Australia, June 1999

Mechanism of c-KIT mediated adhesion in haemopoietic cells.

Sonia Young, Steve Fitter and Leonie Ashman.

12th Lorne Cancer Conference

Lorne, Victoria, 10 - 13th February 2000

To PI 3-K or not to PI 3-K: Role of PI 3-K in oncogenic c-KIT signalling.

Sonia Young, Petranel Ferrao and Leonie Ashman.

2nd International Conference on Signal Transduction

Dubrovnik, Croatia, 26 - 31st May 2000

Constitutive recruitment of PI3-kinase is essential for transformation of haemopoietic cells by D816V mutant KIT.

S. M. Young, P. T. Ferrao, A. C. Cambareri, L. Ronnstrand, D. Linnekin and L. K. Ashman.

11th International Conference on Second Messengers and Phosphoproteins

Melbourne, Victoria, 22 - 26th April 2001

Modulation of receptor internalisation and biological responses by isoforms of c-KIT and a PI 3-K recruitment mutant.

Sonia Young, Tony Cambareri, Ly Nguyen, Petranel Ferrao, Leonie Ashman.

The Hunter Cellular Biology Meeting

Hunter Valley, New South Wales, 10th - 12th April 2002

Modulation of receptor internalisation and biological responses by isoforms of c-KIT and a PI 3-K recruitment mutant.

Sonia Young, Tony Cambareri, Ly Nguyen, Petranel Ferrao, Leonie Ashman.

ABBREVIATIONS

AML	Acute Myeloid Leukaemia
APAAP	Alkaline Phosphatase Anti-Alkaline Phosphatase
ATP	Adenosine Triphosphate
Az	Azide
BAD	Bcl-2/Bcl-X_L-agonist, Causing cell Death
BCA	Bicinchoninic Acid
BSA	Bovine Serum Albumin
CHK	Csk Homologous Kinase
CIP	Calf Intestinal Phosphatase
CML	Chronic Myelogenous Leukaemia
CSF-1	Colony Stimulating Factor-1
Csk	Carboxy Terminal Src Kinase
DAG	Diacylglyercol
DEPC	Diethylpyrocarbonate
DMEM	Dulbecco's Modified Eagle's Medium
DMSO	Dimethylsulphoxide
DNA	Deoxyribonucleic Acid
DTT	1,4-Dithiothreitol
EBV	Epstein Barr Virus
ECF	Enhanced Chemifluorescence
EDTA	Ethylenediaminetetra-acetic acid
EGF	Epidermal Growth Factor
ELISA	Enzyme Linked Immunosorbent Assay
ERK	Extracellular Signal Regulated Kinase
FacsFix	Fluorescence Activated Cell Sorting Fixative
FAK	Focal Adhesion Kinase
FCS	Foetal Calf Serum
FeLV	Feline Leukaemic Virus
FGF	Fibroblast Growth Factor
FITC	Fluorescein Isothiocyanate
FRET	Fluorescent Resonance Energy Transfer
GAB2	Grb2 Associated Binder 2

GAP	GTPase Activating Protein
GDP	Guanosine Diphosphate
GIST	Gastrointestinal Stromal Tumour
GM-CSF	Granulocyte Macrophage Colony Stimulating Factor
GTP	Guanosine Triphosphate
HBSS	Hank's Balanced Salt Solution
HEPES	Hydroxyethylpiperazine N`-2-ethanesulphonic acid
huSCF	Human Stem Cell Factor
HZ4-FeSV	Hardy Zuckerman 4 Strain of Feline Sarcoma Virus
IL	Interleukin
ILK	Integrin Linked Kinase-1
IMDM	Iscove's Modified Dulbecco's Medium
IMVS	Institute of Medical and Veterinary Science
IP_3	Inositol Triphosphate
IRS	Insulin Receptor Subunit
JAK	Janus Kinase
JNK	c-Jun N-terminal Kinase
kDa	kiloDalton
KL	Kit Ligand
LB	Luria Broth
MAPK	Mitogen Activated Protein Kinase
MAPKAP-K1	Mitogen Activated Protein Kinase-activating Protein Kinase 1
MATK	Megakaryocyte-associated Tyrosine Kinase
MFI	Mean Fluorescence Intensity
MGF	Mast Cell Growth Factor
MIHC	Myb Immortalised Haemopoietic Cell
Milli-Q water	Milli-Q purified Water
mMCP-5	Murine Mast Cell Protease - 5
MP1	MEK partner-1
mRNA	Messenger Ribonucleic Acid
muGM-CSF	Murine Granulocyte Macrophage - Colony Stimulating Factor
muIL-3	Murine Interleukin - 3
NGF	Nerve Growth Factor
NP40	Nonidet P 40

NRS	Normal Rabbit Serum
PBS	Phosphate Buffered Saline
PCR	Polymerase Chain Reaction
PDGF	Platelet Derived Growth Factor
PDK1	3' Phosphoinositide-dependent Kinase-1
PE	Phycoerythrin
PH	Pleckstrin Homology
PI 3-K	Phosphoinositide 3-Kinase
PKB	Protein Kinase B
PKC	Protein Kinase C
PLCγ	Phospholipase Cγ
PLD	Phopholipase D
PMSF	Phenylmethylsulfonyl fluoride
PRK2	PKC-related Kinase 2
PTB	Phosphotyrosine Binding
PtdIns	Phosphatidylinositol
PVDF	Polyvinylidene Difluoride
RAC-PK	Related to the A and C Kinases
RNA	Ribonucleic acid
RSV	Rous Sarcoma Virus
RTK	Receptor Tyrosine Kinase
SAPK	Stress Activated Protein Kinase
SCF	Stem Cell Factor
SD	Standard Deviation
SDS	Sodium Dodecylsulphate
SDS-PAGE	Sodium Dodecylsulphate-Polyacrylamide Gel Electrophoresis
SEM	Standard Error of the Mean
SH	Src Homology
Sl	*Steel*
Sl^d	*Steel-Dickie*
SLF	Steel Factor
Socs1	Suppressor of Cytokine Signalling
Sos	Son of Sevenless
STAT	Signal Transducers and Activators of Transcription

TAE	Tris-acetate-EDTA
TBS	Tris Buffered Saline
TE	Tris-EDTA
TLC	Thin Layer Chromatography
TSE	Tris-sodium-EDTA
U	Units
VEGF	Vascular Endothelial Growth Factor
W	*White Spotting*
WT	Wild Type

CHAPTER 1:

INTRODUCTION

1. INTRODUCTION

1.1. SIGNAL TRANSDUCTION AND CANCER

Cancer is a multifactorial disease characterised by unrestrained proliferation resulting from the loss of control of cell growth, cell death and terminal differentiation. Malignant neoplasms have an additional feature in that they are capable of invading and metastasising in foreign tissues (Blume-Jensen and Hunter, 2001). The unrestrained proliferation and ability to metastasise is attributed to an accumulation of two types of mutations in the genome of the cell (Bishop, 1987; Bishop, 1991; Varmus, 1989). The first involves inactivating mutations in tumour suppressor genes that encode proteins whose function is to inhibit the proliferation of cells. The other class involves mutations in growth stimulatory genes resulting in the constitutive activation of the encoded protein. This type of mutation exerts a dominant effect and the protein encoded by the mutant gene is called an oncogene. A recent observation indicates the potential for a third class consisting of mutations to alter telomere maintenance which is important in human tumourigenesis (Hahn *et al.*, 1999).

Oncogenes were initially identified in ribonucleic acid (RNA) tumour viruses, known as retroviruses (Bishop, 1991). In 1910, Peyton Rous was the first to observe that an infectious filtrate obtained from chicken sarcomas was capable of inducing tumour formation in otherwise healthy chickens (Bishop, 1982). The infectious agent was identified as a virus and later called the Rous sarcoma virus (RSV) (Varmus, 1989). Sixty years after the discovery by Rous, the transforming agent carried by RSV was identified as *Src*. A homologue of this gene encoding a protein tyrosine kinase was found in the normal cellular genome (Bishop, 1982; Varmus, 1989).

Oncogenes arise by deoxyribonucleic acid (DNA) mutation, chromosomal translocation or gene amplification of their respective cellular counterparts called proto-

oncogenes (Bishop, 1987; Bishop, 1991; Varmus, 1989). The majority of proto-oncogenes are thought to constitute the signal transduction machinery of a cell which is responsible for the regulation of numerous biological responses including proliferation, differentiation, adhesion, migration and apoptosis (reviewed in Cantley *et al.*, 1991; Varmus, 1989). There are various mechanisms by which proto-oncogenes act. They may trigger phosphorylation on serine, threonine or tyrosine residues either indirectly by growth factors acting on their cognate receptors or by direct catalysis in the case of activated receptors acting on their downstream effectors (Bishop, 1991). Oncogenic versions of these proteins arise from mutations, deletions or chromosomal fusions affecting the primary structure of the protein resulting in deregulated and constitutive kinase activity. Conversely, proto-oncogenes can function by dephosphorylating growth regulatory enzymes such as Cdc25A and B (Nilsson and Hoffmann, 2000; Parsons, 1998). Proto-oncogenes can also exhibit lipid kinase activity as in the case of phosphoinositide 3-kinase (PI 3-K) (see section 1.7 for more details) and sphingosine kinase (Xia *et al.*, 2000). Other proto-oncogenes exhibit GTPase activity (an example being Ras; Bishop, 1991), act as nuclear transcription factors (Bishop, 1991) or act as modifiers of cell death (for example Bcl-2; Adams and Cory, 2001).

Ongoing research into cancer management is concerned with deducing the structure and function of proto-oncogenes and oncogenes. Understanding the differences between proto-oncogenes and their corresponding oncogenes will aid in development of pharmaceutical agents that potently and specifically inhibit activated oncogenes. This project investigated the function of a receptor tyrosine kinase (RTK), c-KIT, and an oncogenic version that has been identified in several leukaemias.

1.2. Receptor Tyrosine Kinases (RTKs)

RTKs comprise a large family of growth factor receptors of which 58 have been identified to date (Blume-Jensen and Hunter, 2001). All have three basic structural

components consisting of a large glycosylated extracellular domain responsible for ligand binding, a single pass hydrophobic transmembrane domain which anchors the receptor in the plasma membrane, and lastly a cytoplasmic domain with intrinsic tyrosine kinase catalytic activity (Schlessinger and Ullrich, 1992; Schlessinger, 2000; Ullrich and Schlessinger, 1990; Yarden and Ullrich, 1988). Based on the sequence similarity and structural characteristics of the RTKs, they have been sub-divided into distinct subclasses (Ullrich and Schlessinger, 1990) of which 20 have been established to date (Blume-Jensen and Hunter, 2001).

The extracellular regions of RTKs are composed of discrete globular domains enabling them to bind ligand. Consistent with the need to create specificity, there is minimal sequence conservation in this region (Yarden and Ullrich, 1988). The transmembrane region is highly hydrophobic, with a conserved length, however its sequence is not conserved even within subclasses (Yarden and Ullrich, 1988). The juxtamembrane domain is a sequence of about 50 amino acids (Yarden and Ullrich, 1988) separating the membrane region from the kinase domain and is divergent between RTK subclasses but appears relatively conserved within (Ullrich and Schlessinger, 1990; Yarden and Ullrich, 1988). The tyrosine kinase domains are the most conserved regions of RTKs (Ullrich and Schlessinger, 1990; Yarden and Ullrich, 1988). These are composed of an adenosine triphosphate (ATP) binding site with a consensus sequence containing a crucial lysine residue (Ullrich and Schlessinger, 1990). The ATP binding site is in the amino terminal region of the kinase domain, while the carboxy terminal remainder contains the tyrosine acceptor site within the activation loop (Yarden and Ullrich, 1988). The carboxy terminal tail has the highest degree of variation both in its length and sequence even within subclasses (Yarden and Ullrich, 1988). Carboxy terminal tails for RTKs are typically composed of hydrophilic residues and small amino acids suggesting that they might be flexible (Yarden and Ullrich, 1988).

The mechanism of activation and the subsequent signal transduction cascades are similar for all sub-classes of RTKs. Firstly, the ligand must bind to the extracellular domain

of the receptor, this results in a change in conformation of the extracellular domain, allowing receptor dimerisation to occur (Ullrich and Schlessinger, 1990). Dimerisation seems to be an important step since it precedes phosphorylation (Schlessinger and Ullrich, 1992) and catalytic activation (Schlessinger, 1995). Dimerisation allows the transphosphorylation of a conserved tyrosine in the activation loop of the catalytic domain which results in increased kinase activity and precedes the autophosphorylation of residues outside the catalytic domain (Heldin, 1995; Hubbard and Till, 2000). These phosphotyrosine-containing motifs then recruit downstream effectors to the receptor.

Analysis of the crystal structures of the insulin receptor, fibroblast growth factor (FGF) receptor-1 and vascular endothelial growth factor (VEGF) receptor-2 has shed light on mechanisms regulating receptor activation (Hubbard and Till, 2000). In the unstimulated form of the receptor, the activation loop of the catalytic domain acts as a negative regulator blocking access of ATP and substrate (Hubbard *et al.*, 1998; Hubbard and Till, 2000; Hunter, 2000). The activation loop is also mobile and the inactive conformation is in equilibrium with the active conformation which has sites accessible for ATP and substrate binding (Figure 1.1) (Blume-Jensen and Hunter, 2001; Hubbard *et al.*, 1998; Hubbard and Till, 2000; Schlessinger, 2000). Ligand induced dimerisation stabilises the active conformation long enough for transphosphorylation of one or more tyrosines in the activation loop to occur (Figure 1.1). Dimerisation alone however is not sufficient for kinase activation, and additional conformational changes induced by ligand are required for full activation (reviewed in Blume-Jensen and Hunter, 2001). In the case of Tek (TIE2) activation also involves the relief of negative regulation by the carboxy terminal tail which partially obstructs the substrate tyrosine binding site (Blume-Jensen and Hunter, 2001). Similarly, the juxtamembrane domain has been reported to have an autoinhibitory function (Blume-Jensen and Hunter, 2001). As well as their inhibitory function, these regions are phosphorylated and act as docking sites for Src

Figure 1.1: Activation of RTKs.

In the unstimulated state, the inactive conformation of the RTK (ATP and substrate inaccessible) (blue) is in equilibrium with the active conformation (ATP and substrate accessible)(green). Juxtamembrane (orange) and carboxy terminal (red) regions negatively regulate the receptor. When ligand is bound, shown on the right, the active conformation is stabilised allowing phosphorylation of the activation loop, relief of negative constraints and general phosphorylation. Reprinted by permission from Nature (Blume-Jensen and Hunter, 2001).

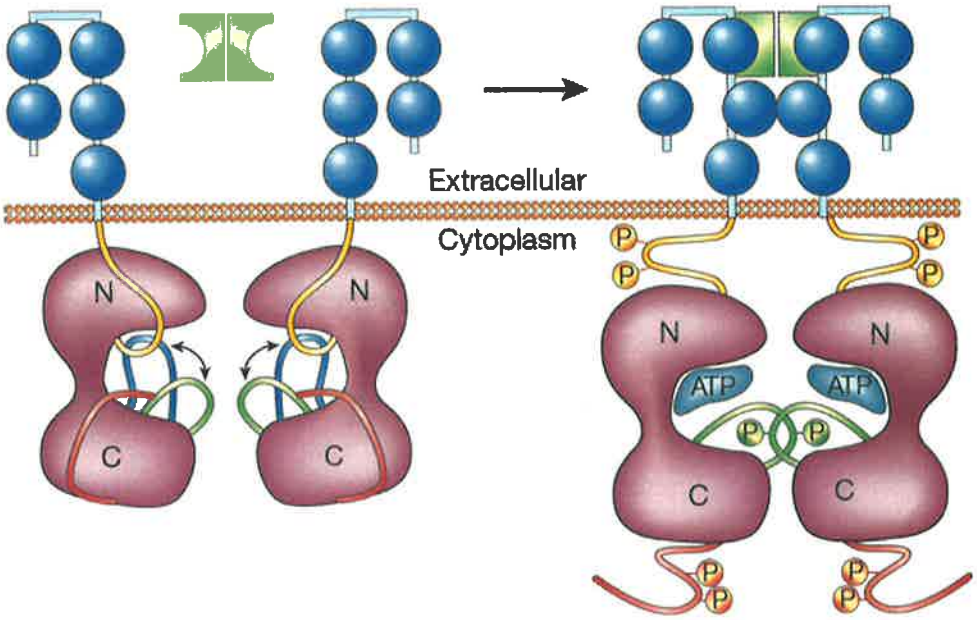
Extracellular
Cytoplasm
N
N
C
C
P
P
P
P
N
N
ATP
ATP
P
P
C
C
P
P
P
P

homology (SH) 2 and protein tyrosine binding (PTB) domain containing proteins, therefore their role in receptor activation is two fold (Blume-Jensen and Hunter, 2001).

RTKs have oncogenic potential and activated forms can be observed in cancer (reviewed in Ullrich and Schlessinger, 1990; Yarden and Ullrich, 1988). A common mechanism of constitutive RTK activation is through autocrine stimulation, by expression of the cognate ligand in the same cell. In addition, overexpression of RTKs resulting in increased dimers can lead to ligand independent activation as has been observed for epidermal growth factor (EGF) receptor and HER2/neu in breast cancer (Blume-Jensen and Hunter, 2001; Yarden and Ullrich, 1988). A key feature of oncogenic conversion of receptors is that mutation or deletions in the receptor must overcome any negative restraints that ligand binding usually relieves (Maehama and Dixon, 1998). Carboxy terminal truncation is a mechanism involved in constitutive activation of various RTK subfamilies (Yarden and Ullrich, 1988), as too are mutations in the juxtamembrane domain for example in c-KIT (Blume-Jensen and Hunter, 2001), confirming the negative regulatory role of these two regions. Point mutations or deletions in the extracellular domain, transmembrane domain and in the kinase domain of RTKs have also been observed in various cancers (Blume-Jensen and Hunter, 2001; Ullrich and Schlessinger, 1990).

1.2.1. Discovery of the c-KIT Proto-oncogene

The viral homologue of the cellular proto-oncogene, *c-Kit* was initially identified in feline leukaemic virus (FeLV), Hardy Zuckerman 4 feline sarcoma virus (HZ4-FeSV) (Besmer *et al.*, 1986). Infectious filtrate obtained from primary feline fibrosarcomas exhibited the ability to transform and induce focus formation in feline embryonic fibroblasts and mink cells (Besmer *et al.*, 1986). Restriction digest analysis and Southern blotting of HZ4-FeSV revealed sequences not homologous to FeLV or to pre-existing oncogenes and therefore the foreign sequence was designated *v-Kit*. The 1.1 kb *v-Kit* sequence fused to a truncated viral

Gag sequence encoded a 370 amino acid fusion protein. Gag-linked myristoylation was presumed to localise *v-Kit* to the plasma membrane.

Through the use of oligonucleotide probes based on the *v-Kit* sequence, *c-KIT* was identified in feline (Herbst *et al.*, 1995a), murine (Qiu *et al.*, 1988) and human (Yarden *et al.*, 1987) cDNA libraries. In the human, the largest quantities were found in a glioblastoma cell line and term placenta (Yarden *et al.*, 1987). Three types of structural modifications were observed in *v-Kit* including: lack of the extracellular domain, lack of the transmembrane domain and the first 17 amino acids of the intracellular juxtamembrane region (Herbst *et al.*, 1995a; Yarden *et al.*, 1987) and finally the deletion of 50 amino acids in the carboxy terminal domain and their replacement with five non-related amino acids (Herbst *et al.*, 1995a). Three point mutations located in the juxtamembrane and kinase insert not attributable to species divergence were also identified (Herbst *et al.*, 1995a). These modifications are believed to be in part responsible for the deregulated oncogenic activity observed in *v-Kit* and give clues as to the regulation and function of c-Kit.

In parallel to these studies, c-KIT was identified at the protein level. A search for myeloid leukaemia associated antigens using monoclonal antibodies identified a surface marker on acute myeloid leukaemia (AML) cells that was absent in an autologous Epstein Barr Virus (EBV) transformed B cell line (Gadd and Ashman, 1985). The expression (or overexpression) of this marker on AML, detected with monoclonal antibody YB5.B8, was associated with a poor prognosis (Ashman *et al.*, 1988; Gadd and Ashman, 1985). It was later determined that the antigen recognised by YB5.B8 was c-KIT, a 145 kDa protein expressed in immature haemopoietic cells and tissue mast cells (Ashman *et al.*, 1991; Cole *et al.*, 1987; Lerner *et al.*, 1991; Mayrhofer *et al.*, 1987).

1.2.2. c-KIT is a Receptor Tyrosine Kinase

The cellular homologue of *v-Kit*, c-KIT was determined to be a 976 amino acid protein (Yarden *et al.*, 1987). Based on cell surface iodination studies of transfected NIH-3T3 fibroblasts, the protein was shown to be expressed on the cell surface (Yarden *et al.*, 1987). Deductions made concerning the primary amino acid sequence (Andre *et al.*, 1992; Giebel *et al.*, 1992; Vandenbark *et al.*, 1992) and the presence of a 24 amino acid signal peptide located at the amino terminus (Yarden *et al.*, 1987) supported this observation. The molecular weight of c-KIT was predicted to be about 110 kiloDalton (kDa), however potential N-linked glycosylation sites in the extracellular domain (Qiu *et al.*, 1988) increase the molecular weight to 125 kDa and 145 kDa (Reith *et al.*, 1991; Yarden *et al.*, 1987) for immature and mature c-KIT respectively. Homology of c-KIT with other RTKs and its amino acid sequence suggested that it has an extracellular domain, a transmembrane domain and an intracellular kinase domain (Vandenbark *et al.*, 1992) (Figure 1.2). Based on structural similarity (Blechman *et al.*, 1993b) and sequence homology (Herbst *et al.*, 1995a; Qiu *et al.*, 1988; Yarden *et al.*, 1986), c-KIT was assigned to RTK subclass III along with platelet derived growth factor (PDGF) receptor and colony stimulating factor-1 (CSF-1) receptor. Characteristic structural features of this subclass include five immunoglobulin like repeats in the extracellular domain and a kinase domain that is split by an interkinase sequence (Fantl *et al.*, 1993).

The extracellular domain contains 491 amino acid with 12 irregularly spaced cysteine residues, 10 of which are involved in disulphide bonding required to form the 5 immunoglobulin like repeats (Qiu *et al.*, 1988; Yarden and Ullrich, 1988). Only about 25% amino acid homology exists in the extracellular domain for receptors in this subclass (Qiu *et al.*, 1988) consistent with different functional requirements for binding ligand (Lev *et al.*, 1993). The extracellular domain has more species divergence than the intracellular domain, highlighting its importance in regulation of activation (Herbst *et al.*, 1995a).

Figure 1.2: Schematic diagram of human c-KIT.

Numbered circles represent the five immunoglobulin like domains with the first three representing the ligand binding domain. The split tyrosine kinase is denoted by red boxes. Location of the alternate splice sites in the juxtamembrane and interkinase region are indicated. The ligand for c-KIT, stem cell factor is abbreviated as SCF

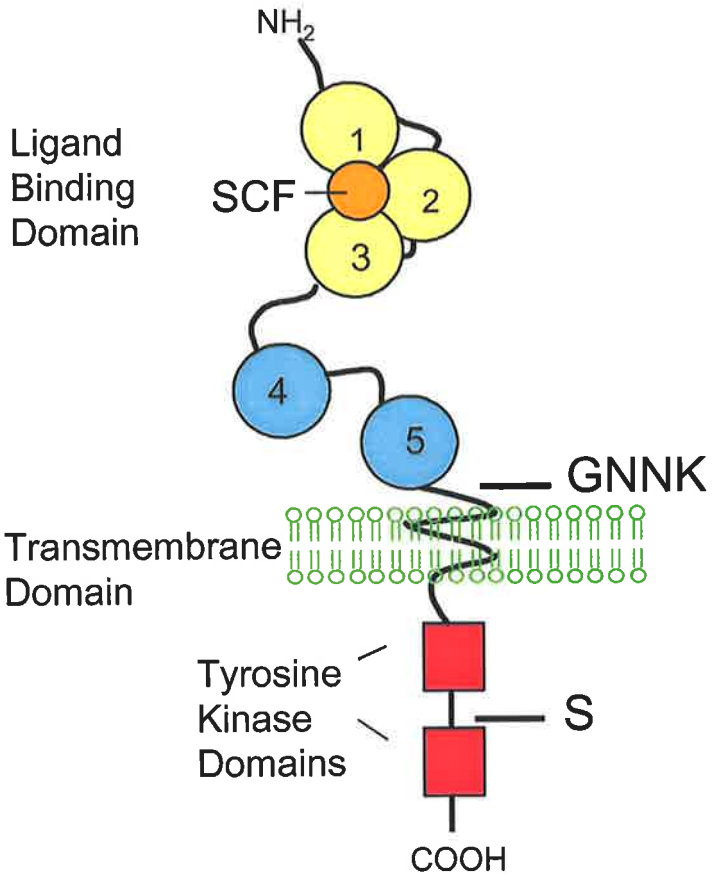
NH2
Ligand
Binding
Domain
SCF
1
2
3
4
5
GNNK
Transmembrane
Domain
Tyrosine
Kinase
Domains
S
COOH

Unlike the extracellular domain, the 439 amino acid intracellular domain contains a high amount of homology with other subclass III members (Blechman *et al.*, 1993b; Qiu *et al.*, 1988; Yarden *et al.*, 1987). The intracellular kinase domain is split by a hydrophilic insert sequence (Qiu *et al.*, 1988; Yarden *et al.*, 1986). The interkinase region is variable between members of the family and its length ranges from 70 to 100 amino acids (Qiu *et al.*, 1988; Yarden *et al.*, 1987). The amino terminal kinase domain is characterised by an ATP binding motif while the carboxy terminal kinase domain contains sequences consistent with kinase activity as well as the conserved autophosphorylation site in the activation loop at Y821 (equivalent to Y823 in human c-KIT) (Qiu *et al.*, 1988).

The carboxy terminal tail varies in length and is divergent between receptors in the family (Herbst *et al.*, 1995a; Yarden *et al.*, 1987), however some tyrosines that may recruit downstream signalling proteins are conserved (Qiu *et al.*, 1988). The carboxy terminal tail is deleted in *v-Kit* supporting its possible involvement in receptor down modulation (Qiu *et al.*, 1988).

1.2.3. Naturally Occurring Isoforms of c-KIT

In humans, four naturally occurring isoforms of c-KIT resulting from differential splicing at two distinct sites have been identified (Figure 1.2). The first occurs due to alternate splicing at the 3' end of exon 9, the exon encoding the region immediately prior to the transmembrane domain (Giebel *et al.*, 1992; Gokkel *et al.*, 1992; Hayashi *et al.*, 1991; Reith *et al.*, 1991; Vandenbark *et al.*, 1992). This results in an in-frame insertion or deletion of twelve base pairs encoding glycine-asparagine-asparagine-lysine, abbreviated as GNNK+ or GNNK- throughout this thesis. The second site for alternate splicing occurs at the 3' end of exon 15 (Crosier *et al.*, 1993). This results in the insertion or deletion of three base pairs encoding serine 715 in the interkinase sequence, abbreviated as S+ or S- respectively. Transcripts containing the serine residue have not been identified in mice (Crosier *et al.*,

1993) and analysis of the genomic structure revealed only the one acceptor site in contrast to the two in the human genomic sequence (Qiu *et al.*, 1988). All human c-KIT isoforms have been shown to have an equivalent affinity for their ligand (Caruana *et al.*, 1999).

The isoforms of *c-KIT* are co-expressed in tissues and their relative levels have been analysed in a number of different tissues and cell lines. In melanocytes, bone marrow and haematopoietic tumour cell lines, the GNNK- isoform appears to be dominant (Crosier *et al.*, 1993; Giebel *et al.*, 1992; Piao *et al.*, 1994). Similarly in AML there is higher expression of GNNK- *c-KIT* transcript relative to GNNK+ however the ratio of GNNK-:GNNK+ was quite heterogeneous and did not appear to depend on the AML subtype or correlate with colony forming ability in conditioned medium containing low levels of c-KIT ligand (Piao *et al.*, 1994). Supporting the observation in human cells, murine placenta and mast cells show co-expression of the isoforms with a dominance of GNNK- (Reith *et al.*, 1991). Analysis of messenger ribonucleic acid (mRNA) for the serine isoform indicates that in human bone marrow cells, melanocytes, and various tumour cell lines the S+ isoform is dominant (Crosier *et al.*, 1993).

Research investigating the role of murine GNNK-/+ isoforms in ligand mediated responses in mast cells indicated that both isoforms were able to promote proliferation to an equivalent extent with a half-maximal response at 25 ng/ml of ligand, however the GNNK- isoform induced a slightly stronger effect on adhesion (Serve *et al.*, 1995). Further analysis into the differential effects of c-KIT isoforms on ligand mediated biological responses was performed in NIH-3T3 fibroblasts transfected with cDNA encoding isoforms of human *c-KIT* (Caruana *et al.*, 1999). Analysis of the transformation efficiency of the isoforms revealed that GNNK-S+ induced potent transformation as shown by focus formation, anchorage independent growth and the ability to produce tumours in nude mice. The GNNK+S+ isoform promoted anchorage independent growth but only weak focus formation and no tumour formation in mice (Caruana *et al.*, 1999). The GNNK+S- isoform induced only focus

formation, while the GNNK-S- isoform could not be detected by indirect immunofluorescence or immunochemistry using the alkaline phosphatase anti-alkaline phosphatase (APAAP) method, despite the presence of mRNA transcripts (Caruana *et al.*, 1999).

Investigation of the downstream signalling pathways activated by murine c-Kit revealed that both isoforms became phosphorylated in a ligand dependent manner accompanied by an increased association with downstream substrates (Reith *et al.*, 1991). The GNNK- isoform had slightly increased autophosphorylation (Serve *et al.*, 1995) and constitutive activity (Reith *et al.*, 1991) as compared to GNNK+ c-Kit. Expression of human c-KIT in NIH-3T3 cells revealed differences between the activation kinetics of the GNNK-S+ and GNNK+S+ isoforms over a time course of ligand stimulation (Caruana *et al.*, 1999). Unlike murine c-Kit, human GNNK- c-KIT did not exhibit detectable basal phosphorylation, which may be due to serum starvation, differences between cell types or the levels of expression. Ligand activation of the GNNK-S+ isoform resulted in rapid and transient phosphorylation of c-KIT peaking at two minutes, while the GNNK+S+ isoform exhibited delayed but sustained phosphorylation of c-KIT peaking at seven minutes (Caruana *et al.*, 1999). The absence of the serine residue in c-KIT did not alter the kinetics of ligand activation, nor did it alter its ability to recruit PI 3-K whose binding site is only a few residues downstream (Caruana *et al.*, 1999).

1.2.4. Inactivation of c-Kit in *White Spotting* (*W*) Mutant Mice

The RTK c-Kit, has been described as being allelic to the *white spotting* (*W*) locus in mice (Chabot *et al.*, 1988; Nocka *et al.*, 1989). Mice with mutations in the *W* locus have developmental abnormalities in germ cells, melanocytes, haematopoietic progenitor cells as well as cells of the erythroid and mast cell lineages, resulting in an absence of coat colour, macrocytic anaemia and in more severe cases sterility or death. Based on the observations

from the *W* mutant mice, a large amount of data about the involvement and function of c-Kit in the development of these lineages has been obtained.

Several lines of evidence have linked *c-Kit* to the *W* locus. It was observed that the expression patterns of c-Kit closely reflected the tissues that were affected in *W* mutant mice (Andre *et al.*, 1992; Ikeda *et al.*, 1991; Keshet *et al.*, 1991; Kitamura *et al.*, 1978; Lammie *et al.*, 1994; Manova and Bachvarova, 1991; Nocka *et al.*, 1989; Ogawa *et al.*, 1991b; Ratajczak *et al.*, 1992). At the genetic level, *in situ* hybridisation and hybrid cell lines localised the *c-Kit* gene to mouse chromosome 5, which is the same as the *W* locus (Chabot *et al.*, 1988). Sequencing and restriction fragment length polymorphism of DNA from *W* mice revealed base pair transitions or creation of novel fragments in *c-Kit* (Chabot *et al.*, 1988; Reith *et al.*, 1990). Functional involvement of mutant c-Kit in the *W* phenotype was confirmed by the observation that c-Kit kinase activity was affected in *W* mice (Nocka *et al.*, 1989) and also that introduction of wild type (WT) *c-Kit* cDNA into *W* mutant cells rescued the responses of these cells to the c-Kit ligand (Alexander *et al.*, 1991).

Multiple independent mutations or deletions within *c-Kit* and the surrounding regions involved in regulating gene expression are affected in the *W* phenotype (Berrozpe *et al.*, 1999; Hayashi *et al.*, 1991; Koshimizu *et al.*, 1994; Nocka *et al.*, 1989; Reith *et al.*, 1990; Reith *et al.*, 1991; Rottapel *et al.*, 1991; Tan *et al.*, 1990). The various mutations alter c-Kit kinase activity in a way that is correlated with the overall severity of the phenotype (Nocka *et al.*, 1989; Nocka *et al.*, 1990b; Reith *et al.*, 1990). Deletion or truncation mutants of *c-Kit* appear to have a relatively mild phenotype in the heterozygous state, however in the homozygous state, they are severe and can be lethal (Chabot *et al.*, 1988). Point mutations in the conserved region of the kinase domain resulting in impaired or no kinase activity exert a 'dominant negative' effect in the heterozygous form (Herbst *et al.*, 1992; Nocka *et al.*, 1990b; Reith *et al.*, 1991; Tan *et al.*, 1990) due to sequestering active receptor into inactive dimerised complexes (Adachi *et al.*, 1992; Tan *et al.*, 1990). In the homozygous form, these *W*

mutations generally result in viable progeny due to the presence of a low residual kinase activity (reviewed in Bernstein *et al.*, 1991). The phenotype of the mutant mice shows that c-Kit dimerisation and kinase activity are important for its function (Herbst *et al.*, 1992).

Piebaldism is an autosomal dominant disorder affecting humans which has a similar phenotype to *W* mice (reviewed in Vliagoftis *et al.*, 1997). It is diagnosed by congenital patching of white skin and white hair on the scalp, forehead, chest, abdomen and the extremities and is present from birth (Giebel and Spritz, 1991). Due to the correlations of this disease with the *W* locus in mice, parallels were made and it was shown to be dependent on missense mutations and deletions in the *c-KIT* gene (Fleischman *et al.*, 1991; Giebel and Spritz, 1991).

1.3. THE LIGAND FOR C-KIT

The ligand for c-KIT was simultaneously identified by several research laboratories in murine, human and rat systems and was named mast cell growth factor (MGF) (Anderson *et al.*, 1990; Boswell *et al.*, 1990; Williams *et al.*, 1990), steel factor (SLF) (Williams *et al.*, 1992), kit ligand (KL) (Flanagan and Leder, 1990; Huang *et al.*, 1990; Nocka *et al.*, 1990a) and stem cell factor (SCF) (Martin *et al.*, 1990; Zsebo *et al.*, 1990a; Zsebo *et al.*, 1990b), of which the latter terminology has been used throughout this thesis.

The ligand for c-KIT is a 248 amino acid transmembrane polypeptide with an extracellular domain of 189 amino acids, a hydrophobic transmembrane domain of 23 amino acids and an intracellular domain consisting of 36 amino acids (Flanagan and Leder, 1990). Alternate splicing of both murine and human SCF (huSCF) results in the formation of two membrane bound isoforms, with one lacking exon 6 that encodes 28 amino acids of the extracellular domain (Flanagan *et al.*, 1991). This splicing event is tissue specific, with the brain and bone marrow expressing about five fold more of the long form (248 amino acids), while the spleen expresses an equal amount of both splice variants (Flanagan *et al.*, 1991).

A soluble form of SCF was identified in murine stromal supernatant (Williams *et al.*, 1990) and in conditioned medium from buffalo rat liver cells (Martin *et al.*, 1990; Zsebo *et al.*, 1990a) and Balb/c 3T3 fibroblasts (Nocka *et al.*, 1990a). This soluble form is produced due to the presence of a serine protease site at amino acid 165 in exon 6 (Longley *et al.*, 1997) absent in the alternately spliced variant (Flanagan *et al.*, 1991). Another site for cleavage is between amino acids 158 - 159 and is cleaved by chymase, a chymotrypsin like protease derived from human mast cells, resulting in a product 7 amino acids shorter than the previously reported form of soluble SCF (Longley *et al.*, 1997). In murine SCF, an alternate cleavage site in exon 7 utilised in the absence of the exon 6 site allows formation of soluble SCF from both transmembrane forms (Majumdar *et al.*, 1994) This site is absent in human SCF (Majumdar *et al.*, 1994). Both the transmembrane and soluble forms of SCF have been shown to be biologically active (Anderson *et al.*, 1990).

SCF has been determined to exist as a non-covalent homodimer, however under physiological conditions, most of it is present as a monomer (Hsu *et al.*, 1997). The first structural information was obtained from a crystal structure of the receptor binding core encoded by amino acids 1 – 141 (Zhang *et al.*, 2000b). The SCF dimer was found to be joined head to head through an extensive hydrophobic region that covered about 20% of the total surface area of each monomer (Zhang *et al.*, 2000b). The presence of SCF in dimeric form appears to be required for function since dimerisation defective SCF had minimal activity (Hsu *et al.*, 1997) while disulfide linked dimers had enhanced (Hsu *et al.*, 1997) or no activity (Zhang *et al.*, 2000b) dependent on the location of the disulfide link. Unlike soluble SCF, the majority of membrane bound SCF exists in a dimer formation as was shown by cross-linking studies (Tajima *et al.*, 1998). Deletion of the majority of the cytoplasmic domain did not seem to affect the dimerisation ability, however replacement of this region with extraneous amino acids diminished dimerisation capabilities (Tajima *et al.*, 1998).

SCF belongs to the short chain helical cytokine family (Bazan, 1991). It differs from PDGF and CSF-1, both ligands for subclass III RTKs, in that they both form disulphide linked homodimers. Other ligands also exist in a transmembrane form, for example TNFα which also has roles as a growth factor as well as serving adhesive functions (Massague, 1990).

1.3.1. *Steel* Mutant Mice Lack Functional c-KIT Ligand

The finding that SCF mapped to mouse chromosome 10 (Copeland *et al.*, 1990; Zsebo *et al.*, 1990a) led to the identification of SCF being allelic with the *Steel* (*Sl*) locus. Alterations in the SCF gene are the cause of the *Sl* phenotype with deletions having the most dramatic phenotype including death *in utero* or shortly after birth due to a complete loss of SCF function (Zsebo *et al.*, 1990a). Mutations in SCF generally result in a milder phenotype with defects in pigmentation, haematopoietic cells, melanocytes and germ cells (Flanagan *et al.*, 1991; Zsebo *et al.*, 1990a).

The phenotype of *Sl* mutant mice is similar to that of *W* mutant mice, in that they have severe macrocytic anaemia, are sterile and lack pigmentation (Copeland *et al.*, 1990; Flanagan and Leder, 1990). Transplantations studies elucidated the involvement of the *Sl* locus in haemopoiesis and its relationship to the *W* locus in mice (Kitamura and Go, 1978; Kitamura *et al.*, 1978). Adult mice mutant for the *Sl* locus (Sl/Sl^d) have only 1% of normal mast cell numbers in the skin as compared to WT, while no mast cells were present in the stomach, caecum, bone marrow, spleen, thymus, heart, lung, kidney, liver and brain (Kitamura and Go, 1978). Similarly, W/W^v mutant mice displayed a similar distribution of mast cells (Kitamura *et al.*, 1978). Bone marrow transplantation from WT donors showed that mast cells in the *Sl* mutant mice could not be rescued (Kitamura and Go, 1978), in contrast to *W* mutant mice that were partially rescued (Kitamura *et al.*, 1978). Skin grafts further elucidated the roles of *Sl* and *W* (Kitamura and Go, 1978). Grafting *W* mutant skin onto a WT mouse resulted in increased mast cells up to 100 fold at the site of engraftment whereas there was no change

when *Sl* skin was grafted onto a WT mouse. However, grafting of *W* skin onto *Sl* mice resulted in mast cell rescue at the engraftment site but the converse did not result in rescue. This indicated a link between the *W* and *Sl* locus, suggesting that *Sl* provided a microenvironmental cue to support the growth of these cells while *W* provided a signal intrinsic to the cells affected. This led to the notion that the *Sl* gene product encoded the ligand for the *W* gene product. Further, SCF has been shown to be expressed in complementary tissues to c-KIT (Lammie *et al.*, 1994).

The functional requirement for the transmembrane form of SCF has been highlighted in the *Steel-Dickie* (Sl^d) mutant (Flanagan *et al.*, 1991). The Sl^d mutation results in the deletion of the transmembrane and intracellular region, producing a soluble protein capable of stimulating proliferation (Flanagan *et al.*, 1991). Mice with this mutation have impaired development of haemopoietic cells, melanocytes and germ cells, although the phenotype is less severe than other types. It is of interest to note this phenotype because it shows a requirement of transmembrane SCF in supporting haemopoiesis, germ cell development and pigmentation. The functional requirement of the cytoplasmic region of SCF in dimerisation has been shown in Sl^{17H} mutant mice (Tajima *et al.*, 1998). In this mutation the cytoplasmic domain is replaced with 27 extraneous amino acids which allows surface expression, however its stability, rate of transport and dimerisation is affected (Tajima *et al.*, 1998). Mice with this genotype have decreased tissue and peritoneal mast cells, white spotting with residual pigmentation, and the males are infertile (Tajima *et al.*, 1998). Observation of Sl^d and Sl^{17H} mutant mice indicate the importance of the transmembrane and intracellular regions of SCF for its function. The transmembrane form of SCF is required for adhesion of cells to stroma (Tajima *et al.*, 1998) and is also important in the homing of transplanted haemopoietic cells to irradiated Sl^{17H} spleen (Tajima *et al.*, 1998).

1.4. ACTIVATION OF C-KIT

1.4.1. Ligand Binding

The affinity of huSCF for its receptor is $3x10^{-8}$ M (Flanagan and Leder, 1990; Lev *et al.*, 1992c) without exhibiting preference for c-KIT isoforms (Caruana *et al.*, 1999). Analysis of SCF action between species revealed that huSCF is only active on human c-KIT, since it shows negligible affinity for murine c-Kit (Martin *et al.*, 1990; Zsebo *et al.*, 1990a). Rat SCF, on the other hand, is active on both species of c-KIT (Martin *et al.*, 1990), showing about 10 - 100 fold reduced affinity for human c-KIT relative to murine c-Kit (Lev *et al.*, 1992c).

The species divergence exhibited with human and rat SCF enabled mapping of the ligand binding site. By the use of chimeric c-KIT composed of human and murine portions, and using either human or rat SCF, the ligand binding site was mapped to the second immunoglobulin like domain of human c-KIT (Lev *et al.*, 1993). Studies using antibody displacement techniques also confirmed these results (Blechman *et al.*, 1993a). The two immunoglobulin like domains flanking the second were found to be important in ligand recognition with the first having an inhibitory effect on SCF binding while the third enhanced the affinity, possibly by stabilising the interaction (Blechman *et al.*, 1993a; Lev *et al.*, 1993). It is of interest to note that RTKs containing immunoglobulin like domains in the extracellular region (those from sub-class III and V) bind ligand within the first three immunoglobulin like domains, and where this has been defined further, to either the second or third (Jiang *et al.*, 2000).

The site of interaction for c-KIT on SCF has been identified by the use of chimeric interspecies and epitope mapping to three distinct regions on SCF (Matous *et al.*, 1996). Modelling of SCF by crystal structure have shown that these regions on SCF are also non-contiguous in the primary sequence, but are contiguous on the surface of SCF (Jiang *et al.*, 2000).

1.4.2. Dimerisation and Activation of Downstream Pathways

The binding of ligand to RTKs results in dimerisation, which appears to be an important step for their activation since it correlates with kinase activity (Blume-Jensen *et al.*, 1991). It is also highlighted by the dominant negative action of various *W* mutants in mice (Nocka *et al.*, 1990b; Reith *et al.*, 1991; Tan *et al.*, 1990). The dimeric conformation consists of two molecules of SCF monomer complexed to two molecules of c-KIT (Philo *et al.*, 1996). Controversy exists over the mechanism by which ligand induces dimerisation. One view is that ligand is the driving force since the addition of SCF to soluble c-KIT consisting of the first three immunoglobulin like domains resulted in dimerisation (Lemmon *et al.*, 1997). However, this does not seem likely since excess SCF did not disrupt c-KIT dimer formation (Lemmon *et al.*, 1997; Lev *et al.*, 1992c) which would be expected if the ligand was solely responsible. Others have proposed that the binding of SCF induces a conformational change in c-KIT revealing sites critical for dimer formation (Blechman *et al.*, 1995). A more plausible explanation is a combination of the two models, where the dimeric nature of SCF initiates receptor dimerisation and a conformational change in the receptor stabilises the dimer. Upon the binding of ligand, the extracellular region of c-KIT undergoes conformational changes in the secondary and tertiary structure (Narhi *et al.*, 1998). Expression of the extracellular domain alone is sufficient to allow dimerisation (Blechman *et al.*, 1995; Lev *et al.*, 1992b; Narhi *et al.*, 1998; Philo *et al.*, 1996). It is thought that the fourth immunoglobulin like domain is important in supporting dimerisation since its deletion abolished dimerisation as well as c-KIT auto kinase activity (Blechman *et al.*, 1995).

Dimerisation is an important step since it precedes tyrosine phosphorylation of intracellular residues within the dimers by a process called transphosphorylation or autophosphorylation (see section 1.2). Transphosphorylation in the kinase domain precedes kinase activity as well as phosphorylation at other sites of the receptor (Heldin, 1995). In the human PDGF receptor, one phosphorylated tyrosine residue Y857, resides in the activation loop of the catalytic kinase domain (Claesson-Welsh, 1994). This residue in the activation

loop is conserved in human and murine c-KIT as Y823 and Y821 respectively (Serve *et al.*, 1995). Phosphorylation of residues outside the kinase domain serve as docking sites for downstream signalling molecules, triggering multiple signalling cascades (Heldin, 1995). Signalling pathways have important roles in contributing to the numerous biological responses, and the duration/strength of signalling through c-KIT may modulate the mixture of downstream cascades triggered, and determine which of the many biological outcomes of SCF/c-KIT signalling are activated.

1.4.3. Biological Responses Mediated by c-KIT

Ligand binding and receptor dimerisation are important prerequisites for eliciting the biological response. For example, *W* mice with c-Kit incapable of binding SCF or dimerising correctly have defects in various biological responses including proliferation, adhesion and chemotaxis of mast cells, melanocytes and natural killer cells (Dastych *et al.*, 1998; Nocka *et al.*, 1989).

The interaction of SCF with c-KIT has been found to induce the proliferation of many haemopoietic cell types including both mature and immature mast cells (Tsai *et al.*, 1991), natural killer committed precursors (Colucci and Di Santo, 2000), over half of AML cases (Ikeda *et al.*, 1993) and a human megakaryocytic cell line, MO7e (Kuriu *et al.*, 1991). The effect of SCF on proliferation has been dissected from its survival response, showing that SCF increases the survival of certain cells expressing c-KIT (Bendall *et al.*, 1998; Colucci and Di Santo, 2000; Ricotti *et al.*, 1998). Adhesion is also mediated by SCF interacting with c-KIT. This can be due to direct interaction of c-KIT with the transmembrane form of SCF expressed on fibroblasts (Kinashi and Springer, 1994), or indirect with the interaction of SCF and c-KIT stimulating integrin mediated adhesion to the extracellular matrix (Kinashi and Springer, 1994; Levesque *et al.*, 1995; Levesque *et al.*, 1996; Yuan *et al.*, 1997). Direct adhesion through the interaction of c-KIT with membrane bound SCF is independent of c-KIT kinase

activity, however integrin mediated adhesion is dependent on an active kinase since a kinase inhibitor, genistein inhibited the adhesion (Kinashi and Springer, 1994). This suggests that the kinase activity of c-KIT is required in an inside-out signalling mechanism to modify the functional state of the integrins (Levesque *et al.*, 1995). A role of c-KIT in chemotaxis has been observed both in bone marrow derived mast cells (Meininger *et al.*, 1992) and in c-KIT transfected cells (Blume-Jensen *et al.*, 1993). In bone marrow derived mast cells, c-KIT signalling has been shown to promote secretion (Damen *et al.*, 2001), degranulation (Vosseller *et al.*, 1997), membrane ruffling (Vosseller *et al.*, 1997) and actin assembly (Blume-Jensen *et al.*, 1993; Vosseller *et al.*, 1997). SCF is also capable of inducing differentiation of immature mast cells (Tsai *et al.*, 1991), Myb immortalised haemopoietic cell(s) (MIHC) derived from murine foetal liver (Ferrao *et al.*, 1997), and melanocytes in the embryo as well as in adult human skin xenografts (Ricotti *et al.*, 1998). However, in other cases such as natural killer cells, SCF is not required for the commitment of haemopoietic stem cells to the lineage, instead, it is important in increasing the numbers of this population (Colucci and Di Santo, 2000). All of these responses including proliferation, survival, adhesion, chemotaxis, differentiation and secretion can be seen in mast cells with a more restricted range of responses occurring in other cell types.

While stimulation of c-KIT with SCF can in some cases act alone to elicit biological responses, it can also act in concert with other RTKs and cytokine receptors to augment the response obtained (Martin *et al.*, 1990; Zsebo *et al.*, 1990b). In most cell types, SCF exerts little proliferative effect on its own, however, it synergises with other cytokines such as interleukin (IL)-6, IL-3 and IL-7 to exert a dramatic effect on proliferation (Martin *et al.*, 1990; Zsebo *et al.*, 1990b). Synergy of SCF with extracellular matrix proteins acting via integrins has also been observed where the presence of fibronectin enhanced SCF mediated proliferation of AML cells (Bendall *et al.*, 1998).

While the role of c-KIT kinase activity in eliciting biological responses is clear, the precise signalling pathways that couple c-KIT activation to specific responses are unknown. Ongoing research is investigating how signal transduction downstream of c-KIT and other RTKs regulates the outcome.

1.5. Aberrant c-KIT Kinase Activity and its Role in Neoplasia

The first oncogenic version of c-KIT, v-Kit, was identified as the transforming element of the HZ4-FeSV responsible for fibrosarcoma formation in cats (Besmer *et al.*, 1986). The transforming activity of v-Kit and the oncogenic potential of other RTKs (Ullrich and Schlessinger, 1990) suggested that aberrant activation of c-KIT had the potential to be involved in neoplasia. c-KIT has subsequently been found to have a role in haemopoietic associated neoplasms including mastocytosis, AML, myeloproliferative disorders as well as gastrointestinal stromal tumours (GISTs).

Mastocytosis is a sporadic disease characterised by mast cell hyperplasia in the bone marrow, liver, spleen, lymph nodes, gastrointestinal tract and skin (Nagata *et al.*, 1998). The most common c-KIT anomaly involved in mastocytosis is mutation of aspartate at position 816, located in the phosphotransferase region of the kinase domain to a valine residue (D816V) (Worobec *et al.*, 1998), however mutations to tyrosine or phenylalanine have also been reported (Longley *et al.*, 1999). The D816V mutation was observed in 25% of mastocytosis patients (n=65) (Worobec *et al.*, 1998), while in another study all (n=15) patients with adult sporadic mastocytosis contained the mutation (Longley *et al.*, 1999). Patients presenting with this mutation are generally of an older age and exhibit more severe disease patterns associated with haemopoietic disorders, including mast cell lesions in bone marrow, chronic neutropenia, acute non-lymphocytic leukaemia, myelodysplastic syndrome and myelodysplastic disease (Nagata *et al.*, 1995; Worobec *et al.*, 1998). This suggests that the D816V c-KIT mutation is associated with worse prognosis. Another constitutively active

c-Kit mutation identified in a murine mastocytoma cell line (FMA3) results from an in frame deletion of 21 base pairs at the juxtamembrane domain (Tsujimura *et al.*, 1996) indicating an important role of this region in regulating kinase activity. Upregulation of c-KIT transcription may also have a role since an increase in c-KIT mRNA was identified in all (n=6) patients with mastocytosis as determined by quantitative polymerase chain reaction (PCR) (Nagata *et al.*, 1998).

The presence of D816V was first identified in association with V560G as a heterozygous mutation in HMC-1, a human mast cell leukaemic line (Furitsu *et al.*, 1993; Kanakura *et al.*, 1994). These mutations induce constitutive tyrosine phosphorylation on c-KIT as well as its constitutive association to a downstream substrate, PI 3-K (Furitsu *et al.*, 1993; Kanakura *et al.*, 1994). Introduction of the corresponding murine mutants V559G and D814V or the human equivalents, either separately or together, into factor dependent cell lines rendered the cells factor independent and tumourigenic in mice (Ferrao *et al.*, 1997; Hashimoto *et al.*, 1996; Kitayama *et al.*, 1995; Tsujimura *et al.*, 1994). This suggests that both mutations are transforming events. An equivalent mutation (D814Y) observed in P815, a murine mastocytoma cell line, also induces constitutive c-Kit phosphorylation and kinase activity (Tsujimura *et al.*, 1994).

Most amino acids, when substituted at D814, result in constitutive phosphorylation and factor independent growth indicating the critical role of the aspartate residue in regulating enzyme activity (Moriyama *et al.*, 1996). Investigation into the mechanism by which D816V may act revealed that it induced degradation of SHP1, a phosphatase involved in dephosphorylating c-KIT and hence regulating its activity (Piao *et al.*, 1996). The D816V mutation also causes a difference in the phosphorylation selectivity and substrate specificity of c-KIT (Piao *et al.*, 1996). The constitutive activity of D816V c-KIT appears to be due to ligand independent dimerisation, since a dimerised form of the recombinant intracellular kinase domain was detected by gel filtration, unlike WT c-KIT which was present as a

monomer (Lam *et al.*, 1999). Further, the constitutive phosphorylation of D814Y c-Kit and factor independent growth observed when expressed in Ba/F3 cells was abrogated with the co-expression of a *W* mutant version of c-Kit (Tsujimura *et al.*, 1999). Although no constitutively dimerised complex has been detected in cross linking studies (Kitayama *et al.*, 1995), it is thought that D816V may induce a conformational change in the receptor allowing self association at sites distinct from those required for ligand mediated dimerisation (Tsujimura *et al.*, 1999).

Aberrant activation of c-KIT may play a role in AML with 7 out of 12 patients in one study showing constitutive c-KIT phosphorylation (Ikeda *et al.*, 1991). Mutations involving a loss or replacement of aspartate at 419 in the extracellular domain of c-KIT have been observed in 7.7% (n=60) of AML cases (Gari *et al.*, 1999). The D816V mutation also occurs in occasional cases of AML (Ashman *et al.*, 2000; Beghini *et al.*, 1998). Overexpression of c-KIT does not appear to be a causative agent since c-KIT protein and mRNA levels were generally less than or equal to those found in normal CD34+ cells (Cole *et al.*, 1996). Autocrine activation of c-KIT as a common means of transformation has also been excluded (Cole *et al.*, 1996). Myeloproliferative disorders are a group of haemopoietic neoplasms at the myeloid stem cell level and mutation of c-KIT at aspartate 52 has been observed in 3 of 25 cases (Kimura *et al.*, 1997; Nakata *et al.*, 1995).

The most common mesenchymal tumours in the human digestive tract are GISTs (Hirota *et al.*, 1998) of which a major proportion contain mutations in c-KIT (Moskaluk *et al.*, 1999; Taniguchi *et al.*, 1999). Similarly to D816V in mastocytosis, GIST patients presenting with c-KIT mutations are generally older and have tumours of a more malignant phenotype including metastasis and invasion of adjacent tissues (Taniguchi *et al.*, 1999). The majority of c-KIT mutations in GIST are located in exon 11 encoding the intracellular juxtamembrane region and consist of in frame insertions, deletions and missense mutations (Moskaluk *et al.*, 1999; Taniguchi *et al.*, 1999). Where further defined, these mutations encompass amino acids

550 to 560 (Moskaluk *et al.*, 1999; Taniguchi *et al.*, 1999), located in a region thought to encode a regulatory α-helix. Expression of several juxtamembrane mutant forms of c-KIT in Ba/F3 factor dependent cells results in factor independent growth, tumour formation and constitutive kinase activity (Hirota *et al.*, 1998). Additional types of mutations identified in GIST include a 6 nucleotide duplication in exon 9 encoding the carboxy terminal end of the extracellular region as well as a missense mutation, K642E in the amino terminal kinase domain (Hirota *et al.*, 2001; Lux *et al.*, 2000). Unlike mastocytosis, no mutations have been observed in the exon where D816V is located (Taniguchi *et al.*, 1999).

The above research highlights that types of c-KIT mutations are similar within but different between the types of neoplasms. In mastocytosis, mutations are mostly located in the enzymatic pocket, such as D816V, while in GIST mutations are mainly in the juxtamembrane region and considered to be a regulatory type mutation (Longley *et al.*, 2001). Identification of these differences may aid in potential therapeutic treatments (Longley *et al.*, 2001), with an example being Imatinib (Glivec, formerly STI-571). Imatinib is a potent inhibitor of abl kinase, PDGF receptor, c-KIT and bcr-abl (Buchdunger *et al.*, 1996; Buchdunger *et al.*, 2000; Druker *et al.*, 1996) due to its ability to stabilise the inactive conformation of the kinase (Shah *et al.*, 2002). It is currently in phase II trials for the treatment of chronic myelogenous leukaemia (CML) (Kantarjian *et al.*, 2002; Sawyers *et al.*, 2002) of which 95% of patients contain the bcr-abl oncogene (Sawyers, 1999). Imatinib is also active against various c-KIT mutations found in GIST (Tuveson *et al.*, 2001). In a phase I study, administration of Imatinib to patients with GIST resulted in improved clinical symptoms in 24 of the 27 studied, while in 25 of 36, tumour regression was observed (van Oosterom *et al.*, 2001). Interestingly, Imatinib is not active on the D816 kinase domain mutant as judged by phosphorylation and cell growth, although the V560G mutant was strongly inhibited (Frost *et al.*, 2002; Ma *et al.*, 2002). Co-expression of the D816V mutant with V560G as present in one subline of HMC-1 abolishes the response to Imatinib. Therefore, Imatinib is active on regulatory type mutations

in c-KIT, however this is overcome by the addition of kinase domain mutations. The differential effect of Imatinib on regulatory and kinase domain mutations in c-KIT further illustrates that they lead to constitutive receptor activation by different mechanisms. Three indolinones have recently been identified as inhibitors of catalytic and regulatory type c-KIT mutations and may therefore be useful in the treatment of mastocytosis (Liao *et al.*, 2002).

1.6. SIGNAL TRANSDUCTION PATHWAYS

Activation of signal transduction by RTKs is a complex process involving cascades of protein and lipid phosphorylation, culminating in various biological responses. Receptor dimerisation triggered by ligand binding promotes the autophosphorylation of one receptor by its neighbour. This causes displacement of the activation segment from the active site (Blume-Jensen and Hunter, 2001) to allow further phosphorylation on tyrosines outside the kinase domain (Pawson and Nash, 2000). These phosphorylated residues then act as docking sites allowing the binding and activation of downstream substrates (reviewed in Pawson and Schlessinger, 1993). Although common signal transduction pathways are activated by RTKs, different biological responses can be obtained depending on the cellular makeup and the strength and duration of the signal (Fantl *et al.*, 1993).

1.6.1. Protein Modules Involved in Signal Transduction

Various modular domains are involved in signal transduction, each having a unique role. Two of these were originally identified in the non-receptor tyrosine kinase Src, but later found in unrelated proteins and were labelled SH2 and SH3 (reviewed in Pawson, 1995). Other modular structures also present in proteins are the pleckstrin homology (PH) domain (which contains homology to pleckstrin a major substrate of protein kinase C (PKC) in platelets) (Lemmon and Ferguson, 1998), and the PTB domain (Pawson, 1995). More details on these domains follows.

The SH2 domain specifically recognises phosphotyrosine in the context of a small amino acid peptide (Pawson, 1995). The affinity and specificity of the association is created by approximately three amino acids carboxy terminal to the phosphorylated tyrosine. As an example, the SH2 domain of the adaptor subunit of PI 3-K recognises the sequence pY-X-X-M where pY represents tyrosine phosphorylation and X represents any amino acid (Pawson and Schlessinger, 1993). The 100 amino acid SH2 domain (Pawson and Schlessinger, 1993) has a structure analogous to a two pin electric socket and the phosphopeptide is analogous to a two pin plug (Smithgall, 1995). The pocket responsible for binding phosphotyrosine contains the only invariant amino acid, arginine, which is important for binding oxygen atoms in the phosphate group (Pawson, 1995). The second, more variable pocket is involved in binding amino acids carboxy terminal to the phosphorylated tyrosine (Pawson and Schlessinger, 1993; Pawson, 1995). The effect of a SH2 domain binding its target sequence can be three fold (Schlessinger, 2000). Firstly, the association can cause an increase in the phosphorylation of the protein, for example, phospholipase Cγ (PLCγ) binding to a RTK (Pawson and Schlessinger, 1993; Schlessinger, 1994). Secondly, it can cause translocation of the protein to the membrane localising it near its substrates, and finally, it can stimulate enzyme activity by inducing a conformational change in the protein, for example PI 3-K (Pawson and Schlessinger, 1993).

The SH3 domain specifically recognises proline residues usually present in a sequence X-P-X-X-P, where the second X tends to be a proline and the third X an aliphatic residue (Pawson, 1995; Smithgall, 1995). Unlike the SH2 domain, SH3 mediated association is not induced by phosphorylation, but instead is mainly involved in stable protein-protein interactions (Pawson and Schlessinger, 1993). The SH3 domain has a more regulatory role in signal transduction (Pawson and Schlessinger, 1993) being involved in subcellular localisation, cytoskeletal interactions and in linking signals (Pawson, 1995). It is composed of approximately 50 amino acids (Pawson and Schlessinger, 1993) and has a barrel like structure

with a hydrophobic pocket (Schlessinger, 1994; Smithgall, 1995) containing the signature sequence A-L-Y-D-Y responsible for binding proline rich sequences (Smithgall, 1995).

Less is known about PH domains and their involvement in intracellular signalling and cytoskeletal organisation (reviewed in Lemmon and Ferguson, 1998). The substrates to which they bind include the βγ subunits of G proteins, some PKC isoforms and phosphoinositides (Lemmon and Ferguson, 1998; Pawson, 1995). Associations with 3' phosphorylated phosphoinositides have been characterised in respect to the PI 3-K pathway (see section 1.7 for more detail). PH domains form important associations with phosphoinositides (Vanhaesebroeck and Alessi, 2000) and the affinity and specificity for binding varies. As an example, the PH domain of Akt binds with high affinity to phosphatidylinositol (PtdIns)-3,4-P_2 whereas 3' phosphoinositide-dependent kinase-1 (PDK1) prefers PtdIns-3,4,5-P_3 (Martin, 1998).

PTB domains, like SH2 domains, bind phosphorylated tyrosines in the context of N-P-X-pY (Pawson, 1995). This association is important for interactions with activated receptors, and examples of proteins with PTB domains are Shc and the insulin receptor substrate(IRS) (Pawson, 1995). The suggested purpose of these domains is to amplify signals from a given receptor by creating multiple docking sites for signalling proteins (Pawson and Nash, 2000).

Proteins have various combinations of these domains and can be grouped into two classes. The first are adaptors that lack any intrinsic enzyme activity and are composed of a number of these domains (eg. Grb2) (Pawson, 1995). The other class have these domains in conjunction with their own intrinsic catalytic activity (Schlessinger, 1994).

1.6.2. The Complexity of Cellular Signalling

Signal transduction pathways downstream of RTKs are complex. There are multiple components forming a cascade of phosphorylation events thought to provide amplification of

the initial signal, such that increased numbers of the more downstream components are activated than would occur in a single activation step (Brown *et al.*, 1997). Multi-level cascades increase the sensitivity to a stimulus and allow for the switch like responses (Brown *et al.*, 1997; Ferrell, 1996; Ferrell, 1997).

The strength of signal down a particular pathway dictates the response obtained (reviewed in Marshall, 1995). In the PC12 phaeochromocytoma cell line, activation of the trkA RTK by its ligand, nerve growth factor (NGF) results in neurite extension (Qui and Green, 1992; Traverse *et al.*, 1992; Traverse *et al.*, 1994). Accompanying this is sustained Ras activation, prolonged extracellular signal regulated kinase (ERK) activation and nuclear translocation (Qui and Green, 1992; Traverse *et al.*, 1992; Traverse *et al.*, 1994). Activation of endogenous EGF or insulin receptors results in weak mitogenic responses associated with transient Ras and ERK activation without nuclear translocation (Dikic *et al.*, 1994; Qui and Green, 1992; Traverse *et al.*, 1992; Traverse *et al.*, 1994). Overexpression of these receptors is capable of generating neurite formation which appears to be due to the prolonged activation of ERK leading to its nuclear translocation (Dikic *et al.*, 1994; Traverse *et al.*, 1994). This indicates that the duration of ERK activation and nuclear translocation is an important parameter in the decision to proliferate or differentiate. Therefore, RTKs that activate the same signal transduction pathway can elicit different biological responses by varying the amplitude and duration of the signal (Pawson and Nash, 2000).

The signal transduction pathways interact and converge on overlapping targets to ensure tight control over biological functions (Pawson and Nash, 2000). An example of this is in cell division where a cell needs to monitor its size and internal state so that it doesn't divide before reaching the appropriate mass (Pawson and Nash, 2000). One means of doing this is by requiring two pathways to converge on the activation of a particular protein. This is illustrated by Rsk which must be phosphorylated by two proteins, PDK1 and ERK for its full activation (Pawson and Nash, 2000).

Compartmentalisation adds to the complexity and control of signal transduction as it segregates proteins within the cell (Weng *et al.*, 1999). Communication between compartments such as the cytosol and plasma membrane can be via translocation or recruitment to an activated receptor. For example, the Grb2/Son of Sevenless (Sos) complex (which is the first step of the Ras-mitogen activated protein kinase (MAPK) cascade; see section 1.6.3) is recruited to the plasma membrane where it acts on Ras (Schlessinger, 1995; Schlessinger and Bar-Sagi, 1997).

Another complexity arises from scaffolding where components assemble into functional complexes in order to increase efficiency and specificity in signalling (Weng *et al.*, 1999). An example of a scaffolding protein in mammalian cells is MEK partner-1 (MP1) which binds MEK and ERK, facilitating the phosphorylation of the latter (Garrington and Johnson, 1999). Given the complexity of signal transduction pathways downstream of RTKs, and the control mechanisms employed, it is clear that more complete characterisation is required to fully understand their roles in cellular responses.

1.6.3. Ras-MAPK Pathway

After activation of RTKs by ligand engagement and tyrosine phosphorylation, a cascade of serine and threonine phosphorylation events follow of which a portion can be attributed to the Ras-MAPK pathway (Avruch *et al.*, 1994). The significance of this pathway in signal transduction is emphasised by two points. Firstly, it is highly conserved between species, since homologous proteins have been found in *Caenorhabditis Elegans* and *Drosophila* (Schlessinger, 1995; Schlessinger and Bar-Sagi, 1997). Secondly, 5 of the 10 components in this pathway are involved in human oncogenesis (Schlessinger and Bar-Sagi, 1997) demonstrating that it is a critical cascade for the regulation of proliferation and differentiation.

The pathway is initially triggered by binding of the SH2 domain of the adaptor protein Grb2 to the tyrosine phosphorylated RTK either directly or via Shc (Figure 1.3) (Schlessinger, 1995; Schlessinger and Bar-Sagi, 1997). The binding of Grb2 to the receptor recruits a guanine nucleotide exchange factor, Sos (Pawson and Schlessinger, 1993) which is stably associated through its proline rich region to the SH3 domain of Grb2 (Claesson-Welsh, 1994; Schlessinger, 1995; Schlessinger and Bar-Sagi, 1997). Although Sos is constitutively active, its actions only become apparent upon translocation to the membrane where its substrate, a GTPase protein termed Ras is located (Schlessinger, 1995; Schlessinger and Bar-Sagi, 1997). Ras is anchored to the plasma membrane by postranslational modification involving farnesylation (Rebollo and Martinez, 1999) and has intrinsic guanosine diphosphate (GDP)/ guanosine triphosphate (GTP) exchange and GTPase activity, but at a lower level than that seen in response to RTK activation (Rebollo and Martinez, 1999). In response to the guanine nucleotide exchange factor, Sos, Ras becomes activated through an exchange of GDP for GTP (Schlessinger and Bar-Sagi, 1997). The binding of GTP to Ras results in a conformational change (Avruch *et al.*, 1994) allowing it to interact with a number of proteins (Rebollo and Martinez, 1999), notably the serine/threonine kinase Raf, also known as MAPK kinase kinase (Avruch *et al.*, 1994). Raf is partially activated through its membrane recruitment by Ras, however full activation may require another protein (Dent *et al.*, 1998). Activation of Raf kinase activity allows it to phosphorylate and activate the dual specificity kinase, MAPK kinase also known as MEK on serine and threonine residues. MEK, a dual specificity kinase is in turn responsible for phosphorylating ERK on tyrosine and threonine residues resulting in its activation (Dent *et al.*, 1998; Garrington and Johnson, 1999).

The kinase ERK, phosphorylates both nuclear and cytoplasmic proteins containing the sequence P-X-S/T-P(Davis, 1993). Cytosolic substrates include Raf1, MAPK-activating protein kinase 1 (MAPKAP-K1) (also known as $p90^{s6kinase}$ and rsk1), mnk1 and 2, EGF receptor, synapsins and integrins (Cohen, 1997; Davis, 1993; Hughes *et al.*, 1997; Vojtek and

Figure 1.3: Activation of the Ras-MAPK pathway by RTKs.

See text for details. Reprinted by permission from Journal of Biological Chemistry (Vojtek and Der, 1998).

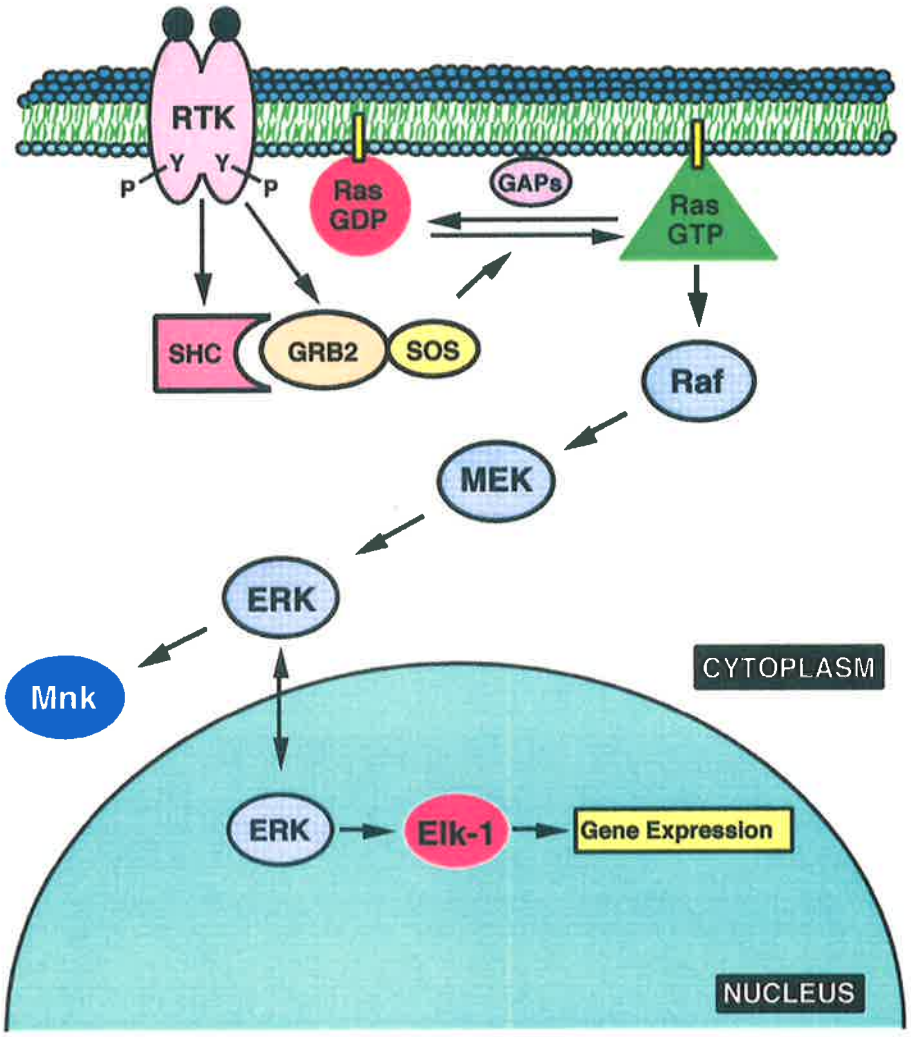
RTK
Y
Y
P
P
Ras
GDP
GAPs
Ras
GTP
SHC
GRB2
SOS
Raf
MEK
ERK
Mnk
CYTOPLASM
ERK
Elk-1
Gene Expression
NUCLEUS

Der, 1998). ERK can also translocate to the nucleus where it phosphorylates numerous transcription factors including Elk1, c-myc, IL-6 and c-jun (Avruch *et al.*, 1994; Davis, 1993; Vojtek and Der, 1998).

To ensure aberrant activation of this pathway does not occur, ERK activates the expression of ERK phosphatases, which down modulate the cascade through negative feedback (Brondello *et al.*, 1997). The phosphorylation of Sos by ERKs (Buday *et al.*, 1995) uncouples the Sos/Grb2 complex from RTKs (Buday *et al.*, 1995) or Sos from Grb2 (Langlois *et al.*, 1995) and results in down regulation (Buday *et al.*, 1995). Phosphorylation of Raf is possibly another mechanism of negative feedback since its hyperphosphorylation correlates with decreased association with the membrane (Wartmann *et al.*, 1997). The GTPase activating protein (GAP) becomes activated by RTKs and has a negative regulatory role by accelerating the intrinsic GTPase activity of Ras, thereby inhibiting its function (Vojtek and Der, 1998).

Ras is a key component of this cascade and its importance is exemplified by the finding that it is mutated in a third of human tumours (Avruch *et al.*, 1994; Vojtek and Der, 1998). Several isoforms of Ras exist and these activate effectors to varying extents. K-Ras prefers to activate Raf, while H-Ras, prefers to activate PI 3-K (Rebollo and Martinez, 1999) through interacting with its p110 subunit (Rodriguez-Viciana *et al.*, 1994).

1.7. PHOSPHOINOSITIDE 3-KINASE (PI 3-K)

The enzyme PI 3-K, is recruited to almost every activated RTK complex (Vanhaesebroeck *et al.*, 1996), suggesting an important role in signal transduction. This family of isoenzymes phosphorylates the inositol ring of phospholipids at the 3' hydroxyl group and is subdivided into classes based on catalytic specificity, structure and likely mode of regulation (reviewed in Vanhaesebroeck *et al.*, 1997). Class I PI 3-K is important in signalling via receptor complexes, with subclass IA being activated by RTKs and subclass IB

activated by βγ subunits of heterotrimeric G proteins. Both subclasses of PI 3-K exist as a heterodimer composed of a regulatory or adaptor subunit associated to a catalytic subunit (Backer, 2000; Vanhaesebroeck *et al.*, 1997). Subclass 1A PI 3-K consists of a p110 catalytic subunit and a p85 regulatory subunit (Vanhaesebroeck and Alessi, 2000). These subunits are constitutively associated through interaction of the amino terminal portion of the p110 catalytic domain with the segment between the two SH2 domains of the p85 subunit (Backer, 2000). The modular structure of the catalytic subunit of class 1B PI 3-K was revealed by X-ray crystallography (Walker *et al.*, 1999). Unlike the other classes, PI 3-K 1A and 1B can phosphorylate PtdIns, PtdIns-4-P and PtdIns-4,5-P_2 to generate PtdIns-3-P, PtdIns-3,4-P_2 and PtdIns-3,4,5-P_3 respectively (Galetic *et al.*, 1999; Vanhaesebroeck *et al.*, 1997). The lipids PtdIns-3,4-P_2 and PtdIns-3,4,5-P_3 have roles as second messengers since they appear only after stimulation with ligand, unlike PtdIns-3-P which is present in quiescent cells and only slightly increases upon RTK activation (Auger *et al.*, 1989).

Activation of the PI 3-K pathway occurs through interaction of the p85 adaptor subunit with phosphorylated tyrosines on the receptor (see below), however this is not the sole mechanism. Ras can directly interact with the catalytic subunit of PI 3-K to increase its activity (Vanhaesebroeck *et al.*, 1997). Another example is Grb2 associated binder 2 (Gab2), which activates PI 3-K in response to IL-3 (Gu *et al.*, 2000). This is mediated by an interaction of Gab2 with PI 3-K and is dependent on the recruitment of Shc and Grb2 to the receptor (Gu *et al.*, 2000). Similarly, PI 3-K interacts with phosphotyrosines on another scaffolding adaptor family member, Gab1 as observed in EGF stimulated cells (Zhang *et al.*, 2002).

Interaction of the p85 subunit with receptor phosphotyrosines results in the activation of the PI 3-K pathway (Figure 1.4) (Vanhaesebroeck *et al.*, 1997; Yu *et al.*, 1998). The p85 subunit of PI 3-K binds via its SH2 domains to phosphorylated tyrosines in the Y-X-X-M motif (Backer *et al.*, 1992; Duronio *et al.*, 1998; Gillham *et al.*, 1999). This results in

Figure 1.4: Activation of the PI 3-K pathway by RTKs.

See text for details. Solid arrows indicate the movement of Akt from the cytosol to the membrane through an interaction of its PH domain with the lipids and then release to the cytosol and nucleus to phosphorylate downstream effectors (in blue). A line with a perpendicular bar indicates an inhibitory role of Akt mediated phosphorylation.

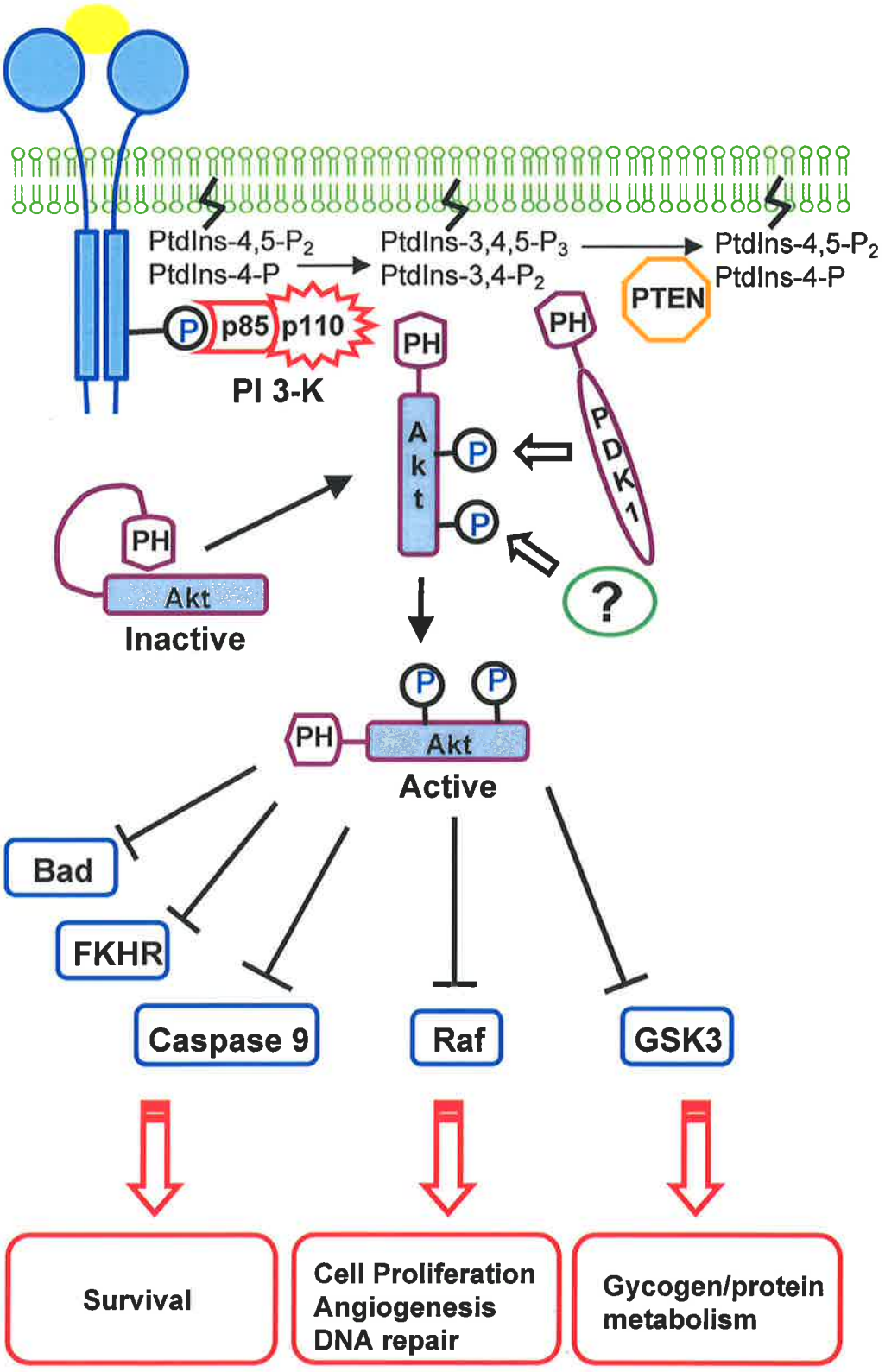
PtdIns-4,5-P2
PtdIns-4-P
PtdIns-3,4,5-P3
PtdIns-3,4-P2
PtdIns-4,5-P2
PtdIns-4-P
PTEN
P
p85
p110
PI 3-K
PH
Akt
PDK1
?
Inactive
Active
Bad
FKHR
Caspase 9
Raf
GSK3
Survival
Cell Proliferation
Angiogenesis
DNA repair
Gycogen/protein
metabolism

membrane localisation (Gillham *et al.*, 1999) bringing the catalytic subunit into close proximity with its substrate, allowing phosphorylation of PtdIns, PtdIns-4-P and PtdIns-4,5-P_2 (Vanhaesebroeck *et al.*, 1997). Although PI 3-K activated by RTKs can phosphorylate three substrates, it has higher affinity for PtdIns-4,5-P_2 (Carpenter *et al.*, 1990). Lipids generated by PI 3-K activity behave as second messengers to elicit various biological responses through the recruitment of proteins containing PH domains (reviewed in Toker and Cantley, 1997). Along with its lipid kinase function, PI 3-K, has serine/threonine kinase activity and has been reported to phosphorylate both PI 3-K subunits and IRS (reviewed in Rameh and Cantley, 1999).

1.7.1. Effectors of the PI 3-K Pathway

Effectors of the PI 3-K pathway are recruited to the plasma membrane through an interaction of their PH domain with 3' phosphorylated phosphoinositides (Lemmon and Ferguson, 1998). A well-characterised effector of the PI 3-K pathway is Akt.

1.7.1.1.Akt

The 57 kDa serine/threonine kinase Akt, was identified in 1991 by three independent groups and given the names c-Akt (Bellacosa *et al.*, 1991), protein kinase B (PKB) (Coffer and Woodgett, 1991) and Related to the A and C kinases (RAC-PK) (Jones *et al.*, 1991). This protein will be referred to as Akt throughout this thesis. Upon activation of the PI 3-K pathway, Akt translocates to the plasma membrane (Andjelkovic *et al.*, 1997) through interaction of its PH domain with PtdIns-3,4-P_2 (Figure 1.4) (Klippel *et al.*, 1997). The association of Akt with PtdIns-3,4-P_2 increases its kinase activity and allows dimerisation to occur (Klippel *et al.*, 1997; Marte and Downward, 1997; Toker and Cantley, 1997). For full activation, Akt must be phosphorylated at two distinct sites, T308 and S473 (Andjelkovic *et al.*, 1997; Vanhaesebroeck *et al.*, 1997) which occur independently (Vanhaesebroeck and Alessi, 2000). The PH domain has an important regulatory role in Akt activation (Franke *et*

al., 1995; Stokoe *et al.*, 1997) as it masks the T308 phosphorylation site in the activation loop when not in contact with lipid (Stokoe *et al.*, 1997). Binding of the PH domain to lipid relieves this constraint (Stokoe *et al.*, 1997) and Akt becomes phosphorylated on T308 located in the activation loop by PDK1, a serine/threonine kinase (Figure 1.4) (Galetic *et al.*, 1999; Marte and Downward, 1997; Rameh and Cantley, 1999; Stokoe *et al.*, 1997). PDK1 is constitutively active, but requires lipids generated by PI 3-K for its recruitment to its substrate (Rameh and Cantley, 1999). In response to growth factor stimulation, PDK1 translocates to the membrane (Anderson *et al.*, 1998) via its PH domain, binding PtdIns-3,4,5-P_3 (Stokoe *et al.*, 1997), and phosphorylates membrane localised Akt (Galetic *et al.*, 1999; Marte and Downward, 1997; Rameh and Cantley, 1999). The other site phosphorylated on Akt, S473, is located in the carboxy terminal regulatory region of the kinase domain and is phosphorylated by an unidentified kinase (Leevers *et al.*, 1999; Vanhaesebroeck and Alessi, 2000). Sequences surrounding both phosphorylation sites are different suggesting the involvement of two kinases (Galetic *et al.*, 1999; Marte and Downward, 1997). A candidate for phosphorylation at S473 is integrin-linked kinase-1 (ILK) (Persad *et al.*, 2001). Alternatively, PDK1 associated with the carboxy terminal of PKC-related kinase 2 (PRK2) has been reported to phosphorylate Akt at S473, indicating a dual role (reviewed in Vanhaesebroeck and Alessi, 2000). In addition, two sites of tyrosine phosphorylation in Akt have been identified and substitution of these abolished kinase activity stimulated by RTKs (Chen *et al.*, 2001).

Once Akt has been phosphorylated it is released from the plasma membrane and can phosphorylate numerous substrates in the cytosol. It also translocates to the nucleus where it can phosphorylate nuclear targets (Meier *et al.*, 1997). Substrates of Akt (Figure 1.4) have the motif R-X-R-X-X-S/T (Marte and Downward, 1997). Some targets of Akt are involved in survival through the regulation of apoptosis (Kelley *et al.*, 1999; Kulik and Webber, 1998). Akt phosphorylates Caspase-9, inhibiting it and hence blocking apoptosis (Stambolic *et al.*,

1999; Vanhaesebroeck and Alessi, 2000). It can also phosphorylate Bcl-2/Bcl-X_L-agonist causing cell death (BAD) on S136 (Blume-Jensen *et al.*, 1998; Datta *et al.*, 1997). Phosphorylation of BAD at two sites is important to induce an association with 14-3-3 which leads to its sequestration in the cytosol, preventing its association to apoptotic proteins such as Bcl-X_L and Bcl-2 (Datta *et al.*, 1997; Stambolic *et al.*, 1999; Zha *et al.*, 1996). Translocation of Akt to the nucleus allows it to phosphorylate Forkhead transcription factors (Vanhaesebroeck and Alessi, 2000). This promotes nuclear export where they interact with 14-3-3 preventing them from interacting with target genes (Vanhaesebroeck and Alessi, 2000). Another target of Akt includes Raf which becomes phosphorylated at S259 resulting in inhibition of the Ras-MAPK pathway (reviewed by Vanhaesebroeck and Alessi, 2000). Akt also has various insulin dependent roles such as an involvement in glycolysis regulation and glycogen synthesis (Galetic *et al.*, 1999; Vanhaesebroeck *et al.*, 1997; Vanhaesebroeck and Alessi, 2000).

1.7.1.2. Other Effectors of PI 3-K

PI 3-K has other effectors besides Akt. It activates some novel and atypical PKC proteins through 3' phosphorylated lipids (reviewed in Toker and Cantley, 1997) and phosphorylates $p70^{s6kinase}$, a protein involved in the cell cycle, although this may be downstream of Akt (reviewed in Grammer *et al.*, 1996). Other proteins include Rho/Rac (small GTP binding proteins) which have roles in actin cytoskeletal reorganisation (Leevers *et al.*, 1999).

Another downstream protein indirectly activated by PI 3-K is c-Jun N-terminal kinase (JNK) also known as stress activated protein kinase (SAPK). Activation of JNK was observed in cells stimulated with various haemopoietic cytokines including SCF (Foltz and Schrader, 1997). JNK activation in cells stimulated with EGF is inhibited by expression of a dominant negative adaptor subunit of PI 3-K and treatment with wortmannin (Logan *et al.*,

1997). The mechanism by which PI 3-K activates JNK is unknown, although it may be mediated by activation of Rac (Mainiero *et al.*, 1997).

1.7.2. Downregulation

The PI 3-K pathway is tightly regulated to ensure aberrant activation does not occur. A negative regulatory mechanism potentially activated when lipids reach a threshold level involves the ability of PtdIns-3,4,5-P_3 to bind directly to the carboxy terminal SH2 domain of p85 (Ching *et al.*, 2001; Rameh *et al.*, 1995). This blocks the ability of the p85 subunit to bind phosphotyrosines on the receptor (Rameh *et al.*, 1995).

Upon PI 3-K activation by RTKs the p85 subunit can become phosphorylated modifying the amino terminal SH2 domain (Kavanaugh *et al.*, 1992). This does not affect binding to the PDGF receptor which is mainly mediated via the carboxy terminal SH2 domain, but it may regulate PI3-K activity by other means, or alter its interaction with other proteins (Kavanaugh *et al.*, 1992). Others have observed that decreased kinase activity of PI 3-K is associated with p85 phosphorylation supporting a role in negative regulation (Rameh and Cantley, 1999).

Probably the major mechanism of control is through the action of phosphatases. A recently discovered phosphatase PTEN, removes the 3' phosphate group on the inositol ring, converting PtdIns-3,4,5-P_3 to PtdIns-4,5-P_2, reversing the reaction catalysed by PI 3-K and preventing the activation of Akt and other effectors (Maehama and Dixon, 1998; Myers *et al.*, 1998).

1.7.3. Deregulation of the PI 3-K Pathway and its Involvement in Cancer

The first suggestion of the role of PI 3-K in cancer came from observations of viral oncogene products, polyoma middle-T antigen and v-src. It was observed that the transforming ability of polyoma middle-T antigen was mediated by its association with the Src tyrosine kinase, which in turn was associated with PI kinase activity (Whitman *et al.*, 1985).

Correlation of middle-T transformation with PI kinase activity was observed (Whitman *et al.*, 1985), and since the p85 subunit of PI 3-K directly associates with Src (Carpenter *et al.*, 1990), it was considered to be PI 3-K dependent. Studies with PI 3-K inhibitors indicated that its activation is required for Ras mediated transformation (Rodriguez-Viciana *et al.*, 1997). Constitutive PI 3-K activity has also been observed in 86% of colorectal tumour tissues (Phillips *et al.*, 1998). PI 3-K has a role in transformation once activated by other proteins, however it also has a role in its own right. A mutant version of the catalytic subunit of PI 3-K, v-p3k was found in avian sarcoma virus 16 (Chang *et al.*, 1997). Expression of this protein, or the proto-oncogene when fused to retroviral Gag resulted in transformation (Aoki *et al.*, 2000). In humans, an oncogenic version of the catalytic subunit has not been detected to date, however, upregulation of this subunit by increased copy number and resultant increased PI 3-K activity has a role in ovarian cancer (Shayesteh *et al.*, 1999). A mutant version of the adaptor subunit in a cell line derived from thymic lymphoma has also been reported (Jimenez *et al.*, 1998).

Akt has also been implicated in carcinogenesis. An oncogenic version of Akt was first identified as a retroviral oncogene, v-Akt, which encoded a 105 kDa protein fused to Gag (Bellacosa *et al.*, 1991). Subsequently, overexpression of Akt due to amplification has been observed in pancreatic carcinomas, human ovarian carcinoma cell lines, primary ovarian tumours as well as breast carcinomas (Bellacosa *et al.*, 1995; Cheng *et al.*, 1992; Cheng *et al.*, 1996). Mutation of Akt does not appear to have a role in carcinogenesis (Bellacosa *et al.*, 1995).

PTEN is now known to be one of the most common targets of mutation in human cancer, with a frequency approaching that of p53 (reviewed in Cantley and Neel, 1999). It functions as a tumour suppressor gene and has been mapped to chromosome 10q23, a site mutated in various cancer types (reviewed in Cantley and Neel, 1999; Smith and Ashworth, 1998). Mutations in PTEN cause an ablation of phosphatase activity and have been identified

in various carcinomas including glioblastoma, prostate cancer cell lines, endometrial and breast tumours (Li *et al.*, 1997; Rasheed *et al.*, 1997). No mutations have been detected in low grade adult gliomas or childhood gliomas, indicating an involvement in progression rather than as the primary transforming event (Rasheed *et al.*, 1997). In addition to its role in sporadic carcinomas, germ line mutations are involved in hereditary diseases and cause rare autosomal dominant inherited cancer syndromes (reviewed in Cantley and Neel, 1999). These are characterised by multiple hamartomas that are benign tumours where cellular differentiation is normal but highly disorganised. These include Cowden disease, Lhermitte-Duclos disease, Bannayan-Zonana syndrome and Juvenile polyposis syndrome (Cantley and Neel, 1999; Liaw *et al.*, 1997; Smith and Ashworth, 1998). Mice heterozygous for this mutation also exhibit an increased incidence of tumours involving a loss of heterozygosity (Podsypanina *et al.*, 1999; Suzuki *et al.*, 1998).

Besides being a lipid phosphatase, PTEN may have other roles contributing to its tumour suppressor function. Mice with mutations in both copies of PTEN die at day 9.5 of gestation (Suzuki *et al.*, 1998). These mice display patterning defects in cephalic and caudal regions similar to focal adhesion kinase (FAK) knockout mice, which die at the same time (Ilic *et al.*, 1995). Since it is known that PTEN interacts with FAK causing its dephosphorylation, and also that overexpression of PTEN inhibits cell migration and cell spreading (Tamura *et al.*, 1998), the embryonic lethality of PTEN may be due to its effects on the cytoskeleton resulting from an inability to dephosphorylate FAK.

1.8. Signal Transduction Activated by c-KIT

In response to binding its ligand, SCF, c-KIT dimerises, exhibits increased kinase activity and undergoes rapid dose-dependent phosphorylation (Funasaka *et al.*, 1992; Kuriu *et al.*, 1991; Lev *et al.*, 1991; Rottapel *et al.*, 1991). Only the mature 145 kDa form of c-KIT, is phosphorylated in response to SCF in mast cells presumably because the 125 kDa form is

intracellular and inaccessible to ligand (Rottapel *et al.*, 1991). Phosphorylation of c-KIT on tyrosines creates docking sites for SH2 containing proteins enabling them to interact and become phosphorylated. Known tyrosine residues involved in substrate association are shown in Figure 1.5, others have yet to be identified. In response to SCF, at least 12 proteins are phosphorylated (Miyazawa *et al.*, 1991) suggesting that a complex array of signal transduction pathways become activated.

1.8.1. PI 3-K

One protein to become associated with c-KIT in a ligand dependent manner is PI 3-K (Lev *et al.*, 1991; Rottapel *et al.*, 1991) (see section 1.7 for details on the activation and function of PI 3-K). The p85 adaptor subunit of PI 3-K interacts with c-KIT via its carboxy terminal SH2 domain (Sattler *et al.*, 1997). Interaction of PI 3-K with c-KIT has been narrowed down to the kinase insert by way of deletion mutants, anti peptide antibodies and expression of the kinase insert in bacteria (Lev *et al.*, 1992a). The residue responsible for this association has been mapped to Y719 and Y721 in mouse and human c-KIT respectively (Herbst *et al.*, 1995b; Serve *et al.*, 1994). Controversy exists as to whether p85 becomes tyrosine phosphorylated in response to c-KIT stimulation (Blume-Jensen *et al.*, 1994; Lev *et al.*, 1991; Serve *et al.*, 1994), however if phosphorylation is observed, it is weak suggesting it does not have a major role in signal transduction.

By the use of Y719F and Y721F mutants that no longer directly recruit PI 3-K and also use of PI 3-K inhibitors LY294002 and wortmannin, the role of PI 3-K activation in response to c-KIT stimulation has been assessed. In murine bone marrow mast cells, mutation of the tyrosine 719 to phenylalanine abolished adhesion (Serve *et al.*, 1994; Serve *et al.*, 1995). Further effects observed in bone marrow derived mast cells include a partial decrease in DNA synthesis and survival, inhibition of degranulation, impaired membrane ruffling and reduced actin assembly (Timokhina *et al.*, 1998; Vosseller *et al.*, 1997). Investigation of PI 3-K in

Figure 1.5: Phosphorylation sites in human c-KIT known to recruit SH2 domain containing proteins.

Schematic diagram of c-KIT focusing on the intracellular domain. Y823 is in the activation loop. Green bar represents the plasma membrane.

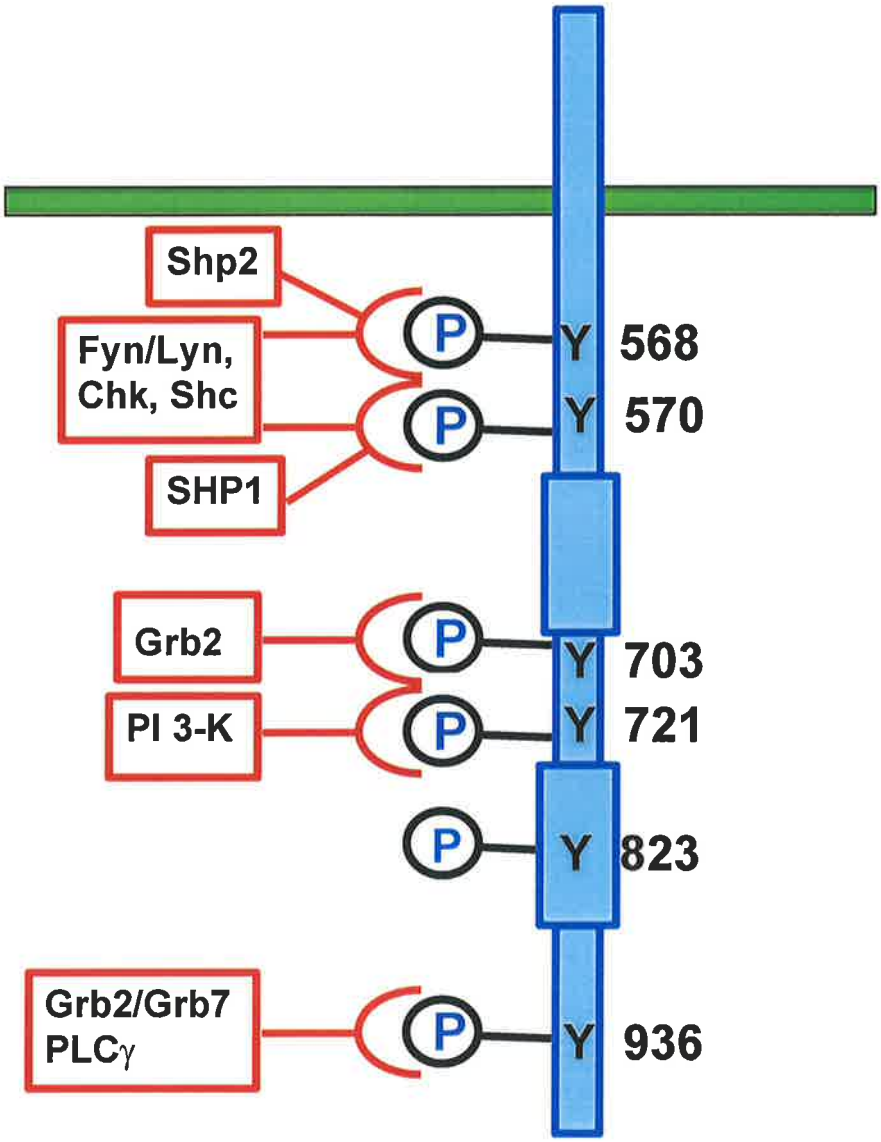
Shp2
Fyn/Lyn,
Chk, Shc
SHP1
Grb2
PI 3-K
Grb2/Grb7
PLCγ
P
Y
568
570
703
721
823
936

spermatogonia, another cell population where c-KIT is expressed, revealed that it was important in proliferation (Feng *et al.*, 2000). The proliferation was mediated by activation of Akt, which phosphorylated $p70^{s6kinase}$ resulting in an increase in cyclin D3 expression and phosphorylation of Retinoblastoma protein. The activation of PI 3-K by c-KIT has also been observed to have a role in cellular differentiation (Kubota *et al.*, 1998).

Once activated by c-KIT, PI 3-K exists in a multimeric complex. The adaptor protein CRKL associates with the p85 subunit of PI 3-K and is thought to be involved in recruiting signalling molecules (Sattler *et al.*, 1997). Similarly, c-Cbl associates with the p85 subunit of PI 3-K (Sattler *et al.*, 1997), suggesting that PI 3-K may be responsible for the recruitment of proteins to c-KIT as well as in the activation of Akt.

1.8.2. Ras-MAPK Pathway

Activation of the Ras-MAPK pathway occurs after stimulation of c-KIT (Miyazawa *et al.*, 1991) (for details regarding the Ras-MAPK pathway, see section 1.6.3). The adaptor protein, Grb2 complexes with c-KIT at Y703 and Y936 upon SCF stimulation with Y703 providing the link to the Ras-MAPK pathway (Thommes *et al.*, 1999). Another adaptor, Grb7 binds specifically to Y936 on c-KIT via its SH2 domain (Thommes *et al.*, 1999). Grb2 recruits Sos, a guanine nucleotide exchange factor (Brizzi *et al.*, 1996), leading to the activation of Ras (Duronio *et al.*, 1992). Alternately, Grb2/Sos can be indirectly recruited to c-KIT by interaction with an adaptor protein Shc that binds in its own right and becomes phosphorylated by Src (Lennartsson *et al.*, 1999). Ras stimulation results in its association and recruitment of Raf to the plasma membrane (Tauchi *et al.*, 1994). This increases Raf phosphorylation on serine (Hallek *et al.*, 1992; Lev *et al.*, 1991) but not on tyrosine (Herbst *et al.*, 1991; Miyazawa *et al.*, 1991), and increases its intrinsic kinase activity (Miyazawa *et al.*, 1991). Downstream of Raf are ERK1 and ERK2 whose phosphorylation and activation

correlate with increased kinase activity of c-KIT (Funasaka *et al.*, 1992; Miyazawa *et al.*, 1991).

A negative regulator of the Ras-MAPK pathway, GAP forms a weak association to c-KIT in human embryonic kidney fibroblast cells (Herbst *et al.*, 1991) and haemopoietic cells (Duronio *et al.*, 1992). No association has been observed in mast cells (Duronio *et al.*, 1992; Herbst *et al.*, 1995b; Rottapel *et al.*, 1991) possibly because it was below the limits of detection. Similarly there is controversy over phosphorylation of GAP in response to c-KIT stimulation (Duronio *et al.*, 1992; Funasaka *et al.*, 1992; Herbst *et al.*, 1991; Miyazawa *et al.*, 1991; Rottapel *et al.*, 1991).

1.8.3. Others

Recruitment of PLCγ to activated RTK complexes allows close localisation to its substrate, inositol phospholipids (reviewed in Berridge, 1993). PLCγ hydrolyses inositol phospholipids into inositol triphosphate (IP_3) and diacylglycerol (DAG) which are involved in calcium mobilisation and PKC recruitment and activation respectively (Berridge, 1993). Some studies have shown weak association of PLCγ to c-KIT (Herbst *et al.*, 1995b; Rottapel *et al.*, 1991), however others disagree, possibly because the level was below limits of detection (Blume-Jensen *et al.*, 1994; Herbst *et al.*, 1991; Lev *et al.*, 1991). The weak recruitment may be due to partial indirect competition with p85 which binds with high affinity to c-KIT (Herbst *et al.*, 1995b). The residue Y728 in murine c-Kit is required for the activation of PLCγ (Gommerman *et al.*, 2000). Accompanying recruitment of PLCγ to the activated c-KIT complex is weak phosphorylation, possibly on tyrosine residues (Blume-Jensen *et al.*, 1994; Herbst *et al.*, 1991; Lev *et al.*, 1991).

Downstream of PLCγ is PKC which is activated by c-KIT (Blume-Jensen *et al.*, 1993; Vosseller *et al.*, 1997). PKC has roles in c-KIT mediated degranulation, membrane ruffling, actin assembly (Vosseller *et al.*, 1997) as well as a role in the negative regulation of c-KIT

(for more details see section 1.8.4). It has been proposed that the c-KIT mediated activation of PKC is through the activation of phospholipase D (PLD) and not via PLCγ, since IP_3 is not produced in response to SCF (Koike *et al.*, 1993). Activation of PLD is PI 3-K dependent (Kozawa *et al.*, 1997).

In response to SCF, Src family kinases, by virtue of their SH2 domain, interact with phosphorylated tyrosines on c-KIT resulting in an increase in their kinase activity (Linnekin *et al.*, 1997). The tyrosines involved in this association for Lyn and Fyn have been identified as Y568 and Y570 in human c-KIT (Y567 and Y569 are the murine equivalents) (Linnekin *et al.*, 1997; Timokhina *et al.*, 1998). The activation of Src family kinases in conjunction with PI 3-K induces proliferation due to their ability to stimulate Rac resulting in the activation of JNK (Timokhina *et al.*, 1998). Src also has a role in the phosphorylation of the adaptor protein Shc, leading to the activation of the Ras-MAPK pathway (Lennartsson *et al.*, 1999).

A negative feedback mechanism exists in which Src kinase activity is inhibited by phosphorylation of a carboxy terminal tyrosine (Avraham *et al.*, 1995). This is performed by carboxy terminal Src kinase (Csk) homologous kinase (CHK) formerly referred to as megakaryocyte-associated tyrosine kinase (MATK) (Jhun *et al.*, 1995). CHK is activated in response to SCF through an interaction with Y568 and Y570 of c-KIT, the same tyrosines involved in recruiting Src (Timokhina *et al.*, 1998).

In response to SCF, increased tyrosine phosphorylation and activation of a cytoplasmic related kinase Tec, is observed (Tang *et al.*, 1994). Phosphorylation of Tec is partly dependent on the activity of PI 3-K and the Src family kinase Lyn (van Dijk *et al.*, 2000). Tec can associate with c-KIT, however a low concentration of detergent was used (Tang *et al.*, 1994) suggesting that the interaction may be indirect (van Dijk *et al.*, 2000). For example, Tec interacts with a scaffolding protein, Dok, whose association is stabilised by Lyn (van Dijk *et al.*, 2000). Dok is phosphorylated via a PI 3-K dependent mechanism in response to SCF and can interact with numerous SH2 containing proteins (van Dijk *et al.*, 2000).

Activation of receptors lacking intrinsic kinase activity such as members of the cytokine receptor superfamily induce signal transduction via members of the Janus family of protein tyrosine kinases (JAKs). A member of the JAK family, JAK2 has a role in SCF mediated proliferation (Linnekin *et al.*, 1996). Interaction of JAK2 with c-KIT was constitutive with further association observed upon SCF treatment (Weiler *et al.*, 1996). Stimulation of c-KIT with SCF also resulted in rapid and transient phosphorylation of JAK2 (Linnekin *et al.*, 1996). JAKs are involved in activating signal transducers and activators of transcription (STAT) which become activated by treatment of cells with SCF (Brizzi *et al.*, 1999).

A protein, suppressor of cytokine signalling (Socs1) becomes inducibly associated via its SH2 domain to c-KIT upon SCF stimulation (De Sepulveda *et al.*, 1999). Its role in c-KIT signalling is two fold, it suppresses c-KIT mediated proliferation while maintaining survival signals (De Sepulveda *et al.*, 1999). It also acts as an adaptor type protein since it interacts with both Grb2 and the rho-family guanine nucleotide exchange factor, Vav (De Sepulveda *et al.*, 1999).

1.8.4. Down Modulation of c-KIT Function

To ensure tight regulation of c-KIT function, numerous down-modulatory pathways are employed and activated upon SCF binding. These consist of ubiquitination, internalisation, degradation and activation of negative feedback loops involving the function of phosphatases as well as PKC mediated phosphorylation of c-KIT.

In response to ligand, c-KIT is lost from the surface through endocytosis and undergoes degradation (Lev *et al.*, 1991). Extensive research into internalisation revealed that inactivation of receptor kinase activity decreased the rate of internalisation of c-KIT (Yee *et al.*, 1993) and CSF-1 receptor (Carlberg *et al.*, 1991). Investigation into the role of downstream substrates in internalisation revealed that mutation of the PI 3-K binding site in

c-KIT did not affect internalisation (Gommerman *et al.*, 1997; Yee *et al.*, 1993). Similar results have been obtained with other RTKs belonging to subclass III (Carlberg *et al.*, 1991; Joly *et al.*, 1995). Therefore PI 3-K in its own right does not have a role, however lack of PI 3-K recruitment in concert with a lack of calcium influx during c-KIT activation perturbs internalisation (Gommerman *et al.*, 1997). Src family kinases also have a role in SCF mediated internalisation of c-KIT (Broudy *et al.*, 1999; Jahn *et al.*, 2002a).

Degradation of RTKs is dependent on their kinase activity (Carlberg *et al.*, 1991; Yee *et al.*, 1993) and phosphorylation (Ohtsuka *et al.*, 1990). Unlike internalisation, ligand mediated degradation is dependent on PI 3-K activity, as shown by removal of its binding site in c-KIT (Gommerman *et al.*, 1997; Yee *et al.*, 1993), CSF-1 receptor (Carlberg *et al.*, 1991; Murray *et al.*, 2000) and PDGF receptor (Joly *et al.*, 1995). PI 3-K appears to have a role in the late endocytic steps of degradation since mutant c-KIT incapable of recruiting PI 3-K internalises normally but remains in vesicles at the periphery of the cell (Gommerman *et al.*, 1997). Similar observations have been made with the activation of the CSF-1 receptor in the presence of wortmannin (Murray *et al.*, 2000).

Prior to internalisation and degradation, c-KIT is ubiquitinated on lysine residues (Miyazawa *et al.*, 1994). Ubiquitin serves to tag proteins for degradation (reviewed in Hicke, 1999). In response to SCF stimulation, c-KIT becomes ubiquitinated as demonstrated by upward smearing and retarded migration by Sodium Dodecylsulphate-Polyacrylamide Gel Electrophoresis (SDS-PAGE) analysis (Miyazawa *et al.*, 1994). This ubiquitination is dependent on the receptors intrinsic kinase activity and also on the presence of ligand but not on PI 3-K activity (Miyazawa *et al.*, 1994; Yee *et al.*, 1993). c-Cbl has a role in ubiquitination since it functions as an E3 ubiquitin protein ligase involved in conjugating ubiquitin to its substrate (Ettenberg *et al.*, 2001). Phosphorylation of c-Cbl is observed upon SCF stimulation and it associates with c-KIT potentially by virtue of its constitutive interaction with Grb2

(Brizzi *et al.*, 1996). It also complexes with the SH3 domain of p85 (Kanagasundaram *et al.*, 1996; Sattler *et al.*, 1997).

Phosphatases are an important family of proteins involved in down-regulating signal transduction pathways activated by RTKs. A balance between phosphatase and kinase action needs to be established otherwise aberrant signalling may occur. It was initially thought that phosphatases were constitutively activated, exerting a negative effect in the absence of stimulus due to their significant basal activity, however it has been shown that their activity is also regulated by RTKs (Hunter, 1995). A phosphatase predominantly expressed in haemopoietic cells, SHP1, transiently associates to c-KIT after SCF stimulation (Yi and Ihle, 1993). This results in a slight increase in tyrosine phosphorylation of SHP-1 and a subsequent dephosphorylation of c-KIT *in vitro* (Yi and Ihle, 1993). Interaction of SHP-1 on murine c-Kit is via Y569 (Y570 human equivalent) although Y567 (Y568 human equivalent) contributes to this association (Kozlowski *et al.*, 1998). SHP-1 also constitutively associates with Vav and Grb2/Sos, and this is increased upon stimulation with SCF (Kon-Kozlowski *et al.*, 1996). The negative regulatory role of SHP-1 is highlighted in knockout mice, which have a *motheaten* phenotype with significantly elevated levels of myeloid cells (Paulson *et al.*, 1996). Homozygous *W* and *motheaten* mice crosses have a less severe phenotype than either mutation on its own, lending support to the role of SHP-1 in the negative regulation of c-KIT function (Paulson *et al.*, 1996). A ubiquitously expressed phosphatase, SHP-2 associates with murine c-KIT at Y567 (Y568 in human c-KIT) upon SCF binding (Kozlowski *et al.*, 1998). Mutation of both tyrosines required to recruit SHP-1 and SHP-2 results in increased proliferation in response to SCF (Kozlowski *et al.*, 1998), further supporting a negative role of these proteins. SHP-2 also becomes tyrosine phosphorylated in response to SCF allowing it to complex directly with Grb2 (Tauchi *et al.*, 1994). It is considered that SHP-2 potentiates the action of RTKs and other cytokine receptors since it is incapable of dephosphorylating c-KIT (Tauchi *et al.*, 1994) and secondly, its mutation suppresses growth factor induced mitogenesis

(Kharitonenkov *et al.*, 1997) and haemopoietic development (Qu *et al.*, 1997). Lack of functional SHP-2 suppresses c-KIT mediated induction of ERK (Qu *et al.*, 1997) which maybe due to its ability of linking Grb2 to c-KIT (Tauchi *et al.*, 1994).

A protein activated downstream of c-KIT, involved in a negative feedback loop is PKC. Inhibition of PKC results in increased mitogenicity (Blume-Jensen *et al.*, 1993). It mediates its effect of inhibiting c-KIT kinase activity and tyrosine phosphorylation by inducing direct phosphorylation of c-KIT on S741 and S746 in the kinase insert (Blume-Jensen *et al.*, 1993; Blume-Jensen *et al.*, 1995) These sites are constitutively phosphorylated, however the presence of SCF upregulates their phosphorylation (Blume-Jensen *et al.*, 1995). PKC also appears to be involved in downregulation of c-KIT by causing proteolytic cleavage near the transmembrane domain (Yee *et al.*, 1993). Similar observations of the inhibitory effect of PKC have been made with other receptors (Downing *et al.*, 1989; Nishizuka, 1986; Schlessinger, 1986) implying a universal role of PKC as a negative feedback inhibitor of RTK activity.

1.9. AIMS

The objectives of this research are to address the mechanisms by which c-KIT mediates its cellular responses in relevant factor dependent immature haemopoietic cells, to aid in the understanding of signalling pathways induced by RTKs and to contribute to correlating cellular responses with the activation of signal transduction pathways.

Part of this objective will be fulfilled by the analysis of two human c-KIT isoforms, which either contain or lack GNNK in the extracellular juxtamembrane domain. Expression of these isoforms in NIH-3T3 fibroblasts resulted in significant differences in the activation kinetics of c-KIT as well as the biological responses obtained (Caruana *et al.*, 1999). Therefore it was of interest to determine if these differences could also be observed in cells in which c-KIT is normally expressed. This will provide useful information regarding the

function of c-KIT in haemopoietic cells and correlation of its activation kinetics in response to huSCF with biological responses. Further, it will identify any differences of c-KIT function in two cellular systems.

In response to ligand binding to c-KIT, various signal transduction proteins are activated, with one of the key proteins being PI 3-K. PI 3-K is recruited directly to c-KIT via Y721 and is responsible for eliciting various biological responses including survival, adhesion, degranulation, membrane ruffling and actin assembly as observed in mast cells (Serve *et al.*, 1994; Serve *et al.*, 1995; Timokhina *et al.*, 1998; Vosseller *et al.*, 1997). The aim of this section was to determine the involvement of direct PI 3-K recruitment in c-KIT signal transduction and its ability to elicit biological responses in an alternate physiologically relevant cell model, the haemopoietic progenitor cells.

Oncogenic forms of c-KIT have been found in various malignancies and it is of interest to deduce differences between these oncogenic forms and the proto-oncogenic versions. This will be important to aid in the development of future cancer therapies. One oncogenic form of c-KIT that induces factor independent growth and tumour formation results from a single base pair change, D816V (Ferrao *et al.*, 1997; Hashimoto *et al.*, 1996; Kitayama *et al.*, 1995; Tsujimura *et al.*, 1994). This mutation results in constitutive activation of c-KIT as well as a constitutive association with the p85 subunit of PI 3-K (Furitsu *et al.*, 1993; Kanakura *et al.*, 1994). The mechanisms employed to mediate factor independent growth are largely unknown, and it was hypothesised that the direct recruitment of PI 3-K may play an important role. The aim of this section was to determine the involvement of direct PI 3-K recruitment by D816V c-KIT in factor independent growth and tumourigenicity by constructing c-KIT containing the D816V mutation but lacking the PI 3-K binding site. This research will aid in identifying key components involved in the oncogenesis by c-KIT. Further, it will elucidate the role of PI 3-K in both oncogenic and WT c-KIT function.

CHAPTER 2:

MATERIALS AND METHODS

2. MATERIALS AND METHODS

2.1. TISSUE CULTURE

Reagents used were of analytic grade unless specified otherwise. All solutions were prepared using Milli-Q purified water (Milli-Q water) generated by deionising distilled water using a Milli-Q RO60 system (Millipore Corporation, Bedford, MA) and then further purified by passing through two beds of ion exchange resins, a carbon filter and an organic filter using a Milli-Q system (Millipore).

2.1.1. Tissue Culture Media and Solutions

Dulbecco's Modified Eagle's Medium (DMEM) was prepared by mixing one sachet of DMEM powder (GibcoBRL, Rockville, MD, Cat. No. 12800-017) and 3.7 g $NaHCO_3$ (BDH, USA, Cat. No. 10247) in 900 ml of Milli-Q water. To the solution, N-2-Hydroxyethylpiperazine N`-2-ethanesulphonic acid (HEPES) pH 7.2 (Boehringer-Mannheim, Australia, Cat. No. 737151) was added from sterile stock solutions for a final concentration of 15 mM. Likewise, penicillin (Sigma, St Louis, MO, Cat. No. P3032) and streptomycin sulphate (Sigma, St Louis, MO, Cat. No. S9137) was added for final concentrations of 100 IU/ml and 100 µg/ml respectively. The pH of the solution was adjusted to 7 by the addition of 4 ml 1 M hydrochloric acid (HCl) and the volume adjusted to 1 L with Milli-Q water. The medium was filter sterilised using an Acrocap TM 0.22 µm filter unit (Gelman Sciences, Ann Arbor, MI, Cat. No. 4480) and a Millipore pump with a filling bell (Millipore, Bedford, MA, Cat. No. SVGB1010) and stored at 4°C. Prior to use, medium was supplemented with 10-20% foetal calf serum (FCS) (CSL, Parkville, Victoria, Australia, Cat. No. 09702301) which had previously been heat inactivated at 56°C for 30 minutes. To medium that had been stored at 4°C for more than 7 days, glutamine was added to yield a final concentration of 2

mM. DMEM with pyruvate and high glucose without glutamine (JRH Biosciences, Lenexa, KS, Cat. No. 45042301) was supplemented with 15 mM HEPES (JRH Biosciences, Lenexa, KS, Cat. No. 44811901), 50 U/ml penicillin, 50 µg/ml streptomycin sulphate (JRH Biosciences, Lenexa, KS, Cat. No. 05081901) and 200 mM glutamine (JRH Biosciences, Lenexa, KS, Cat. No. 44831901).

Iscove's Modified Dulbecco's Medium (IMDM) was prepared by adding one sachet of IMDM powder (GibcoBRL, Rockville, MD, Cat. No. 12200-036) and 2 g of $NaHCO_3$ in 900 ml of Milli-Q water. As with DMEM, sterile stock solutions of HEPES, penicillin and streptomycin sulphate were added to the same final concentrations as above and filter sterilised as previously indicated. The pH was adjusted to 7.4 with 2.5 ml of 1 M HCl and the volume made to 1 L. RPMI 1640 medium was prepared the same way as for IMDM using RPMI 1640 powder (GibcoBRL, Rockville, MD, Cat. No. 31800-02).

Double strength IMDM was prepared by dissolving one sachet of IMDM powder (Cytosystems, Australia, Cat. No. 50-016-PA) and 0.2 g L-asparagine in 390 ml of Milli-Q water. Sterile stocks of penicllin, streptomycin sulphate, DEAE-Dextran (Pharmacia, Sweden, Cat. No. 17-0350-01) were added to give a final concentrations of 200 IU/ml, 200 µg/ml and 0.19 mg/ml respectively. Medium was filter sterilised and stored up to 6 months at 4°C.

Hank's balanced salt solution (HBSS) contained 0.14 M NaCl, 5 mM KCl, 0.3 mM $Na_2HPO_4.12H_2O$, 0.4 mM KH_2PO_4, 4.2 mM $NaHCO_3$, 5.5 mM glucose, 1% Phenol Red (in 0.1 M NaOH) in Milli-Q water, with a final pH of 7.4. The solution was sterilised by autoclaving at 130°C for 20 minutes and stored at 4°C. Hanks without calcium and magnesium, with phenol red from JRH Biosciences (Lenexa, KS, Cat. No. 55021-500M) was also used.

Tissue culture grade phosphate buffered saline (PBS) contained 0.14 M NaCl, 3 mM KCl, 8 mM $Na_2HPO_4.12H_2O$ and 1 mM KH_2PO_4 in sterile tissue culture grade Milli-Q water,

with a final pH of 7.4. Solution was sterilised by autoclaving and stored at 4°C. A sterile 10x stock of PBS without calcium and magnesium (JRH Biosciences, Lenexa, KS, Cat. No. 45312301) diluted in Milli-Q water sterilised by autoclaving and stored at 4°C was also used.

A solution used for removing adherent cells from the base of tissue culture flasks and dishes consisted of 0.054% w/v trypsin and 0.54 mM ethylenediaminetetra-acetic acid (EDTA) in HBSS. Once dissolved, the solution was filtered through a low protein binding 0.22 μm filter (Millipore, Bedford, MA, Cat. No. SLGV025LS). To prevent inactivation of the trypsin, the solution was stored at –20°C. In some cases, 0.05% trypsin with 0.02% EDTA from JRH Biosciences (Lenexa, KS, Cat. No. 59417) was used.

Semi-solid medium containing methylcellulose was used for colony growth. To sterilise methylcellulose, 8.1 g of A4M premium grade 400 centipose methylcellulose powder (DOW Chemical Company, Midland, MI), was added to a 500 ml bottle with a tissue culture flea and autoclaved at 15 psig (121°C) for 15 minutes. When cool, 270 ml of sterile single strength IMDM (double-strength diluted 1:1) was added to the bottle while stirring and the mixture left to stir at room temperature in the dark for 3 days with occasional shaking. During this time, bovine serum albumin (BSA) solution was made by dissolving 20 g BSA (Sigma, St Louis, MO, Cat. No. 2153) in 88.4 ml Milli-Q water in a conical flask at 4°C overnight. Duolite mixed resin beads (BDH, Australia, Cat. No. 55057) were used to deionise the BSA solution at 4°C. This involved the addition of 4 g of beads to the BSA solution, with mixing every 15 minutes for about 2 hours or until beads became yellow. The solution was decanted into a fresh conical flask to remove existing beads. The process was repeated twice or until the beads did not change to yellow after incubation for 2 hours. The BSA solution was decanted and an equal volume of double-strength IMDM was added, and the solution filter sterilised. Aliquots were stored at -20°C if not used immediately, with a small aliquot collected to check for sterility. To the dissolved methylcellulose, 60 ml of the BSA solution

and 180 ml of FCS was added and left to stir for a further 4 hours. The methylcellulose mixture was aliquoted and stored at –20°C until required. Small aliquots of methylcellulose were set aside for sterility checks and batch testing to ensure comparative batches were used.

2.1.2. Cytokines and Growth Factors

Cytokine units are defined such that 50 Units results in 50% of the maximal number of colonies in soft agar cultures containing $5x10^4$ murine bone marrow cells. Purified recombinant huSCF produced in E. *coli*, was supplied by Amgen Corporation (Thousand Oaks, CA). Recombinant murine granulocyte macrophage - colony stimulating factor (muGM-CSF) ($5x10^5$ U/ml) synthesised by insect cells infected with a recombinant baculovirus vector was a gift from Dr. T. Gonda (Division of Human Immunology, Hanson Centre for Cancer Research, Adelaide). Recombinant murine interleukin-3 (muIL-3) ($7.5x10^5$ U/ml) synthesised by insect cells infected with a recombinant baculovirus vector was a gift from Dr. T. Gonda (Division of Human Immunology, Hanson Centre for Cancer Research, Adelaide). Recombinant murine CSF-1 (5000 U/ml) synthesised by insect cells infected with a recombinant baculovirus vector was donated by Elizabeth MacMillan (Division of Human Immunology, Hanson Centre for Cancer Research, Adelaide). Conditioned medium containing either recombinant human GM-CSF or IL-3 was obtained from cultured CHO cells transfected with the respective mammalian expression plasmids, kindly provided by Dr. A. Lopez (Division of Human Immunology, Hanson Centre for Cancer Research, Adelaide, Australia).

2.1.3. Culture Maintenance of Cells

Tissue culture work was performed in Class II Biosafety Cabinets, using reagents prewarmed to 37°C in a water bath. Bottles from the water bath were sprayed with 70% ethanol to prevent contamination. Cell cultures were maintained in tissue culture flasks or wells in tissue culture medium (see section 2.1.1) and were incubated in a humidified

atmosphere containing 5% CO_2 in air at 37°C. Cell density and viability were determined from an aliquot diluted 1:2 in 0.8% w/v trypan blue (in saline). Cell counts were performed using a haemocytometer, where cells excluding trypan blue were deemed viable. Cell cultures were maintained for approximately three weeks before referring back to the cryopreserved stocks.

The murine fibroblast cell line, psi2 (Mann *et al.*, 1983) was obtained from Dr. T. Gonda (Division of Human Immunology, Hanson Centre for Cancer Research, Adelaide). The psi2 packaging cell line produces empty ecotropic retrovirus. Upon transfection with plasmid, the introduced retroviral constructs were packaged into these viral particles. Transfected cells producing virus particles were used to infect target cells with plasmid by co-cultivation. Cells were maintained as sub-confluent monolayers in DMEM containing 10% FCS. Cultures that were approximately 70% confluent were harvested and subcultured into a new flask. To harvest cells, the adherent monolayer was rinsed once in HBSS and then incubated for 1 minute in trypsin diluted 1/2 in HBSS. After incubation, the sides of the tissue culture flask were hit several times to dislodge any remaining adherent cells. Trypsin activity was inhibited by the addition of FCS diluted in DMEM to 10%. Cells were then seeded into new flasks at appropriate densities.

The non-adherent factor dependent cell line, FDC-P1 (Dexter *et al.*, 1980) obtained from Dr. T. Gonda (Department of Human Immunology, Hanson Centre for Cancer Research, Adelaide, Australia) was maintained in DMEM containing 10% FCS supplemented with 62.5 U/ml baculovirus derived muGM-CSF. Cells were maintained at densities between $5x10^4$/ml to $1x10^6$/ml and were sub-cultured every 2 - 3 days.

Non-adherent myb immortalised haemopoietic cells (MIHC) were obtained from Dr. P. Ferrao (Division of Haematology, Hanson Centre for Cancer Research, Adelaide) (Ferrao *et al.*, 1997). These cells were created by transducing day 14 foetal livers with pRuf with inserted "truncated myb" (pRuf CT3-*Myb*) and selected for long term factor dependent growth

selection. Cells were grown in DMEM supplemented with 20% FCS with 250 U/ml baculovirus derived muGM-CSF alone or further supplemented with 46.9 U/ml muIL-3. Cells were maintained at densities between $1x10^5$/ml to $1x10^6$/ml and were sub-cultured every 2 - 3 days. For some experiments, MIHC infected with human D816V c-KIT or GNNK+S+ c-KIT created by Dr. P. Ferrao (Division of Haematology, Hanson Centre for Cancer Research, Adelaide, Australia) (Ferrao *et al.*, 1997) were used as controls. D816V c-KIT MIHC serving as a control were maintained in DMEM with 20% FCS without exogenous factor, while GNNK+S+ c-KIT MIHC control cells were maintained in DMEM with 20% FCS supplemented with 100ng/ml huSCF.

The factor dependent human megakaryocytic leukaemic cell line, MO7e (Avanzi *et al.*, 1988) was obtained from Dr. P. Crozier (Department of Molecular Medicine, School of Medicine, University of Auckland, Auckland, New Zealand). Cells were maintained at log phase in DMEM with 10% FCS supplemented with conditioned medium from CHO cells transfected with either human GM-CSF or human IL-3 cDNA.

2.1.4. Cryopreservation of Cells

Cells were cryopreserved in the presence of 10% dimethylsulphoxide (DMSO) as cryoprotectant to prevent fracturing of the cellular membranes. Cells in mid-log phase were passaged as above and resuspended in the appropriate growth medium to approximately $1x10^7$/ml. Immediately prior to freezing, an equal volume of "freezing mix" (30% FCS, 20% analytical grade DMSO (BDH, Merck, Victoria, Australia, Cat. No. 10323) and 50% RPMI-1640) was added dropwise to the cells. 1 ml aliquots of the cell suspension were dispensed into cryotubes (Nunc, Denmark, Cat. No. 3-66656) which were wrapped in cotton wool and placed at -70°C overnight to allow for gradual freezing. The next day, vials were transferred to liquid nitrogen filled tanks, for long term storage.

2.1.5. Thawing of Cryopreserved Cells

Cryotubes removed from liquid nitrogen were snap thawed in a 37°C water bath. The contents were transferred to a 10 ml centrifuge tube and 4 ml medium was added dropwise while shaking the tube. The tube was left for 3 minutes and 3 ml medium was added dropwise prior to centrifuging (200 g for 5 minutes at 25°C). The supernatant was removed and cells were seeded into the appropriate growth medium.

2.2. CYTOLOGY, CYTOCHEMISTRY AND HISTOLOGY

Smears containing $5x10^4$ cells were prepared from cultured cells. Cells were harvested, pelleted and resuspended in 100% filtered FCS such that the final amount of FCS present was greater than 80%. Aliquots of 75 µl were cytocentrifuged at 28 g at room temperature for 5 minutes on ethanol cleaned glass microscope slides in a cytospin 3 (Shandon Scientific, Cheshire, England). Cell smears were allowed to air dry before being stored at 4°C in air tight slide boxes in the presence of 2 - 4 mm self indicating silica gel (Ajax Chemicals, Australia, Cat. No. 3681).

To observe cellular morphology, tumour specimens were fixed in 10% formalin. The specimen samples were then paraffin embedded and sectioned at 5 µm at the Division of Histopathology (Institute of Medical and Veterinary Sciences (IMVS), Adelaide). The sections were stored at room temperature and stained with Haematoxylin/Eosin as detailed in section 2.2.1.

To detect specific markers in tumour specimens, fresh frozen sections prepared by immersion in Tissue TeK OCT compound (ProSciTech, Queensland, Australia, Cat. No. 1A018), were frozen with isopentane pre-cooled in liquid nitrogen and stored at -70°C. Sections (5 µm) thick were prepared on a cryostat machine with the help of Llew Spargo (Arthritis Research Laboratory, IMVS, Adelaide) and stored at -20°C in air tight slide boxes in the presence of self indicating silica gel until required for staining.

2.2.1. Morphological Characterisation of Cells

To observe general cellular morphology, cell smears prepared using the Cytospin Centrifuge, were stained with Wright-Giemsa through the automated system by the Diagnostic Services Laboratory, Division of Haematology, IMVS. Briefly, the slides were immersed in Jerner's stain for 2 minutes, Giemsa stain for 6 minutes and washed in a buffer of pH 7, before air drying. For photography, slides were mounted in glycerol-glycine mountant (Appendix 8.1).

To observe the morphology of tissue samples, paraffin embedded sections were stained with Haematoxylin/Eosin at the Division of Histopathology, IMVS and then mounted in DePX.

2.2.2. Phenotypic Characterisation of Cells

To determine the phenotype of cells in culture, the expression of lineage specific esterases was analysed. Mature macrophages express 'non-specific' (α-naphthyl acetate) esterase while mature neutrophils express naphthol-AS-D-chloroacetate esterase. The method used to detect these lineage specific enzymes was adapted from a technique described by (Yam *et al.*, 1971). Cytocentrifuged cell smears were fixed in ice cold esterase fixative (see section 8.1) for 30 seconds in a Coplin jar and then washed in distilled water with 3 changes over 5 minutes. The slides were then allowed to stain for 45 minutes at room temperature in a freshly made solution of 'non-specific' esterase substrate solution (see appendix 8.1). The slides were washed as above and stained for 1 hour at room temperature in a freshly made 'chloroacetate' esterase substrate solution (see appendix 8.1). Slides were washed as above and counterstained in Dako® methylgreen solution (Dako, Carpinteria, CA, Cat. No. S1962) from which the contaminating methyl violet had been removed by two extractions with an equal volume of chloroform. For photography, slides were mounted in glycerol-glycine mountant (see section 8.1). Cells expressing 'non-specific' (α-naphthyl acetate) esterase were

detected by a red-brown colouring and those expressing 'chloroacetate' (naphthol-AS-D-chloroacetate) esterase by a blue colouring.

2.3. IMMUNOASSAYS

2.3.1. Antibodies

Antibodies specific for human c-KIT included murine monoclonal 1DC3 (1gG1) (Aylett *et al.*, 1995) which was produced in our laboratory. An isotype matched negative control murine monoclonal antibody, 1B5 specific for *Giardia* (provided by Professor G. Mayrhofer, Department of Microbiology and Immunology, University of Adelaide, Australia) was run in parallel to 1DC3 in indirect immunofluorescence assays.

Antibodies to murine surface expressed proteins for MIHC phenotyping by immunofluorescence were ACK2 raised against murine c-KIT (donated by Dr. M. Ogawa, Department of Pathology, Institute of Medical Immunology, Kumamoto University Medical School, Japan) (Ogawa *et al.*, 1991a), F4/80 raised against mature macrophages (Austyn and Gordon, 1981) (donated by Dr. A. Hapel, John Curtin School of Medical Research, Canberra, Australia), biotinylated RB6 8C5 raised against GR-1 to detect mature neutrophils (Holmes *et al.*, 1986) and M1/70 raised against MAC-1 to detect monocytes (donated by Dr. I. Bertoncello, Peter MacCallum Institute, Melbourne) (Springer *et al.*, 1979) and 30H12 raised against Thy1 (Ledbetter and Herzenberg, 1979) (obtained from Dr. I. Kotlarski, University of Adelaide). Antibody was diluted in 10% normal human serum in PBS containing 1% BSA (Sigma, St Loius, MO, Cat. No. A-7906) and 0.1% w/v sodium azide (Az) (Sigma, St Louis, MO, A-7906) (PBS/BSA/Az) as follows: ACK2, 1μg/ml; F4/80, undiluted; RB6 8C5, 1/160; M1/70, 1/320 and 30H12, 1/160, all prior to a 1/2 dilution in the indirect immunofluorescence assay. A rabbit polyclonal antibody raised against a synthetic peptide of murine mast cell protease-5 (mMCP-5) provided by Dr. Patrick McNeil, University of New South Wales,

Sydney (McNeil *et al.*, 1992) was used at 1/50 in 10% normal goat serum to detect murine mast cells.

Murine monoclonal antibodies, 1DC3 and 1B5 were detected using affinity-isolated fluorescein isothiocyanate (FITC)-labelled F(ab')2 sheep antibody to mouse immunoglobulin (Silenus, Australia, Cat. No. DDF) or affinity purified R-phycoerythrin (PE) - labelled goat F(ab')2 anti-mouse Ig (Southern Biotechnology Associates, Inc. Birmingham, AL, Cat. No. 1030-09) both diluted 1/50 in 10% normal rabbit serum. Rat monoclonal antibodies ACK2, F4/80, M1/70 and Thy1 were detected with goat anti-rat IgG-R-PE (Southern Biotechnology Associates, Birmingham, AL, Cat. No. 3030-09) diluted 1/100 in 10% normal human serum. Biotinylated RB6 8C5 was detected with 1/50 dilution of streptavidin-R-GPE (Caltag Laboratories, SA 1001-4) in 10% normal human serum.

2.3.2. Indirect Immunofluorescence Assay

Target cells were harvested and washed twice in 2 ml ice cold PBS/BSA/Az by centrifuging at 200 g for 5 minutes at 4°C. Cells were then resuspended to approximately $1x10^7$ cells/ml in PBS/BSA/Az supplemented with 10% heat inactivated normal rabbit serum (NRS) or 10% normal human serum in order to block antibodies binding to surface Fc receptors. Aliquots of 50 µl were dispensed into round-bottomed plastic tubes and placed on ice. Saturating levels of antibody or culture supernatant (50 µl) were added to cell suspensions, vortexed and then incubated on ice for 60 minutes. Cells were washed twice in 2 ml PBS/BSA/Az and after the final wash the supernatant was removed leaving about 50 µl in the tube. Tubes were vortexed prior to the addition of 50 µl of secondary antibody diluted in PBS/BSA/Az supplemented with 10% NRS or 10% normal human serum. Cell suspensions were vortexed and incubated on ice for 60 minutes in the dark. Following the incubation, cells were washed twice with 2 ml PBS/BSA/Az and fixed in 0.5 ml of fluorescence activated

cell sorting fixative (FacsFix) (see section 8.1). The samples were stored for up to three weeks at 4°C in the dark.

Samples were analysed by flow cytometry using either a Profile II or EPICS XL flow cytometer (Coulter, Hialeah, FL). To ensure reproducibilty of mean fluorescence intensity on the flow cytometers from day to day, FL1 (detecting FITC) and FL2 (detecting R-PE) photomultiplier tube sensitivities were calibrated using Standard-Brite™ calibration beads (Coulter, Cat. No. PN 6604146).

2.3.3. Fluorescence Activated Cell Sorting

Cells were washed in HBSS containing 5% FCS and stained as above (see section 2.3.2) in 10% NRS in PBS under sterile conditions in the absence of Az and resuspended to $5x10^6$/ml in HBSS containing 5% FCS. Cells were run through the FACStar^{PLUS} cell sorter (Becton-Dickinson, Moutainview, CA). Pools of cells expressing a similar level of c-KIT were collected in sterile tubes. Cells were washed and seeded in appropriate medium in 25 cm^2 growth area flasks. For clonal isolation, cells were sorted individually into 96 well plates. Wells containing a single cluster were selected for amplification to ensure only one cell had been deposited in the well. Sorted cells were expanded until analysis by indirect immunofluorescence could be performed to confirm surface expression.

2.3.4. Alkaline Phosphatase Anti-Alkaline Phosphatase (APAAP) Technique

Further details of reagents used for this technique are in the appendix section 8.1.

The APAAP technique used to detect the expression of both intracellular and membrane bound antigens and was a derivation of that described by Erber *et al.*, (1984).

Slides were prepared as detailed in section 2.2. Using a wax pen (Dakopatts, Glostrup, Denmark, S2002), a ring was drawn around the cell smear to localise the applied solutions. Cells were fixed for 30 seconds in ice cold standard fixative (see appendix 8.1) then immediately washed by agitation in tris buffered saline (TBS) (see appendix 8.1) with three

changes over a 5 minute duration. To avoid high background staining, cell smears were not allowed to dry out from this point on. Excess TBS was removed with a paper towel and 50 µl of hybridoma supernatant diluted 1/2 in 10% NRS in PBA was added to the wax ring. This was incubated overnight in a humidified box at 4°C.

Primary antibody was removed by three washes in TBS over a 5 minute duration. To the cell smear 30 µl of rabbit anti-mouse Ig bridging antibody (Dakopatts, Glostrup, Denmark, Z259) diluted 1/50 in 10% NRS in PBS/BSA/Az was added and incubated for 1 hour at room temperature. Slides were washed as above then incubated with 30 µl of APAAP complex (Dakopatts, Glostrup, Denmark, D0651) diluted 1/100 in 10% NRS in PBS/BSA/Az. Smears were washed and incubated with two more rounds of bridging antibody and APAAP complex with 10 minute incubations for each. After the final wash, slides were incubated upright in a Coplin jar with APAAP substrate (see section 8.1) for 20 minutes and then rinsed with distilled water. Slides were either dried or counterstained immediately.

For counter staining, pre-wet slides were immersed in Dako® Mayer's Hematoxylin (Lillie's Modification) (Dako Carpinteria, CA, Cat. No. S3309) for 5 to 10 minutes. Slides were briefly rinsed in a large volume of distilled water prior to a 3 second immersion in acid water (0.5% HCl in distilled water). Slides were again rinsed in a large volume of distilled water prior to immersion in Scott's gentle alkaline solution (see section 8.1) for 2 minutes. Slides were rinsed in water and the mounted with glycerol-glycine (see section 8.1) and stored at room temperature. Cells exhibiting antibody binding had faint red colouring with the Haematoxylin stained nucleus appearing purple.

A variation on the above technique was performed by Ms Ly Nguyen (Division of Haematology, Hanson Centre for Cancer Research, Adelaide) to detect murine mast cells. Cells fixed as above were incubated with anti-mMCP-5 diluted 1/50 in 10% normal goat serum in PBS/BSA/Az and incubated for 1 hour in a humidified chamber at room temperature. Slides were washed as above and incubated with biotinylated swine anti-rabbit

Ig (Dako, Carpinteria, CA) diluted 1/500 in 20% normal human serum for 2 hours at room temperature. Washed slides were then incubated with neat streptavidin alkaline phosphatase (Zymed Laboratories, CA, Cat. No. P50231) for one hour then incubated with APAAP substrate (detailed in section 8.1) for 20 minutes. Slides were counterstained with haematoxylin as above and mounted in glycerol/glycine (see section 8.1).

2.4. TUMOURIGENICITY STUDIES

Cells in log phase growth were harvested and washed three times in DMEM. During the last wash, cells were counted and resuspended to $1x10^7$/ml in serum free DMEM. Aliquots of $2x10^6$ cells (200 µl) were injected into the hind flank of 8 week old female syngeneic (CBA strain) mice. Mice were monitored for tumour development daily.

Once mice presented with tumours measuring 5 to 10 mm in diameter, the mouse was sacrificed and the skin around the tumour removed. The exposed tumour was excised and divided into four sections. One section used for tissue culture was homogenised in DMEM using sterile apparatus. This sample was counted and seeded in DMEM supplemented with FCS to ensure factor independent growth. Other portions were used for fresh frozen sections (see section 2.2), fomalin fixation (see section 2.2) and the final portion was snap frozen in liquid nitrogen and stored at -70°C.

2.5. PROLIFERATION ASSAYS

Cells were passaged and seeded in fresh medium at $3x10^5$/ml a day prior to the assay to ensure that all clones were of an equivalent density.

2.5.1. PI 3-K Reagents

LY294002 (Sigma, St Louis, MO, Cat. No. L-9908) was dissolved in DMSO to a stock concentration of 6.5 mM and stored at -20°C. The final concentration of DMSO in culture was 0.15%.

Wortmannin (Sigma, St Louis, MO, Cat. No. W-1628) was diluted to 5 mM in DMSO and stored at -70°C. The final concentration of DMSO in the assay was 0.007%.

2.5.2. Analysis of Cell Number by Absorbance

This procedure was performed using CellTitre™ Assay reagent (Promega, Madison, WI, Cat. No. G5421) according to the manufacturer's instructions. It is based on the cellular conversion of a tetrazolium salt to a coloured formazan product, which is measured by absorbance at 490 nm to determine the number of viable cells.

Cells were harvested and washed three times in DMEM lacking serum and resuspended in DMEM supplemented with either 10 or 20% FCS. Densities used were either $5x10^4$ or $2.5x10^4$ cells/ml. Triplicate 50 µl aliquots of cells were seeded into wells of a 96 well tissue culture tray already containing 50 µl DMEM with appropriate FCS and growth factors and incubated for 2 - 6 days in a humidified chamber in a tissue culture incubator at 37°C. Total cell yield was determined after culture by the addition of 10 µl dye solution and incubation at 37°C for 3.5 hours, after which 25 µl of 10% sodium dodecylsulphate (SDS) (stop solution) was added and left for 30 minutes at 37°C. The absorbance at 490 nm was measured on an enzyme linked immunoabsorbent assay (ELISA) plate reader (Biorad, model 3550) with the reference wavelength set at 655 nm. To serve as background controls, triplicate wells containing medium only were included on all trays.

2.5.3. Analysis of Cell Survival, Proliferation and Growth by PKH Assay

The technique and data analysis was essentially carried out as described by Ashley *et al.,* (1994). The procedure relies on the incorporation of a fluorescent lipophilic dye into the cellular membrane. Cellular division results in equal distribution of the dye between the two daughter cells, hence the level of fluorescence on a given cell is an indication of the number of divisions undergone (Figure 2.1). The total yield of fluorescence in the viable population

Figure 2.1: Schematic diagram showing the distribution of PKH-26 dye amongst daughter cells.

The division of one cell stained with PKH-26 dye results in the equal distribution of PKH-26 dye amongst the daughter cells. Therefore, the fluorescent dye distribution serves as a measure of proliferation in the culture. For example, one division reduces the fluorescence level of a cell by half, and a further division will reduce this to a quarter. The rate of survival during culture is calculated based on the total fluorescence yield in the viable population and the number of cells present. Diagram shown where pink represents live cells stained with PKH-26 and the blue cell represents cell death.

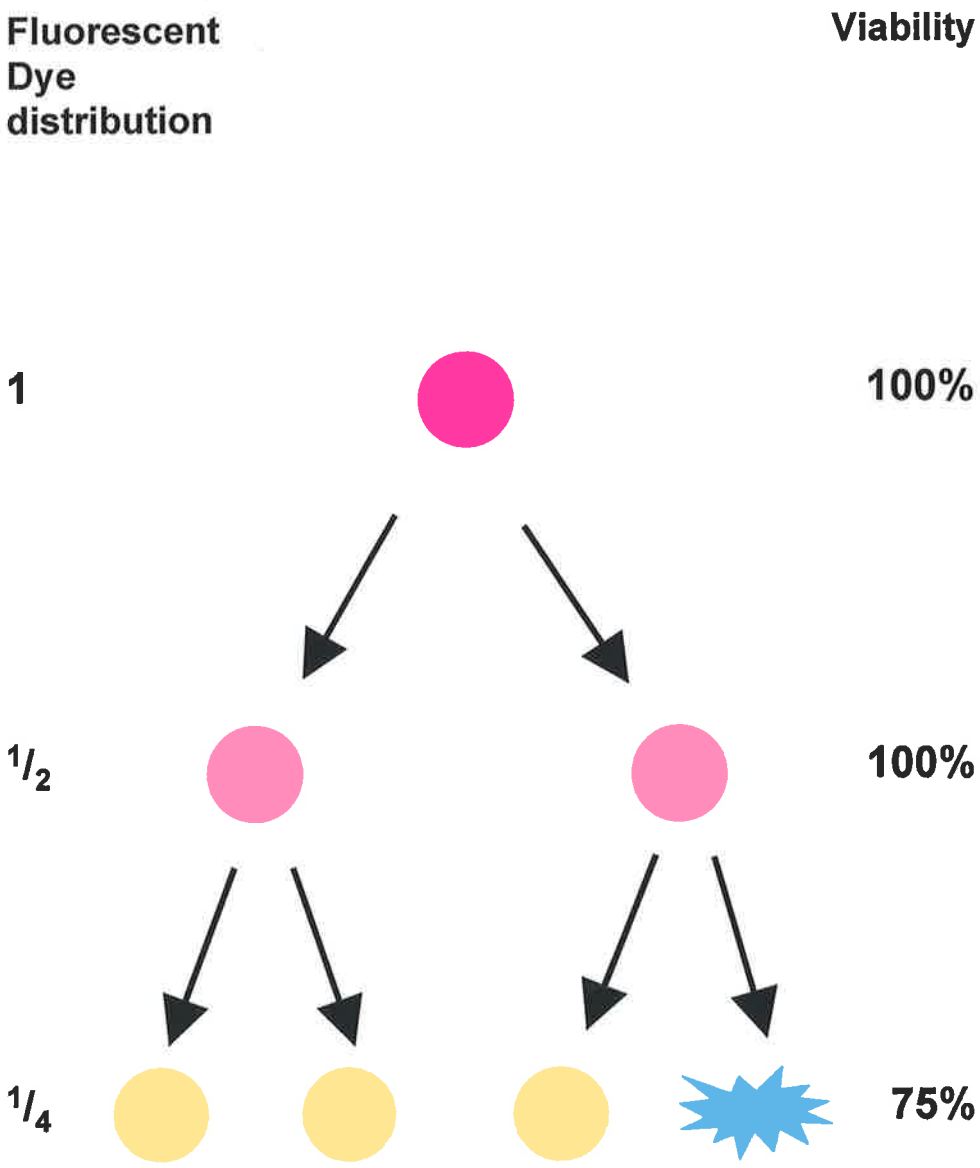
Fluorescent
Dye
distribution
Viability
1
100%
1/2
100%
1/4
75%

indicates cellular survival (Figure 2.1). A standard number of fluorescently labelled beads are mixed into each sample and they are used to calculate the total number of cells present.

Cells were labelled using the PKH-26 Red Fluorescent Cell Linker Kit (Sigma, St Louis, MO, PKH26-GL) as per the manufacturer's instructions. Cells were harvested from culture at equivalent densities and washed three times in serum free DMEM and then resuspended to $2x10^7$/ml in Diluent C (supplied in kit). The staining procedure was optimised for each cell line used to maximise staining whilst maintaining cell yields from the procedure. For FDC-P1 cells, an equal volume of $2x10^{-5}$ M PKH-26 dye diluted in diluent C was added to the cells and incubated at room temperature for 3 minutes with gentle mixing every 30 seconds. For MIHC, an equal volume of $1x10^{-5}$ M PKH26 dye diluted in diluent C was added to the cells and incubated at room temperature for 3 minutes with gentle mixing every 30 seconds. To stop dye incorporation, an equal volume of 100% FCS was added and incubated for 1 minute followed by the addition of an equal volume of 10 or 20% FCS in DMEM with a further incubation of 1 minute. The volume was made to 10 ml and viability and number of cells were determined using a haemocytometer and trypan blue exclusion. Cells were centrifuged and resuspended to $3x10^5$/ml (for FDC-P1) and $4x10^5$/ml (for MIHC) in appropriate growth medium and incubated overnight to stabilise the cells before commencing analysis.

FDC-P1 cells were harvested 15 hours post staining and washed three times in serum free DMEM and then resuspended to $1x10^6$/ml in serum free DMEM for 2 hours at 37°C. Cells were counted and resuspended to $2x10^5$/ml in DMEM with 10% FCS and 100 µl aliquoted in triplicate into 96 well tissue culture trays already containing factors to give a final volume of 200 µl and a final density of $1x10^5$/ml. For titration of huSCF a half-medium change was performed after 24 hours to maintain the sub-optimal concentrations of huSCF in the wells. After 48 hours culture, the contents of the wells were harvested (200 µl) and 400 µl FacsFix (see section 8.1), was added. Samples were vortexed before storage at 4°C in the

dark. To analyse the effect of LY294002 on proliferation and survival of cells, cells were incubated in the presence of LY294002 or DMSO control for 1 hour prior to the addition of cytokine or growth factor.

For MIHC, the cells were harvested 15 hours post staining and washed three times in serum free DMEM. Cells were then resuspended to $4x10^4$/ml (for examination of huSCF titration) or $1x10^5$/ml and $2x10^5$/ml (to examine the effect of LY294002) in DMEM with 20% FCS. Aliquots of 500 µl were added to wells already containing either factor or LY294002 titrations to give a final volume of 1 ml and a final density of $2x10^4$/ml, $5x10^4$/ml or $1x10^5$/ml. After 2 and 4 days of culture, the entire contents of the wells were harvested (1 ml). Since MIHC can differentiate and adhere to the plastic, wells were washed with 100 µl of medium and incubated with 100 µl trypsin to remove the adherent population. This was added to the tube containing the corresponding non-adherent population. Cultures were vortexed and triplicate 200 µl aliquots were added to round bottomed plastic tubes along with 400 µl of FacsFix (see section 8.1). Samples were vortexed before storage at 4°C in the dark. The volumes added to remove the adherent cells (200 µl) were taken into account during the calculations.

On the day of analysis, $2.5x10^3$ Standard-Brite™ calibration beads diluted in PBS (Coulter, Hialeah, FL, Cat. No. PN 660414) was added to the tubes immediately prior to analysis. The cell count, bead count and the mean fluorescence intensity (MFI) for each sample was analysed on a flow cytometer. The total cell number was calculated using the formula: Cell Density (cells/ml) = (viable cell count ÷ bead count) x (volume of the beads ÷ volume of the cells) x (concentration of the beads). Since each division results in halving of the fluorescence of individual cells, the average number of divisions was calculated based on the MFI at each time point relative to the MFI at day 0. The formula used was: Number of Divisions = (log (MFI at day 0 ÷ MFI at that day)) ÷ log (2). The survival or maintenance as

the percentage retention of fluorescence relative to day 0 was calculated by the formula: Cell maintenance = (MFI at that day x total viable cells at that day) ÷ (MFI at day 0 x total cells at day 0) x 100. This calculation is possible as no dye from dead cell membranes is able to re-incorporate into live cells and dead cells are excluded from analysis on the flow cytometer.

2.5.4. Statistical Analysis of Data

All statistical analysis was performed using a two sample students t-test assuming unequal variance unless otherwise indicated. Statistical significance was at the level of $\alpha < 0.05$.

2.6. DIFFERENTIATION ASSAYS

The day prior to the assay cells were seeded in fresh medium at $3x10^5$/ml. This ensured that on the day of the assay, cells were at a similar density of about $6x10^5$/ml. Differentiation assays in both liquid culture and semi-solid medium were set up in parallel.

2.6.1. Liquid Culture

Cells were harvested and washed three times in serum free DMEM and resuspended to $2x10^4$/ml in DMEM with 20% FCS. 2 ml aliquots were placed into wells containing no factor, 100ng/ml SCF or 250 U/ml muGM-CSF and 46.9 U/ml IL-3. Cytocentrifuge smears of this population were made to enable comparison. Throughout the assay the density was monitored and cultures amplified similarly. On day 7, the contents of the wells were harvested. The non-adherent fraction was pooled with the adherent fraction which had been removed by trypsinisation. Cytocentrifuge smears of samples were made with $5x10^4$ per slide (as in section 2.2). Slides were stained with esterase or Wright-Giemsa stain (see section 2.2.2 and 2.2.1 respectively for details).

2.6.2. Semi-solid Medium

Frozen aliquots of methylcellulose (see section 2.1.1) were thawed at 37°C in a waterbath. To the 42.5 ml aliquot of methylcellulose, 7.5 ml IMDM and 500 µl of glutamine was added and mixed well before use.

The experiment was performed in triplicate with $5x10^3$ cells per dish. A 1 ml aliquot of culture was taken and the volume was made up to 10 ml with serum free DMEM. Samples were centrifuged and resuspended in 2 ml serum free DMEM. Samples were counted and $2x10^4$ cells were added to 5 ml tubes already containing factors. Using a 5 ml pipette and 16G 1½ gauge needle, 4 ml of methylcellulose solution was added to the 5 ml sterile tube, and pipetted up and down repeatedly to disperse cells and factors throughout the methylcellulose. Aliquots of 1ml were dispensed into triplicate 3.5 mm dishes. Dishes were stored for 1 week at 37°C in a humidified box in an incubator, after which the number of colonies on each plate were counted. Colonies counted contained greater than 50 cells.

2.7. PROTEIN ANALYSIS

2.7.1. Antibody Details

See Table 2.1 for antibodies used for immunoprecipitation, Table 2.2 for primary antibodies used to probe Western blots and Table 2.3 for secondary antibodies conjugated to alkaline phosphatase activity.

2.7.2. Biotinylation of Cell Surface Antigens

Cells harvested from log phase cultures were washed three times in PBS/BSA/Az. During the last wash cells were counted and resuspended to $2x10^7$/ml in PBS (pH 7.4). To each 1ml of cells, 0.5 mg of 10 µg/µl membrane impermeant NHSS-spacer-biotin (Pierce, Rockford, IL, Cat. No. 21217) freshly made in PBS was added and incubated with occasional mixing for 30 minutes at room temperature. After incubation, cells were washed three times

Table 2.1: Antibodies used for Immunoprecipitation

Specificity	Monoclonal Name	Isotype	Species	Produced by	City/ Country	Cat. No./ Reference
c-KIT (extra cellular)	Kit4.G12	IgG2a	Murine	A. C. Cambareri, L. Ngyuen, L. K. Ashman	Division of Haematology, Hanson Centre for Cancer Research, Adelaide, Australia	Unpublished data
PI 3-K p85 subunit		Polyclonal	Rabbit	Upstate Biotechnology	Lake Placid, NY	06-195
Salmonella	1D4.5	IgG2a	Murine	O'Connor and Ashman	Dept of Microbiology and Immunology, The University of Adelaide	(O'Connor and Ashman, 1982)

Table 2.2: Primary antibodies used for Immunoblotting
Cell Signalling was based in Bevery, MA, Santa Cruz Biotechnology in Santa Cruz, CA, Upstate Biotechnology in Lake Placid, NY, Transduction Laboratories in Lexington, KY, Zymed in San Francisco, CA and Promega based in Madison, WI. 1C1.HF was kindly donated by Dr H-J. Bühring (Transplantation Immunology and Immunohaematology, University of Tubingen, Germany).

Specificity	Monoclonal Name	Isotype	Species	Dilution	Produced by	Cat. No./ Reference
Akt		Polyclonal	Rabbit	1/1000	Cell Signaling	9272
Akt-Phospho (S473)		Polyclonal	Rabbit	1/1000	Cell Signaling	9271S
c-KIT (carboxy terminus)		Polyclonal C19	Rabbit	1/1000	Santa Cruz Biotechnology	sc-168
c-KIT (extracellular)	1C1.HF	IgG1	Murine	1/2	Dr H-J. Bühring	(Bühring *et al.*, 1993)
ERK1		Polyclonal	Rabbit	1/1000	Santa Cruz Biotechnology	Sc-094
ERK2		Polyclonal	Rabbit	1/1000	Santa Cruz Biotechnology	Sc-154
ERK-phospho (T202, Y204)	E10	IgG1	Murine	1/1000	Cell Signaling	9106S
JNK		Polyclonal	Rabbit	1/1000	Cell Signaling	9252
JNK-phospho (pTPpY)		Polyclonal	Rabbit	1/2000	Promega	V7931/2
JNK-phospho (T183, Y185)	G9	Not listed	Murine	1/2000	Cell Signaling	9255S
Phosphotyrosine	4G10	1gG2bk	Murine	1/2000	Upstate Biotechnolgoy	05-321
Phosphotyrosine	PY20	IgG2b	Murine	1/5000	Transduction Laboratories	P11120
PI 3-K p85 subunit		Polyclonal	Rabbit	1/1000	Upstate Biotechnology	06-195
Ubiquitin	Ubi-1 [MAB1510]	IgG1κ	Murine	1/1000	Zymed	13-600

Table 2.3: Secondary reagents for Immunodetection on Western blots
All secondary reagents were conjugated to alkaline phosphatase

Specificity (anti-)	Source	Dilution	Produced by	City/Country	Cat. No.
Mouse	Sheep	1/1000	Silenus	Victoria, Australia	985034010
Rabbit	Sheep	1/2000	Silenus	Victoria, Australia	984134010
Biotin	Streptavidin	1/4000	Molecular Probes	Eugene, OR	S-921

with PBS. During the final wash, cells were counted, resuspended to $1x10^7$/ml in PBS and lysed as in section 2.7.3.

2.7.3. Preparation of Cellular Lysates

Cells grown in log phase were harvested and starved of growth factors in DMEM without serum at $1x10^6$/ml for 2 hours at 37°C. After serum and factor deprivation, FDC-P1 cells were resuspended to $1x10^7$/ml in serum free DMEM, while MIHC were resuspended to $2x10^7$/ml in serum free DMEM. Cells were pulsed with or without 100 ng/ml huSCF at 37°C and then pelleted in a microcentrifuge by pulsing to 15000 g. Tubes were immediately placed on ice, the supernatant aspirated and cells lysed in 1 ml of lysis buffer (see section 8.2) by trituration and vortexing. Lysed cells were incubated on ice for 30 minutes with vortexing every 5 minutes to assist in lysis. Tubes were then centrifuged at 15000 g for 30 minutes at 4°C to remove nuclei. The clarified lysate was transferred to a fresh tube and a small portion was removed and stored at -20°C for protein determination and whole cell lysate analysis. The remainder was immunoprecipitated (see section 2.7.4).

2.7.4. Immunoprecipitation

Immunoprecipitation of lysates was performed with 5 μg of primary antibody (see section 2.7.1) and 25 μl of a 50% slurry of Protein A Sepharose (in PBS with 0.1% Az) at 4°C on a rotating platform for 2 hours at 4°C. Immunoprecipitates of the same treatments were pooled and washed five times in the corresponding detergent supplemented with 5 mM sodium orthovanadate. After the final wash, the Protein A Sepharose pellet was resuspended in an equal volume of double strength reduced loading buffer (see section 8.2). Samples were boiled for 2 minutes and then either loaded onto gels or stored frozen at -20°C. If frozen, samples were reboiled for 2 minutes prior to loading on gels.

2.7.5. Determination of the Protein Content in Lysates

Protein determination was carried out on whole cell lysates using Micro BCA Protein Assay Reagent Kit (Pierce, Rockford, IL, 23235) according to the manufacturer's instructions. The assay relies on the presence of bicinchoninic acid (BCA) and Cu^{2+}. In the presence of peptides and amino acid side chains, a purple reaction product is obtained absorbing at 562 nm. BSA (supplied with kit) was serially diluted in PBS with concentrations ranging from 1.56 μg/ml to 200 μg/ml. Protein determination was performed on frozen lysates after centrifugation for 15 minutes at 15000 g at 4°C. Samples were diluted 1/20 or 1/30 in PBS. For the correction of background absorbance, blanks consisting of PBS only or 1% Nonidet P 40 (NP40) or 1% Triton diluted 1/20 or 1/30 dilution in PBS were used. Standards, lysates and blanks (75 μl) were loaded in triplicate into wells of 96 well trays. Standards and blanks were replicated on all trays used. To the wells, 75 μl of BCA reagent (50% reagent MA, 48% reagent MB, 2% reagent MC) was added and trays incubated at 37°C for 2 hours in a humidified box. Microtitre plates were read on a Biorad microtiter plate reader (Bio-Rad, model 3550) at absorbance 570 nm.

2.7.6. Size Determination of Proteins

The molecular weight of proteins was calculated by comparing their relative electrophoretic mobility with proteins of known size. The commercially available molecular weight markers used were Prestained SDS-PAGE Standards, High Range (Biorad Laboratories, Hercules, CA, Cat. No. 161-0309) and SeeBlue® Pre-Stained Standard (Invitrogen, Carlsbad, CA, Cat. No. LC5625). The estimated sizes of these molecular weight markers in kDa are as follows:

Prestained SDS-PAGE Standards, High Range: 204; 123; 80; 48

SeeBlue® Pre-Stained Standard: 250; 98; 64; 50; 36; 30; 16; 6; 4

2.7.7. Sodium Dodecylsulphate-Poly Acrylamide Gel Electrophoresis (SDS-PAGE)

Immunoprecipitates as described in section 2.7.4 above were size fractionated under reducing conditions on 8% polyacrylamide gels (see section 8.2) overlayed with a stacking gel (see section 8.2). Gels were assembled in Hoefer gel tank apparatus, according to the manufacturer's instruction, and immersed in protein electrophoresis buffer (see section 8.2). Boiled immunoprecipitates were loaded onto gels using cut tips to ensure Protein A Sepharose was loaded. Samples were electrophoresed at 15 mA/gel through the stacking gel and 20 mA/gel through the resolving gel.

Whole cell lysates (15 µl) diluted 1/2 in double strength reduced loading buffer were size fractionated under reducing conditions on 10% polyacrylamide gels (see section 8.2) overlayed with a stacking gel (see section 8.2). Samples were boiled for 2 minutes prior to loading and were electrophoresed at 15 mA/gel through the stacking gel and 20 mA/gel through the resolving gel.

2.7.8. Transfer of Proteins to Nitrocellulose and Polyvinylidene Difluoride (PVDF)

Proteins size fractionated on 8% or 10% gels by SDS-PAGE were transferred to either polyvinylidene difluoride (PVDF) Hybond membrane (Amersham Pharmacia, Buckinghamshire, England, Cat. No. RPN 303F) prewetted in 100% methanol, or onto nitrocellulose (Advantec MFS, Pleastanton, CA, Cat. No. A045A330R) using a fully submerged electrophoretic transfer technique with 20% or 10% methanol for PVDF or nitrocellulose respectively (see section 8.2 for transfer buffer details). For transfer to nitrocellulose, gel and membrane were allowed to equilibriate in transfer buffer for 15 minutes prior to setting up transfer. Proteins were transferred at 30 mA overnight or 250 mA for 2 hours.

2.7.9. Western Blotting Technique

Membranes to be probed were washed twice in 1x TBS (see section 8.2 for 10x stock) with 0.1% Tween20 for 10 minutes. To prevent non-specific antibody binding, the membranes were incubated in 2.5% membrane blocking solution (Amersham Pharmacia, Buckinghamshire, England, NIF833) in TBS for 1 hour whilst rocking slowly. The membrane was washed in TBS with 0.1% Tween20 (2 quick rinses followed by a 15 minute incubation and two 5 minute incubations) on a fast rocking platform. The membrane was then incubated with primary antibody (see Table 2.2) diluted in 2.5% membrane blocking solution for at least 2 hours in a covered container on a slow rocking platform at room temperature. After washing as above, the membrane was incubated with secondary reagent (see Table 2.3) for at least 1 hour in a covered container on a slow rocking platform at room temperature. Membranes were then washed as above followed by two rinses and an incubation for 5 minutes in TBS. The membrane was incubated protein side down on enhanced chemifluorescence (ECF) substrate (Amersham Pharmacia, Buckinghamshire, England, Cat. No. RPN 5785) for 30 seconds to 1 minute then placed protein side down on the glass plate of the FluorImager (Molecular Dynamics) and scanned immediately using a 570 nm filter. For strong signals, ECF was diluted 1/2 in TBS.

Blots were maintained wet and stored at 4°C in TBS with 0.1% Tween20 on a rocking platform. After probing, all blots were dried between two pieces of Whatman paper and stored in the dark.

2.7.10. Quantitation of Protein Bands

Data produced by the FluorImager or PhosphorImager was quantitated using ImageQuantTM software (Molecular Dynamics). Background values for each band were determined using an equivalent size analysis region in the same lane. The background value in relative fluorescence units was subtracted from the intensity of the band of interest.

2.8. ASSESSMENT OF PI 3-K ACTIVITY

2.8.1. Antibody Details

See section 2.7.1 (Table 2.1) for details.

2.8.2. Preparation of Lipid

The lipids used in this procedure included PtdIns, a substrate for PI 3-K and phosphatidylserine, added to increase the specificity of the reaction. Lipids were prepared in chloroform/methanol (95:5 v/v) at 10 mg/ml and 5 mg/ml stock for PtdIns and phosphatidylserine respectively and stored aliquoted at -70°C.

To make 400 µl of resuspended lipid, 20 µl of PtdIns (10 mg/ml) and 10 µl of phosphatidylserine (5 mg/ml) were carefully dried under a stream of nitrogen until just dry. Lipids were then resuspended in 400 µl of lipid resuspension buffer (see section 8.2) with a probe sonicator on ice by 2 quick 30 second pulses. Once in suspension, lipid was kept at room temperature and used within 2 hours of preparation.

2.8.3. Preparation of Cellular Lysates

Cellular lysates were prepared as described in section 2.7.3. Immunoprecipitations were performed as in 2.7.4, with 60 µl of 50% Protein A Sepharose slurry and 5 µg of antibody. After two hours rotation at 4°C, immunoprecipitated pellets were washed 3 times with ice cold Tris saline (see section 8.3) and 3 times with ice cold 1x kinase buffer (see section 8.3).

2.8.4. *In vitro* Kinase Assay

To the 30 µl Protein A Sepharose pellet 20 µl of 5x kinase buffer, 50 µl of resuspended lipid, 2 µl of 2.5 mM ATP and 10 µCi of γ^{32}P-ATP (specific activity 3000 Ci/mM) (PerkinElmer, Boston, MA, Cat. no. NEG002A) were added and the reaction allowed

to proceed at room temperature for 20 minutes. The reaction was terminated by the addition of 100 µl of 1 M HCl. Lipids were extracted with the addition of 200 µl chloroform:methanol (1:1 v/v) and 500 µl of 2 M KCl saturated with chloroform (10% v/v final). Tubes were vortexed briefly and centrifuged for 2 minutes at 15000 g to separate the mixture out into two phases, the top aqueous phase and the lower organic phase. The organic phase was collected with a fine pipette tip and placed into a fresh tube.

To inhibit PI 3-K activity, wortmannin (see section 2.5.1), at a final concentration of 70 nM was added to the kinase mix, just prior to the addition of γ^{32}P-ATP. The final concentration of DMSO in the reaction was 0.007%.

2.8.5. Thin Layer Chromatography

Samples were spotted 2 cm from the base of a thin layer chromatography (TLC) plate (aluminium sheet precoated with silica gel 60; Merck, Darmstadt, Germany, 5553) that had been immersed in potassium oxalate solution (see section 8.3) for 30 seconds and let to dry at room temperature overnight. Plates were then placed in a tank containing chloroform:methanol:acetic acid:water (43:38:5:7 v/v) that had equilibrated overnight and run until the solvent front was near the top of the TLC plate. The plate was then removed and allowed to dry. It was covered in plastic wrap and developed overnight on phosphorimaging plates. Plates were read on a PhosphorImager (Molecular Dynamics, Sunnyvale, CA).

2.8.6. Quantitation of PhosphorImager Results

Quantitation of PhosphorImager results was performed as in section 2.7.10 above.

2.9. MANIPULATION OF DNA

2.9.1. Restriction Endonuclease Digestion

Plasmid DNA was digested with 2 - 3 fold excess restriction endonuclease in a final volume of 10 - 40 µl. Digests were performed for 1 - 3 hours in 1x digestion buffer (supplied with enzyme as a 10x concentrated stock) at the optimal temperature as indicated by the manufacturer. The extent of digestion was determined by visualisation of the DNA fragments by gel electrophoresis (see section 2.9.2). Following digestion, enzymes were inactivated as specified by the manufacturer. If DNA was to be digested by multiple enzymes, then this was done simultaneously if the enzymes required compatible buffer conditions. If not, the DNA was purified by phenol chloroform extraction (section 2.9.4.2) after digestion with the first enzyme and before digestion with the subsequent enzyme.

2.9.2. Electrophoresis of DNA

DNA was separated by electrophoresis on agarose gels made in 1x Tris-acetate-EDTA (TAE) (see section 8.4) with the percentage of the gel dependent on the size of the DNA products to be detected. Generally, 1% agarose gels were used. For the analysis of PCR products 1% and 2% agarose and 4% low melting point Sea Plaque (FMC BioProducts, Rockland, ME Cat. No. 50111) gels were used. To the DNA, gel loading buffer (see section 8.4) was added and the samples loaded on horizontal gels immersed in an electrophoresis tank containing 1x TAE. Gels were electrophoresed at 80 - 100 V until the bromophenol blue dye front was three quarters along the gels. Gels were then removed, stained with ethidium bromide solution (2 µg/ml in water) for 5 minutes and destained in water for 5 minutes. DNA bands were visualised using a FluorImager 595 (Molecular Dynamics) with a 610 nm filter.

2.9.3. Size Determination and Quantitation of DNA Fragments

The size of DNA fragments were calculated by comparing their relative mobilities in agarose with DNA of known size. The commercially available molecular weight markers used were *Bacillus subtilis* bacteriophage SPP1 DNA digested with *Eco*RI (GeneWorks, Adelaide, Australia, Cat. No. DMW-S1) and plasmid pUC19 DNA digested with *HpaII* (GeneWorks, Adelaide, Australia, Cat No. DMW-P1) The estimated sizes of these molecular weight markers in kilobases are as follows:

*Eco*RI digested SPP1 DNA: 8.51; 7.35; 6.11; 4.84; 3.59; 2.81; 1.95; 1.86; 1.51; 1.39; 1.16; 0.98; 0.72; 0.48; 0.36

*Hpa*II digested pUC19 DNA: 0.501; 0.489; 0.404; 0.331; 0.242; 0.190; 0.147; 0.111; 0.110; 0.067; 0.034; 0.026

The concentration of DNA in solution was determined by spectrophotometry with absorbance at 260 nm based on the assumption that an absorbance value of 1 was equivalent to 50 µg/ml (1 cm light path). Alternatively, DNA was electrophoresed and the intensity of the ethidium bromide stained bands was compared to those with known molecular weight markers.

2.9.4. Purification of DNA

Two techniques were used in the purification of DNA. Firstly, GENECLEAN® was used to purify DNA excised from agarose gels. The second technique was phenol chloroform extraction used for purifying DNA after restriction enzyme digests.

For purification of the target DNA fragment from contaminating DNA fragments after restriction endonuclease digestion, samples were electrophoresed and stained with ethidium

bromide as in section 2.9.2. The gel was then scanned on the FluorImager and a printout the same size as the gel was obtained. This printout was placed beneath a glass plate the gel was resting on and the fragment of interest was excised from the gel. The gel was then rescanned to ensure all the band had been excised.

2.9.4.1.GENECLEAN®

This method was used to purify DNA between 0.3 and 5 kb from molten agarose and was a modification of the manufacturer's instructions (BIO 101, La Jolla, CA, Cat. No. 3105). It relied on the affinity of a specially formulated silica matrix termed 'GLASSMILK' to bind double stranded DNA. The excised gel slice containing the DNA fragment was placed into a microcentrifuge tube and weighed (assuming 1 mg is equivalent to 1 ml). To this, 2.5 - 3 volumes of sodium iodide (NaI) solution (supplied by manufacturer) was added and the agarose melted at 55°C. To the molten agarose, 5 µl of glassmilk suspension (supplied by manufacturer) (for 5 µg or less of DNA) was added and the sample rotated at 4°C for 15 to 30 minutes. DNA bound to the silica matrix was pelleted in a microcentrifuge for 5 seconds and the NaI supernatant was removed. The pellet was resuspended and washed 3 times with 'NEW WASH' (NaCl/Ethanol/Water; as supplied by the manufacturer) and resuspended in 10 - 20 µl Milli-Q water by heating the tube at 55°C for 10 minutes. The glassmilk was pelleted and the supernatant containing the DNA was transferred to a fresh tube.

2.9.4.2.Phenol Extraction

The DNA to be purified was made up to a minimum volume of 100 µl. To this, 2 µl of glycogen (2 mg/ml) (Roche, Mannheim, Germany, Cat. No. 901393) was added as a carrier to aid in visualisation of the purified DNA. An equal volume of phenol/chloroform (50% phenol, 50% chloroform) was added, vortexed and incubated on ice for 2 minutes to allow separation of the two phases. The solution was then centrifuged at 4°C at 15000 g for 5

minutes and the top aqueous phase transferred to a new centrifuge tube. To precipitate the DNA, 0.1 volumes of 3 M sodium acetate (pH 5.2) and 2.5 volumes of 100% ethanol was added and incubated on ice for 20 minutes prior to centrifuging at 15000 g for 20 minutes at 4°C. The precipitated DNA was washed once with 500 µl of 70% ethanol and allowed to air dry or dry under vacuum and then resuspended in water or Tris-EDTA (TE) (see section 8.4 for 100x stock).

2.9.5. Dephosphorylation of DNA

Dephosphorylation of vector DNA was performed to stop vector religation. This procedure used calf intestinal alkaline phosphatase (CIP) (Amersham Pharmacia, Buckinghamshire, England, E2250Y) which removed the 5' phosphate of DNA. Phosphatase treatment was performed in a reaction volume of 10 µl comprising DNA, 1x OnePhorAll buffer (Amersham Pharmacia, Buckinghamshire, England, 27-0901-02) and 1 U of CIP per 1 µg of DNA. Phosphatase reactions for 'sticky ends' were carried out at 37°C for 30 minutes and then terminated by the addition of EDTA (pH 8) to a final concentration of 5 mM and incubation at 75°C for 10 minutes. DNA was purified using the GENECLEAN® method (see section 2.9.4.1).

2.9.6. Ligation

Ligation of DNA was performed using T4 DNA ligase (Amersham Pharmacia, Buckinghamshire, England, E70005Y). Ligation reactions were performed with a 1 - 3 fold molar excess of insert DNA to vector DNA in the presence of 10 mM ATP, 66 mM Tris HCl (pH 7.6), 6.6 mM $MgCl_2$, 10 mM 1,4-Dithiothreitol (DTT), 150 mM NaCl, and 6 U of T4 ligase to a final volume of 10 µl and incubated at 4°C overnight. To terminate the reaction, it was heated at 65°C for 10 minutes and DNA was then purified using phenol chloroform procedure (see section 2.9.4.2).

2.9.7. Production of Electrocompetent Bacterial Cells

Bacterial *Escherichia coli* DH10β strain used for transformation were made electrocompetent by the following procedure. Bacterial cells from glycerol stocks were streaked onto a Ψa agar plate (see section 8.4) and incubated overnight at 37°C. A single colony was used to inoculate 10 ml of Luria Broth (LB) (see section 8.4) and was incubated with shaking at 37°C overnight. This was subcultured 1:100 into 1 L of prewarmed superbroth (see section 8.4) and grown until an OD_{600nm} of 0.4 - 0.6 (1 cm light path) was achieved. The cells were then chilled on ice for 15 to 30 minutes and centrifuged in a cold rotor at 5000 g for 15 minutes. The pellets were washed three times in ice cold water and then resuspended in 20 ml of 10% glycerol. Cells were centrifuged at 5000 g for 15 minutes at 4°C and resuspended in 1ml of 10% glycerol. The competent cells were aliquoted (45 µl) into cold 1.5 ml microcentrifuge tubes on dry ice and stored at -70°C until required.

2.9.8. Transformation of Electrocompetent Cells

Electrocompetent cells were thawed to room temperature and placed on ice. In a cold 1.5 ml tube, 40 µl of cells were mixed with 1 - 2 µl of purified ligated DNA and incubated on ice for 1 minute. This mixture was transferred to an ice-cold 0.2 cm cuvette and pulsed at 25 µF, 1.6 kV and 200 Ω with a Bio-Rad Gene Pulser. A time constant of approximately 4.5 µseconds was obtained after each electroporation. Immediately after the pulse, 500 µl of ice cold SOC medium (see section 8.4) was added to the cuvette using a glass pasteur pipette, mixed and the contents transferred to 10 ml polypropylene tubes and incubated for 1 hour at 37°C with gentle shaking. Dilutions of the culture were then plated onto Luria agar plates (see section 8.4) containing 100 µg/ml ampicillin.

2.9.9. Expansion of Plasmid DNA

2.9.9.1.Small Scale Plasmid Preparation

Single colonies were plucked aseptically from agar plates and grown overnight in 10 ml microcentrifuge tubes containing 3 ml of Luria broth (see section 8.4) with 100 µg/ml ampicillin. Cultures were chilled on ice and 1.5 ml transferred to microcentrifuge tubes. The bacterial cells were pelleted in a microcentrifuge at 9000 g for 1 minute. The supernatant was aspirated and the pellet resuspended in 250 µl of fresh lysis buffer (see section 8.4), vortexed and incubated on ice for 5 minutes. To this, 20 µl of lysozyme (10 mg/ml) was added, vortexed for 3 seconds, boiled in a waterbath for 1 minute and immediately placed on ice for 15 minutes. Chromosomal DNA and protein was pelleted by centrifugation at 15000 g for 20 minutes at 4°C. The supernatant containing the plasmid DNA was transferred to a fresh tube and precipitated with 2 volumes of 100% ethanol and vortexing. The plasmid DNA was pelleted at 15000 g for 15 minutes at 4°C. The pellet was washed with 1 ml of 70% ethanol, dried under vacuum and resuspended in 30 µl of Milli-Q water.

2.9.9.2.Midiprep DNA Preparation

Midiprep DNA preparation was carried out using a QIAGEN Midi Kit (QIAGEN, Germany, Cat. No. 12143) with slight modifications to the manufacturer's instructions. A 100 ml 2x YT bacterial culture (see section 8.4) containing 100 µg/ml ampicillin was inoculated with bacterial culture using a sterile loop and incubated overnight at 37°C with shaking. The culture was centrifuged at 4°C for 10 minutes at 5000 g. The supernatant was removed and the pellet resuspended in 4 ml Buffer P1 containing RNase A. Cells were lysed by the addition of 4 ml Buffer P2, mixed and incubated for 5 minutes at room temperature. The chromosomal DNA and protein were precipitated by the addition of 4 ml Buffer P3 with gentle inversion and incubated on ice for 15 minutes. Samples were centrifuged at 27000 g for 30 minutes at 4°C. The supernatant was transferred to a fresh plastic tube and centrifuged at 27000 g for 10 minutes at 4°C and then applied to a QIAGEN-tip that had been pre-equilibrated with 10 ml of Buffer QBT. The column was washed twice with 10 ml of Buffer

QC before the elution of plasmid DNA using 5 ml Buffer QF. Eluted DNA was precipitated with 0.7 volumes of room temperature isopropanol and centrifuged at 27000 g for 30 minutes at 4°C. The supernatant was removed and the DNA pellet air dried briefly. The pellet was then resuspended in 400 µl of TE (see section 8.4) and transferred to a microcentrifuge tube. The DNA was then re-precipitated with the addition of 40 µl 3 M sodium acetate and 1 ml of 100% ethanol and microcentrifuged at 15000 g for 30 minutes at 4°C. The pellet was washed in 70% ethanol, centrifuged for 10 minutes at 15000 g at 4°C and dried under vacuum. The pellet containing the plasmid DNA was resuspended in 100 µl of TE.

Glycerol stocks were made of all midiprep cultures. 3 ml of culture was centrifuged at 2500 g for 10 minutes at 4°C and supernatant removed. The pellet was resuspended in 1 ml of 20% glycerol in Luria Broth (see section 8.4) and transferred to a 1ml cryotube for storage at -20°C.

2.9.10. Primers used for Polymerase Chain Reaction (PCR) and Sequencing

Table 2.4 summarises the location of the oligonucleotide primers used to sequence or amplify human c-KIT. The location of these oligonucleotide primers is based on the c-KIT sequence published by Yarden *et al.*, (1987).

Table 2.4: Oligonucleotide Primers

Name	Oligonucleotide Sequence *	Location	Orientation
447	5'-*GGGGGATCC* GATGTGGGCAAGACTTCT-3'	1506-1524	sense
1003	5'-GCAGGAAGACTCCTTTGAATGC-3'	2142-2163	anti-sense
1002	5'-GATAGTACTAATGAGTACATGG-3'	2167-2188	sense
1004	5'-TCATCCTCCATGATGGCG-3'	2283-2300	anti-sense
SRC-09	5'-TTGGCAGCCAGAAATATC-3'	2400-2418	sense
SRC-03	5'-TTAGAATCATTCTTGATG-3'	2470-2487	anti-sense
SRC-10	5'-AACTTAGAATCGACCGGC-3'	2642-2660	anti-sense
SRC-05	5'-GAATGGTCTACCACGGGC-3'	2865-2882	anti-sense

*Italicised sequence in oligonucleotide primer 447 encodes an endonuclease restriction site.

2.9.11. Purification of Oligonucleotide Primers

Primers were synthesised on an Applied Biosystems 391 DNA synthesiser in the Division of Haematology, IMVS, Adelaide by Mr A. Mangos and were obtained still attached to the synthesis column. The below procedure was used to remove and purify primers. A 1 ml syringe was inserted into one end of the column and into the other end another 1 ml syringe containing 500 µl of ammonium hydroxide (25% ammonia solution, MERCK, Melbourne, Victoria, Australia, Cat. No. 1.05428) was inserted. The plungers of the syringes were moved backwards and forwards in order to fill the column with ammonium hydroxide and left to stand for 20 minutes. The ammonium hydroxide was then drawn into one syringe and the contents placed in a 2 ml screw-capped tube. The above procedure was repeated three more times until a volume of 2 ml was obtained. The primer/ammonium hydroxide solution was incubated overnight at 56°C. The vials were allowed to cool and the primer dried down by vacuum. The pellet was dissolved in 100 µl of sterile distilled water and the concentration

determined by spectrophotometry $A_{260}1$ = 33µg/ml (1 cm light path) or to determine the molarity (M) the following formula was used:

$$\text{concentration of oligo(M)} = \frac{\text{weight (g)}}{\text{oligo molecular weight} \times \text{volume (L)}}$$

molecular weight of dNTPs: A = 347.2, T = 332.2, G = 363.2, C = 323.2

2.9.12. Polymerase Chain Reaction (PCR)

All reagents were aliquoted using non-aerosol tips in order to reduce contamination. Reactions were prepared in 0.5 ml microcentrifuge tubes to a final volume of 50 µl and overlayed with 50 µl of mineral oil. For amplification of plasmid DNA, reactions containing 0.5 to 1 ng DNA, 100 ng each of forward and reverse primers, 0.2 mM each of dATP, dTTP, dCTP and dGTP (Pharmacia, Sweden, Cat. No. 27-20(5-8)0-02), 50 mM KCl, 10 mM Tris HCl (pH 8.3), 1.5 mM $MgCl_2$ and 2.5 U of AmpliTaq DNA Polymerase (Perkin Elmer, Boston, Massachuesetts, Cat. No. N801-0060) made to the final volume with sterile Milli-Q water were prepared.

DNA was amplified using a DNA Thermal Cycler (Perkin Elmer, Boston, Massachuessetts) with an initial 7 minute denaturation step at 94°C followed by 30 rounds of denaturation, primer annealing and elongation, finishing with a final extension at 72°C for 7 minutes. Completed reactions were stored at 4°C.

The temperature selected for the annealing of primers was 1 - 5°C lower than the average melting temperature for the two oligonucleotide primers. The melting temperature was calculated using the formula:

Melting Temperature (°C) = 2(A+T)+4(C+G)

Optimised PCR conditions for each set of primers are detailed in Table 2.2 below.

Table 2.5: Optimised PCR conditions

Primers	Denaturation	Annealing	Elongation
447 and 1004	94°C / 1 minute	52°C / 1 minute	72°C / 1.5 minutes
SRC-09 and SRC-10	94°C / 1 minute	52°C / 1 minute	72°C / 1 minute
447 and SRC-10	94°C / 1 minute	51°C / 1 minute	72°C / 2 minutes

2.9.13. Sequencing of DNA

The ABIPRISM Dye Terminator Cycle Sequencing Reaction Kit (Perkin Elmer, Boston, MA) was used to sequence DNA purified using the QIAGEN midi kit. For a sequencing reaction, 8 µl of Terminator Ready Reaction Mix (A, G, C, T-Dye Terminator, dGTP, dATP, dCTP, dTTP, Tris-HCl, pH 9; $MgCl_2$; thermostable pyrophosphatase AmpliTaq polymerase) was added to 2 µg of template DNA and 3.2 pmol of sequencing primer. The volume was made up to 20 µl with Milli-Q water. The reaction was cycled using a Perkin Elmer GeneAmp PCR System 9600 using the following program: [96°C 10 seconds, 50°C 5 seconds, 60°C 4 minutes] x 25 cycles, followed by a 4°C hold step. Following cycle sequencing the DNA was precipitated with 2 µl 3M sodium acetate (pH 4.6) and 50 µl 95% ethanol and incubated on ice for 10 minutes. The DNA was pelleted at 15000 g for 30 minutes at 4°C, washed with 250 µl 70% ethanol and air dried. The sequence was then determined using a Perkin Elmer automated sequencer by the sequencing laboratory in the Division of Haematology, IMVS, Adelaide).

2.10. INTRODUCTION OF RECOMBINANT DNA INTO EUKARYOTIC CELLS

2.10.1. cDNA and Expression Vectors

Human *c-KIT* cDNA, according to the sequence published by Yarden *et al.*, (1987) inserted between the Asp 718 - Not I sites of the pBluescript M13 - (SK) vector was provided by Dr. D. Williams (Immunex Corporation, Seattle, WA).

Human *c-KIT* cDNA containing a single point mutation A2813T, inserted in the *Bam*HI site of the pcDNA3 polylinker, was provided by Dr. L. Ronnstrand (Ludwig Institute for Cancer Research, Uppsala, Sweden).

The retroviral vector pRUFMC1*neo* was provided by Drs J. Rayner and T. Gonda, (Hanson Centre for Cancer Research, Adelaide, Australia) (Rayner and Gonda, 1994) and contained 5' and 3' LTRs and the neomycin gene was driven by the f9 polyoma enhancer. The vector is shown in Figure 2.2.

Human GNNK+S+ and GNNK-S+ isoforms of *c-KIT* inserted into the *Hpa*I site of pRUFMC1*neo* was created previously by Dr. G. Caruana (Caruana *et al.*, 1999). Human *c-KIT* containing the substitution A2468T, resulting in the D816V mutation, was inserted into the *Hpa*I site of pRUFMC1*neo* by Dr. P. Ferrao (Ferrao *et al.*, 1997).

Required cDNA fragments were purified and cloned into the polylinker of the retroviral expression vector, pRUFMC1*neo*. DNA plasmids containing retroviral expression constructs were expanded by midiprep DNA preparations (see section 2.9.9.2) for transfection into the psi2 packaging cell line.

2.10.2. Calcium Phosphate Transfection into psi2 Packaging Cells

The viral packaging fibroblast cell line psi2 was transfected with retroviral plasmid constructs as described by Lang *et al.,* (1985). Briefly, a day prior to transfection, 6 cm dishes were each seeded with $1x10^5$ psi2 cells in DMEM supplemented with 10% FCS. In a 10 ml

Figure 2.2: Schematic of the pRUFMC1*neo* retroviral vector.

The pRUFMC1*neo* vector was created by inserting MC1*Neo* cassette between *Bgl*II and *Cla*I sites of pRUF. U3, R and U5 represent repeat sequences within the LTR in which *Kpn*I and *Sma*I sites have been omitted from the figure. A unit proviral length is 3259 bp. Amp^R represents gene encoding resistance to ampicillin while ORI refers to the origin of plasmid replication. 'SD' and 'SA' represent the splice donor and splice acceptor sites respectively. In the polylinker, *Bam*HI, *Xho*I, HpaI , *Hind*III and *Bgl*II are all unique.

pRUFNeo (5650 bp)

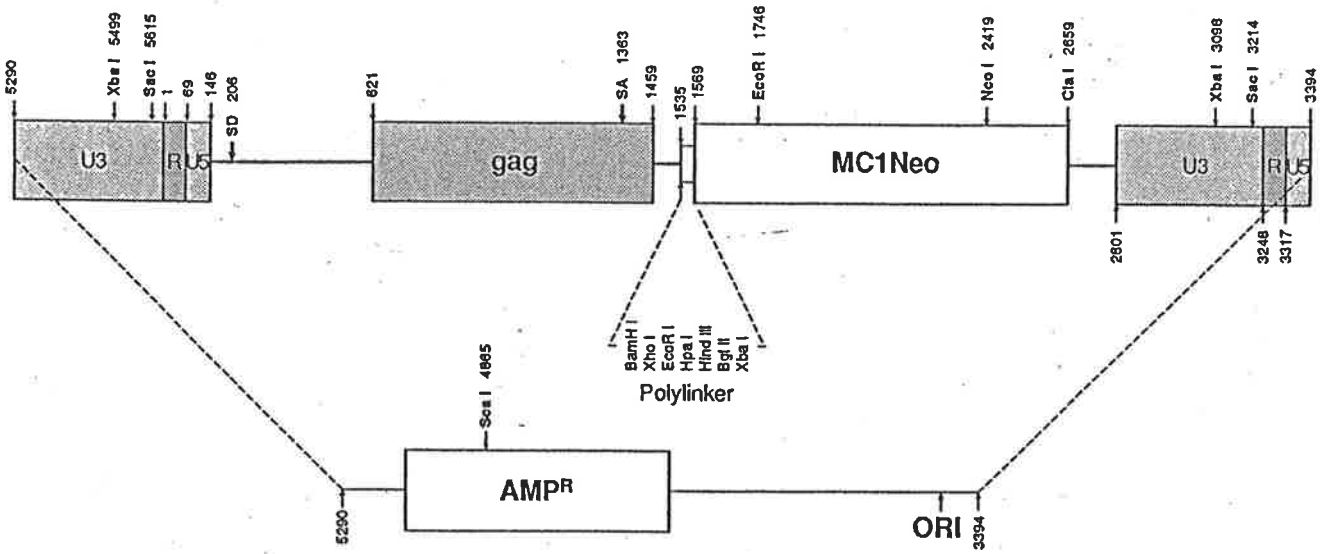

polystyrene tube, a 0.5 ml solution containing 20 µg DNA and 250 mM $CaCl_2$ was prepared. A second solution of equal volume was freshly prepared in a 20 ml conical polystyrene tube and consisted of 250 mM NaCl, 1.5 mM $NaPO_4$ pH 7 and 50 mM HEPES pH 7.1. The DNA solution was added dropwise to the second solution while bubbling air through the second solution with a 1 ml pipette. The combined solution was incubated at room temperature for 30 minutes until a visible precipitate had formed. 500 µl of the precipitate was added dropwise to a duplicate set of dishes and cultures incubated at 37°C. After 24 hours, cells were 'glycerol shocked'. Medium was removed from dishes and 1 ml of 15% glycerol in DMEM was added and rocked gently every 30 seconds. After 4 minutes the glycerol/DMEM was removed and cells were gently washed with 5 ml DMEM. After the wash, DMEM containing 10% FCS was added and cells incubated overnight. The following day, cells were harvested and seeded into DMEM containing 10% FCS and 400 µg/ml geneticin. Medium was changed twice weekly. Geneticin was maintained in the culture medium for about 1 week until all mock transfected cells died.

2.10.3. Retroviral Infection of Suspension Cells by Co-cultivation

Semi-confluent monolayers of psi2 transfectants were irradiated at 30 Grays, harvested and seeded at $1x10^6$ in 25 cm^2 growth area flasks. Non-adherent cells to be infected were added at various densities depending on the cell line in a final volume of 5 ml. After 2 days co-cultivation, the non-adherent cells were collected, washed and cultured in 5 ml DMEM with FCS, muGM-CSF and 1 mg/ml geneticin. Medium was changed twice weekly until all mock infected cells had died.

2.11. Manipulation of RNA

For RNA procedures, materials were maintained free from RNase contamination, and gloves were always worn. Plasticware and autoclaved glassware was pretreated with 0.5 M

NaOH to remove RNase contamination. All Milli-Q water used was treated with 0.1% v/v diethylpyrocarbonate (DEPC) (Sigma, St Louis, MO, Cat. No. D-5758) at 37°C overnight and autoclaved to inactivate the DEPC. All other solutions used were prepared in 'RNase-free' plasticware or glassware. Plugged tips were used to prevent contamination.

2.11.1. Total RNA Extraction

Total RNA extraction was performed using TRIzol according to the manufacturer's instructions (GibcoBRL, Gaithersburg, MD, Cat. No. 15596-026). Cells in log phase growth ($1.25x10^7$total) were harvested and washed in tissue culture grade PBS. The supernatant was removed and 1 ml TRIzol reagent was added to the pellet and mixed by pipetting. The samples were left at room temperature for 5 minutes, before transferring them to microcentrifuge tubes and storing frozen at -70°C.

To 1 ml samples that had been thawed to room temperature, 0.2 ml chloroform was added and vigorously shaken before incubation for 3 minutes. Samples were centrifuged at 12000 g for 15 minutes at 4°C which resulted in the presence of three phases, a lower red phase, a phenol-chloroform interphase and an upper colourless aqueous phase containing RNA. The aqueous phase was transferred to a fresh tube and the RNA was precipitated with 0.5 ml isopropyl alcohol by incubation at room temperature for 10 minutes. The samples were centrifuged at 12000 g for 10 minutes at 4°C. The supernatant was removed and the pellet washed with 1 ml 75% ethanol. Samples were incubated at room temperature for 10 minutes then centrifuged for 5 minutes at 7500 g at 4°C. Pellets were air dried then dissolved in DEPC treated water by pipetting and incubation at 60°C for 10 minutes.

2.11.2. Quantitation of RNA

Quantitation of RNA was performed using a spectrophotometer to measure absorbance at A260 and A280. The concentration was determined on the assumption that an absorbance

at 260 nm of 1 is equivalent to 40 μg/ml (1 cm light path) of RNA. The ratio of A260/A280 was determined to ensure freedom from protein contamination.

2.11.3. Probes

A probe for human *c-KIT* was created by digesting GNNK+S+ *c-KIT* cDNA contained in pRUFMC1*neo* with *Eco*RI. A fragment encoding the first 700 base pairs of *c-KIT* was gel purified. A 780 base pair fragment of the human glyceraldehyde 3-phosphate dehydrogenase (GAPDH) cDNA excised from pHcGAP (ATCC, Rockville, MD) was provided by Mr G. Casey (Division of Haematology, IMVS, Adelaide).

2.11.4. Random Oligonucleotide Priming

The double stranded DNA probe from 2.11.3 above was labelled using the GIGAprime DNA Labelling Kit (Bresatec, Adelaide, Australia, Cat. No. GPK-1) according to the manufacturer's instructions with minor modifications. 50 - 100 ng of template DNA was made to 7 μl with sterile Milli-Q water and heated at 95°C for 5 minutes to denature the DNA, and then placed on ice to cool. To this was added 6 μl of decanucleotide solution, 6 μl of nucleotide/buffer cocktail, 50 μCi of α^{32}P-dATP (specific activity 3000 Ci/mM) (Bresatec, Adelaide, Cat. No. ADA-2) and 1 μl (5 U) of Klenow DNA polymerase. The solution was mixed and briefly centrifuged before incubation at 37°C for 15 minutes. The reaction was terminated by the addition of 1 μl of 0.5 M EDTA and the volume adjusted to 50 μl with sterile Milli-Q water. The final volume was then adjusted to 50 μl with sterile Milli-Q water. The probe was purified from the label using Microbio-spin 6 chromatography columns (Biorad, Hercules, CA, Cat. No. 732-6221). Columns were inverted to resuspend the gel and the tip snapped off and placed in a 2 ml microcentrifuge tube with the top cap removed to allow flow. The column was centrifuged for 2 minutes at 1000 g and then placed in a clean tube. Samples were applied to the column and centrifuged at 1000 g for 4 minutes, to elute

the purified labelled probe. The counts per minute of the DNA probe was determined by diluting 1 µl of the probe in 100 µl Milli-Q water and placing into a Bioscan QC-2000.

2.11.5. Northern Blot Transfer

RNA samples (10 µg) isolated as described in section 2.11.1 were dried in a speedivac and then resuspended in 12 µl of sample buffer (see section 8.5) with 0.2 mg/ml ethidium bromide and mixed. RNA was denatured at 65°C for 5 minutes and then 1 µl of loading buffer (see section 8.5) was added to the tubes. Samples were electrophoresed in a 1% agarose gel (see section 8.5) in formaldehyde running buffer (Appendix 8.5). The gels were washed by rocking in DEPC treated water for 30 minutes and then ethidium bromide stained RNA contained in the gel was visualised using a FluorImager at an excitation wavelength of 610 nm. This was performed to determine the quality of the RNA. The gel was then blotted onto Hybond N+ filters (Amersham, Buckinghamshire, England, Cat. No. RPN303B) and the RNA transferred by capillary action in 10x SSC (see section 8.5) overnight. The nylon membrane was rinsed in 2x SSC and allowed to air dry prior to cross-linking the RNA to the filter by exposure to UV light (0.4 J/cm2 in a Hybaid UV crosslinker).

Nylon membranes were placed in 2x SSC, rolled and placed in glass hybaid bottles. Prior to hybridisation with radiolabelled probes, filters were incubated at 68°C for 30 minutes in 10 ml of pre warmed Express Hyb solution (Clontech, Palo Alto, CA, 8015-1) Probes for a final activity of $5x10^6$ cpm/ml were denatured by incubation at 95°C for 10 minutes and then added to 3 ml ExpressHyb. This was added to the bottle containing the membrane and incubated for 1 hour at 68°C whilst rotating.

Filters were washed twice with 2x SSC containing 0.05% SDS with the final wash incubated for 30 minutes at room temperature, whilst rocking. Filters were then washed once in a more stringent solution (0.1x SSC with 0.1% SDS) at 50°C for 30 minutes while shaking. Filters were dried and wrapped in plastic wrap. Hybridisation signals were detected on

phosphor storage screens which were exposed overnight and analysed using a Molecular Dynamics PhosphorImager with ImageQuantTM software (Molecular Dynamics, Sunnyvale, CA). Hybridisation signals were quantified using the GAPDH signals as a loading control. To reprobe, nylon membranes were stripped by submersion in a 90°C solution of 0.5% SDS for 10 minutes and dried on Whatman paper.

CHAPTER 3:

DIFFERENTIAL FUNCTION OF c-KIT ISFOFORMS IN HAEMOPOIETIC PROGENITOR CELLS

3. DIFFERENTIAL FUNCTION OF C-KIT ISOFORMS IN HAEMOPOIETIC PROGENITOR CELLS

3.1. INTRODUCTION

Activation of the RTK, c-KIT by its ligand SCF results in haemopoietic cell proliferation, survival, differentiation, adhesion and chemotaxis (Bendall *et al.*, 1998; Kinashi and Springer, 1994; Meininger *et al.*, 1992; Ricotti *et al.*, 1998; Tsai *et al.*, 1991). Receptor dimerisation, transphosphorylation and the activation of downstream pathways including PI 3-K and Ras-MAPK are important aspects of c-KIT function (Lev *et al.*, 1991; Miyazawa *et al.*, 1991; Rottapel *et al.*, 1991).

Human c-KIT has four naturally occurring isoforms, which arise from differential splicing at two distinct sites. Alternate splicing results in the insertion/deletion of GNNK in the extracellular juxtamembrane region, or the insertion/deletion of a single serine residue in the interkinase sequence (Crosier *et al.*, 1993; Giebel *et al.*, 1992; Gokkel *et al.*, 1992; Hayashi *et al.*, 1991; Vandenbark *et al.*, 1992). The presence or absence of GNNK on a S+ background of c-KIT had significant effects on the biological responses and activation kinetics in response to huSCF, which was not attributable to differences in ligand binding affinity (Caruana *et al.*, 1999). These studies performed in NIH-3T3 fibroblasts revealed that the GNNK- isoform was more transforming in the presence of huSCF as shown by focus formation, anchorage independent growth and the ability to produce tumours in nude mice. The GNNK+ isoform also promoted anchorage independent growth but only weak focus formation and no tumours in mice. The kinetics of c-KIT activation in response to huSCF stimulation were also different between the two isoforms with GNNK- exhibiting rapid transient responses, while GNNK+ exhibited a slower more sustained response.

Considering the behavioural differences of the c-KIT isoforms in response to huSCF in NIH-3T3 fibroblasts, it was of interest to evaluate these parameters in physiologically relevant haemopoietic cells. Two factor dependent haemopoietic models were chosen. One was an immature murine myeloid cell line, FDC-P1, dependent on muGM-CSF for growth and survival. The other was a factor dependent early haemopoietic cell population, MIHC. These cells derived from murine foetal liver are capable of differentiating along the macrophage and granulocyte lineages (Ferrao *et al.*, 1997).

3.2. EXPRESSION OF C-KIT ISOFORMS IN FDC-P1

The role of human c-KIT isoforms in huSCF mediated biological responses and signal transduction was examined in the factor dependent murine myelomonocytic cell line, FDC-P1. The factor dependent nature of these cells allowed analysis of survival and proliferation in response to growth factor stimulation. FDC-P1 cells express endogenous c-Kit at low levels, however huSCF has little affinity for murine c-Kit (Martin *et al.*, 1990; Zsebo *et al.*, 1990a) therefore its presence will not affect observations.

The human *c-KIT* cDNA encoding the GNNK+S+ isoform was obtained from Dr. D. Williams (Immunex Corporation, Seattle, WA) in pBluescript(SK). GNNK-S+ *c-KIT* was created previously from the 3 kb GNNK+S+ cDNA insert in pBluescript(SK) vector, by PCR site directed mutagenesis using primers flanking the area to be deleted and then ligation (Caruana *et al.*, 1999). The construct was validated by sequencing (Caruana *et al.*, 1999). The *c-KIT* cDNA inserts were excised from pBluescript(SK) using restriction endonucleases *Asp*718 and *Not*I, end filled and inserted into the *Hpa*I site of the pRUFMC1*neo* retroviral vector (Caruana *et al.*, 1999). *c-KIT* constructs in pRUFMC1*neo* were transfected into the virus packaging cell line, psi2 by the calcium phosphate method (see section 2.10.2). Transfected cells were selected for resistance to geneticin.

MuGM-CSF dependent FDC-P1 were infected by co-cultivation with psi2 cells producing virus containing cDNA encoding either GNNK-S+ or GNNK+S+ human c-KIT (see section 2.10.3 for method). Infected cells were selected with 1 mg/ml geneticin until control cells died. To obtain c-KIT expression within a physiological range, cells were sorted based on their surface expression using fluorescence activated cell sorting. Antibody used in these studies (1DC3) bound to the first immunoglobulin like domain of c-KIT, exhibiting no preference for the isoforms (unpublished data). The sorted population was used to create a series of clones to ensure that observations were not due to a clonal artefact of the infected population. These were created by single cell deposition using fluorescence activated cell sorting and were expanded and characterised in regard to their surface expression.

3.2.1. Analysis of c-KIT Expression by Indirect Immunofluorescence

Indirect immunofluorescence performed on FDC-P1 clones used 1DC3, an IgG1 antibody specific for c-KIT, and an isotype matched negative control, 1B5, specific for *Giardia*. Parental FDC-P1 did not express human c-KIT (Figure 3.1A). Expression of c-KIT was observed in all clones as a single peak shift of fluorescence above background. Four clones of each isoform, displayed in Figure 3.1A, were selected based on their surface expression. Selected clones exhibited a range of surface c-KIT which was paired between the isoforms. These clones were amplified and cryopreserved (see section 2.1.3 and 2.1.4). For subsequent experiments, cells were maintained in medium supplemented with muGM-CSF (refer to section 2.1.3 for details).

Saturation binding analysis previously performed in our laboratory on FDC-P1 cells transduced with human *c-KIT* cDNA, gave an estimate of the number of surface expressed receptors (Caruana *et al.*, 1999). To determine the relative copy numbers of c-KIT on FDC-P1 clones, an indirect immunofluorescence assay was performed on clones, in parallel to FDC-P1 populations that had been characterised by saturation binding analysis (Caruana *et*

Figure 3.1: Surface expression of c-KIT isoforms by indirect immunofluorescence assay.

Surface expression of c-KIT was determined by indirect immunofluorescence using monoclonal antibody 1DC3 (anti-c-KIT) and an isotype matched negative control 1B5 (anti-*giardia*). **A:** Histogram of mean ± standard deviation (SD) from a duplicate experiment shows the relative surface expression profiles of GNNK- and GNNK+ c-KIT in FDC-P1 clones after correction for background levels. **B:** Comparison of c-KIT copy number previously obtained from saturation binding analysis in FDC-P1 (see reference Caruana *et al.*, 1999) with mean fluorescence intensity for the same populations. ΔMFI represents the change in mean fluorescence intensity after correction for background.

A

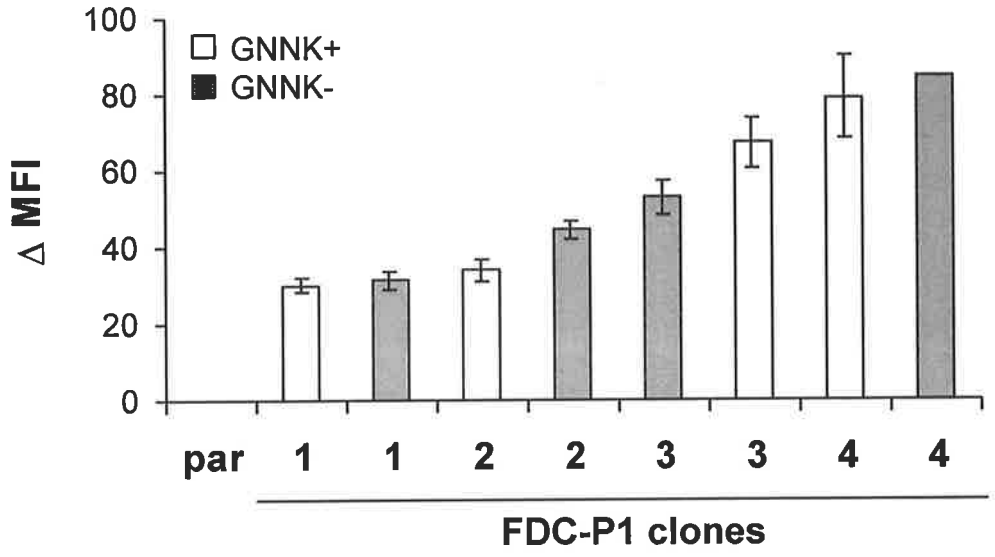
100
80
60
40
20
0
Δ MFI
GNNK+
GNNK-
par
1
1
2
2
3
3
4
4
FDC-P1 clones

B

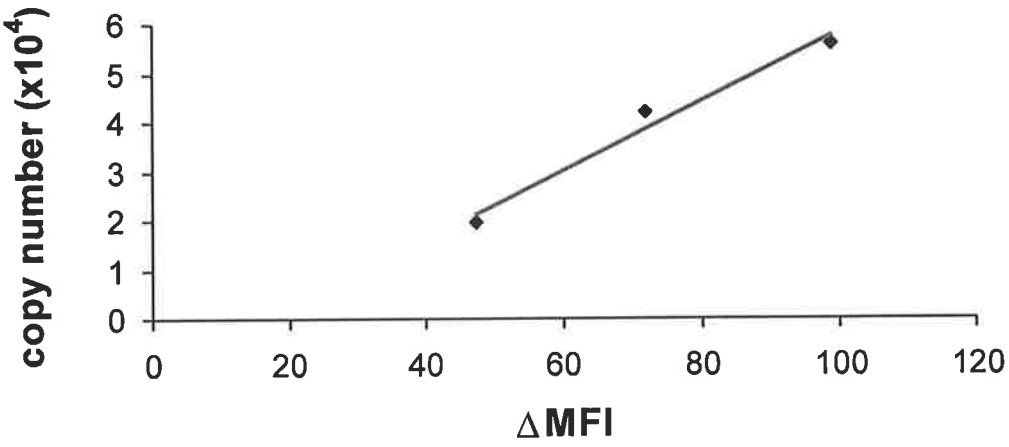
copy number (x10⁴)
6
5
4
3
2
1
0
0
20
40
60
80
100
120
ΔMFI

al., 1999). Good correlation (r = 0.99) was observed between mean fluorescence intensity and the saturation binding data obtained on FDC-P1 cells (Figure 3.1B). Using the linear equation obtained from Figure 3.1B, the copy number for each of the clones was determined to be in the range 1 - $5x10^4$ receptors per cell. This level is comparable to $2x10^4$ c-KIT molecules per cell expressed on CD34+ cells from human bone marrow (Cole *et al.*, 1996) and is therefore within the physiological range.

3.2.2. Analysis of c-KIT Expression by Immunohistochemistry.

The expression of c-KIT in each of the clones was further examined by immunohistochemistry using the APAAP technique (see section 2.3.4 for details). Both internal and external c-KIT was detected, unlike the indirect immunofluorescence assay, which only detected surface expressed c-KIT. Cells permeabilised with fixative were incubated with 1DC3 antibody or an isotype matched negative control, 1B5. Expression of c-KIT was indicated by red staining, with haematoxylin staining the nucleus purple (Figure 3.2). Parental FDC-P1 remained unstained with antibody to c-KIT (Figure 3.2A). Similarly no staining was observed with the negative control antibody for any of the clones (representative clone shown in Figure 3.2B). In each of the clones treated with antibody against c-KIT, faint red staining was observed. Two representative clones for each isoform are shown in Figure 3.2C - F.

3.2.3. Analysis of c-KIT Expression by Immunoprecipitation and Western Blot

Another technique employed to determine the expression of c-KIT within FDC-P1 clones was by immunoprecipitation and Western blot. c-KIT was immunoprecipitated from lysed FDC-P1 clones using a purified monoclonal antibody (KIT4.G12) directed against the extracellular region. Samples were electrophoresed under reducing conditions and transferred to membrane, which was probed with an antibody raised against the extracellular region of c-KIT, 1C1. Two bands were present after probing for c-KIT (Figure 3.3A). The first band at

Figure 3.2: Immunohistochemical analysis of c-KIT on representative FDC-P1 clones.

Cells cytocentrifuged onto glass slides were fixed and incubated with an anti-c-KIT antibody (1DC3) or an isotype matched control. Antibody bound to cells was detected using a bridging rabbit anti-mouse antibody, followed by APAAP complex. Cells were incubated with substrate resulting in c-KIT positive cells staining red and with haematoxylin counterstain staining the nucleus purple. Cells were visualised using an Olympus microscope and photographed with a 20x objective lens. **A:** Uninfected parental FDC-P1 stained with 1DC3. **B:** FDC-P1 GNNK-4 clone stained with isotype matched negative control. **C:** FDC-P1 GNNK+4 clone stained with 1DC3. **D:** FDC-P1 GNNK+1 clone stained with 1DC3. **E:** FDC-P1 GNNK-4 clone stained with 1DC3. **F:** FDC-P1 GNNK-2 clone stained with 1DC3.


A

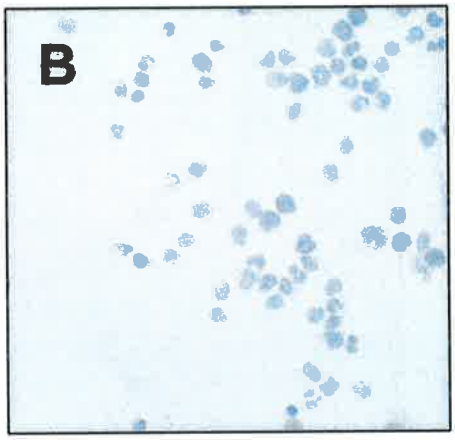
B

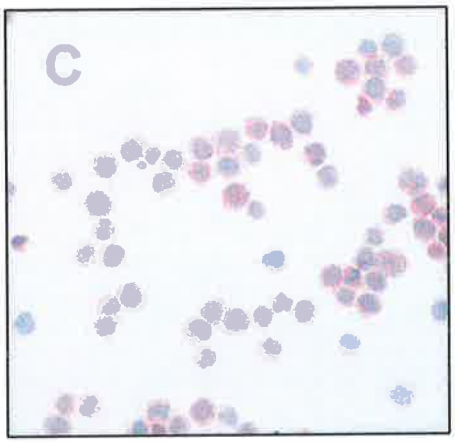
C

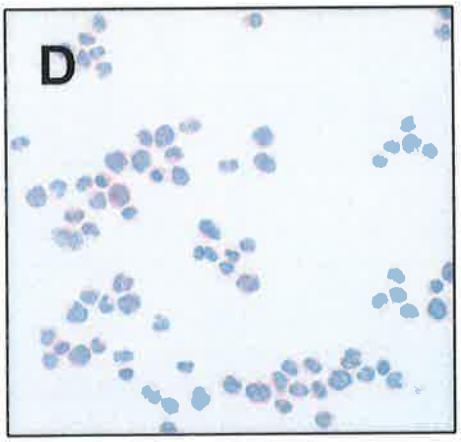
D

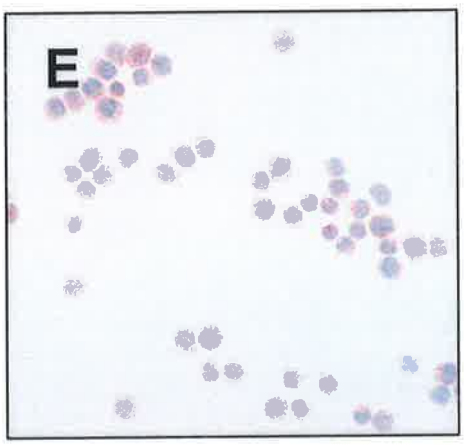
E

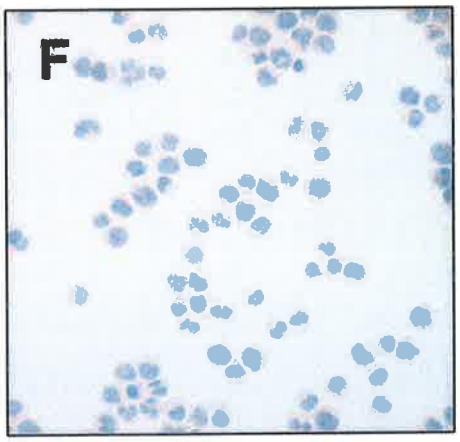
F

Figure 3.3: Detection of degraded c-KIT in FDC-P1.

A: Detection of c-KIT in FDC-P1 clones. Indicated FDC-P1 GNNK+ clones were starved of serum and factor for 2 hours and lysed at $1x10^7$/ml. Clarified lysates were immunoprecipitated with KIT4.G12 antibody and Protein A Sepharose for 2 hours and samples resolved by reduced SDS-PAGE. Proteins were transferred to PVDF and blotted for c-KIT with a murine monoclonal antibody, 1C1 and visualised by ECF on the FluorImager (Molecular Dynamics). **B:** Detection of surface expressed c-KIT by Western analysis. Cell surface biotinylation was performed on indicated FDC-P1 clones. Cells were then lysed, c-KIT immunoprecipitated and resolved by reduced SDS-PAGE. Proteins were transferred to PVDF and blotted for biotin using streptavidin conjugated to alkaline phosphatase or for c-KIT with 1C1 and visualised by ECF on the FluorImager. **C:** Use of additional protease inhibitors and different antibodies for the detection of c-KIT. FDC-P1 GNNK+1 clone was lysed in 1% NP40 with commercial protease inhibitor cocktail or with additional protease inhibitors (+) including 10 μg/ml aprotinin and leupeptin and 1 mM PMSF in the presence (+) or absence (-) of a caspase inhibitor, VAD-fmk. Blots were probed with 1C1 or a rabbit polyclonal antibody raised against the carboxy terminal region of c-KIT (C-ter c-KIT). Proteins were visualised by ECF on the FluorImager.

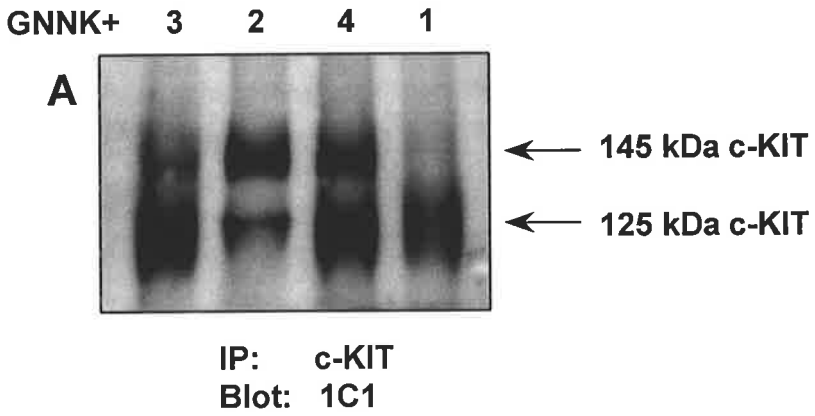
GNNK+ 3 2 4 1
A
145 kDa c-KIT
125 kDa c-KIT
IP: c-KIT
Blot: 1C1

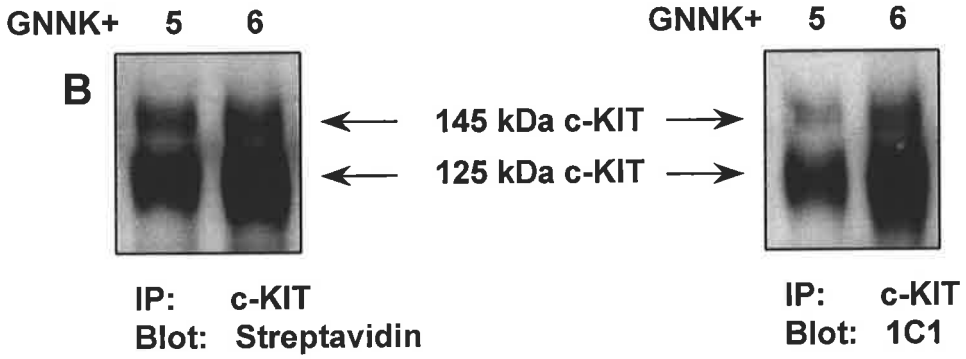
GNNK+ 5 6
B
145 kDa c-KIT
125 kDa c-KIT
IP: c-KIT
Blot: Streptavidin
GNNK+ 5 6
IP: c-KIT
Blot: 1C1

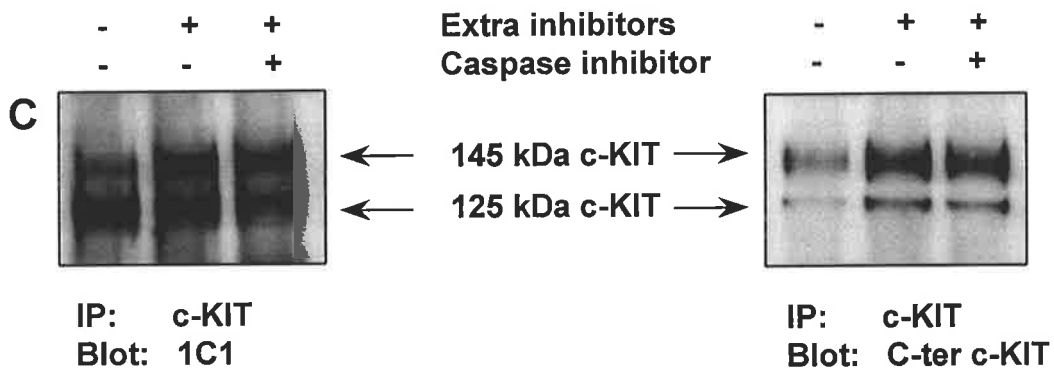
- + +
- - +
Extra inhibitors
Caspase inhibitor
- + +
- - +
C
145 kDa c-KIT
125 kDa c-KIT
IP: c-KIT
Blot: 1C1
IP: c-KIT
Blot: C-ter c-KIT

approximately 145 kDa represented fully glycosylated c-KIT, whereas the band at 125 kDa corresponded to the immature unglycosylated form (Figure 3.3A). Only the 145 kDa version of c-KIT is expressed on the surface since the immature form undergoes further glycosylation prior to its plasma membrane localisation (Yarden *et al.*, 1987). Surprisingly, there was great variation in the intensity of the 125 kDa band and a trend suggested that clones with increased surface expression had higher levels of the 125 kDa protein. This possibly suggested that varied intracellular pools of immature c-KIT existed in the clones, or that the 125 kDa protein was expressed on the surface, contributing to the immunofluorescence data.

To investigate if the 125 kDa protein could be expressed on the surface and therefore contribute to the immunofluorescence result, cell surface proteins were biotinylated (see section 2.7.2), cells lysed and c-KIT immunoprecipitated. Samples were electrophoresed under reducing conditions and transferred to membrane. The resultant duplicate blots were probed with streptavidin, to detect biotin or with an antibody against the extracellular region of c-KIT, 1C1 (Figure 3.3B). In two representative clones, biotinylation of the 125 kDa band was detected (Figure 3.3B). The biotinylated 125 kDa band was at an equivalent intensity to blots probed for c-KIT. These results suggested that the 125 kDa protein was present on the cell surface since it was biotinylated. As a control, antibodies specific for intracellular proteins (p85 and MAPK) were used to confirm only the surface of the cell had been biotinylated (data not shown).

It was surprising that the 125 kDa band was biotinylated since it is considered to be intracellular due to its partial maturation (Yarden *et al.*, 1987). Both antibodies used to detect c-KIT were raised against the extracellular domain, therefore it was possible that a portion of the 125 kDa band was a degradation product of c-KIT. To examine this further, c-KIT was immunoprecipitated with KIT4.G12 and blots were probed with either an antibody to the extracellular region of c-KIT, 1C1, or else a polyclonal antibody raised against the carboxy terminal tail of c-KIT (Figure 3.3C). Less 125 kDa c-KIT was detected when the antibody

generated against the intracellular domain was used as compared to 1C1, suggesting that a large portion of the 125 kDa band was a degraded extracellular fragment of c-KIT. To address this problem, the addition of increased protease inhibitors in the lysis buffer as well as the effect of a caspase inhibitor was analysed. The lysis buffer used for the previous experiment contained a commercial protease inhibitor cocktail (Roche Diagnostics, Mannheim, Germany, Cat. No. 1836145). The effect of 10 μg/ml leupeptin and aprotinin and 1 mM phenylmethylsulfonyl fluoride (PMSF) as included by Hu *et al.,* (1993) and/or a caspase inhibitor, 50 μM VAD.fmk (Calbiochem, San Diego, CA, Cat. No. 62 7610) in addition to the commercial protease inhibitor cocktail were compared. The addition of extra protease inhibitors resulted in increased amounts of the 145 kDa band with an associated decrease in the level of the 125 kDa band (Figure 3.3C). Blotting with the carboxy terminal antibody resulted in increased levels of the 145 kDa band in the presence of extra protease inhibitors (Figure 3.3C). The caspase inhibitor made little difference to the ratio of 145:125 kDa (Figure 3.3C). From these studies it can be concluded that degradation of c-KIT was a problem and this was addressed by the addition of extra protease inhibitors.

In order to compare the levels of functional c-KIT in each of the clones by Western blot analysis, it was decided that the lysis buffer containing extra protease inhibitors should be used in conjunction with antibody raised against the intracellular domain of c-KIT for blotting. To compare c-KIT protein levels between the clones, cells were lysed and lysates immunoprecipitated and blotted for c-KIT. No c-KIT was detected in parental FDC-P1 however it was present in FDC-P1 clones infected with c-KIT constructs (Figure 3.4A). Quantitation of the 145 kDa band was performed using ImageQuantTM software (Molecular Dynamics) and results were standardised to the number of cells in the lysates (Figure 3.4B). Little similarity in c-KIT expression was observed when the results from Western analysis were compared to the indirect immunofluorescence assay (Figure 3.4B). This may be partially due to the degradation problem identified in Figure 3.3.

Figure 3.4: Presence of c-KIT in FDC-P1 clones.

A: Detection of c-KIT expression by Western blot analysis. Cells starved of serum and factor for 2 hours were resuspended to $1x10^7$/ml and lysed in 1 ml of 1% NP40 in the presence of protease and phosphatase inhibitors. c-KIT was immunoprecipitated with 5 μg KIT4.G12 antibody and 25 μl Protein A Sepharose. Immunoprecipitates were resolved by reduced SDS-PAGE and proteins transferred to PVDF and probed for c-KIT using a commercial rabbit polyclonal antibody against the carboxy terminal tail. Primary antibody was detected with sheep anti-rabbit alkaline phosphatase and enzyme activity was visualised using ECF on the FluorImager. In the figure, par represents parental FDC-P1. **B:** Comparison of c-KIT detection techniques. Results from **A** were quantitated using ImageQuantTM software and expressed as a ratio of the number of cells present in the lysate. c-KIT levels detected by Western blot analysis (bar graph) were compared to the change in mean fluorescence intensity (ΔMFI) obtained from the indirect immunofluorescence assay see Figure 3.1 (line graph). Relative fluorescence units is represented by rfu.

A

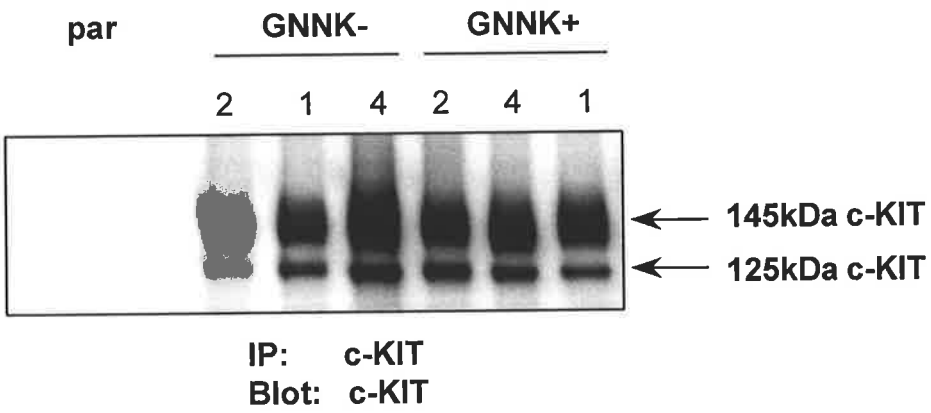
par
GNNK-
GNNK+
2 1 4 2 4 1
145kDa c-KIT
125kDa c-KIT
IP: c-KIT
Blot: c-KIT

B

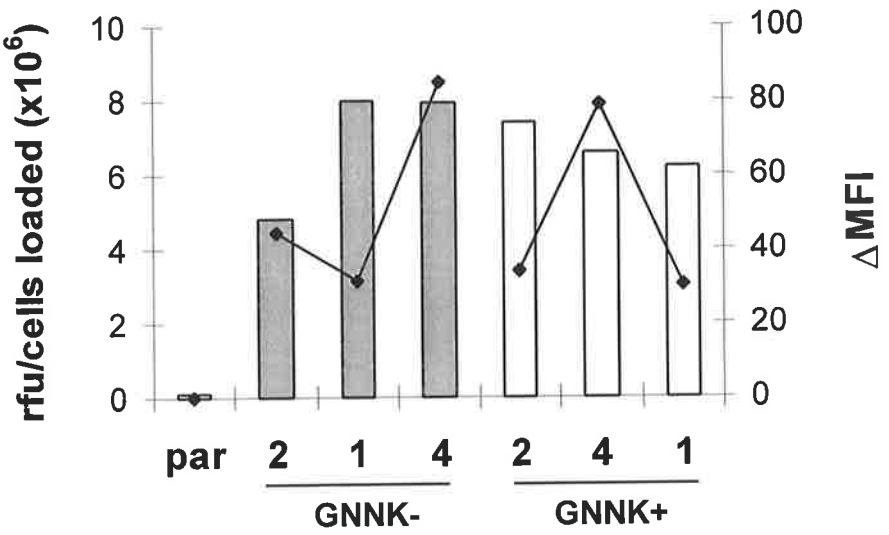
rfu/cells loaded (x10^6)
10
8
6
4
2
0
100
80
60
40
20
0
ΔMFI
par 2 1 4 2 4 1
GNNK-
GNNK+

3.3. GROWTH OF C-KIT EXPRESSING FDC-P1 CLONES IN HUSCF

FDC-P1 cells are dependent on muGM-CSF for growth. To determine if the expression of c-KIT could allow growth in huSCF, FDC-P1 clones were seeded at $5x10^4$/ml in either saturating levels of huSCF (100 ng/ml), muGM-CSF, or in the absence of factor and their growth assessed over three days by MTT assay (see section 2.5.2). Results confirmed that cells were factor dependent since no growth in the absence of factor was observed (Figure 3.5A and B). Only clones expressing c-KIT were capable of growth in huSCF (Figure 3.5C and D) confirming that this was due to the presence of introduced human c-KIT and not endogenous murine c-KIT. The expression of c-KIT did not alter growth in muGM-CSF since all clones grew to an equivalent extent as the parental control (Figure 3.5E and F). Thus, the introduction of both c-KIT isoforms into FDC-P1 allowed for growth in the presence of huSCF.

3.3.1. Effect of c-KIT Surface Expression on Growth in huSCF

Interestingly, the clones exhibited a range of growth in huSCF even though they grew at a consistent rate in muGM-CSF (Figure 3.5). Therefore, the relationship between the level of c-KIT expression (Figure 3.1A) and growth in huSCF was investigated (Figure 3.5). Linear regression analysis suggested a strong relationship between the two variables (r^2 = 0.97 and 0.99 for GNNK- and GNNK+ respectively) such that an increase in surface expression resulted in an increase in huSCF mediated growth (Figure 3.6A). Comparing growth in muGM-CSF to c-KIT surface expression did not result in any relationship indicating that the introduction of c-KIT did not disrupt normal cellular growth (Figure 3.6B).

Growth in huSCF was dependent on the level of surface expression for both isoforms of c-KIT. Interestingly, at low levels of c-KIT expression, growth in huSCF was equivalent, however at higher levels, a difference was observed with the GNNK- expressing clones requiring less surface expression for an equivalent growth response as compared to GNNK+

Figure 3.5: Cellular growth in the presence of huSCF.

Uninfected FDC-P1 or FDC-P1 clones expressing c-KIT isoforms, seeded at a density of $5x10^4$/ml were assessed for total number of cells by MTT assay at days 0, 1, 2 and 3 in the absence of factor **(A, B)**, in the presence of 100 ng/ml huSCF **(C, D)** or in the presence of muGM-CSF **(E, F).** Growth analysed by absorbance at 490 nm from a triplicate experiment is shown as mean ± standard error of the mean (SEM). Due to overgrowth, data for muGM-CSF cultures at day 3 have been omitted.

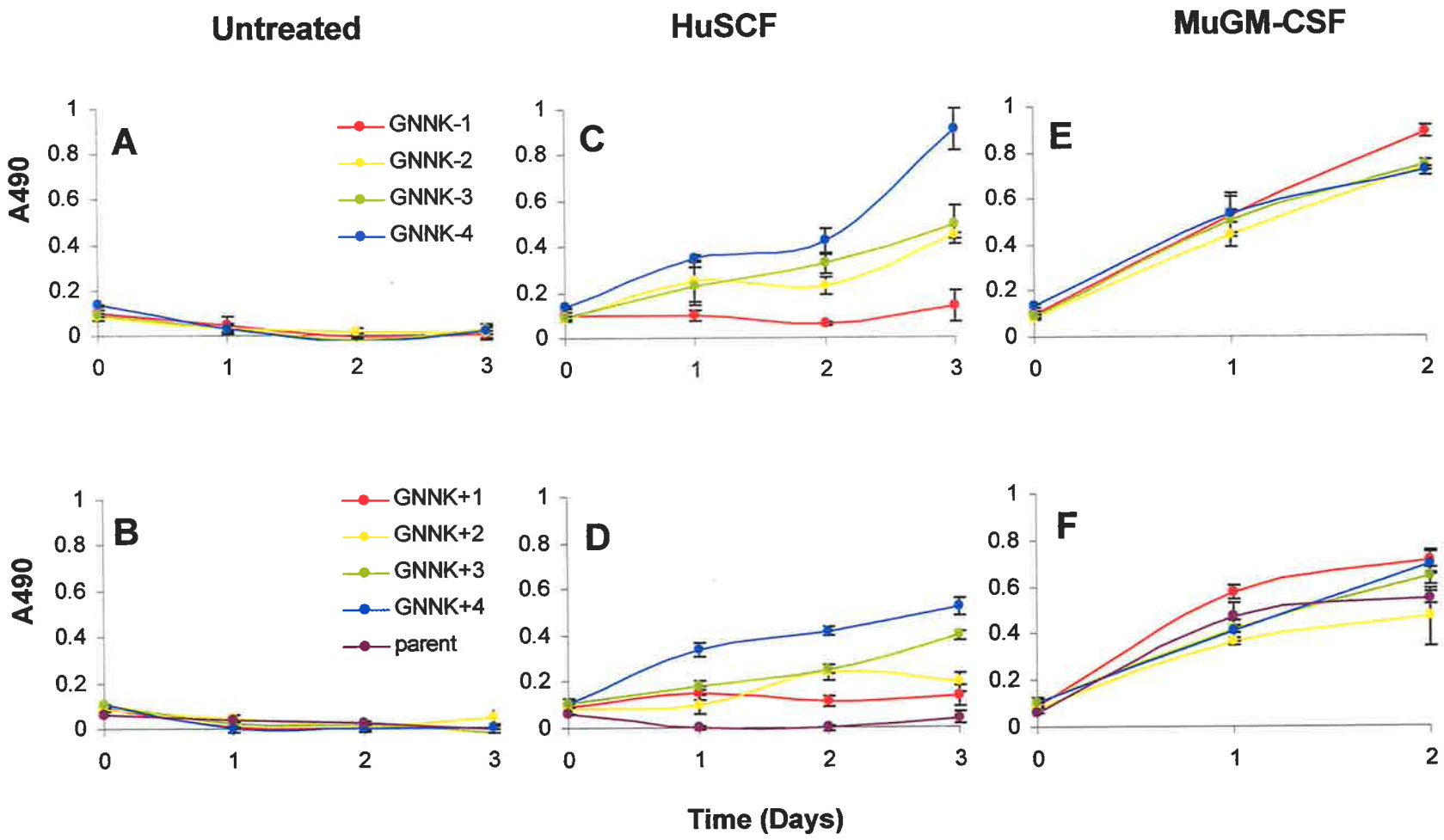
Untreated
HuSCF
MuGM-CSF
A
B
C
D
E
F
A490
GNNK-1
GNNK-2
GNNK-3
GNNK-4
GNNK+1
GNNK+2
GNNK+3
GNNK+4
parent
Time (Days)

Figure 3.6: Comparison of cellular growth in huSCF or muGM-CSF to surface expression.

Cellular growth data (A490) from Figure 3.5 were plotted against surface expression of c-KIT (change in mean fluorescence intensity, ΔMFI) (Figure 3.1). Cells were cultured in 100 ng/ml huSCF **(A)** or muGM-CSF **(B)** for 3 days. Points plotted were mean ± SEM for cellular growth and mean ± SD for surface expression. Solid line (GNNK+ c-KIT) and hashed line (GNNK- c-KIT) shown in **A** were determined by linear regression analysis. Statistical significance ($\alpha < 0.05$) is represented by a *.

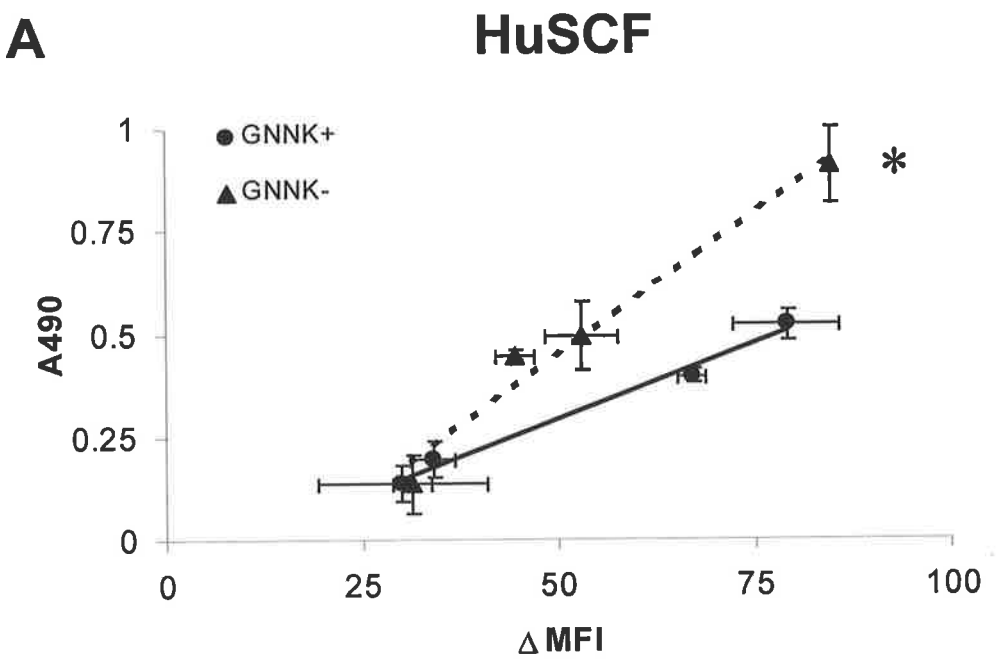
A
HuSCF
GNNK+
GNNK-
*
A490
1
0.75
0.5
0.25
0
0
25
50
75
100
Δ MFI

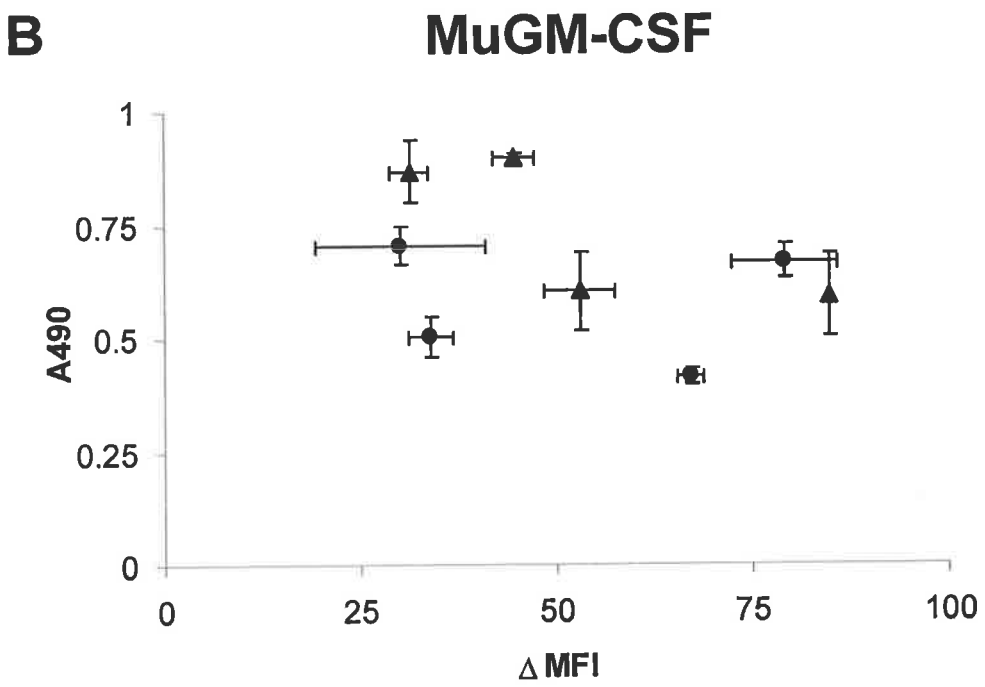
B
MuGM-CSF
A490
1
0.75
0.5
0.25
0
0
25
50
75
100
Δ MFI

expressing clones. Linear regression was used to calculate the slope estimate for each line. A two sample t-test on these values allowing for adjusted expression for degrees of freedom indicated that the slope for the GNNK- clones was statistically higher than that for GNNK+ clones ($p = 0.03$). Therefore growth in huSCF was dependent on surface expression however the relationship between these two variables was different for the c-KIT isoforms.

To determine the contribution of proliferation and survival to the growth advantages caused by increased surface expression, cellular membranes were stained with a lipophilic dye, PKH-26 (see section 2.5.3 for details). The number of divisions undergone by viable cells could be traced based on the amount of dye present on the cells since the dye is distributed equally among the daughter cells. Cellular survival was calculated based on the total yield of fluorescence. Stained cells were seeded at $1x10^5$/ml in either saturating levels of huSCF (100 ng/ml) or muGM-CSF and were harvested after two days culture. Confirming results from the cell growth assay, the total cell yield correlated with surface expression ($r = 0.9$) (data not shown). Proliferation and survival in huSCF were also dependent on c-KIT expression ($r^2 > 0.7$) (Figure 3.7). With changes in surface expression levels, less difference in proliferation was observed as compared to survival, which ranged from 15 to 70%. In these experiments, the differences in the slope of the regression lines for cells expressing the two isoforms were not significant as shown by a two sample t-test allowing for adjusted degrees of freedom ($p > 0.05$). Even though statistical significance was not observed, the trend was similar to results obtained from the MTT assay (Figure 3.6).

3.3.2. Proliferation and Survival in Limiting Concentrations of huSCF

In the previous section, analysis of proliferation and survival were performed using saturating levels of huSCF. To determine if titration of huSCF differentially affected the isoforms, a PKH assay was performed as detailed in section 3.3.1. Cells were seeded at $1x10^5$/ml in sub-saturating levels of huSCF and cultured for 48 hours. After 24 hours, a

Figure 3.7: Comparison of proliferation and survival in huSCF or muGM-CSF to surface expression.

Proliferation **(A, C)** or survival **(B, D)** in either 100ng/ml huSCF **(A, B)** or muGM-CSF **(C, D)** as determined by PKH assay after 2 days culture were plotted against surface expression (ΔMFI, change in mean fluorescence intensity) (Figure 3.1). Points plotted were mean ± SEM for proliferation and survival and mean ± SD for surface expression.

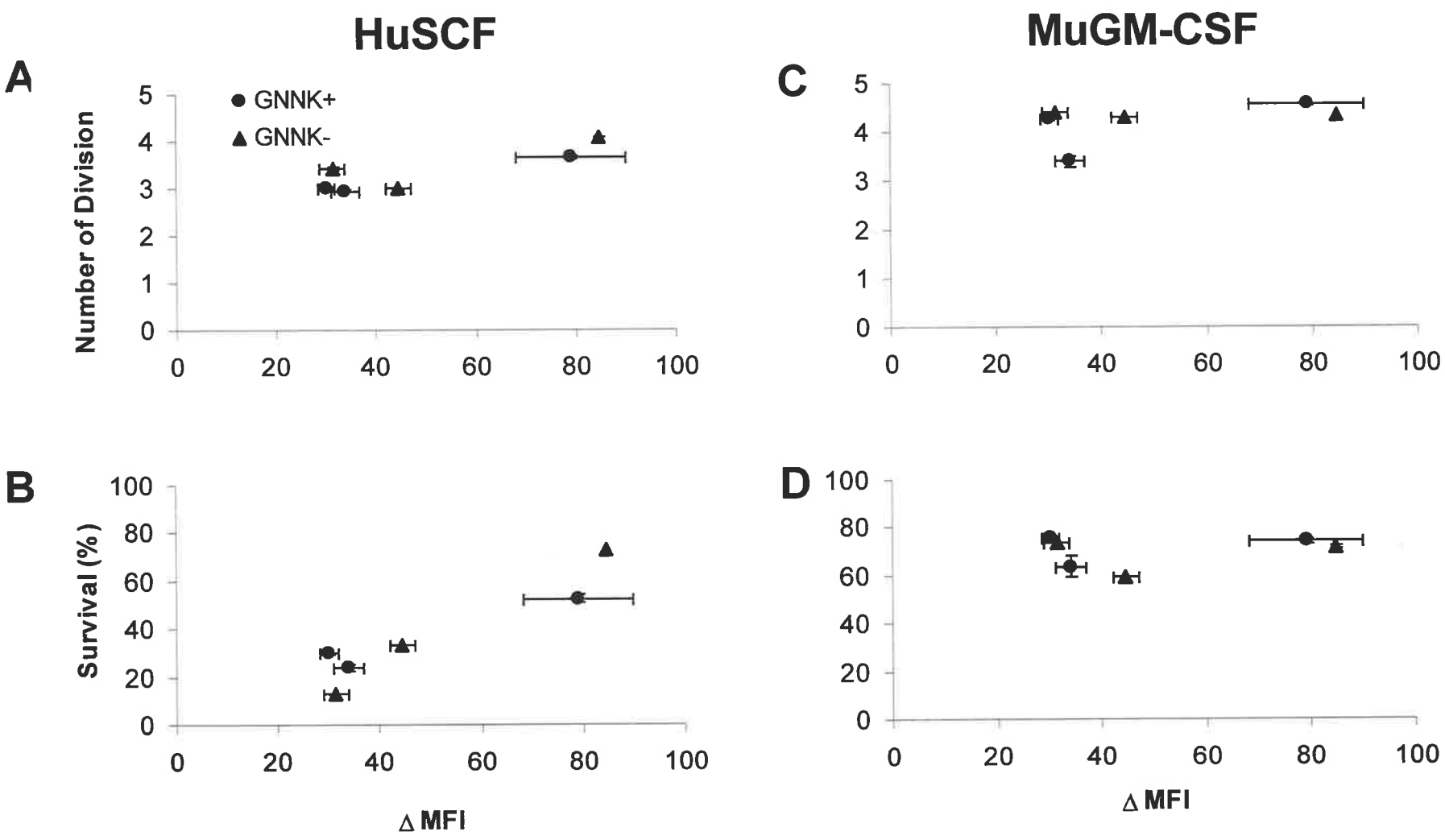
HuSCF
MuGM-CSF
A
B
C
D
GNNK+
GNNK-
Number of Division
Survival (%)
Δ MFI
Δ MFI
0
1
2
3
4
5
0
20
40
60
80
100

half-medium change was performed with medium of the appropriate concentration of huSCF to maintain limiting concentrations. Three clones paired for surface expression of GNNK- and GNNK+ c-KIT were analysed (GNNK-1 paired with GNNK+1, GNNK-2 paired with GNNK+2 and GNNK-4 paired with GNNK+4). These pairs of clones were used in all subsequent experiments. Data of proliferation, survival and total cells obtained are presented in Figure 3.8. The total cell yield varied substantially between the clones being dependent on the surface expression (Figure 3.8A). The calculated level of huSCF giving half-maximal cell yield did not appear to be dependent on the level of c-KIT, nor was it dependent on the isoform expressed (average values for GNNK- and GNNK+ clones were 8.5 ± 2.6 ng/ml and 12.4 ± 2.4 ng/ml with $p = 0.17$). For both isoforms, survival appeared to be more dependent on the concentration of huSCF as compared to proliferation as measured by the number of divisions undergone by surviving cells. For example, at low levels of huSCF, proliferation was near maximal whereas survival was substantially decreased. Overall, the concentration of huSCF required for a half-maximal response did not seem to be influenced by the c-KIT isoform or receptor level. However, consumption of huSCF at the lower levels during the assay could have masked any differences.

3.4. KINETICS OF SCF MEDIATED ACTIVATION OF C-KIT ISOFORMS

Interestingly, the above studies showed that the GNNK- isoform supported cell growth to a greater extent than the GNNK+ isoform in huSCF. Similar results were obtained in NIH-3T3 fibroblasts (Caruana *et al.*, 1999), therefore it was of interest to investigate the biochemical events following stimulation with huSCF in FDC-P1. Analysis of receptor phosphorylation, degradation and ubiquitination following huSCF treatment of cells expressing c-KIT isoforms were carried out by immunoprecipitation and Western blot (see section 2.7). FDC-P1 clones starved of serum and growth factor for 2 hours were stimulated with 100 ng/ml huSCF in triplicate and lysed. Lysates were immunoprecipitated with a

Figure 3.8: Effect of huSCF titration on cell yield, proliferation and survival.

FDC-P1 cells infected with c-KIT constructs were seeded at a density of $1x10^5$/ml and assessed for cell yield, proliferation and survival as described in section 2.5.3 in sub-optimal levels of huSCF. Cells were harvested after 48 hours culture with a half-medium change performed after 24 hours culture to aid in the maintenance of sub-optimal concentrations of huSCF. Data from triplicate experiments are represented as mean ± SEM. **A:** The total number of viable cells present. **B:** The average number of cell divisions of viable cells. **C:** The percentage of fluorescent yield in the viable population. Data points for the number of divisions where less than 1000 viable cells remained were considered unrealistic and have been omitted.

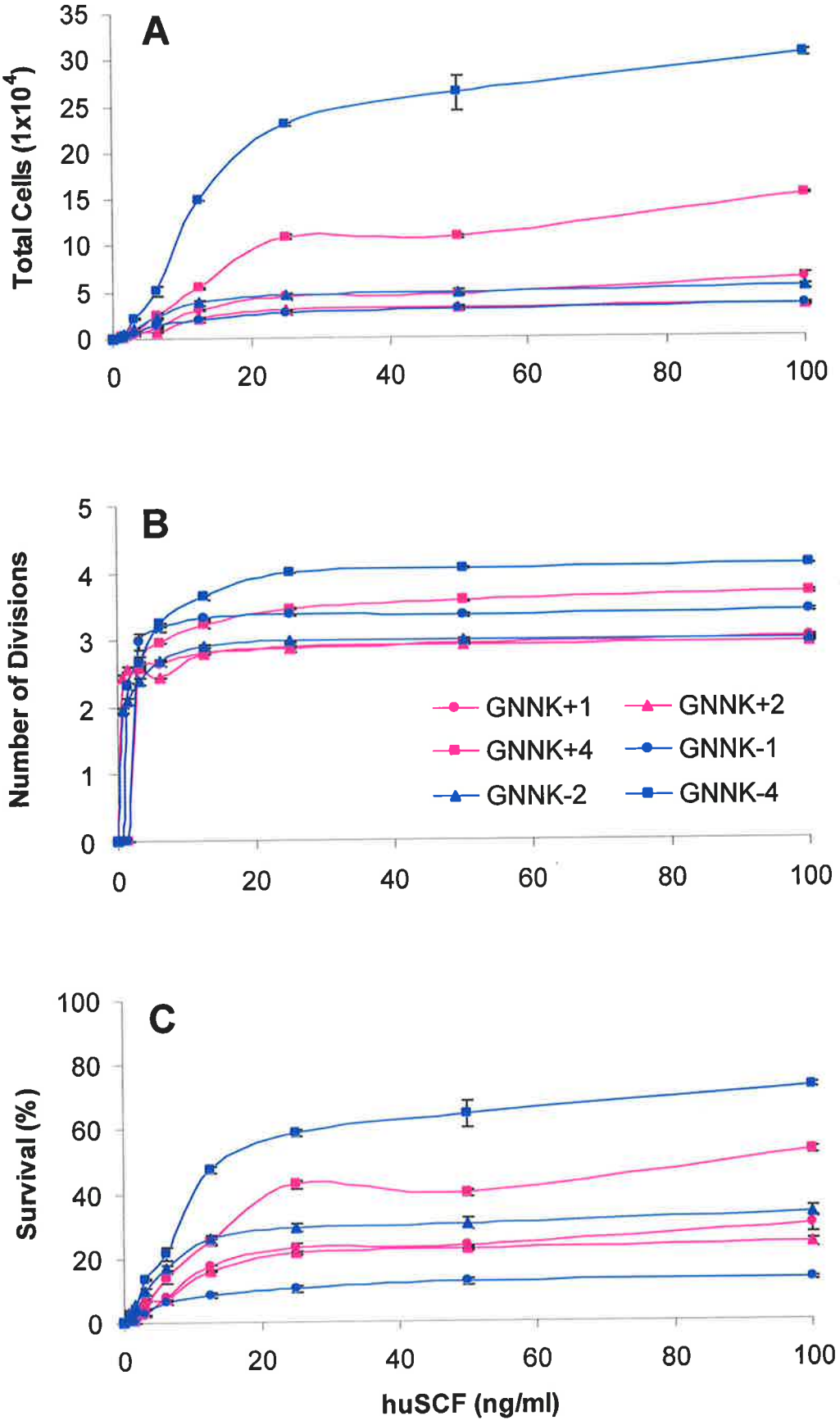
A
Total Cells (1x10^4)
35
30
25
20
15
10
5
0
0
20
40
60
80
100
B
Number of Divisions
5
4
3
2
1
0
GNNK+1
GNNK+2
GNNK+4
GNNK-1
GNNK-2
GNNK-4
C
Survival (%)
100
80
60
40
20
0
huSCF (ng/ml)

purified monoclonal antibody against the extracellular region of c-KIT (KIT-4.G12) and Protein A Sepharose. Immunoprecipitates were resolved on 8% polyacrylamide gels and proteins transferred to membrane. Triplicate membranes were used to detect phosphotyrosine, total c-KIT and p85, or ubiquitin. A separate membrane was used for each detection method because signal is diminished with stripping and reprobing (T. Cambareri, personal communication).

As a control standard for each of the blots, cells of the human megakaryocytic cell line MO7e, which expresses high levels of c-KIT were treated with or without huSCF for 2.5 minutes. Standard aliquots of immunoprecipitates equivalent to $1.8x10^6$ cells were run on each gel to serve as an internal standard to control for variation in transfer and detection processes.

3.4.1. Phosphorylation of c-KIT

In response to huSCF, c-KIT is phosphorylated on tyrosine residues (Rottapel *et al.*, 1991). The phosphorylation of c-KIT isoforms was analysed after varying duration in huSCF and the results are presented in Figure 3.9A and B for a representative GNNK- and GNNK+ clone respectively. Minimal or no phosphorylation of c-KIT was observed for either isoform in the absence of huSCF. In the presence of huSCF both isoforms were rapidly phosphorylated to levels that could be detected within 1 minute. Peak phosphorylation for GNNK- and GNNK+ isoforms occurred after 2.5 and 5 minutes of huSCF stimulation respectively.

The intensity of phosphorylation varied greatly between the two isoforms. Figure 3.9c shows the average phosphorylation of three clones for each isoform as a ratio to the amount of c-KIT present (taken from Figure 3.10). These results indicated that GNNK- c-KIT was phosphorylated six times as much as the GNNK+ isoform when peak levels were compared. The average relative ratio of phosphorylated to total c-KIT for the GNNK- isoform at peak

Figure 3.9: Phosphorylation of c-KIT isoforms in response to huSCF stimulation.

FDC-P1 clones expressing GNNK+/- c-KIT isoforms were starved of serum and factor for 2 hours, stimulated with 100 ng/ml of huSCF at a density of $1x10^7$/ml and lysed. Clarified lysates were immunoprecipitated with 5 μg/ml KIT4.G12 antibody and 25 μl of Protein A Sepharose for 2 hours. Washed immunoprecipitates were loaded onto 8% gels, electrophoresed, transferred to membrane and probed with two antibodies to phosphotyrosine (see table 2.2). Primary antibody was detected with sheep anti-mouse alkaline phosphatase conjugate. Alkaline phosphatase activity was visualised using ECF and FluorImager analysis. Included on the gels was an aliquot of c-KIT immunoprecipitate from MO7e cells that had been treated with (+) or without (-) 100 ng/ml huSCF for 2.5 minutes. **A:** Data from a representative GNNK- clone, GNNK-2. **B:** Data from a representative GNNK+ clone, GNNK+2. **C:** Quantitation of c-KIT phosphorylation in FDC-P1 clones. Results from each of the clones was quantitated using ImageQuantTM software, standardised against the MO7e controls loaded onto the gel and then further standardised to the amount of c-KIT present (Figure 3.10). Results are expressed as an average of the three clones analysed for each isoform, shown as mean ± SEM. Statistical significance ($\alpha < 0.05$) between peak phosphorylation values is shown by a *.

A

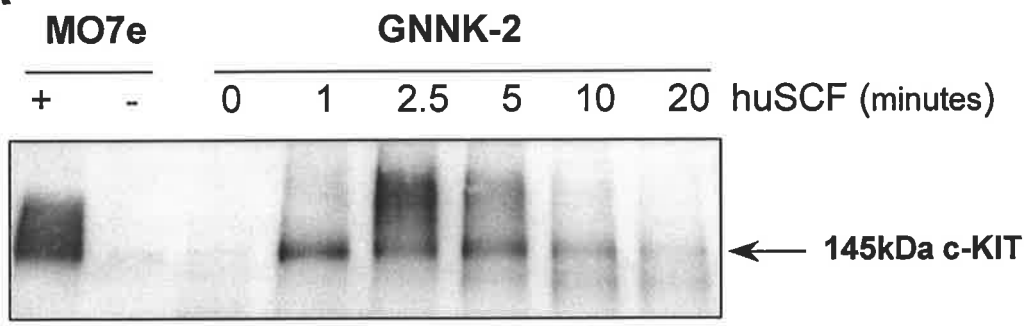

IP: c-KIT
Blot: Phosphotyrosine

B

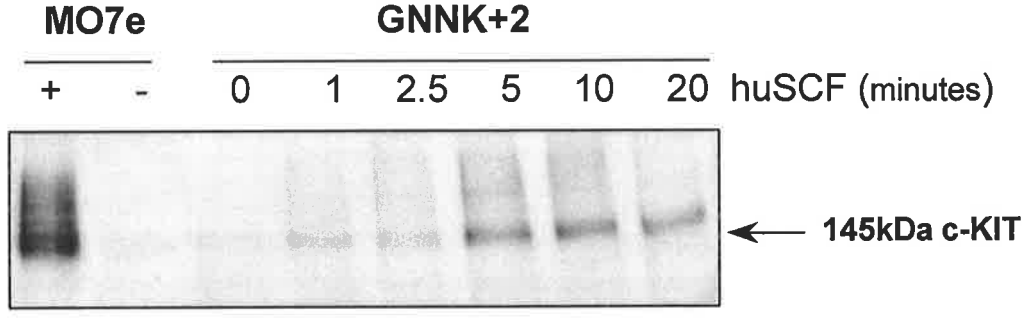

IP: c-KIT
Blot: Phosphotyrosine

C

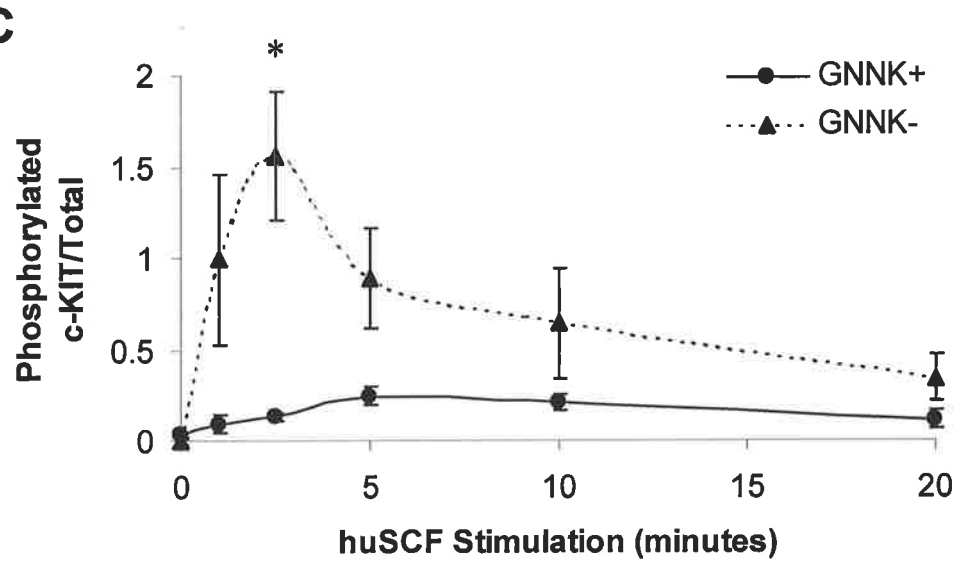

levels was 1.5 whereas peak phosphorylation for the GNNK+ isoform at 5 minutes was only 0.24. Peak phosphorylation of the GNNK- isoform was significantly higher than the GNNK+ isoform ($p = 0.02$).

The duration of c-KIT phosphorylation was also different between the two isoforms. Phosphorylation of the GNNK- isoform appeared to be transient, with less than a quarter of phosphorylated c-KIT remaining after 20 minutes huSCF stimulation. On the other hand, huSCF stimulation of the GNNK+ isoform for 20 minutes resulted in about 50% reduction in c-KIT phosphorylation at peak levels. Therefore the kinetics and intensity of c-KIT phosphorylation differed between the two isoforms of c-KIT after huSCF stimulation.

3.4.2. Degradation of c-KIT

To determine the degradation of c-KIT over a time course of huSCF stimulation, blots were probed with a commercial rabbit polyclonal antibody directed against the carboxy terminal tail of c-KIT (see Table 2.2). Results shown in Figure 3.10A and B are representative of a GNNK- and GNNK+ clone respectively. c-KIT was detected in the presence and absence of huSCF. With increasing duration of huSCF treatment, levels of the mature 145 kDa band of c-KIT decreased for the GNNK- isoform, however this was not evident upon stimulation of the GNNK+ isoform. Upward smearing of the 145 kDa band was evident as early as 1 minute after huSCF stimulation for the GNNK- isoform and persisted throughout the time course. It was also noticeable in cells expressing GNNK+ however not as prominent. This smearing reflects ubiquitination of c-KIT as ubiquitin groups are added resulting in an increase in the molecular weight (Miyazawa *et al.*, 1994).

Standardisation of c-KIT levels as a ratio to the MO7e controls loaded on each blot enabled comparisons between each of the clones. Further, standardisation of the differences in c-KIT expression levels exhibited by the clones was performed by expressing the results as a ratio of c-KIT levels in the absence of huSCF (Figure 3.10C). An initial slight increase in

Figure 3.10: Degradation of c-KIT in response to huSCF stimulation.

FDC-P1 clones were treated as described in Figure 3.9. Membranes were probed using an antibody against the carboxy terminal tail of c-KIT and detected with sheep anti-rabbit immunoglobulin alkaline phosphatase conjugate. Alkaline phosphatase activity was visualised using ECF and FluorImager analysis. **A:** Data from a representative GNNK- clone, GNNK-2. **B:** Data from a representative GNNK+ clone, GNNK+2. **C:** Quantitation of c-KIT in FDC-P1 clones. Results for each of the clones were quantitated using ImageQuantTM software, standardised against the MO7e control loaded onto the gel and further standardised to the level of c-KIT in the absence of huSCF. Results are expressed as an average of three clones for each isoform, shown as mean ± SEM.

A

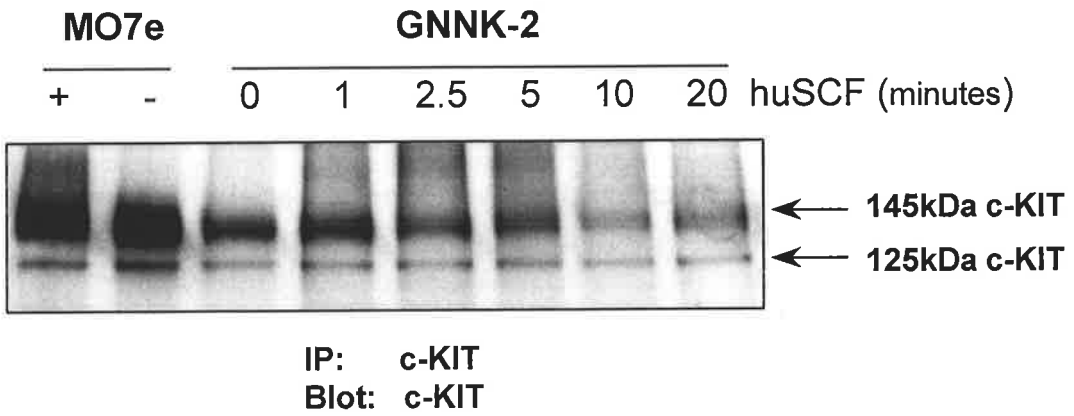
MO7e
GNNK-2
+
-
0
1
2.5
5
10
20
huSCF (minutes)
145kDa c-KIT
125kDa c-KIT
IP: c-KIT
Blot: c-KIT

B

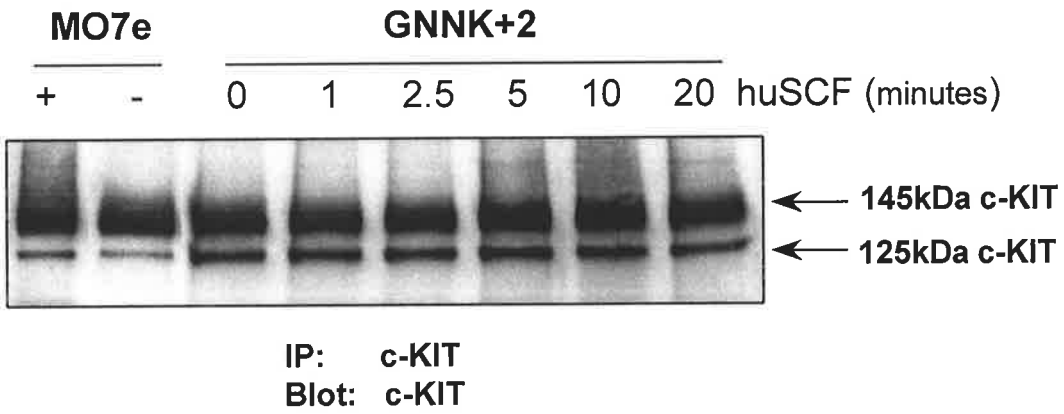
MO7e
GNNK+2
+
-
0
1
2.5
5
10
20
huSCF (minutes)
145kDa c-KIT
125kDa c-KIT
IP: c-KIT
Blot: c-KIT

C

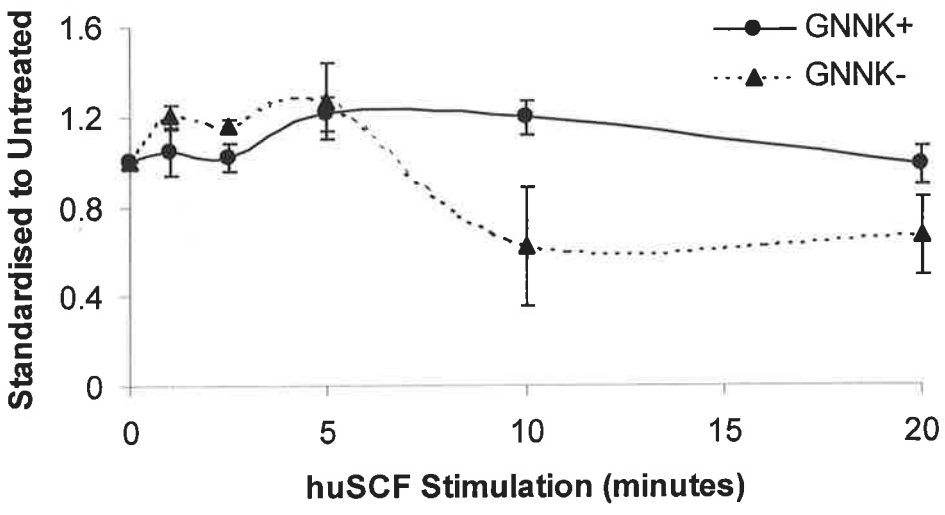
Standardised to Untreated
1.6
1.2
0.8
0.4
0
0
5
10
15
20
huSCF Stimulation (minutes)
GNNK+
GNNK-

the levels of c-KIT was regularly observed possibly due to the immunoprecipitation being more efficient in the presence of huSCF when c-KIT is dimerised. With increasing huSCF stimulation, the level of c-KIT decreased; this was more noticeable for the GNNK- isoform where only 60% of c-KIT remained after treatment with huSCF for 10 minutes. No degradation of the GNNK+ isoform was observed since levels at 20 minutes were comparable to that observed in resting cells. The increased degradation of the GNNK- isoform relative to the GNNK+ isoform followed the same pattern in NIH-3T3 cells (Caruana *et al.*, 1999) although in this instance the difference was not statistically significant ($p = 0.1$).

3.4.3. Ubiquitination of c-KIT

The upward smearing observed in the c-KIT blots (Figure 3.10) was thought to be due to ubiquitination, therefore Western blotting with anti-ubiquitin antibody was carried out after stimulation of cells with huSCF. Results indicated that both isoforms of c-KIT were ubiquitinated (Figure 3.11). Ubiquitination of GNNK- and GNNK+ c-KIT was present after 2.5 and 5 minutes respectively. Quantitative comparisons of c-KIT ubiquitination were not performed because the intensity detected was too low for quantitation and further it was not present in all MO7e samples.

3.5. HuSCF Induced Internalisation of c-KIT

Due to the different kinetics observed in phosphorylation and degradation of the c-KIT isoforms, it was of interest to analyse the rate of internalisation induced by huSCF and this was done by flow cytometry. Cells starved of serum and factor were stimulated with either huSCF or muGM-CSF at 37°C for an indicated duration. Reactions were terminated by incubation on ice and the addition of an equal volume of ice cold PBS/BSA with 0.2% Az. Samples were labelled for c-KIT using indirect immunofluorescence and analysed by flow

Figure 3.11: Ubiquitination of c-KIT in response to huSCF.

FDC-P1 clones were treated and immunoprecipitated as described in Figure 3.9. Membranes were blotted using a mouse monoclonal antibody raised against ubiquitin that was detected with anti-mouse alkaline phosphatase. Alkaline phosphatase activity was visualised using ECF and FluorImager analysis. **A:** Data from a representative GNNK- clone, GNNK-2. **B:** Data from a representative GNNK+ clone, GNNK+2.

A

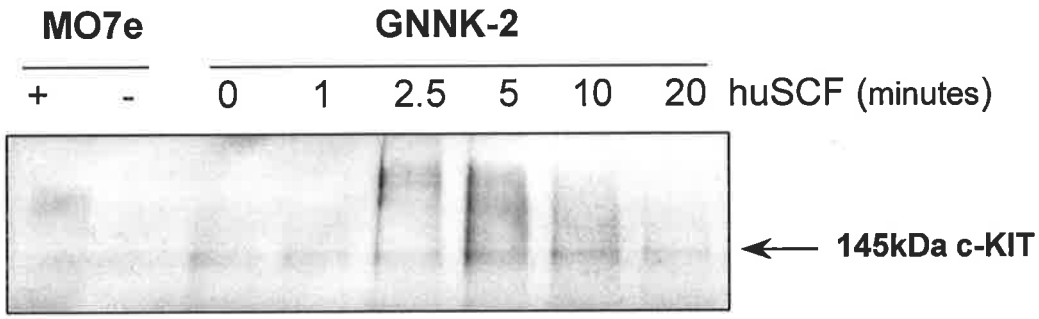

IP: c-KIT
Blot: Ubiquitin

B

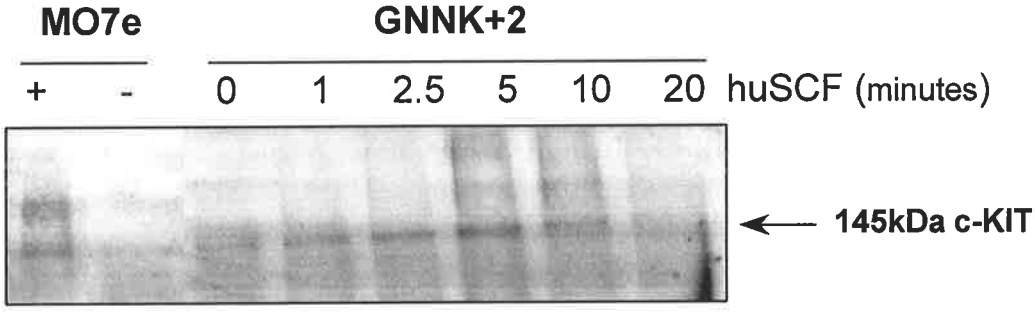

IP: c-KIT
Blot: Ubiquitin

cytometry. Antibodies used were 1DC3, an antibody to c-KIT and the isotype matched negative control, 1B5.

To determine the inhibition in antibody binding (1DC3) due to the presence of huSCF, a portion of cells were incubated on ice in DMEM with 0.1% Az prior to the addition of huSCF or muGM-CSF. The reaction was allowed to proceed for 5 or 30 minutes and then terminated by the addition of an equal volume of ice cold PBS/BSA/Az. This was performed in triplicate at both time points. The inhibition in antibody binding due to the presence of huSCF was calculated by expressing c-KIT levels in the presence of huSCF as a fraction of that in muGM-CSF. The duration in huSCF did not affect the inhibition in antibody binding. Averaging the results from the triplicate experiments at both time points for the three clones indicated that huSCF inhibited binding of 1DC3 by about 20%. The inhibition was not isoform specific with residual binding for GNNK- and GNNK+ at 82.9% ± 5.4 and 80% ± 4.4 respectively. This decrease in 1DC3 binding in the presence of huSCF supports existing data (Aylett *et al.*, 1995) and is not surprising since huSCF binds to domain 1 - 3 of c-KIT and 1DC3 binds to domain 1.

Data from the indirect immunofluorescence assay are presented in Figure 3.12A and B for a representative GNNK+ and GNNK- clone and shows that increased duration in huSCF resulted in decreased c-KIT surface expression. The GNNK- isoform appeared to internalise to a greater extent as compared to GNNK+ c-KIT expressing cells. To enable comparisons, results were expressed as a percentage of c-KIT remaining on the surface (Figure 3.12C). In the absence of huSCF, the mean fluorescence intensity after correction for background was taken as 100%. For huSCF stimulated time points, the inhibition in antibody binding was taken into account, therefore, values were expressed as a fraction of c-KIT surface expression when cells were incubated with huSCF on ice in the presence of Az. HuSCF induced rapid internalisation of GNNK- as compared to GNNK+ c-KIT with half-maximal internalisation occurring at 2.5 and 10 minutes respectively (Figure 3.12C). The GNNK- isoform was

Figure 3.12: Internalisation of c-KIT isoforms in response to huSCF.

Cells starved of serum and factor for 2 hours were stimulated with huSCF at 37°C. Reactions were terminated at various time points by incubation on ice and the addition of an equal volume of ice cold PBS/BSA with 0.2% Az. Samples were labelled for c-KIT using indirect immunofluorescence and analysed by flow cytometry. **A:** Primary data from a representative GNNK- clone, GNNK-2 showing the amount of surface c-KIT after huSCF stimulation. **B:** Primary data from a representative GNNK+ clone, GNNK+2 showing the amount of surface c-KIT after huSCF stimulation. **C:** Changes in c-KIT surface expression in the presence of huSCF or muGM-CSF. Average ± SEM of three clones after correction for decreased antibody binding in the presence of huSCF and muGM-CSF. Results are expressed as a percentage of c-KIT remaining on the surface after various times of huSCF and muGM-CSF stimulation. In the Figure, SCF represents huSCF while GM represents muGM-CSF. Statistical significance ($\alpha < 0.05$) between GNNK- and GNNK+ c-KIT expressing cells in the presence of huSCF is shown by a *.

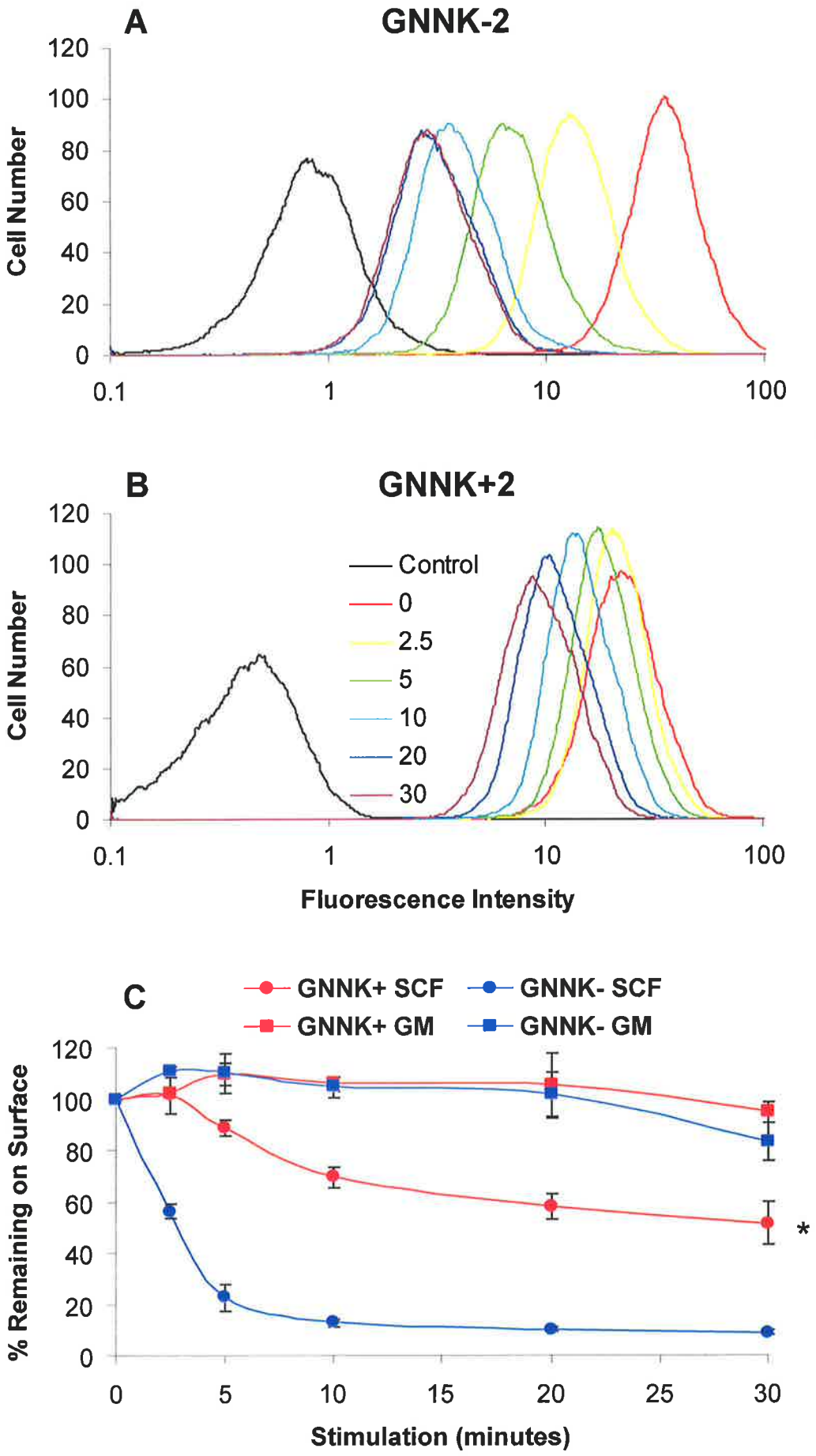
A
GNNK-2
Cell Number
120
100
80
60
40
20
0
0.1
1
10
100
B
GNNK+2
Control
0
2.5
5
10
20
30
Fluorescence Intensity
C
GNNK+ SCF
GNNK- SCF
GNNK+ GM
GNNK- GM
% Remaining on Surface
Stimulation (minutes)
0
5
10
15
20
25
30
*

internalised to a greater extent as compared to the GNNK+ isoform with statistical significance at each time point of huSCF stimulation ($p \leq 0.011$). The addition of muGM-CSF to the cells did not induce internalisation of c-KIT (Figure 3.12C) indicating this was huSCF specific. Therefore huSCF induced more rapid and extensive internalisation of the GNNK- isoform as compared to the GNNK+ isoform as was previously shown in NIH-3T3 fibroblasts (Caruana *et al.*, 1999; Voytyuk *et al.*, 2003).

The parameters of degradation and internalisation in response to huSCF were compared. As might be expected, internalisation preceded degradation for both isoforms of c-KIT (Figure 3.13).

3.6. Activation of Substrates Downstream of c-KIT

3.6.1. Association of PI 3-K to c-KIT

PI 3-K rapidly associates to c-KIT upon stimulation with huSCF as detected by its presence in c-KIT immunoprecipitates (Caruana *et al.*, 1999; Shearman *et al.*, 1993). Its association has been localised in the kinase insert to residues Y719 and Y721 of murine and human c-KIT respectively (Serve *et al.*, 1994). To examine the association kinetics of PI 3-K with c-KIT isoforms after huSCF stimulation, c-KIT immunoprecipitates were resolved by SDS-PAGE under reducing conditions, transferred to membrane and probed with an antibody against the p85 adaptor subunit of PI 3-K. Examples of results from representative GNNK- and GNNK+ clones are shown in Figure 3.14A and B respectively. The presence of p85 in c-KIT immunoprecipitates was detected in all clones after huSCF stimulation however, in its absence, only negligible amounts of p85 were associated.

To standardise results, p85 was expressed as a fraction of the level of c-KIT immunoprecipitated and an average from the three clones was calculated (Figure 3.14C). Upon huSCF stimulation, p85 was rapidly recruited to the GNNK- c-KIT isoform, with levels

Figure 3.13: Comparison of internalisation and degradation in response to huSCF stimulation.

Quantitation of results from the degradation of c-KIT as detected by Western blot analysis (Figure 3.10) was compared to levels of c-KIT remaining on the surface after huSCF stimulation (Figure 3.12). In each case, results are expressed as a percentage of the initial value. **A:** Mean ± SEM for three GNNK- clones analysed. **B:** Mean ± SEM for three GNNK+ clones analysed.

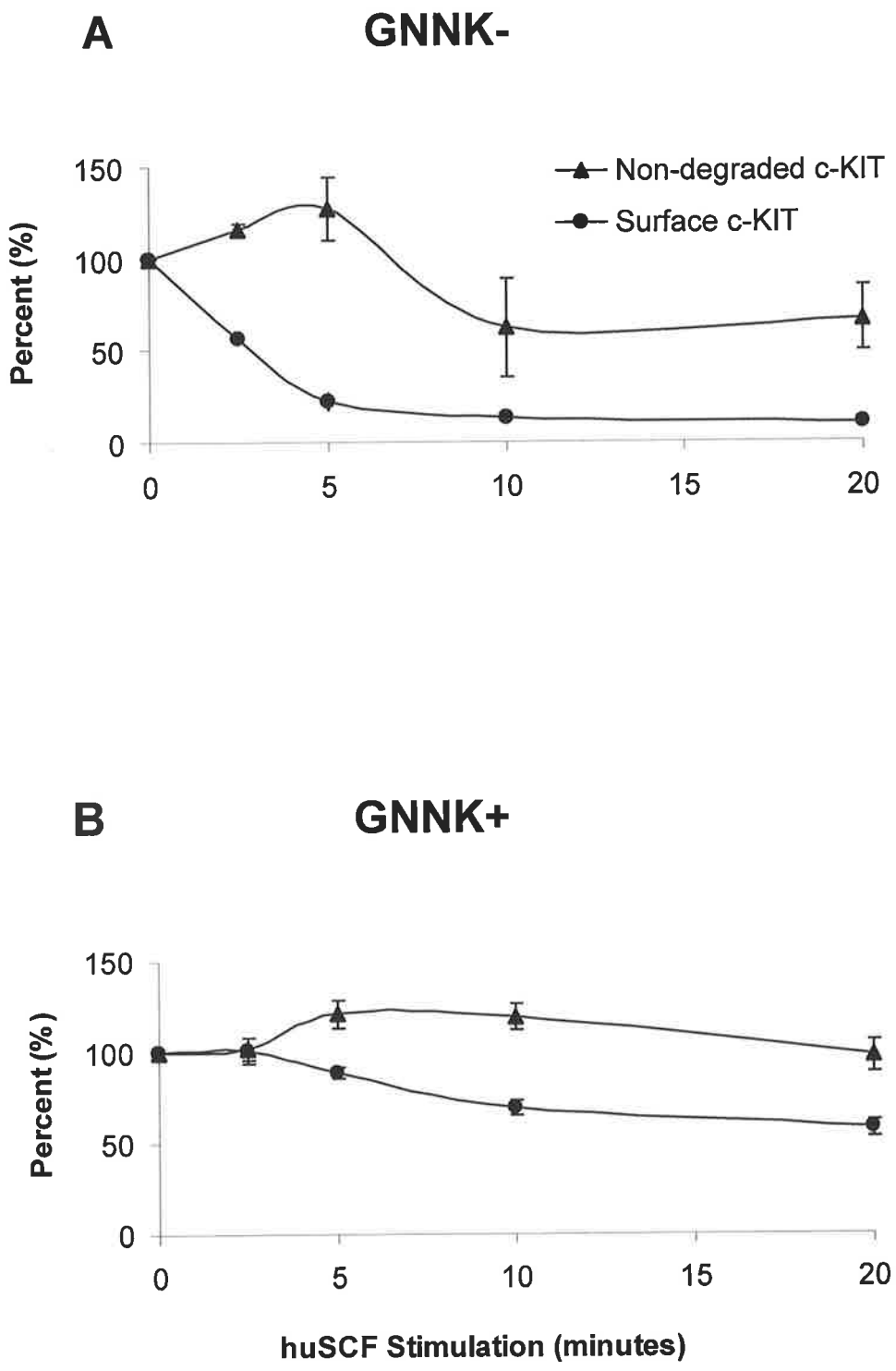
A
GNNK-
Non-degraded c-KIT
Surface c-KIT
Percent (%)
150
100
50
0
0
5
10
15
20
B
GNNK+
Percent (%)
150
100
50
0
0
5
10
15
20
huSCF Stimulation (minutes)

Figure 3.14: Association of p85 to c-KIT in response to huSCF.

FDC-P1 clones were treated as described in Figure 3.9. Membranes were blotted using a rabbit polyclonal antibody raised against the p85 subunit of PI 3-K. Primary antibody was detected with sheep anti-rabbit immunoglobulin alkaline phosphatase conjugate. Proteins were visualised by ECF and FluorImager analysis. **A:** Data from a representative GNNK- clone, GNNK-2. **B:** Data from a representative GNNK+ clone, GNNK+2. **C:** Quantitation of p85 associated to c-KIT. Results from three clones for each isoform were quantitated using ImageQuantTM software. These were standardised against the MO7e controls loaded onto the gel and then further standardised to the amount of c-KIT present (Figure 3.10). Results are expressed as mean ± SEM. Statistical significance ($\alpha < 0.05$) in peak association of p85 to GNNK- and GNNK+ c-KIT is shown by a *.

A

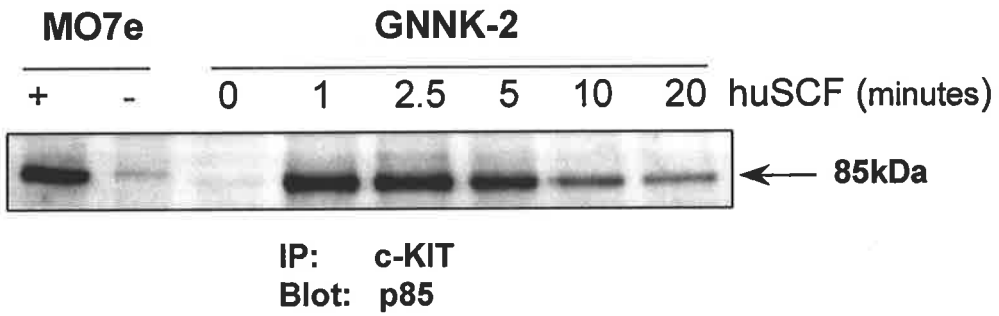
MO7e
GNNK-2
+
-
0
1
2.5
5
10
20
huSCF (minutes)
85kDa
IP: c-KIT
Blot: p85

B

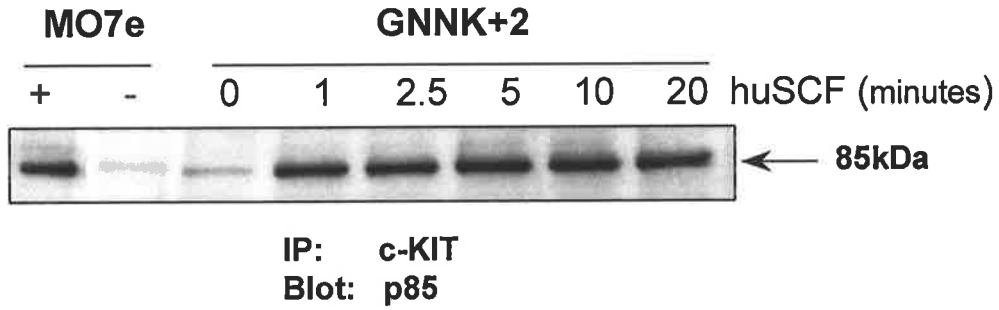
MO7e
GNNK+2
+
-
0
1
2.5
5
10
20
huSCF (minutes)
85kDa
IP: c-KIT
Blot: p85

C

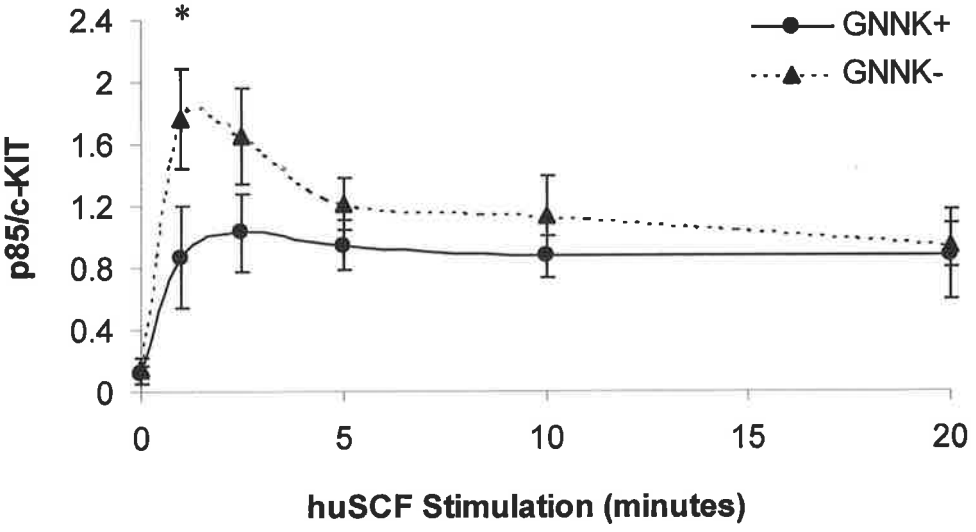
*
GNNK+
GNNK-
p85/c-KIT
2.4
2
1.6
1.2
0.8
0.4
0
0
5
10
15
20
huSCF Stimulation (minutes)

peaking between 1 to 2 minutes (Figure 3.14C). This association was transient with a 50% decrease in associated p85 observed after 5 minutes stimulation and this new level was maintained throughout the remaining time course. The association of p85 with the GNNK+ isoform was also huSCF specific (Figure 3.14C). In response to huSCF, p85 associated to GNNK+ c-KIT reaching peak levels at 2.5 minutes and this was maintained throughout the remainder of the time course. At peak time points, significantly higher amounts of p85 were associated to the GNNK- isoform as compared to GNNK+ ($p = 0.046$). Similarly to c-KIT phosphorylation, the level of association observed at the 20 minute time point was comparable for both isoforms. Therefore both isoforms of c-KIT rapidly associated to p85 on activation and the intensity and rate reflected the phosphorylation of c-KIT.

3.6.2. Akt, a Major Effector of PI 3-K

A well known effector of PI 3-K, Akt, is recruited to the plasma membrane via interaction of its PH domain with 3' phosphoinositides (Rameh and Cantley, 1999). This results in its phosphorylation at T308 and S473, preceding its activation (Leevers *et al.*, 1999; Vanhaesebroeck and Alessi, 2000). By the use of a phospho-specific antibody, raised against a peptide containing phosphorylated S473, the activation state of Akt was indirectly assessed in cellular lysates.

Whole cell lysates from cells stimulated with huSCF were resolved on 10% polyacrylamide gels under reducing conditions and the proteins transferred to membrane. Membranes were immunoblotted with phospho-specific antibody raised against phosphorylated S473 or antibody detecting total Akt protein. As with the immunoprecipitates, a standard of MO7e in the presence or absence of huSCF was included on each gel to enable comparison. Examples of representative blots probed for both total Akt and phosphorylated Akt is shown in Figure 3.15A to D. Phosphorylation of Akt was shown to be dependent on the presence of huSCF (Figure 3.15C and D).

Figure 3.15: Activation of Akt in response to huSCF.

FDC-P1 clones expressing GNNK+/- isoforms were starved of serum and factor for 2 hours, stimulated with 100 ng/ml huSCF at a density of $1x10^7$/ml and then lysed. Clarified lysates (15 µl) were resolved by SDS-PAGE under reducing conditions, transferred to membranes and probed with either Akt **(A, B)** or phosphorylated Akt **(C, D)**. Primary antibody was detected with a secondary antibody conjugated to alkaline phosphatase activity. Alkaline phosphatase activity was visualised using ECF and FluorImager analysis. Included on the gels was an aliquot of MO7e clarified lysate treated with or without 100 ng/ml huSCF for 2.5 minutes. **A, C:** Data from representative GNNK- clone, GNNK-2. **B, D:** Data from a representative GNNK+ clone, GNNK+2. **E:** Quantitation of Akt phosphorylation. Results from three clones for each isoform were quantitated using ImageQuantTM software and standardised against the MO7e loading control. Phosphorylated Akt was expressed as a ratio of the total amount of Akt present and plotted as mean ± SEM.

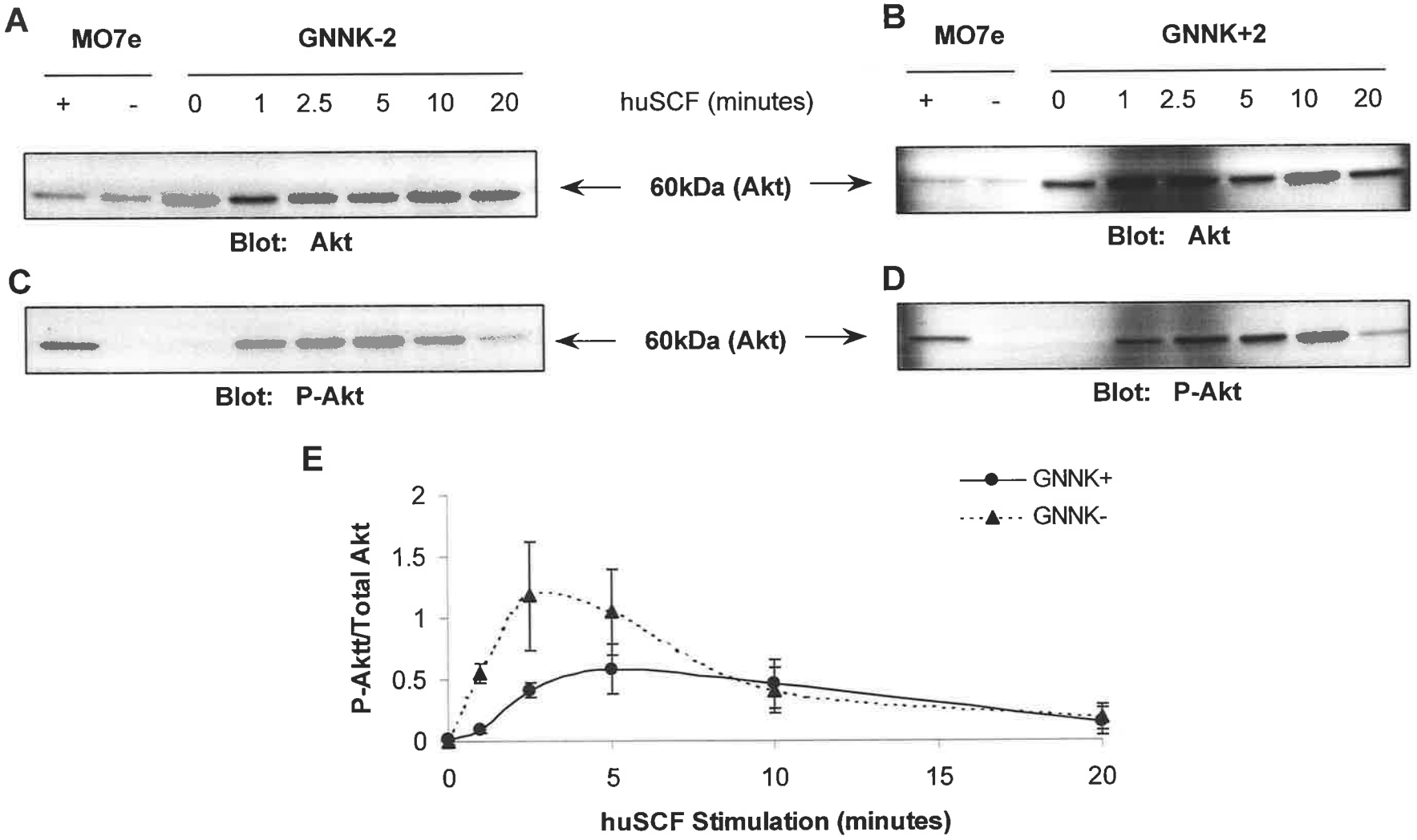
A
MO7e
GNNK-2
+
-
0
1
2.5
5
10
20
huSCF (minutes)
60kDa (Akt)
Blot: Akt
B
MO7e
GNNK+2
+
-
0
1
2.5
5
10
20
Blot: Akt
C
60kDa (Akt)
Blot: P-Akt
D
Blot: P-Akt
E
GNNK+
GNNK-
P-Aktt/Total Akt
2
1.5
1
0.5
0
0
5
10
15
20
huSCF Stimulation (minutes)

To analyse Akt phosphorylation further, results from three clones for each isoform were standardised in regard to MO7e controls and then expressed as a ratio of total Akt present (Figure 3.15E). Akt was phosphorylated to a greater extent in clones expressing the GNNK- isoform and this occurred more rapidly, peaking 2.5 minutes after stimulation as compared to 5 minutes for the GNNK+ isoform. At peak phosphorylation, clones expressing the GNNK+ isoform, had 50% the amount of phosphorylated Akt as compared to those expressing GNNK- however this difference was not statistically significant ($p > 0.1$). The attrition in Akt phosphorylation appeared more rapid for the GNNK- isoform where a six fold decrease was observed after 20 minutes stimulation compared to only a four fold decrease for the GNNK+ isoform. There appeared more variance in the phosphorylation of Akt as compared to the phosphorylation of c-KIT, however the extent of Akt phosphorylation in the clones was not correlated with the level of c-KIT surface expression. These results indicated that the GNNK- isoform induced transient Akt activation while that from the GNNK+ isoform was more sustained.

3.6.3. Activation of ERK Isoforms

Phosphorylation and activation of ERK has been shown to occur in response to growth factor stimulation (Funasaka *et al.*, 1992; Miyazawa *et al.*, 1991). Two isoforms of ERK exist, p42 and p44 (ERK2 and ERK1 respectively) and both are phosphorylated at T202 and Y204 (Dent *et al.*, 1998; Weng *et al.*, 1999). To examine the phosphorylation status of ERK1 and ERK2 in response to the activation of GNNK- and GNNK+ c-KIT, cells were starved of serum for 2 hours, stimulated with huSCF and lysed. Aliquots of lysates were resolved by SDS-PAGE, transferred to membrane and probed for either total ERK (p42 and p44) or dually phosphorylated ERK using phospho-specific antibody. Representative blots for the isoforms are shown in Figure 3.16A to D). No basal phosphorylation in the absence of factor was observed in any of the clones analysed. In response to huSCF stimulation, ERK1 and ERK2

Figure 3.16: Activation of ERK 1 and 2 in response to huSCF.

FDC-P1 clones expressing GNNK+/- isoforms were starved of serum and factor for 2 hours, stimulated with 100 ng/ml huSCF for varying duration at a density of $1x10^7$/ml and then lysed. Clarified lysates were resolved by SDS-PAGE under reducing conditions, transferred to membranes and probed with antibodies to ERK 1 and ERK 2 **(A, B)** or phosphorylated ERK **(C, D)**. Primary antibody was detected with a secondary antibody conjugated to alkaline phosphatase. Alkaline phosphatase activity was visualised using ECF and FluorImager analysis. Included on the gels was an aliquot of MO7e clarified lysate treated with or without 100 ng/ml huSCF for 2.5 minutes. **A, C:** Data from representative GNNK- clone, GNNK-2. **B, D:** Data from a representative GNNK+ clone, GNNK+2. **E:** Quantitation of ERK phosphorylation. Results from three clones for each isoform were quantitated using ImageQuantTM software and standardised against the MO7e loading control. Phosphorylated ERK was expressed as a ratio of the total amount of ERK present and plotted as mean ± SEM.

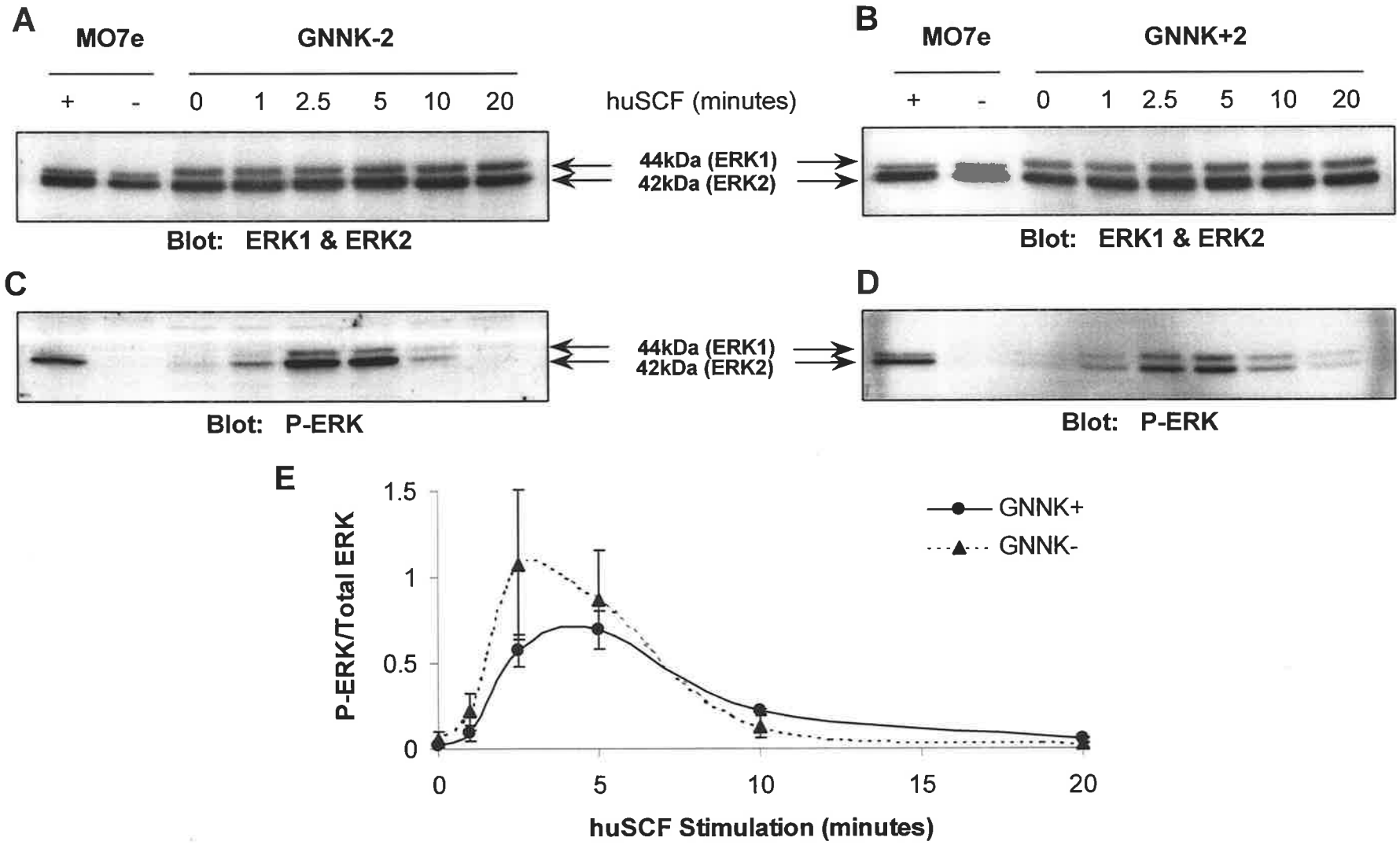
A
MO7e
GNNK-2
+
-
0
1
2.5
5
10
20
huSCF (minutes)
44kDa (ERK1)
42kDa (ERK2)
Blot: ERK1 & ERK2
B
MO7e
GNNK+2
+
-
0
1
2.5
5
10
20
Blot: ERK1 & ERK2
C
44kDa (ERK1)
42kDa (ERK2)
Blot: P-ERK
D
Blot: P-ERK
E
P-ERK/Total ERK
1.5
1
0.5
0
0
5
10
15
20
huSCF Stimulation (minutes)
GNNK+
GNNK-

became phosphorylated with ERK2 phosphorylation being dominant (Figure 3.16C and D). Averages of three clones after standardisation of phosphorylated ERK to total ERK are presented in Figure 3.16E. Peak phosphorylation was observed at 2.5 and 5 minutes for the GNNK- and GNNK+ isoforms respectively (Figure 3.16E). At their peak, the GNNK- isoform resulted in 0.5 fold more phosphorylated ERK as compared to the GNNK+ isoform however this was not significant ($p = 0.2$). Although there was substantial variation in ERK phosphorylation between the clones, this was not correlated with the level of surface c-KIT. The phosphorylation of ERK by both isoforms was transient with substantially decreased levels observed after 10 minutes huSCF stimulation. This is in contrast to p85 and Akt phosphorylation, which appeared to be more sustained (Figure 3.14 and 3.15). Levels of ERK phosphorylation at 10 and 20 minutes were equivalent for both isoforms of c-KIT. This indicated that in these cells both isoforms were capable of phosphorylating ERK 1 and 2 with minimal differences in efficiency.

3.7. Characterisation of MIHC for Analysis of Biological Responses

The myeloid FDC-P1 cell line was useful to analyse proliferative and survival responses induced by huSCF. To evaluate if c-KIT isoforms differed in their ability to induce differentiation in response to huSCF and also to confirm the growth responses observed in FDC-P1, the MIHC model which has previously been studied in our laboratory (Ferrao *et al.*, 1997) was used. Parental MIHC derived from day 14 murine foetal livers were infected with a truncated constitutively active version of the transcription factor, myb (CT3-myb) and selected for long term growth in the presence of muGM-CSF. MIHC remain undifferentiated when maintained in muGM-CSF, while a proportion of cells infected with GNNK+ c-KIT grown in the presence of huSCF differentiated along the monocyte and granulocyte lineages to form macrophages and neutrophils respectively (Ferrao *et al.*, 1997).

The study by Ferrao *et al.*, (1997) grew MIHC in muGM-CSF derived from yeast, however this source was exhausted, therefore lines were maintained in 250 U/ml muGM-CSF derived from baculovirus infected insect cells. Growth in baculovirus derived muGM-CSF resulted in increased numbers of adherent cells in comparison to maintenance in yeast derived muGM-CSF. Further, the non-adherent cells did not tend to grow in clusters as they did when maintained in yeast derived muGM-CSF. To alleviate this problem, 46.9 U/ml muIL-3 derived from baculovirus was added to the culture. This resulted in less adherent cells and more clustering however the population still looked distinct from cells maintained in yeast muGM-CSF. Also affecting the growth of MIHC was FCS, therefore various batches were compared and the one giving optimal growth was used. Since growth conditions of MIHC had changed, the morphology and phenotype of the parental population was examined by the expression of cell surface markers, the expression of macrophage and neutrophil specific esterases, colony morphology in semi-solid medium and Wright-Giemsa staining.

To analyse the phenotype by indirect immunofluorescence, a panel of antibodies specific to murine haemopoietic cell surface proteins at different stages of differentiation were used (see section 2.3.1). The 'early' marker Thy-1 present on progenitor cells was expressed as shown by a peak shift from the negative control (Figure 3.17A), suggesting that cells were immature. Also expressed was MAC-1, a marker found on cells dedicated to the monocyte/macrophage lineage (Figure 3.17B). Heterogeneous expression of F4/80, a marker for mature macrophages was observed with some cells expressing it while others did not (Figure 3.17C). Minimal expression of the neutrophil marker GR-1 was detected (Figure 3.17D).

Because IL-3 induces mast cell formation, it was important to determine that the muIL-3 used to supplement the medium did not induce the outgrowth of mast cells, since the objective was to study haemopoietic progenitor cells capable of differentiating along monocyte/granulocyte lineages. Mast cells express high levels of murine c-Kit, therefore an

Figure 3.17: Analysis of MIHC morphology and phenotype.

A – E: Fluorescence histograms show the expression of cell surface antigens on the parental MIHC population. Indirect immunofluorescence with monoclonal antibodies was used to detect Thy-1 **(A)**, MAC-1 **(B)**, F4/80 **(C)**, GR-1 **(D)** and murine c-Kit **(E)**. Primary antibodies were detected with anti-rat IgG PE or streptavidin IgG PE for biotinylated RB6 8C5 detecting GR1. The negative control in each panel represents cells labelled with the relevant secondary antibody and is representative of background. **F:** Esterase expression of MIHC maintained in muGM-CSF and muIL-3. Brown staining indicates the expression of α-naphthyl acetate esterase while the presence of naphthol-AS-D-chloroacetate esterase is shown by blue staining with methyl green as the counterstain. Photograph is at 20x magnification **G:** Morphology of MIHC maintained in muGM-CSF and muIL-3 as detected by Wright-Giemsa staining. Photograph is at 20x magnification.

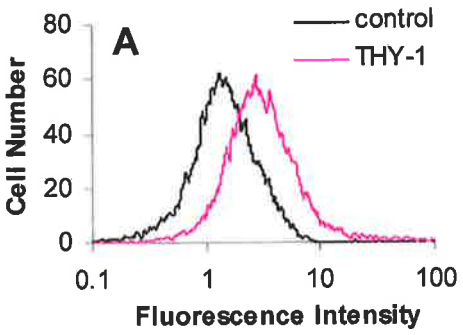
A
control
THY-1
Cell Number
80
60
40
20
0
0.1
1
10
100
Fluorescence Intensity

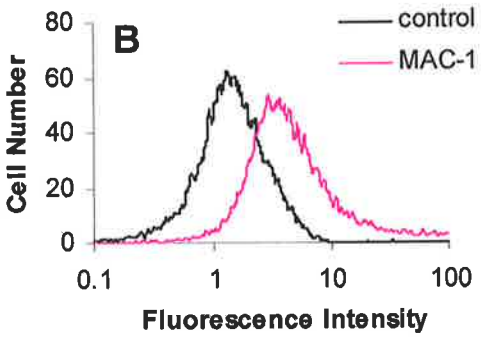
B
control
MAC-1
Cell Number
80
60
40
20
0
0.1
1
10
100
Fluorescence Intensity

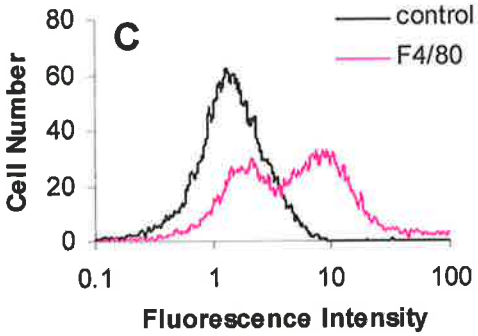
C
control
F4/80
Cell Number
80
60
40
20
0
0.1
1
10
100
Fluorescence Intensity

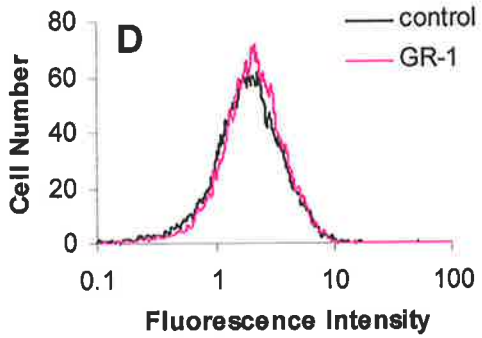
D
control
GR-1
Cell Number
80
60
40
20
0
0.1
1
10
100
Fluorescence Intensity

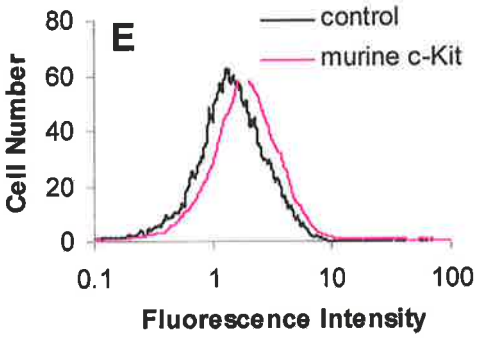
E
control
murine c-Kit
Cell Number
80
60
40
20
0
0.1
1
10
100
Fluorescence Intensity

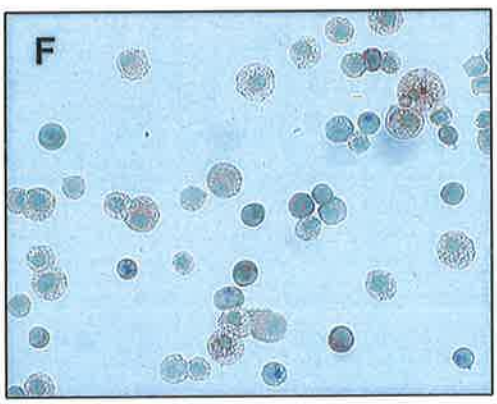
F

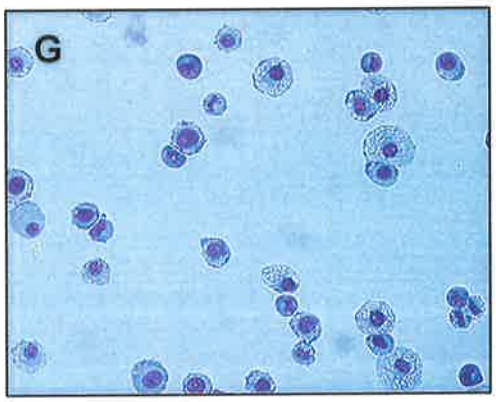
G

indirect immunofluorescence assay was performed to determine the level expressed on parental MIHC. Parental MIHC incubated with ACK-2, an antibody specific to murine c-Kit, showed low level surface staining suggesting that mast cells were not present (Figure 3.17E). To confirm this observation, the presence of the murine mast cell protease, mMCP-5, was determined by immunohistochemistry (refer to section 2.3.4 for details). No red staining above background was evident indicating the absence of mMCP-5 (data not shown). Therefore, the addition of muIL-3 to the medium did not give rise to mast cells in culture and was a suitable supplement to enhance cell growth.

To investigate the differentiation status further, lineage specific esterase staining was performed on cytocentrifuged smears (section 2.2.2), where mature macrophages containing α-naphthyl acetate esterase were stained brown while neutrophils containing naphthol-AS-D-chloroacetate esterase were stained blue (Figure 3.17F). The esterase expression (Figure 3.17F) as well as the morphology as assessed by Wright-Giemsa staining (Figure 3.17G) highlighted that a large proportion of cells were monocyte/macrophage with few blast cells. This confirmed observations from the expression of differentiation markers. An independently derived MIHC population, maintained in baculovirus derived muGM-CSF and muIL-3 was of similar maturity confirming these results. Therefore, parental MIHC were composed of a heterogeneous mix of cells undifferentiated and partially differentiated along the myeloid lineage.

In semi-solid media, MIHC form three morphologically distinct types of colonies dependent on their differentiation status. Highly proliferative cells form compact colonies, partially differentiated immature cells form mixed colonies, while differentiated cells form diffuse colonies (Figure 3.18). Two independent colony assays, performed in triplicate on parental MIHC, indicated that cells mainly formed compact colonies (67%) with about 24% forming mixed colonies and only 8% forming diffuse colonies. The level of compact colonies

Figure 3.18: Morphology of colonies formed in semi-solid medium.

Examples of MIHC colonies formed in methylcellulose after culture for one week. Colonies were defined as 'compact' consisting of rounded cells in close contact **(A)**; 'mixed' consisting of diffuse type colonies with a compact centre **(B)** and 'diffuse' consisting of spread colonies with minimal cell contact **(C)**. Photographs were at an initial magnification of 10x.

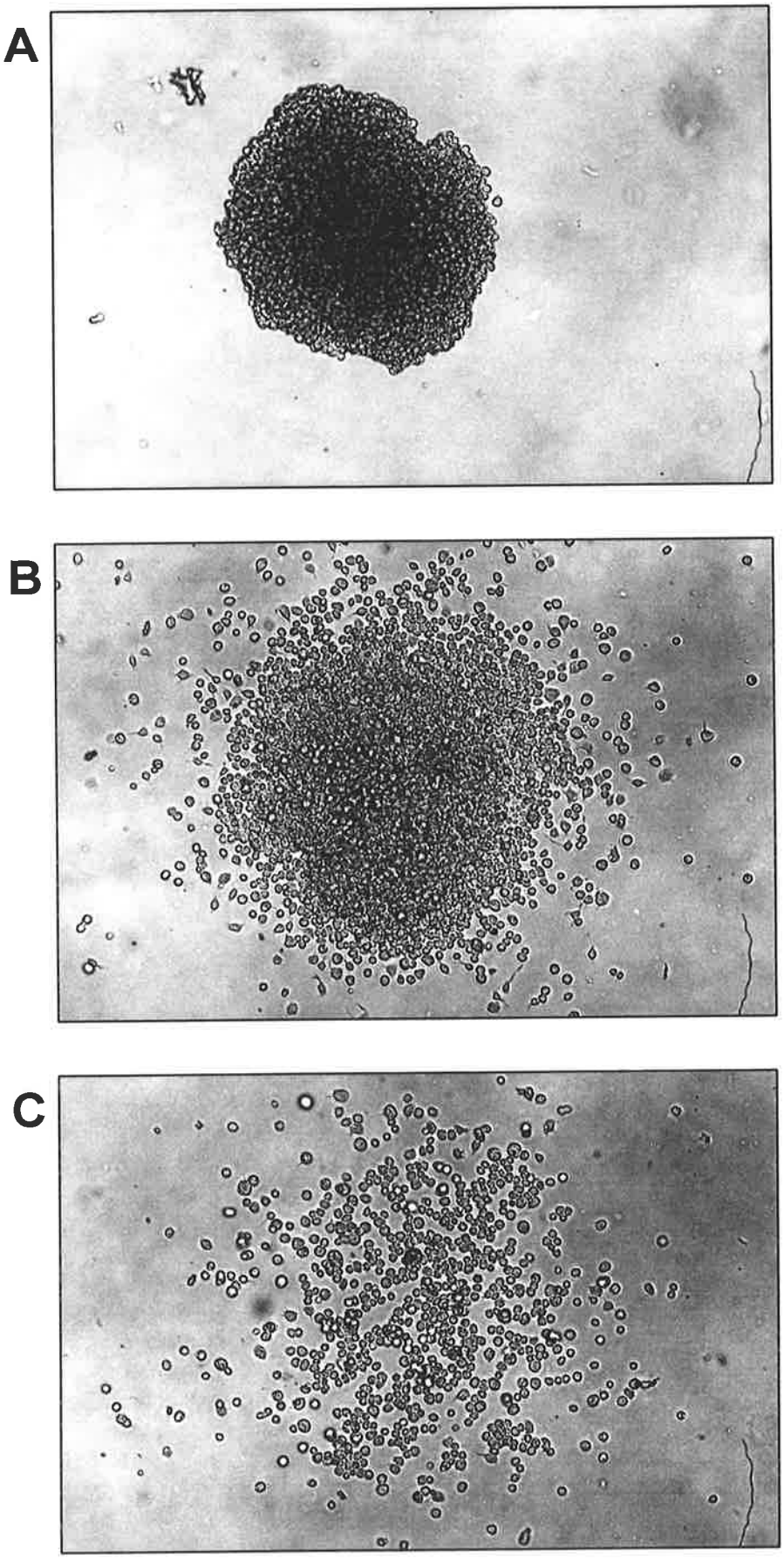
A
B
C

was lower than that observed in yeast muGM-CSF where 79% of cells were of compact morphology (Ferrao *et al.*, 1997) suggesting that the cells were at a more differentiated state.

In summary these results tend to suggest that the parental population maintained in muGM-CSF and muIL-3 derived from baculovirus was composed of cells partially differentiated along the monocyte/macrophage lineage. These were more differentiated than the cells maintained in yeast derived muGM-CSF that had been studied previously (Ferrao *et al.*, 1997).

3.8. Expression of c-KIT Isoforms in MIHC

Parental MIHC maintained in muGM-CSF and muIL-3 were super-infected with *c-KIT* constructs contained in pRUFMC1*neo* by co-cultivation with psi2 virus packaging cells. Based on the surface expression of c-KIT as detected by monoclonal antibody 1DC3, individual cells were sorted into 96 well tissue culture trays using the automated cell deposition facility of the fluorescence activated cell sorter. Clones were amplified and a portion was used for indirect immunofluorescence and flow cytometry while the remaining cells were cryopreserved. Of the derived clones, five for each isoform were selected and their surface expression analysed in duplicate (Figure 3.19). These cells were maintained in medium supplemented with muGM-CSF and muIL-3. To determine the approximate receptor level expressed by MIHC, FDC-P1 populations previously used to determine the copy number of surface c-KIT were included in the immunofluorescence assay. The surface expression of c-KIT in MIHC clones was at a much lower level than the FDC-P1 standards. Therefore, the copy number could not be reliably determined because it required major extrapolation from the FDC-P1 standards. The range of surface c-KIT copy number for the clones was estimated to be 7.3×10^3 to 1.2×10^4 molecules per cell.

Expression of c-KIT was also examined by APAAP (see section 2.3.4 for method). Uninfected or cells incubated with a control antibody remained unstained (Figure 3.19B),

Figure 3.19: Expression of c-KIT in MIHC clones.

MIHC infected with GNNK- and GNNK+ c-KIT and maintained in muGM-CSF and muIL-3 were sorted into clones based on the surface expression of c-KIT. **A:** After expansion, surface expression of c-KIT was determined for each clone by indirect immunofluorescence using monoclonal antibody 1DC3 (anti-c-KIT) and an isotype matched negative control 1B5 (anti-*giardia*). The histogram shows the relative surface expression of GNNK- and GNNK+ c-KIT in MIHC clones after correction for background levels (where ΔMFI represents the change in mean fluorescence intensity). Results are mean ± SD from a duplicate experiment. In the Figure, Par represents parental MIHC. **B to D:** Expression of c-KIT as determined by immunohistochemistry. Cells cytocentrifuged onto glass slides were fixed and incubated with anti-c-KIT antibody (1DC3) or an isotype matched negative control (1B5). Detection of 1DC3 or 1B5 was performed using a bridging rabbit anti-mouse antibody, followed by APAAP complex. Cells were incubated with substrate causing c-KIT positive cells to be stained red. A haematoxylin counterstain stained the nucleus purple. Cells were visualised on an Olympus microscope and photographed with a 20x objective lens. **B**: Parental cells stained with 1DC3. **C**: MIHC GNNK-3 clones stained with 1DC3. **D**: MIHC GNNK+2 clone stained with 1DC3.

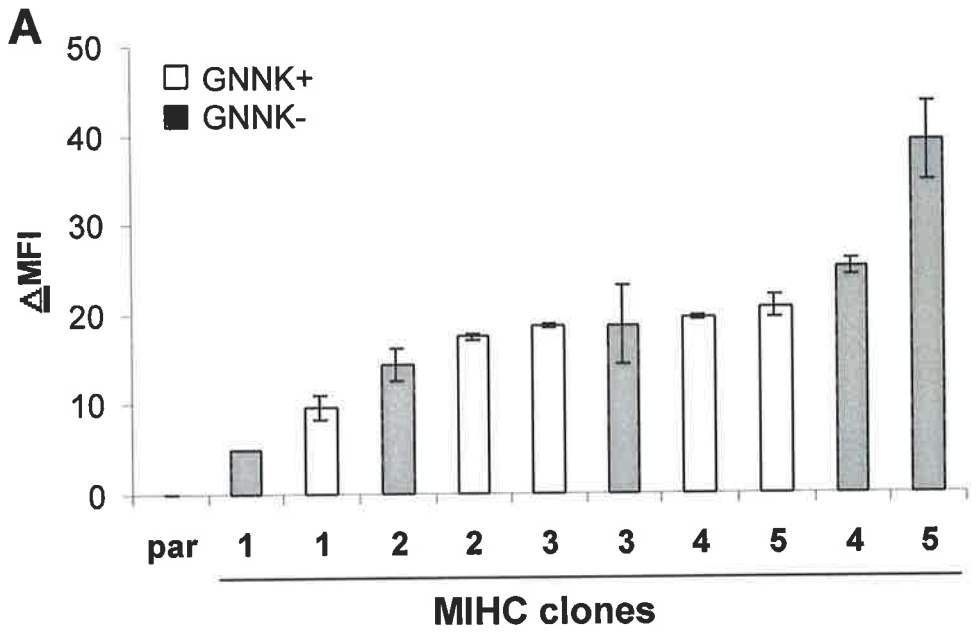
A
50
40
30
20
10
0
ΔMFI
GNNK+
GNNK-
par
1
1
2
2
3
3
4
5
4
5
MIHC clones

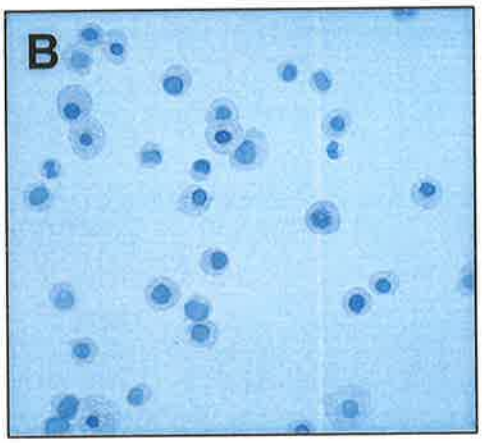
B

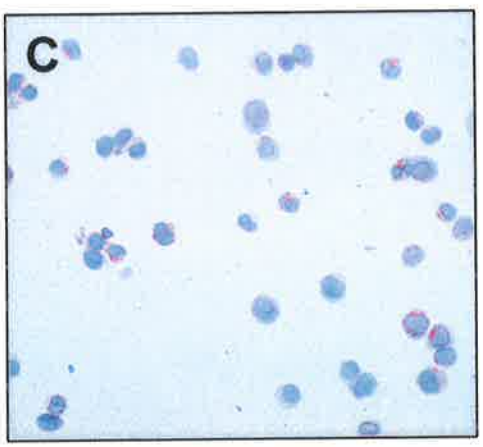
C

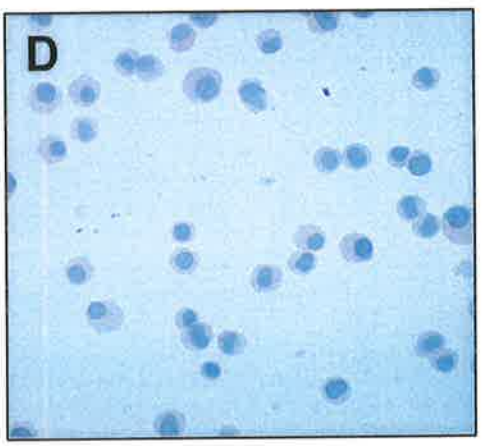
D

while faint red staining indicative of the presence of c-KIT was present in all cells infected with c-KIT constructs (representative GNNK- and GNNK+ clones are shown in Figure 3.19C and D). A high proportion of c-KIT staining appeared to be intracellular.

3.9. PHENOTYPING MIHC CLONES

The parental population infected with c-KIT was partially differentiated along the monocyte/macrophage lineage. Clones expressing c-KIT were selected from a heterogeneous population, therefore they were all phenotyped and their morphology assessed. Analysis of the expression of cell surface markers by indirect immunofluorescence indicated that MAC-1 detecting monocyte/macrophages was highly expressed in all clonal populations, as was F4/80, a marker for mature macrophages (Table 3.1). A peak shift was observed in most cases for immature and mature macrophages. There was low expression of Thy-1 and barely detectable levels of neutrophils (Table 3.1). Supporting the results from the parental line, low expression of murine c-Kit was detected with ACK2 antibody (Table 3.1), an antibody which may also bind human c-KIT to some extent. The absence of mast cells was confirmed by the analysis of mMCP-5 expression in two clones (data not shown). Results from esterase and Giemsa staining revealed heterogeneity between the clones with a high proportion of cells partially differentiated along the monocyte/macrophage lineage (data not shown). This supported results regarding the expression of surface marker antigens.

The final method employed to investigate the background differentiation state of the clones was by investigation of colony morphology in semi-solid medium (see section 3.7 for more detail). In most cases the majority of colonies were compact (Figure 3.20) with the minority being diffuse. An exception was in two of the GNNK+ clones where less than half the colonies were of the compact type. By this criterion, most of the colonies consisted of mainly undifferentiated cells. In summary, the above techniques suggested that there was

Table 3.1: Expression of cell surface marker antigens on MIHC clones.

Expression of cell surface antigens on parental MIHC, GNNK+ and GNNK- c-KIT expressing clones as determined by indirect immunofluorescence. Values are mean fluorescence intensity after correction for background levels. Indirect immunofluorescence with monoclonal antibodies was used to detect Thy-1, MAC-1, F4/80, GR-1 and murine c-Kit (ACK2). Primary antibodies were detected with anti-rat IgGPE or streptavidin PE for biotinylated RB6 8C5 detecting GR1. The negative control used to correct for background levels consisted of cells labelled with the relevant secondary antibody.

	Clone	c-Kit	F4/80	MAC-1	THY-1	GR-1
Parent		0.2	5.59	4.78	1.68	0.21
GNNK-	**2**	-0.34	0.97	4.61	1.47	0.15
	3	0.57	3.07	10.46	2.01	-0.24
	4	0.76	2.98	6.24	1.92	-0.1
GNNK+	**2**	0.21	3.96	6.46	1.82	0.12
	4	0.57	2.98	2.57	1.36	-0.1
	5	0.13	2.89	3.88	1.44	-0.01

Figure 3.20: Percentage of compact colonies formed in muGM-CSF and muIL-3.

MIHC clones were seeded at $5x10^3$/ml in methylcellulose and after one week colonies of greater than 50 cells were scored as either 'compact', 'mixed' and 'diffuse'. Results are mean ± SEM from an experiment performed in triplicate.

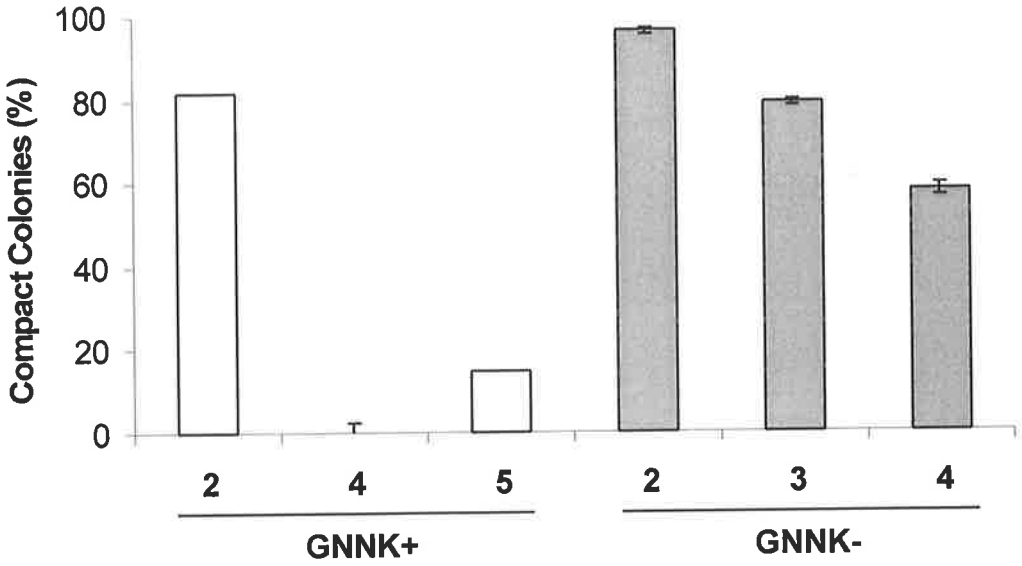
Compact Colonies (%)
100
80
60
40
20
0
2
4
5
2
3
4
GNNK+
GNNK-

substantial clonal variation in the level of background differentiation. These factors would be expected to make it difficult to assess differentiation induced by huSCF.

3.10. Biological Responses Mediated by c-KIT Isoforms in MIHC

3.10.1. Growth in huSCF

To determine if c-KIT expressing MIHC were capable of growth in huSCF, clones were seeded at $2.5x10^4$/ml in either no factor, saturating huSCF (100 ng/ml) or muGM-CSF and muIL-3. Growth was analysed in the various factors after 2, 4 and 6 days using an MTT assay (see section 2.5.2). No growth was observed in the absence of factor confirming that cells remained factor dependent (Figure 3.21A and B). All MIHC clones were capable of growth in huSCF to varying extents (Figure 3.21C and D). Unlike FDC-P1, there was minimal difference in the surface expression of c-KIT between the clones, therefore investigating an association of surface expression with growth rate was not feasible. Interestingly, growth in huSCF for the GNNK- clones at days 4 and 6 was significantly higher than that for GNNK+ clones ($p = 0.02$). Growth in muGM-CSF and muIL3 was also quite heterogeneous indicating clonal variation (Figure 3.21E and F), however no significant difference was observed between the isoforms when analysed after 4 days culture ($p = 0.9$). At optimal conditions in muGM-CSF and muIL-3 the intrinsic growth of the clones was different which could possibly reflect their ability to differentiate. This would affect the growth results in huSCF. To exclude this possibility, the growth of clones in huSCF was standardised relative to growth in muGM-CSF and muIL-3. Results confirmed the above showing a statistically significant increase in growth for the GNNK- isoform as compared to GNNK+ ($p = 0.02$). These results showed that the MIHC clones were capable of growth in huSCF with cells expressing the GNNK- isoform exhibiting better growth rates as compared to the GNNK+ isoform. This supported the previous results in FDC-P1 where the GNNK-

Figure 3.21: Cellular growth in the absence or in the presence of huSCF or muGM-CSF and muIL-3.

Uninfected MIHC or MIHC clones expressing c-KIT isoforms were seeded at a density of $2.5x10^4$/ml and assessed for total number of cells by absorbance after 0, 2, 4 and 6 days of culture in the absence of factor **(A, B)**, in the presence of 100ng/ml huSCF **(C, D)** or in the presence of muGM-CSF and muIL-3 **(E, F)**. Growth was analysed by absorbance at 490 nm. Data are presented as mean ± SEM of a triplicate determination. Due to overgrowth, time points for cultures in muGM-CSF and muIL-3 at day 6 have been omitted. Statistical significance ($\alpha < 0.05$) when comparing MIHC expressing GNNK- to GNNK+ c-KIT is shown by a *.

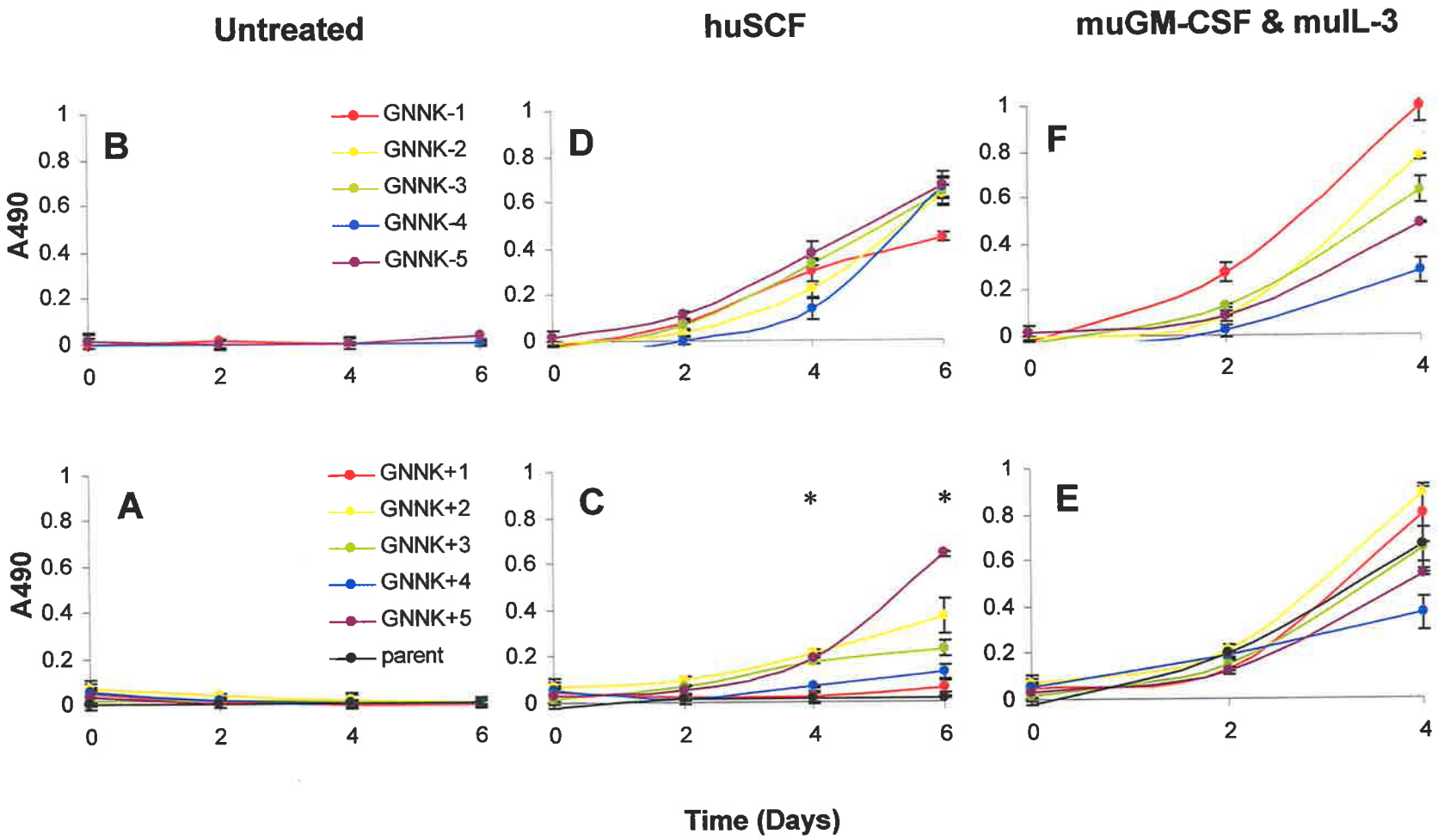
Untreated
huSCF
muGM-CSF & mulL-3
A490
B
D
F
A
C
E
GNNK-1
GNNK-2
GNNK-3
GNNK-4
GNNK-5
GNNK+1
GNNK+2
GNNK+3
GNNK+4
GNNK+5
parent
*
*
0
0.2
0.4
0.6
0.8
1
0
2
4
6
Time (Days)

isoform required lower levels of surface c-KIT as compared to the GNNK+ isoform for an equivalent growth rate.

3.10.2. Examination of Proliferation and Survival in Limiting Concentrations of huSCF

An alternate technique to investigate growth of MIHC clones in huSCF was by PKH assay as described in section 3.3.1. This determined the contributions of proliferation and survival to the overall cell yield. In addition, the dose dependence of huSCF for clones expressing the two isoforms was investigated. Cells stained with PKH-26 were washed three times in serum free medium and then seeded at $2x10^4$/ml into wells containing various concentrations of huSCF. After 24 hours, a half-medium change was performed to maintain limiting huSCF concentrations and after 48 hours, cells were harvested, fixed and analysed by flow cytometry. Three clones for each isoform were analysed based on their expression of c-KIT (GNNK-2, 3, 4 and GNNK+ 2, 4, 5). Calculations of total cell yield, proliferation and survival were made for each clone and since they all expressed similar levels of c-KIT, results were averaged and are presented in Figure 3.22.

Decreased levels of huSCF resulted in reduced cell yield with a half-maximal yield at 5 and 7.5 ng/ml huSCF for GNNK- and GNNK+ expressing cells respectively. Similar to results in FDC-P1, survival appeared to be more dependent on the concentration of huSCF than proliferation. For example, at 5 ng/ml huSCF, the number of divisions undergone by viable cells was near maximal, whereas, survival was approximately half the maximal response.

Although comparison between the isoforms at 10 and 100 ng/ml huSCF revealed a statistically significant increase in cell yield for GNNK- relative to GNNK+ ($p = 0.011$ and 0.024 respectively) (Figure 3.22A), neither the proliferation rate or survival were significantly

Figure 3.22: Effect of huSCF titration on total cell yield, proliferation and survival.

MIHC clones expressing GNNK- and GNNK+ c-KIT were seeded at a density of $2x10^4$/ml and assessed for cell yield, proliferation and survival in sub-optimal levels of huSCF. Cells were harvested after 48 hours culture with a medium change performed after 24 hours to ensure the maintenance of sub-optimal concentrations of huSCF. Data from a triplicate experiment is expressed as mean ± SEM with results obtained from 3 clones for each isoform. Statistical significance ($\alpha < 0.05$) when comparing MIHC expressing GNNK- to GNNK+ c-KIT is shown by a *. **A:** The number of viable cells present. **B:** The average number of cell divisions of the viable population. **C:** The percentage of fluorescence yield in the viable population (survival).

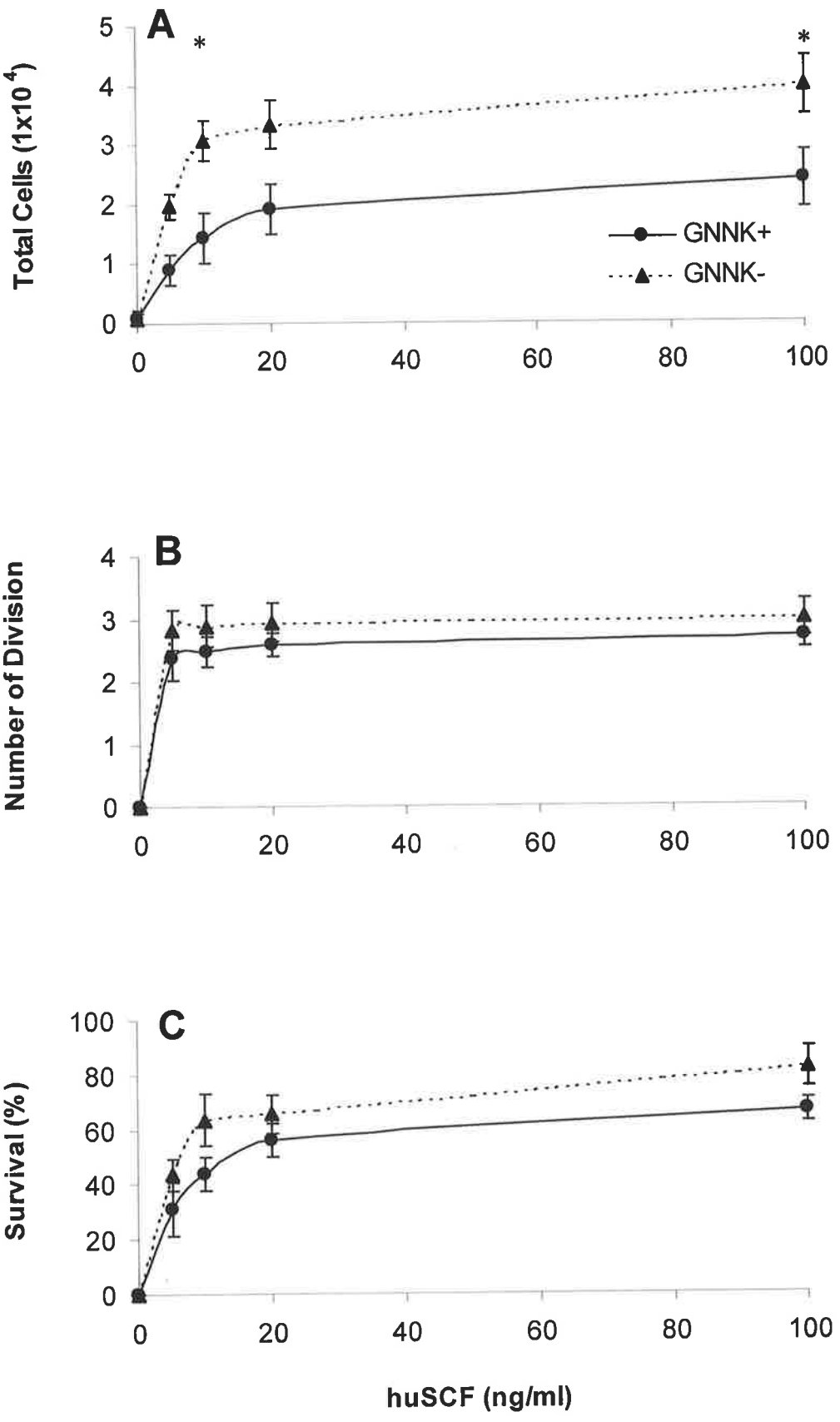
A
B
C
Total Cells (1x10 4)
Number of Division
Survival (%)
huSCF (ng/ml)
GNNK+
GNNK-
*
*
0
1
2
3
4
5
0
20
40
60
80
100

different at either concentration ($p > 0.09$ and 0.07 respectively) (Figure 3.22B and C). This may suggest that both parameters contributed to the difference in cell yield.

3.10.3. Morphology in huSCF

MIHC were chosen for study since they have been shown to serve as a useful model to analyse the effect of huSCF on differentiation (Ferrao *et al.*, 1997), however the substantial level of background differentiation observed in cells grown in muGM-CSF and muIL-3 made it difficult to examine. Nonetheless, differentiation was assessed in semi-solid medium.

Cells were seeded in methylcellulose and colonies formed were counted after one week and scored as compact, mixed or diffuse. As mentioned previously, the proportions of each type of colony formed in muGM-CSF and muIL-3 were quite variable between the clones, although the majority were compact (Figure 3.23A). All three clones expressing GNNK- c-KIT appeared to contain less compact colonies in the presence of huSCF as compared to muGM-CSF and muIL-3 (Figure 3.23A). Two of the four GNNK+ c-KIT expressing clones examined had increased levels of diffuse and mixed colonies in huSCF as compared to muGM-CSF and muIL-3, while another two remained unchanged (Figure 3.23A). These results suggested that huSCF induced differentiation to some extent in most of the clones analysed.

MIHC tend to differentiate when placed under stress. To confirm that the increased differentiation was due to the effect of huSCF and not due to a change in factor, several other factor combinations were examined. To ensure that removal of muGM-CSF was not the cause of the differentiation, colony analysis in muIL-3 and muCSF-1, another cytokine allowing MIHC growth was used. Similarly, to confirm that it was not due to the removal of muIL-3, clones were grown in muGM-CSF alone. Two clones were analysed and results indicated that there was no difference in the proportion of compact, mixed and diffuse colonies in these factor combinations as compared to muGM-CSF and muIL-3 (Figure 3.23B).

Figure 3.23: Colonies formed in semi-solid medium from MIHC clones expressing c-KIT isoforms.

Harvested MIHC ($5x10^3$) uninfected or infected with c-KIT constructs were seeded in triplicate 1 ml methylcellulose cultures with indicated factors. After one week, the number of colonies greater than 50 cells were scored as either 'compact', 'mixed' or 'diffuse'. **A:** Percentage of compact colonies formed in 100 ng/ml huSCF or 250 U/ml muGM-CSF and 46.9 U/ml muIL-3. Results are expressed as mean ± SEM. **B:** Distribution of compact, mixed and diffuse colony types formed by two MIHC clones, GNNK+3 and GNNK-3 in indicated factor combinations. Results are expressed as mean ± SEM from a triplicate experiment. Factor combinations were 100 ng/ml huSCF (SCF), 250 U/ml muGM-CSF and 46.9 U/ml muIL-3 (G/I), 250 U/ml muGM-CSF (GM) and 10 U/ml muCSF-1 and 46.9 U/ml muIL-3 (C/I).

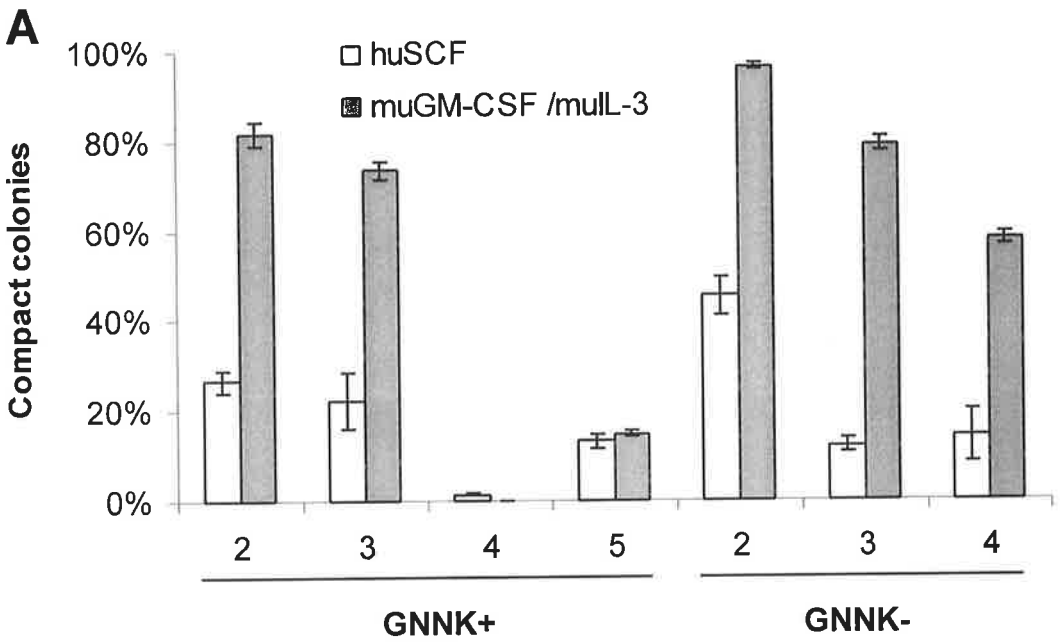
A
100%
80%
60%
40%
20%
0%
Compact colonies
huSCF
muGM-CSF /mulL-3
2
3
4
5
2
3
4
GNNK+
GNNK-

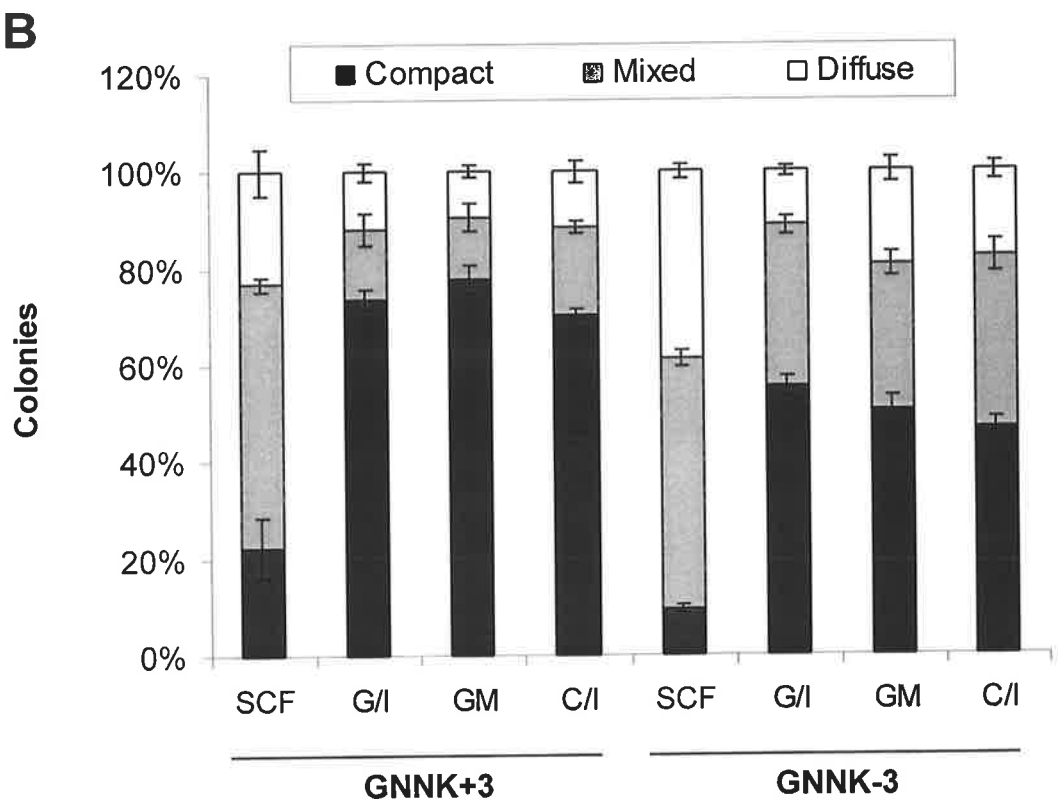
B
120%
100%
80%
60%
40%
20%
0%
Colonies
Compact
Mixed
Diffuse
SCF
G/I
GM
C/I
SCF
G/I
GM
C/I
GNNK+3
GNNK-3

Therefore, the increased differentiation in huSCF was not due to removal of muGM-CSF or muIL-3 and was probably due to the activation of c-KIT.

3.11. DISCUSSION

Previous work in our laboratory has revealed both qualitative and quantitative differences between two c-KIT isoforms in mediating biological responses and signal transduction in response to huSCF in fibroblasts (Caruana *et al.*, 1999). Based on these observations it was of interest to evaluate this in cells in which c-KIT is usually expressed, namely haemopoietic progenitor cells. Comparison of the isoforms in both FDC-P1 and MIHC revealed that cells expressing the GNNK- isoform displayed increased growth as compared to GNNK+ (Figures 3.6, 3.21, 3.22). FDC-P1 clones expressed a range of surface c-KIT (Figure 3.1) with similar growth rates in huSCF between the isoforms being observed at low expression levels. (Figure 3.6). However, at high levels, stimulation of cells expressing the GNNK- isoform resulted in increased huSCF growth as compared to the GNNK+ isoform. A significant difference in the slope coefficient by linear regression analysis was observed suggesting that growth effects due to changes in surface expression of the two isoforms maybe mediated by different means. Therefore the surface expression level of RTKs needs to be taken into account when comparisons are made otherwise an intrinsic difference may not be noted. These differences support the observations in NIH-3T3 fibroblasts in that the GNNK- isoform was more transforming as compared to GNNK+ c-KIT in the presence of huSCF.

Results further confirmed that huSCF stimulation of the GNNK- isoform induced more rapid activation kinetics than the GNNK+ isoform. Specifically, the GNNK- isoform was rapidly phosphorylated, peaking 2.5 minutes after the addition of huSCF, in comparison to the 5 minutes required for GNNK+ c-KIT (Figure 3.9). Associated with this was rapid ubiquitination, internalisation and degradation (Figures 3.10, 3.11, 3,12). These responses were comparable with those in NIH-3T3 fibroblasts (Caruana *et al.*, 1999; Voytyuk *et al.*,

2003). Not only were the activation kinetics of the isoforms similar between the two cellular systems, but also the intensity of these responses. In FDC-P1, the GNNK- isoform was phosphorylated 6 fold more intensely at peak levels as compared to the GNNK+ isoform (Figure 3.9). This is in comparison to the 7 fold difference observed in NIH-3T3 fibroblasts (Caruana *et al.*, 1999). The amount of c-KIT internalised for the isoforms was also similar in both studies, suggesting that the observations in NIH-3T3 were not influenced by inappropriate regulation of c-KIT due to the lack of cell specific key proteins possibly involved. Examples of these may be the SHP-1 phosphatase mainly expressed in haemopoietic cells (Yi *et al.*, 1993), cell specific Src family kinases (for example the dominant haemopoietic Src kinase is Lyn; Linnekin *et al.*, 1997) and also Vav which is a protein specifically expressed by haemopoietic cells (Arudchandran *et al.*, 2000). Therefore the result was not attributable to the cellular background but due to an intrinsic functional difference between the two c-KIT isoforms.

The activation kinetics of Akt and ERK corresponded to phosphorylation of c-KIT where GNNK- induced rapid and transient phosphorylation, peaking at 2.5 minutes in comparison to GNNK+, which peaked at 5 minutes (Figures 3.15 and 3.16). Phosphorylation kinetics of both proteins were similar to those observed in the NIH-3T3 studies, however the intensity of ERK activation appeared different between the cell lines (Caruana *et al.*, 1999; Voytyuk *et al.*, 2003). In NIH-3T3 fibroblasts, phosphorylation of ERK by the GNNK- isoform was of a higher magnitude as compared to the GNNK+ isoform (Caruana *et al.*, 1999; Voytyuk *et al.*, 2003) whereas it was similar in FDC-P1 cells. This difference between FDC-P1 and NIH-3T3 could be dependent on the cellular make up. For example, NIH-3T3 fibroblasts are adherent unlike FDC-P1. Activation of integrins in conjunction with growth factors such as PDGF, EGF and basic FGF results in synergistic activation of ERK (Miyamoto *et al.*, 1996; Schneller *et al.*, 1997). RTKs also localise to focal adhesion complexes (Plopper *et al.*, 1995) and can interact with integrins (Schneller *et al.*, 1997). Therefore potential

integrin engagement in NIH-3T3 fibroblasts may contribute to the different responses. The composition of the cells is likely to be different as well, therefore the specific proteins involved in signal transduction may be limiting in one of the cellular systems as compared to the other.

This study confirmed that expression of the GNNK- isoform induced greater cell growth and also higher intensity phosphorylation of c-KIT after activation by huSCF. Surprisingly, the difference in the intensity of Akt and ERK phosphorylation was not significantly different between the isoforms. Therefore, the activation of signal transduction pathways downstream of c-KIT did not correlate with biological response and receptor phosphorylation. Presumably, other pathways must be involved and one recently discovered protein involved in c-KIT signal transduction in NIH-3T3 cells was Src (Voytyuk *et al.*, 2003). It would be interesting to look at the activation of Src in the FDC-P1 model.

While FDC-P1 cells provided a suitable model to study proliferation and survival, they do not differentiate. To study this aspect of c-KIT function, MIHC were used. However, it was difficult to analyse differentiation in response to huSCF because the parental MIHC population used in this study, unlike that used previously (Ferrao *et al.*, 1997) had a high basal differentiation level (Figure 3.17). Results from lineage surface marker expression, esterase expression and morphology indicated that the parental population was composed of a high proportion of cells partially differentiated along the monocyte/macrophage lineage, with few neutrophils present. This was potentially due to the use of an alternate source of muGM-CSF creating sub-optimal growth conditions. Previous studies used muGM-CSF derived from yeast, however the current studies used muGM-CSF from baculovirus since the original source was exhausted. The concentration used of baculovirus derived muGM-CSF may have been sub-optimal since it was titrated on FDC-P1 cells rather than MIHC. Further, yeast derived muGM-CSF was unpurified, therefore it was possible that it contained other components supplementing the growth of MIHC which were absent in the dialysis purified

baculovirus derived muGM-CSF. Still, muGM-CSF derived from baculovirus was not extensively purified and may have contained growth inhibitory molecules. Batches of FCS also appeared to make a difference in the growth of MIHC. Therefore, conclusions regarding the role of c-KIT isoforms in huSCF mediated differentiation were not made even though the experiments were attempted.

In conclusion, expression of naturally occurring human c-KIT isoforms in haemopoietic cells resulted in profound differences in the kinetics and intensity of signal transduction and biological responses. Results observed correlated with a previous study investigating the role of c-KIT isoforms in NIH-3T3 fibroblasts. It is of interest to deduce the mechanism by which the insertion or deletion of 4 amino acids in the extracellular domain leads to such divergent responses.

CHAPTER 4:

ROLE OF DIRECT PI 3-K RECRUITMENT IN BIOLOGICAL RESPONSES AND SIGNAL TRANSDUCTION MEDIATED BY c-KIT

4. ROLE OF DIRECT PI 3-K RECRUITMENT IN BIOLOGICAL RESPONSES AND SIGNAL TRANSDUCTION MEDIATED BY C-KIT

4.1. INTRODUCTION

PI 3-K is a key protein with varied roles in cellular function including survival, proliferation, differentiation, adhesion and glycolysis regulation (reviewed by Vanhaesebroeck *et al.*, 1996). Recruitment of PI 3-K to the membrane and its subsequent activation is by interaction of the SH2 domain of the p85 subunit with phosphorylated tyrosines of RTKs (Pawson and Schlessinger, 1993). This results in the generation of PtdIns-3,4-P_2 and PtdIns-3,4,5-P_3 (Vanhaesebroeck *et al.*, 1997) which act as second messengers involved in activating proteins with PH domains such as Akt (Toker and Cantley, 1997).

Analysis into the role of PI 3-K in cellular responses has been made feasible by using mutant versions of RTKs lacking the consensus binding site for PI 3-K or by the use of inhibitors, wortmannin and LY294002. The site of association for PI 3-K has been localised to the kinase insert of c-KIT at residue Y721 and Y719 in humans and mice respectively (Herbst *et al.*, 1995b; Serve *et al.*, 1994). Using mutant c-KIT expressed in bone marrow derived mast cells, PI 3-K was shown to be involved in degranulation, adhesion, membrane ruffling and actin assembly (Vosseller *et al.*, 1997). A partial defect in survival and DNA synthesis has also been observed in bone marrow derived mast cells (Serve *et al.*, 1995; Timokhina *et al.*, 1998), while in spermatogonia, a role of PI 3-K and Akt in proliferation has been reported (Feng *et al.*, 2000).

The majority of work investigating the role of signal transduction pathways activated by c-KIT has been done in mast cells (Serve *et al.*, 1994; Serve *et al.*, 1995; Vosseller *et al.*, 1997), however c-KIT is also expressed in haemopoietic progenitor cells. Therefore the aim

of this section was to investigate the role direct PI 3-K recruitment had in haemopoietic progenitor cell growth, proliferation and survival. The activation of PI 3-K and Akt has been implicated in inhibiting apoptosis (Eves *et al.*, 1998; Kennedy *et al.*, 1997; Philpott *et al.*, 1997; Ueno *et al.*, 1997) therefore it was hypothesised that expression of c-KIT lacking PI 3-K recruitment would result in reduced growth and survival. It was also of interest to investigate the role direct PI 3-K recruitment had on the activation of signal transduction downstream of c-KIT.

4.2. Creating and Sequencing of *c-KIT* Containing the Y721F Mutation

Mutation of c-KIT resulting in the substitution of phenylalanine for tyrosine at residue 721 has been shown to prevent PI 3-K recruitment upon huSCF stimulation (Herbst *et al.*, 1995b). Human *c-KIT* cDNA (3 kb coding region and 2 kb 3' untranslated sequence) harbouring an A2813T mutation resulting in the substitution of tyrosine to phenylalanine at residue 721 was obtained in the pcDNA3 vector from Dr. L. Ronnstrand (Ludwig Institute for Cancer Research, Uppsala, Sweden). Digestion of this vector DNA with restriction endonucleases *Acc*III and *Apa*I resulted in the generation of a 666 base pair fragment (residues 2015 - 2681). This fragment was purified by gel electrophoresis. GNNK+S+ isoform termed WT *c-KIT* previously cloned into the *Hpa*I site of the retroviral expression vector pRUFMC1*neo* (Caruana *et al.*, 1999) (see chapter 3) was digested with *Acc*III and *Apa*I, and the complementary fragment separated by gel electrophoresis and purified. The 666 base pair fragment was directionally subcloned into the GNNK+S+ WT *c-KIT* cDNA in pRUFMC1*neo*.

To ensure the presence of the A2813T mutation, diagnostic restriction enzyme digestion was performed. DNA samples purified from bacterial cultures were screened for the mutation by PCR using oligonucleotide primers 447 and 1004 (see section 2.9.10) and digestion with *Rsa*I. Mutation of *c-KIT* at A2813T resulted in the loss of a *Rsa*I site

generating a fragment of 129 base pairs instead of 119 base pairs. This shift, visible in Figure 4.1A revealed that one of the manipulated clones contained the A2813T mutation. To confirm the presence of the A2813T mutation and the lack of additional mutations in this clone, the manipulated region was sequenced using primers 1003, SRC-03 and SRC-05 (see section 2.9.10 for details). Sequencing from the SRC-03 primer is shown in Figure 4.1B with an arrow indicating the A2813T mutation.

All plasmids used for transfection were expanded and purified as outlined in section 2.9.9.2. The virus packaging cell line, psi2, was transfected using calcium phosphate technique (for method, see section 2.10.2) with pRUFMC1*neo* constructs encoding WT or Y721F c-KIT on a GNNK+ background. Transfectants were selected with 400 μg/ml geneticin until untransfected control cells died, which required about a week of treatment. Drug-resistant cells were further selected for c-KIT expression by fluorescence activated cell sorting using monoclonal antibody, 1DC3. Collected cells were expanded and stocks frozen.

4.3. EXPRESSION OF C-KIT IN FDC-P1

Lack of direct PI 3-K recruitment upon c-KIT stimulation results in reduced growth in mast cells in response to SCF (Serve *et al.*, 1995). To investigate this further, and also to examine the types of signal transduction pathways that are activated, the murine factor dependent haemopoietic progenitor cell line, FDC-P1 was chosen. The low level of murine c-Kit expressed by these cells does not interfere with biological responses since huSCF has negligible affinity for murine c-Kit (Martin *et al.*, 1990; Zsebo *et al.*, 1990a).

MuGM-CSF dependent FDC-P1 cells were infected by co-cultivation with psi2 cells expressing either WT or Y721F human *c-KIT* retrovirus (see section 2.10.3). Cells infected with retrovirus containing the various constructs were selected with 1 mg/ml geneticin until uninfected cells died, which required about a week of treatment. For indirect immunofluorescence labelling, 1DC3, an IgG1 antibody specific for the first extracellular

Figure 4.1: Confirmation of the presence of Y721F mutation in c-KIT in pRUFMC1*neo*.

The presence of the A2183T mutation in pRUFMC1neo (Y721F *c-KIT*) was confirmed through the lack of a *Rsa*I restriction endonuclease site **(A)** and through sequencing across the manipulated region **(B)**. **A:** Y721F *c-KIT* cDNA was PCR amplified with primers 447 and 1004 to generate a 794 base pair fragment. PCR fragments were digested and electrophoresed on a 4% low melting point Sea Plaque gel, stained with ethidium bromide and scanned using the FluorImager at 610 nm. As an indication of size *Hpa*II digested pUC19 DNA was run in parallel to the samples and are indicated. Digestion of WT *c-KIT* cDNA, resulted in bands corresponding to 487, 178, 119 and 10 base pairs (indicated by arrows). Mutation of A to T at residue 2813 in Y721F *c-KIT* resulted in the loss of a *Rsa*I site, generating bands at 487, 178 and 129 bp (indicated by arrows). Lane 1 shows digestion of WT *c-KIT* PCR product and lane 2 shows digestion of Y721F *c-KIT* PCR product. The 10 bp fragment was not visible on the gel. **B:** Sequence from the anti-sense primer SRC-03 (2470-2487) corresponding to 2177 - 2196 bp in *c-KIT*. The point mutation of A to T at residue 2183 (indicated by an arrow) resulted in a codon change at 721 of TAC encoding tyrosine to TTC encoding phenylalanine.

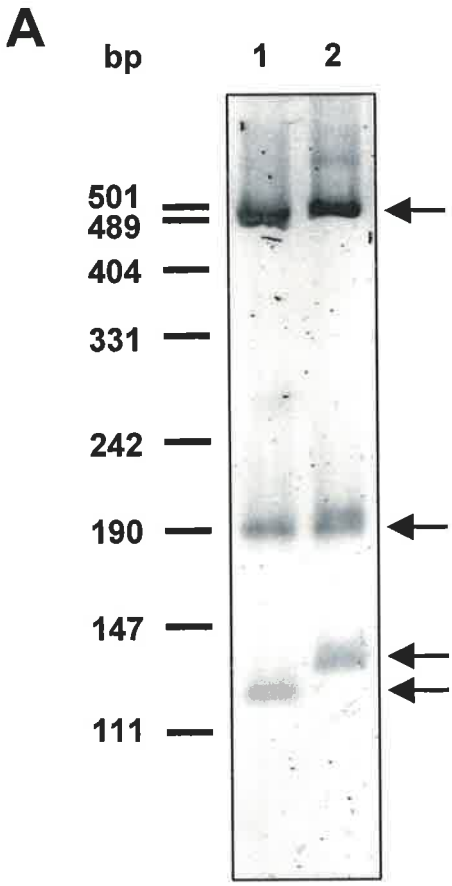
A
bp
1
2
501
489
404
331
242
190
147
111

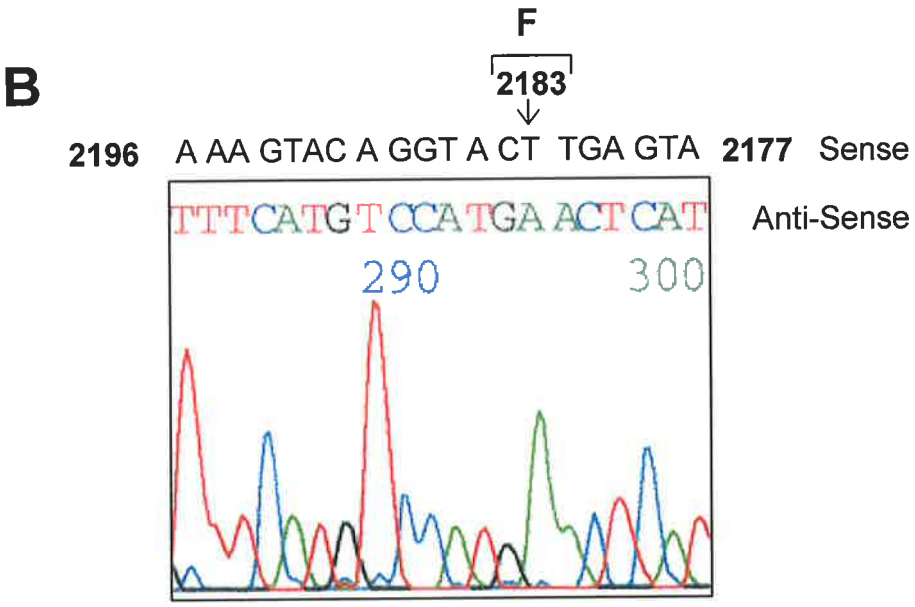
B
F
2183
2196
A AA GTAC A GGT A CT TGA GTA
2177
Sense
TTTCATGTCCATGAACTCAT
Anti-Sense
290
300

domain of c-KIT and 1B5, an isotype matched negative control antibody were used. Immunofluorescence labelling and fluorescence activated cell sorting was used to create a series of clones to ensure results were not due to clonal artefacts of the infected population. These clones, were then expanded and characterised in regard to their surface expression. A range of c-KIT expression levels were identified in each of the clonal series. Four clones with varying levels of c-KIT, but paired between the infectants expressing WT or mutant receptor were selected (Figure 4.2A).

Saturation binding analysis previously performed on FDC-P1 cells infected with c-KIT constructs gave an estimate of the number of receptors expressed per cell (Caruana *et al.*, 1999). As described in section 3.2.1, these cells were analysed in parallel to the indirect immunofluorescence assay on the FDC-P1 clones to give an indication of the number of receptors expressed (Figure 3.1B). Based on the linear equation generated from Figure 3.1B, the copy number for each of the clones was determined to be in the range of 1 - $6x10^4$ receptors per cell which is comparable to $2x10^4$receptor per cell on CD34+ cells from human bone marrow (Cole *et al.*, 1996).

The expression of c-KIT was further identified by immunohistochemistry using the APAAP technique (see section 2.3.4). This technique permeabilised the cellular membrane allowing detection of surface and intracellular c-KIT. In Figure 4.3, faint red staining indicates the expression of c-KIT, while the purple counterstain identifies the nucleus. Parental FDC-P1 cells did not express human c-KIT (Figure 4.3A). Faint red staining was observed in all FDC-P1 clones when an antibody directed against c-KIT was used as compared to the negative control antibody (compare Figure 4.3B with C and D).

A further technique to detect c-KIT was by western blot analysis. Lysed FDC-P1 cells were immunoprecipitated with purified antibody to c-KIT. Immunoprecipitates were resuspended in an equal volume of double strength reduced loading buffer and electrophoresed by SDS-PAGE, transferred to PVDF and the membrane probed with a rabbit

Figure 4.2: Surface expression of c-KIT with and without the PI 3-K binding site.

Surface expression of c-KIT was determined by indirect immunofluorescence using monoclonal antibody 1DC3 (anti-c-KIT) and an isotype matched negative control 1B5 (anti-*giardia*). Histogram of mean ± SD from a duplicate experiment shows the relative surface expression profiles of c-KIT with (WT) and without (Y721F) the PI 3-K binding site in FDC-P1 clones after correction for background levels.

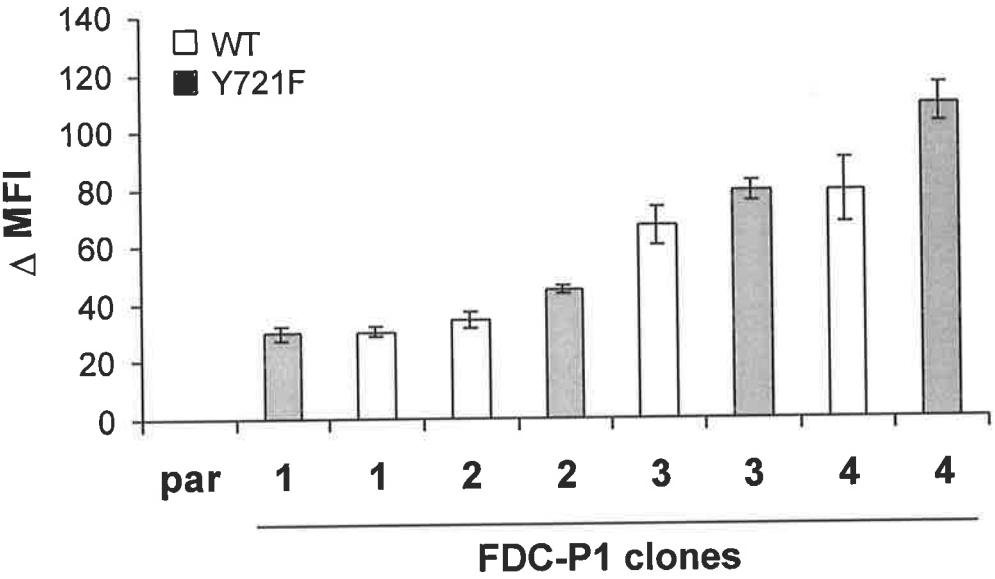
140
120
100
80
60
40
20
0
Δ MFI
WT
Y721F
par
1
1
2
2
3
3
4
4
FDC-P1 clones

Figure 4.3: Immunohistochemical analysis of c-KIT on representative FDC-P1 clones.

Cells cytocentrifuged onto glass slides were fixed and incubated with an anti-c-KIT antibody (1DC3) or an isotype matched control (1B5; anti-*giardia*). Antibody bound to cells was detected using a bridging rabbit anti-mouse antibody, followed by APAAP complex. Cells were incubated with substrate resulting in c-KIT positive cells staining red and with haematoxylin counterstain staining the nucleus purple. Cells were visualised using an Olympus microscope and photographed with a 20x objective lens. **A:** Uninfected parental FDC-P1 stained with 1DC3. **B:** FDC-P1 Y721F3 clone stained with isotype matched negative control. **C:** FDC-P1 WT4 clone stained with 1DC3. **D:** FDC-P1 Y721F3 clone stained with 1DC3.

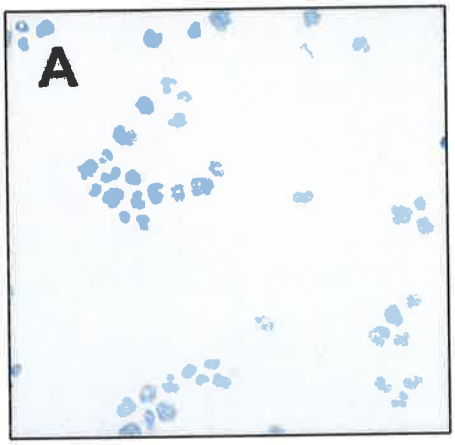
A

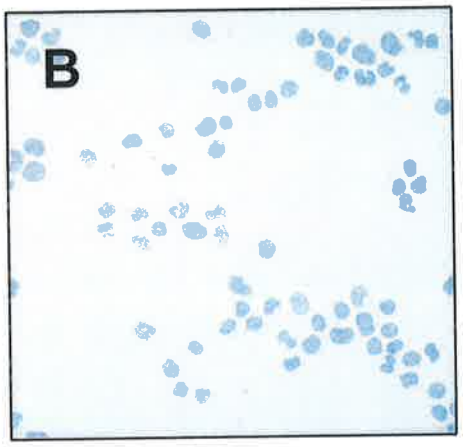
B

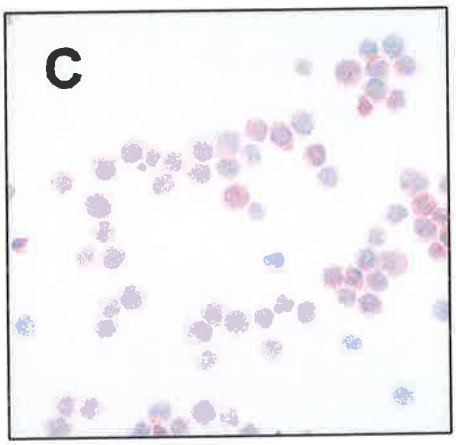
C

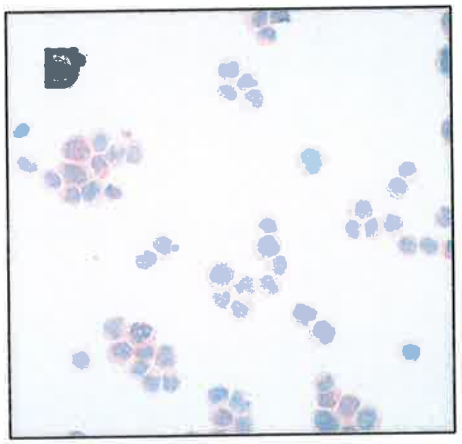
D

polyclonal antibody specific to the carboxy terminal tail of human c-KIT. Results show that all clones expressed detectable levels of c-KIT, appearing as a band at 145 kDa, absent in uninfected FDC-P1 (Figure 4.4A). A band appearing at 125 kDa represented the immature form of c-KIT. Therefore, Y721F c-KIT was of the expected size and normally glycosylated. The band intensity did not correlate with the cell surface levels as detected by immunofluorescence (Figure 4.4B), possibly due to the degradation problem identified in section 3.2.3.

4.4. Association with c-KIT and Activation of PI 3-K After huSCF Stimulation

Mutation of tyrosine at position 721 in c-KIT to phenylalanine has been shown to result in loss of PI 3-K association to the c-KIT complex (Kozawa *et al.*, 1997). To confirm this was the case, cells were lysed after stimulation with huSCF, resolved on polyacrylamide gels and transferred to membrane and probed with an antibody to the p85 subunit of PI 3-K. In response to huSCF, p85 was recruited to WT c-KIT (Figure 4.5A). A trace of residual association was observed for all Y721F c-KIT expressing clones especially at later time points (Figure 4.5B). Results for p85 association were standardised to the level of c-KIT and an average from the three clones plotted (Figure 4.5C). This enabled conclusions to be drawn about changes in the association that were independent of the actual c-KIT levels. In cells expressing WT c-KIT, there was a rapid recruitment of PI 3-K to c-KIT, as was observed in chapter 3. Levels of PI 3-K associated to WT c-KIT only decreased marginally, over the time course with 90% of peak association remaining after 20 minutes of huSCF stimulation. The Y721F mutation decreased p85 recruitment to c-KIT by at least 95%.

The activation of PI 3-K in response to huSCF in c-KIT immunoprecipitates was also investigated. Cells starved for 2 hours were lysed after stimulation with huSCF, and c-KIT was immunoprecipitated. Immunoprecipitates were washed and a kinase reaction with

Figure 4.4: Expression of c-KIT in FDC-P1 clones.

A: Detection of c-KIT by Western blot analysis. Cells starved of serum and factor for 2 hours were resuspended to $1x10^7$/ml and lysed in 1 ml of 1% NP40 in the presence of protease and phosphatase inhibitors. c-KIT was immunoprecipitated with 5 μg KIT4.G12 antibody and 25 μl Protein A Sepharose. Immunoprecipitates were resolved by reduced SDS-PAGE and proteins transferred to PVDF and probed for c-KIT using a commercial rabbit polyclonal antibody against the carboxy terminal tail. Primary antibody was detected with sheep anti-rabbit alkaline phosphatase and enzyme activity was visualised using ECF on the FluorImager. In the figure, par represents parental FDC-P1. **B:** Comparison of c-KIT detection techniques. Results from **A** were quantitated using ImageQuantTM software and expressed as a ratio of the number of cells present in the lysate. c-KIT levels detected by Western blot analysis and standardised to the number of cells lysed (bar graph) were compared to the change in mean fluorescence intensity after correction for background (ΔMFI) obtained from Figure 4.2 (line graph). Relative fluorescence units is represented by rfu.

A

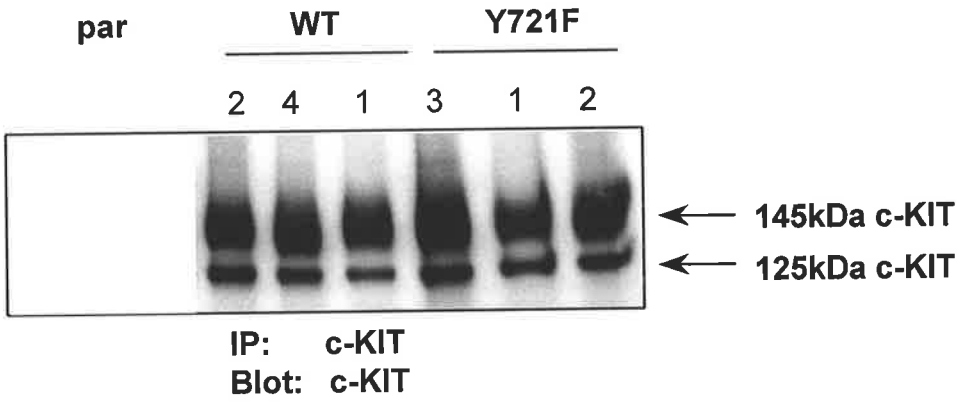
par
WT
Y721F
2 4 1 3 1 2
145kDa c-KIT
125kDa c-KIT
IP: c-KIT
Blot: c-KIT

B

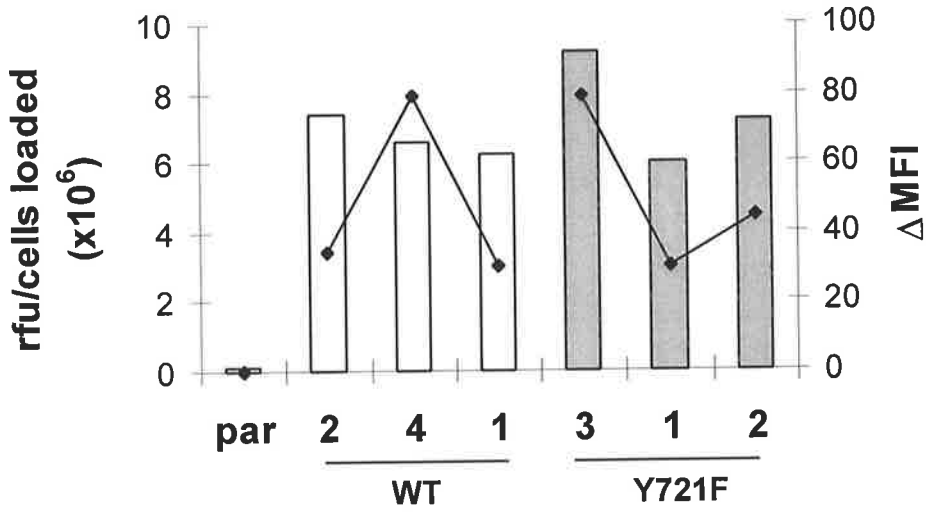
rfu/cells loaded (x10^6)
10
8
6
4
2
0
100
80
60
40
20
0
ΔMFI
par 2 4 1 3 1 2
WT
Y721F

Figure 4.5: Association of p85 to c-KIT in response to huSCF.

FDC-P1 clones expressing c-KIT with (WT) or without(Y721F)the PI 3-K binding site were starved of serum and factor for 2 hours, stimulated with 100 ng/ml of huSCF for varying duration at a density of $1x10^7$/ml and lysed. Clarified lysates were immunoprecipitated with 5 μg/ml KIT4.G12 antibody with 25 μl of Protein A Sepharose for 2 hours. Washed immunoprecipitates were loaded onto 8% gels, electrophoresed, transferred to membrane and probed with a rabbit polyclonal antibody raised against the p85 subunit of PI 3-K. Primary antibody was detected with sheep anti-rabbit immunoglobulin alkaline phosphatase conjugate. Proteins were visualised by ECF and FluorImager analysis. **A:** Data from a representative WT clone, WT4. **B:** Data from a representative Y721F clone, Y721F3. **C:** Quantitation of p85 associated to c-KIT. Results were quantitated using ImageQuantTM software. These were standardised against the MO7e controls loaded onto the gel and then further standardised to the amount of c-KIT present. Results are expressed as mean ± SEM for the three clones.

A

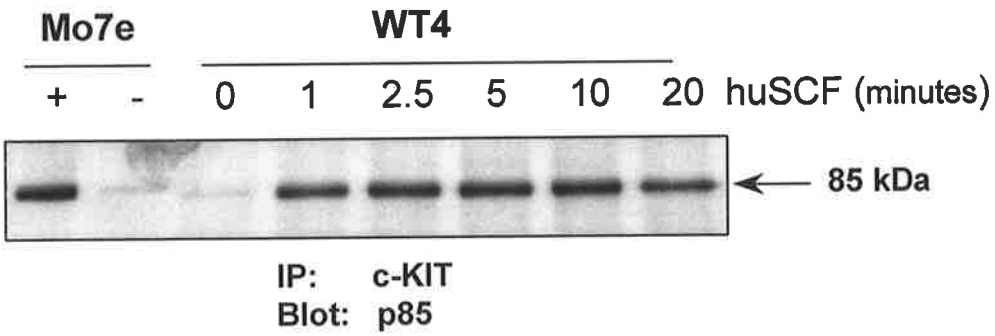
Mo7e
WT4
+
-
0
1
2.5
5
10
20
huSCF (minutes)
85 kDa
IP: c-KIT
Blot: p85

B

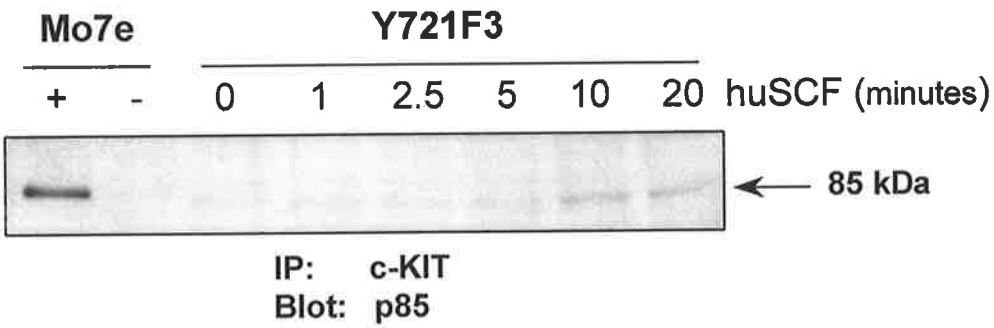
Mo7e
Y721F3
+
-
0
1
2.5
5
10
20
huSCF (minutes)
85 kDa
IP: c-KIT
Blot: p85

C

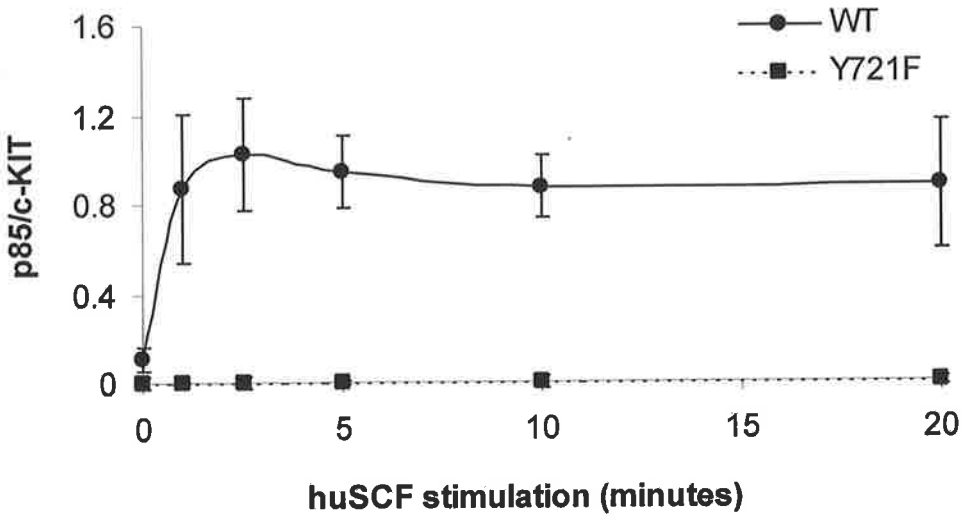
WT
Y721F
p85/c-KIT
1.6
1.2
0.8
0.4
0
0
5
10
15
20
huSCF stimulation (minutes)

^{32}P-ATP and the PI 3-K substrate PtdIns, was performed (see section 2.8.4). The reaction was terminated after 20 minutes incubation at room temperature and the lipid purified and separated by thin layer chromatography and autoradiographed. The presence of PI 3-K activity was shown by phosphorylation of lipid PtdIns to produce PtdIns-3-P, which appeared as a spot above the origin. PI 3-K activity was present in c-KIT immunoprecipitates from WT c-KIT expressing cells in response to huSCF (Figure 4.6A). The lipid phosphorylation was blocked by wortmannin confirming that it was due to PI 3-K activity. In comparison, only trace levels of PI 3-K activity were present in immunoprecipitates from Y721F c-KIT (Figure 4.6A). Average results from two clones of each c-KIT construct were quantitated (Figure 4.6B) confirming results from the representative clones in Figure 4.6A. Similar levels of c-KIT were immunoprecipitated in each case indicating that the lack of PI 3-K activity was due to lack of association and not due to ineffective immunoprecipitation (Figure 4.6C). Although only trace PI 3-K activity was detected in c-KIT immunoprecipitates from Y721F expressing cells, PI 3-K was still active as determined from a p85 immunoprecipitate (Figure 4.6D). This huSCF independent activity was abolished by wortmannin. These results confirmed that the Y721F mutation in c-KIT removed detergent resistant PI 3-K recruitment in response to huSCF.

4.5. GROWTH OF FDC-P1 CLONES IN RESPONSE TO HUSCF

Mutation of the PI 3-K binding site in c-KIT has been reported to decrease SCF mediated growth (Timokhina *et al.*, 1998), therefore it was important to determine whether the Y721F c-KIT expressing clones were capable of growth in saturating huSCF. FDC-P1 clones were seeded at $5x10^4$/ml in either saturating huSCF (100 ng/ml), muGM-CSF or in the absence of factor and their growth assessed over three days in a colourimetric absorbance assay (MTT assay) which measures the total number of viable cells in the culture (see section 2.5.2). Results confirmed that FDC-P1 clones expressing c-KIT remained factor dependent

Figure 4.6: Association and activation of PI 3-K by c-KIT.

A: Detection of PI 3-K activity in c-KIT immunoprecipitates. FDC-P1 clones were stimulated with (+) or without (-) huSCF and lysed at $1x10^7$/ml. Clarified lysates were immunoprecipitated with 5 μg KIT4.G12 and 25 μl Protein A Sepharose for 2 hours. A kinase reaction with (+) or without (-) 70 nM wortmannin (Wm) with PtdIns as the substrate was performed which was terminated after 20 minutes and extracted lipids were resolved by thin layer chromatography. Phosphorimaging screens were exposed to the chromatogram and scanned using a phosphorimager. Two representative clones, WT4 and Y721F3 are displayed. **B:** Quantitation of PI 3-K activity in FDC-P1 clones. Data from **A** of 2 clones each of WT and Y721F c-KIT expressing FDC-P1 cells were quantitated using ImageQuantTM software and are presented as an average ± SD. **C:** Presence of c-KIT and p85 in immunoprecipitates. FDC-P1 clones were treated in parallel to **A** and immunoprecipitates were resolved by reduced SDS-PAGE, transferred to membrane and immunoblotted for c-KIT and p85. Primary antibody was detected with sheep anti rabbit immunoglobulin conjugated to alkaline phosphatase and visualised by ECF using the FluorImager. **D:** PI 3-K activity in p85 immunoprecipitates. As in **A**, however p85 was immunoprecipitated from lysates. Data from two representative clones (WT4 and Y721F3) are presented.

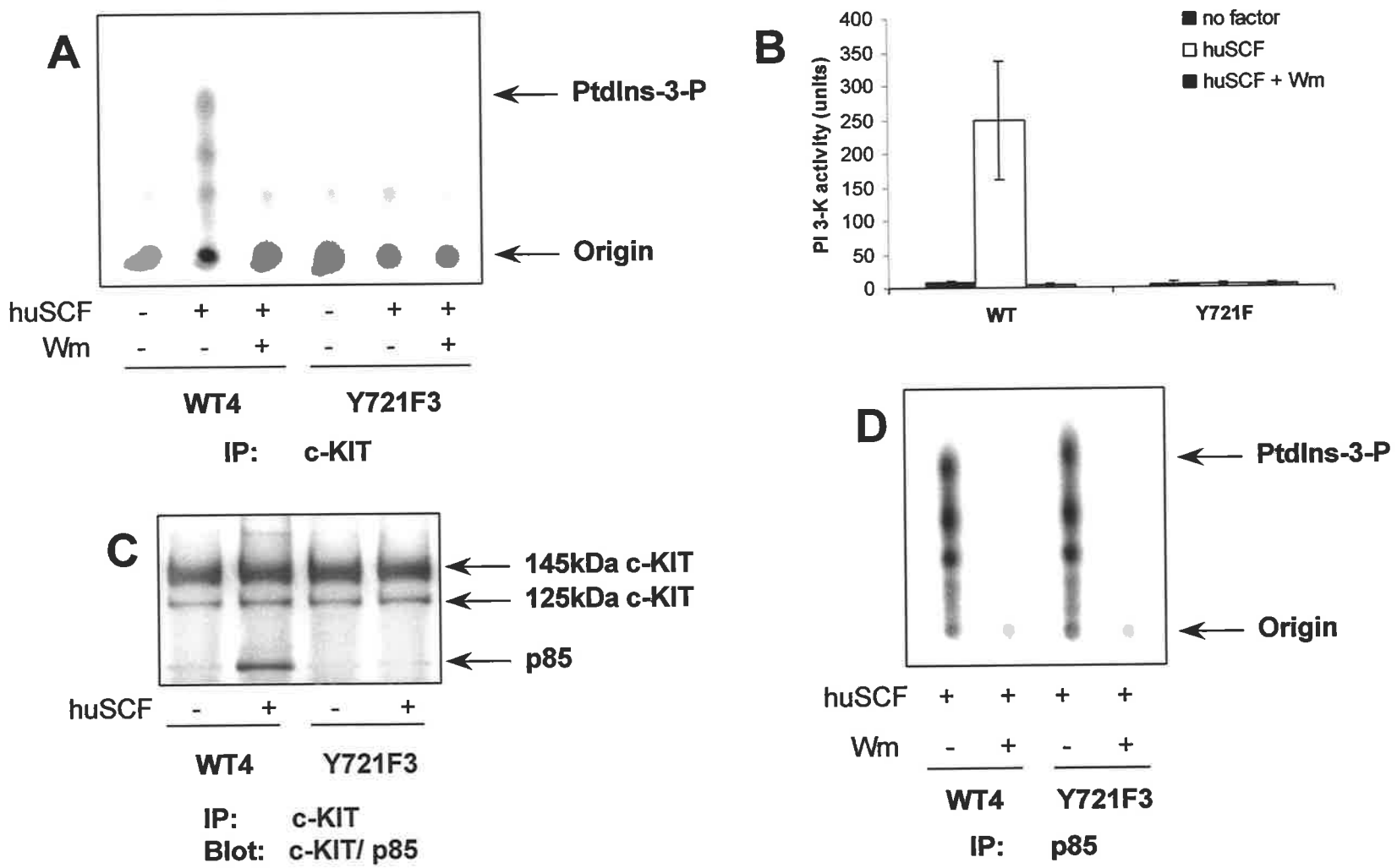
A
PtdIns-3-P
Origin
huSCF - + + - + +
Wm - - + - - +
WT4
Y721F3
IP: c-KIT
B
no factor
huSCF
huSCF + Wm
PI 3-K activity (units)
400
350
300
250
200
150
100
50
0
WT
Y721F
C
145kDa c-KIT
125kDa c-KIT
p85
huSCF - + - +
WT4
Y721F3
IP: c-KIT
Blot: c-KIT/ p85
D
PtdIns-3-P
Origin
huSCF + + + +
Wm - + - +
WT4
Y721F3
IP: p85

since no growth in the absence of factor was observed (Figure 4.7A and B). The addition of huSCF enabled growth of WT c-KIT expressing FDC-P1 (Figure 4.7C). While huSCF did not cause any obvious cellular growth for Y721F c-KIT expressing FDC-P1 (Figure 4.7D) viable cells were present after the three day incubation period unlike cells in the absence of factor. Even though differences in growth rate in huSCF were observed, all clones grew at an equivalent rate in muGM-CSF (Figure 4.7E and F). These results suggested that direct recruitment of PI 3-K was important but not solely responsible for maintenance of cells in huSCF.

The varying extents of growth in huSCF was due to differing levels of surface c-KIT expressed in FDC-P1 clones, with linear regression analysis revealing a strong relationship ($r^2 = 0.99$ and 0.83 for WT and Y721F c-KIT respectively) (Figure 4.8A). At low levels of c-KIT expression, both c-KIT constructs conferred similar rates of growth, however at higher receptor levels, the lack of direct PI 3-K recruitment decreased huSCF mediated growth. Using an approximate t-statistic with adjusted expression for degrees of freedom, the slope coefficient was found to be significantly higher for WT as compared to Y721F c-KIT expressing cells ($p = 0.006$). Therefore, the results suggested that lack of PI 3-K recruitment affected the relationship of huSCF growth to c-KIT surface expression. As was determined in chapter 3, the surface expression of c-KIT did not affect growth in muGM-CSF (Figure 4.8B).

Differences in the growth assay could be due to cell survival, proliferation or both. To determine the involvement of these parameters in the response, a PKH assay was performed as described in section 3.3.1. Cells were seeded at $1x10^5$/ml in either saturating huSCF or muGM-CSF and cultured for 2 days. No difference in huSCF mediated proliferation was observed between the c-KIT constructs (Figure 4.9A) however survival was reduced when the PI 3-K binding site was mutated and also appeared to be more dependent on the level of c-KIT expressed ($r^2 > 0.8$) (Figure 4.9B). These results are a general trend though since no statistical

Figure 4.7: Cellular growth in the presence of huSCF.

Uninfected FDC-P1 or FDC-P1 clones expressing c-KIT with (WT) or without (Y721F) the PI 3-K recruitment site were seeded at a density of $5x10^4$/ml and were assessed for total number of cells by MTT assay after 0, 1, 2 and 3 days of culture in the absence of factor **(A, B)**, in the presence of 100ng/ml huSCF **(C, D)** or in the presence of muGM-CSF **(E, F).** Growth analysed by absorbance at 490 nm from triplicate experiments is presented as mean ± SEM. Due to overgrowth, data for muGM-CSF cultures at day 3 have been omitted.

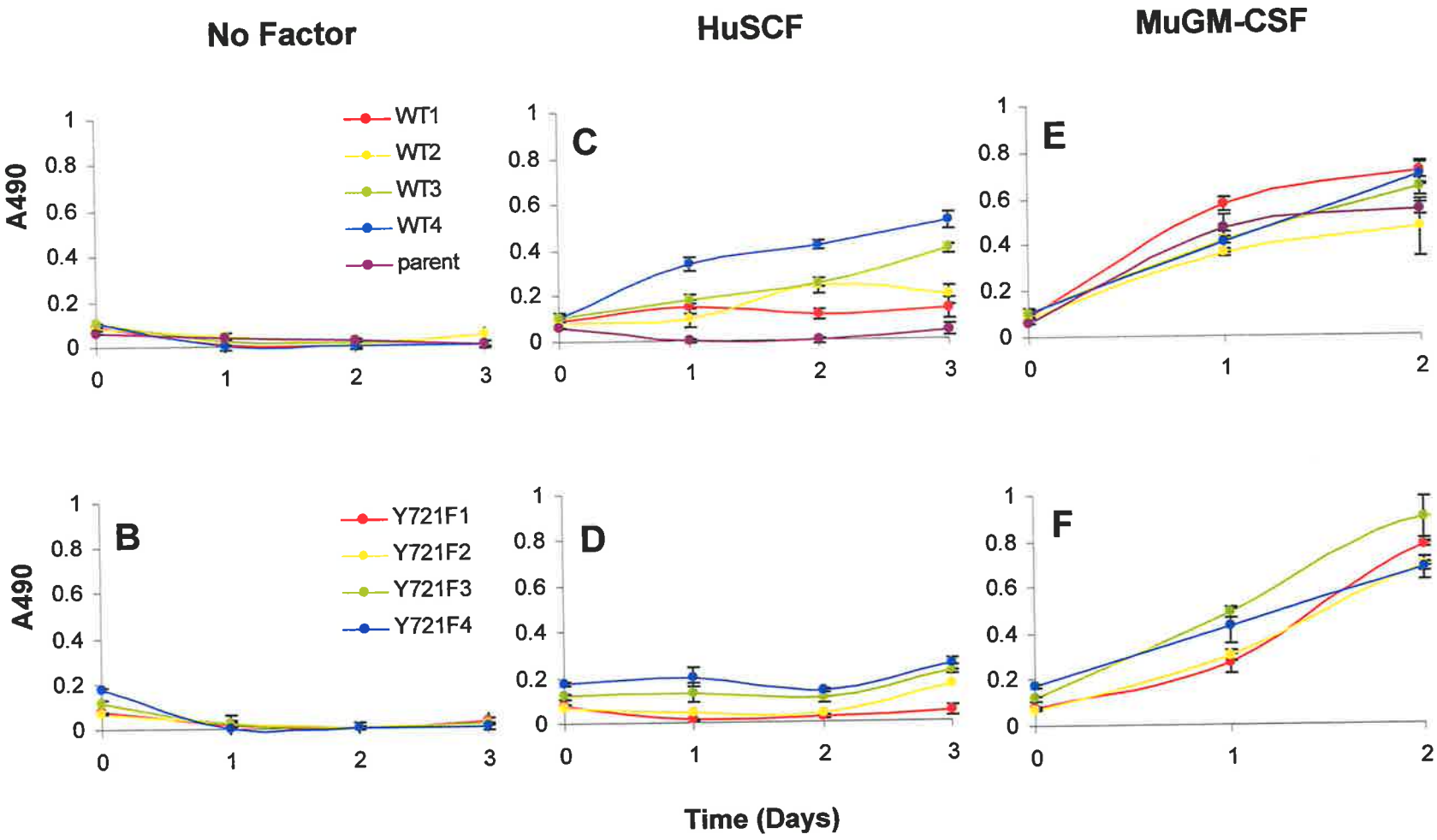
No Factor
HuSCF
MuGM-CSF
A490
WT1
WT2
WT3
WT4
parent
B
Y721F1
Y721F2
Y721F3
Y721F4
C
D
E
F
Time (Days)

Figure 4.8: Comparison of cellular growth in huSCF or muGM-CSF to surface expression.

Cellular growth data (A490) from Figure 4.7 plotted against surface expression of c-KIT (change in mean fluorescence intensity, ΔMFI) (Figure 4.2.). Cells were cultured in 100 ng/ml huSCF **(A)** or muGM-CSF **(B)** for three days. Points plotted were mean ± SEM for cellular growth and SD for surface expression. Solid line (WT c-KIT) and hashed line (Y721F c-KIT) shown in **A** were determined by regression analysis. Statistical significance ($\alpha < 0.05$) is shown by a *.

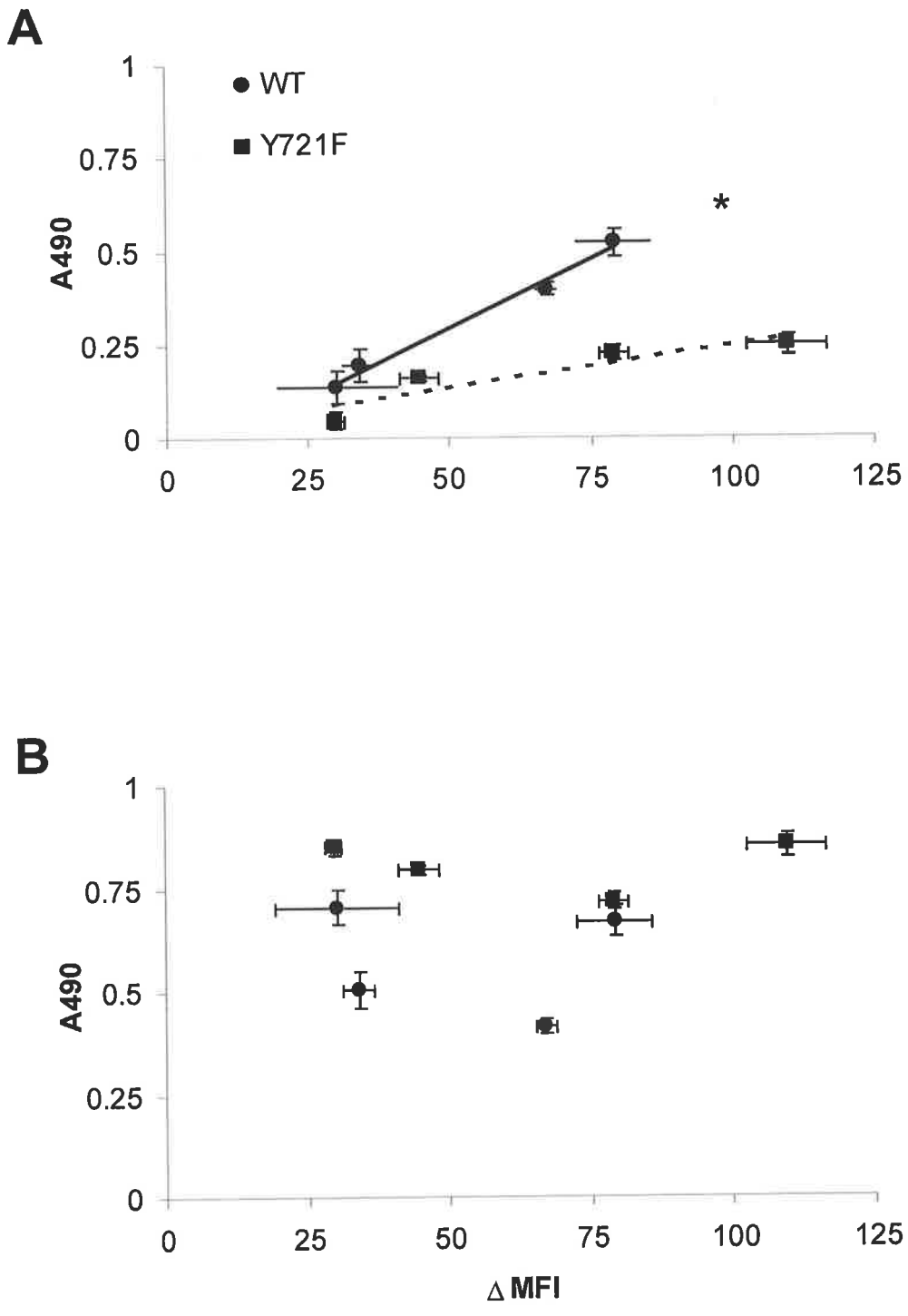
A
WT
Y721F
*
A490
1
0.75
0.5
0.25
0
0
25
50
75
100
125
B
A490
1
0.75
0.5
0.25
0
0
25
50
75
100
125
Δ MFI

Figure 4.9: Comparison of proliferation and survival in huSCF and muGM-CSF to surface expression.

Proliferation **(A, C)** or survival **(B, D)** in either 100 ng/ml huSCF **(A, B)** or muGM-CSF **(C, D)** as determined by PKH assay after 2 days culture was plotted against surface expression (ΔMFI - change in mean fluorescence intensity) (Figure 4.2). Points plotted were mean ± SEM for proliferation and survival and mean ± SD for surface expression.

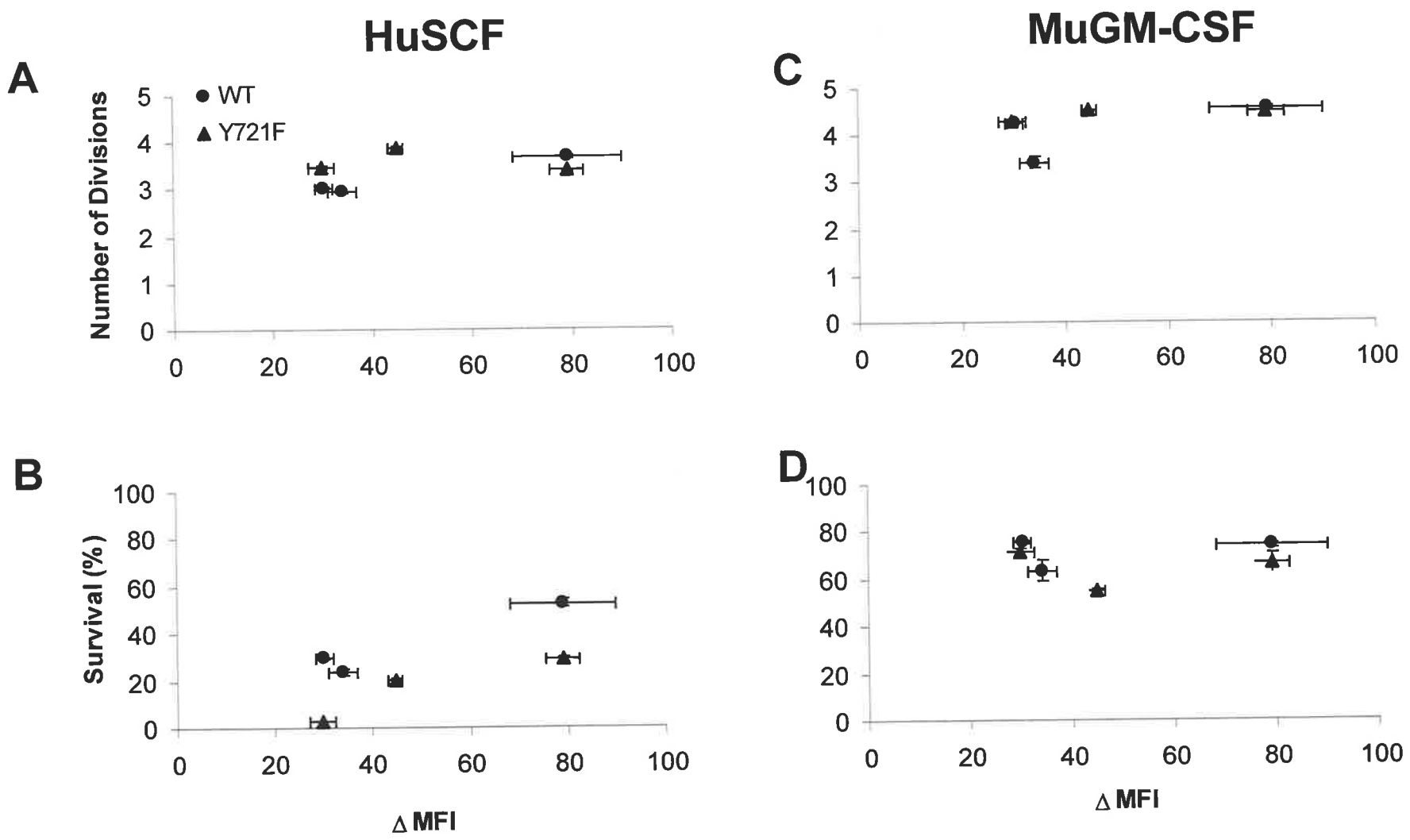
A
HuSCF
WT
Y721F
Number of Divisions
0
1
2
3
4
5
0
20
40
60
80
100
C
MuGM-CSF
B
Survival (%)
0
20
40
60
80
100
Δ MFI
D
Δ MFI

difference was observed in this assay. Proliferation and survival in muGM-CSF was not affected by the level of c-KIT expressed (Figure 4.9C and D).

4.5.1. Examination of Proliferation and Survival in Various Concentrations of huSCF

The experiments in section 4.5 used saturating levels of huSCF. To determine if Y721F c-KIT required higher doses of huSCF for maximal cell yield, proliferation or survival, a PKH assay in sub-saturating levels of huSCF was performed. Cultures were seeded at $1x10^5$/ml and harvested after 48 hours with a half-medium change at 24 hours to maintain sub-saturating levels. Three clones paired for surface expression of WT and Y721F c-KIT were analysed and used in all subsequent experiments (WT1 paired with Y721F1, WT2 paired with Y721F2 and WT4 paired with Y721F3). Results in Figure 4.10 indicated a substantial variation particularly in total cell yield and survival of FDC-P1 clones dependent on the surface expression of c-KIT. A decrease in the concentration of huSCF resulted in a decrease in survival and total cells, while the number of divisions of surviving cells remained relatively constant at all factor concentrations for both sets of clones (Figure 4.10). This was also observed for the isoforms of c-KIT (see section 3.3.2). These results suggested that survival was more dependent on the concentration of huSCF than proliferation as was shown in section 3.3.2. The concentration required for half-maximal cell yield was not altered by the receptor level or the absence of the PI 3-K binding site (average values for WT and Y721F c-KIT expressing clones were 12.5 ± 2.4 and 13.2 ± 1.5 respectively, where $p = 0.4$). A limitation with this experiment however, was that at low levels of huSCF, the concentrations could not always be maintained even though a half-medium change was performed. Therefore lack of PI 3-K recruitment did not appear to affect proliferation although it had an effect on survival.

4.5.2. Analysis of the Role of PI 3-K in Survival and Proliferation by the Use of a PI 3-K Inhibitor, LY294002

Figure 4.10: Effect of huSCF titration on proliferation, survival and total cell yield.

FDC-P1 cells infected with c-KIT constructs were seeded at a density of $1x10^5$/ml and assessed for proliferation, survival and total cell yield as described in section 2.5.3 in various levels of huSCF. Cells were harvested after 48 hours culture with a half-medium change performed after 24 hours to aid in the maintenance of huSCF concentrations. Data from triplicate experiments are represented as mean ± SEM. Data points for the number of divisions where less than 1000 viable cells remained were considered unrealistic and have been omitted. **A:** The total number of viable cells present. **B:** The average number of cell divisions of viable cells. **C**: The percentage of fluorescence yield in the viable population (survival).

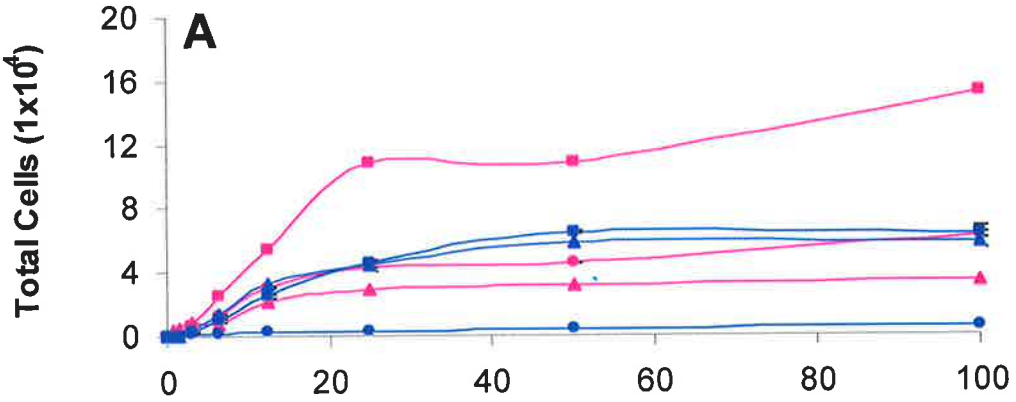
A
Total Cells (1x10⁴)
20
16
12
8
4
0
0
20
40
60
80
100

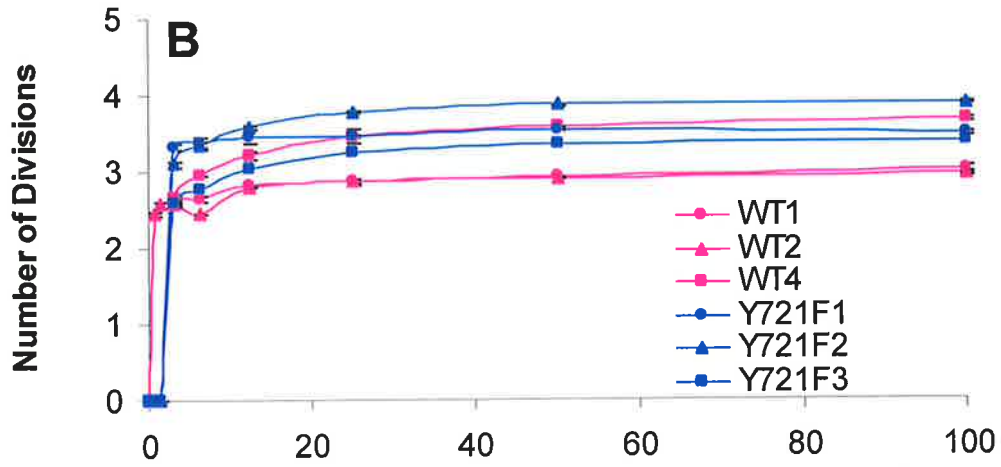
B
Number of Divisions
5
4
3
2
1
0
0
20
40
60
80
100
WT1
WT2
WT4
Y721F1
Y721F2
Y721F3

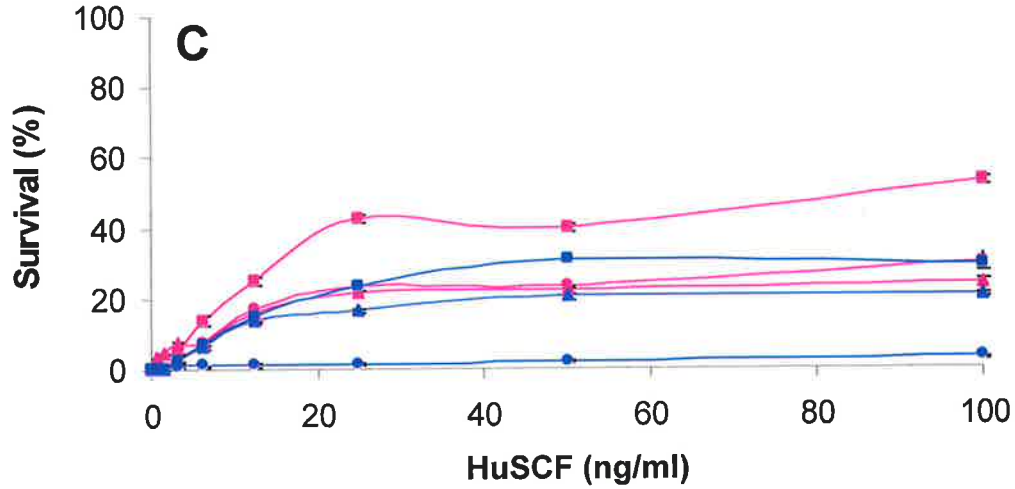
C
Survival (%)
100
80
60
40
20
0
0
20
40
60
80
100
HuSCF (ng/ml)

Direct recruitment of PI 3-K was shown to have a role in huSCF mediated growth (see section 4.5). To investigate this further, a PI 3-K inhibitor, LY294002, was used. LY294002 has been shown to be a specific inhibitor by binding competitively with ATP to PI 3-K in a reversible manner (Vlahos *et al.*, 1994). This inhibitor would block not only direct recruitment, but also any indirect activation of PI 3-K by c-KIT. It has shown to be specific at concentrations as high as 50 μM, exerting little effect on PI 4-K or MAPK activity (Vlahos *et al.*, 1994). The surface membranes of cells were stained with PKH to enable survival and proliferation calculations and were seeded in LY294002 for 1 hour prior to the addition of huSCF or muGM-CSF. Cells were harvested after 2 days and samples analysed by flow cytometry. Results presented in Figure 4.11 have been expressed as a fraction of each parameter in the absence of LY294002. FDC-P1 cells in huSCF appeared to be very sensitive to the presence of the inhibitor with no survival being observed above 5 μM LY294002 (Figure 4.11A and C). Even at the lowest concentration of LY294002 (2 μM), survival in huSCF was decreased four fold for both WT and Y721F expressing FDC-P1, while proliferation at this dose was only slightly affected (Figure 4.11B and C). The results suggested that survival in huSCF was highly dependent on functional PI 3-K. Growth in muGM-CSF also appeared to be dependent on PI 3-K activation however it was due more to an effect on proliferation than survival (Figure 4.11D and F).

4.6. KINETICS OF C-KIT ACTIVATION IN RESPONSE TO HUSCF

Lack of direct PI 3-K recruitment altered c-KIT mediated cell survival in response to huSCF. It was of interest to relate these biological responses with the biochemical events occurring upon huSCF binding, therefore receptor phosphorylation, internalisation, ubiquitination and degradation was assessed on c-KIT with or without the PI 3-K binding site. As described in section 3.4, serum starved FDC-P1 clones were stimulated with 100 ng huSCF, lysed and c-KIT was immunoprecipitated with KIT4.G12, a purified monoclonal

Figure 4.11: Effect of LY294002 on huSCF mediated cell yield, proliferation and survival.

FDC-P1 stained with PKH were seeded at a density of $1x10^5$/ml and assessed for total cell yield **(A, D)**, number of cell divisions of the viable population **(B, E)** and survival **(C, F)** in huSCF **(A, B, C)** and muGM-CSF **(D, E, F)** with varying concentrations of LY294002. Cells were harvested after 48 hours and analysed by flow cytometry. Data (mean ± SEM) from triplicate cultures has been expressed as a ratio of values in LY294002 compared to controls without LY294002. Data points for the number of divisions have been omitted where less than 1000 viable cells remained as it was considered unrealistic.

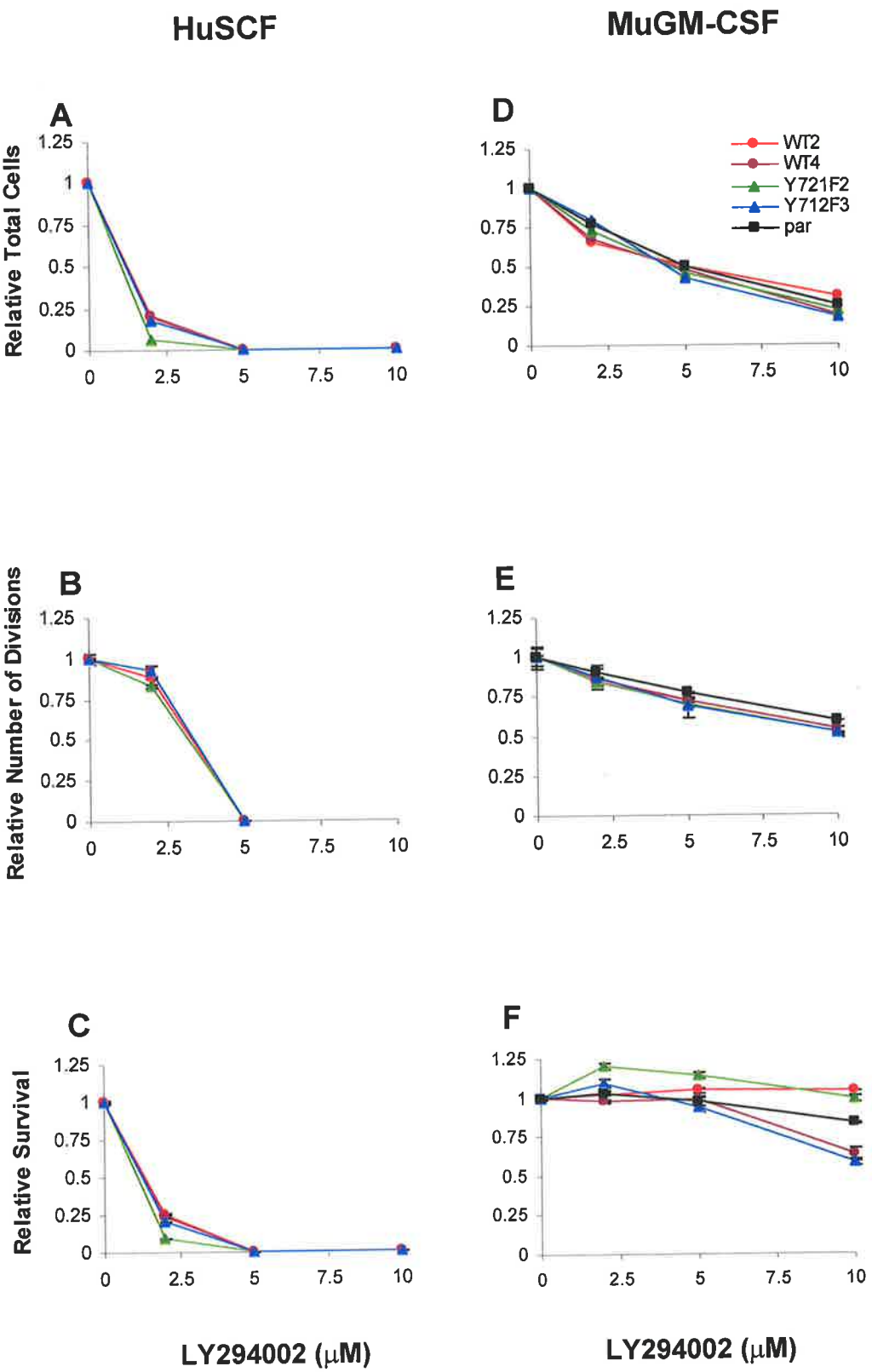
HuSCF
MuGM-CSF
A
D
B
E
C
F
Relative Total Cells
Relative Number of Divisions
Relative Survival
WT2
WT4
Y721F2
Y712F3
par
1.25
1
0.75
0.5
0.25
0
0
2.5
5
7.5
10
LY294002 (μM)
LY294002 (μM)

antibody against the extracellular region of c-KIT. Immunoprecipitates were resolved on polyacrylamide gels, transferred to PVDF and probed for phosphotyrosine, ubiquitin, c-KIT. As described in section 3.4, c-KIT immunoprecipitates from MO7e were included on the blots to control for variation in transfer and detection.

4.6.1. Phosphorylation of c-KIT in Response to huSCF

The kinetics of c-KIT phosphorylation in response to huSCF were examined on three FDC-P1 clones for each construct with a representative clone of each shown in Figure 4.12A and B. The antibody against phosphotyrosine detected a band at 145 kDa corresponding to c-KIT (Figure 4.12A and B), however no extra bands were identified (data not shown). Mutation of the PI 3-K binding site did not alter the dependence of c-KIT on huSCF for phosphorylation. Results for each clone were standardised to the level of c-KIT present and an average of the clones for each construct is shown in Figure 4.12C. Mutation of the PI 3-K binding site did not alter the time taken to reach peak phosphorylation (about 5 minutes). A 50% decrease in the average peak phosphorylation intensity for three clones was observed when the PI 3-K binding site was mutated, however this was not significant ($p = 0.07$). The rate of attrition for phosphorylation was quicker when the PI 3-K binding site was present. The inference from these results was that the Y721 site became phosphorylated rapidly and transiently after huSCF stimulation since the levels of phosphorylation were almost equivalent after stimulation for 20 minutes.

4.6.2. Ubiquitination and Degradation of c-KIT After Stimulation with SCF

Phosphorylation of c-KIT occurred as an upward smear therefore the ubiquitination of c-KIT was assessed. Low levels of ubiquitination of c-KIT was detected in most clones (as shown in section 3.4.3; Figure 3.11) however the signal obtained was too weak to enable accurate quantitation.

Figure 4.12: Phosphorylation of c-KIT in response to huSCF stimulation.

FDC-P1 clones were treated as described for Figure 4.5. Membranes were probed with two antibodies to phosphotyrosine (see Table 2.2). Primary antibody was detected with sheep anti-mouse conjugated to alkaline phosphatase. Alkaline phosphatase activity was visualised using ECF and FluorImager analysis. Included on the gels was an aliquot of c-KIT immunoprecipitate from MO7e that had been treated with (+) or without (-) 100 ng/ml huSCF for 2.5 minutes. **A:** Data from a representative WT clone, WT4. **B:** Data from a representative Y721F clone, Y721F3. **C:** Quantitation of c-KIT phosphorylation. Results for each of the clones were quantitated using ImageQuant. These were standardised against the MO7e controls loaded onto the gel and then further standardised to the amount of c-KIT present (Figure 4.13). Results are expressed as an average of the three clones analysed for each isoform, shown as mean ± SEM.

A

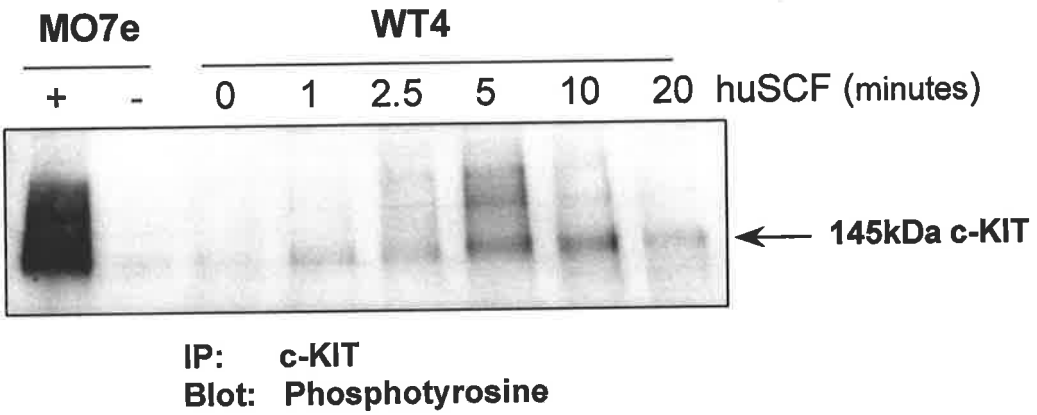

IP: c-KIT
Blot: Phosphotyrosine

B

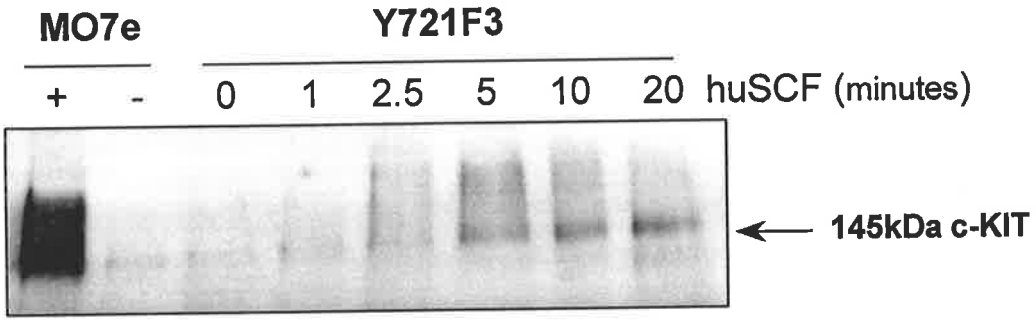

IP: c-KIT
Blot: Phosphotyrosine

C

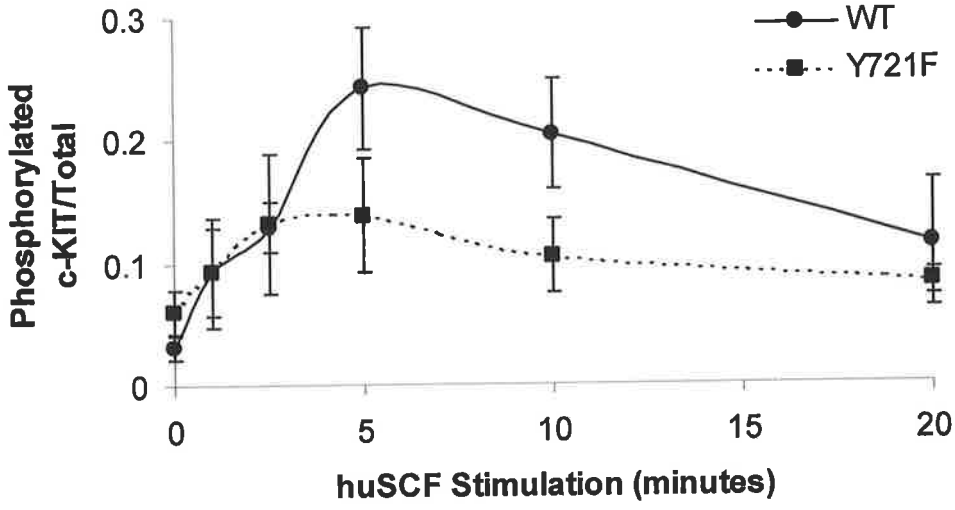

To determine the levels of c-KIT detected in the immunoprecipitates, membranes were blotted with a c-KIT specific antibody (see Figure 4.13A and B for results from two representative clones). The antibody used was shown not to detect degraded c-KIT (see section 3.2.3). Analysis was performed on three clones expressing WT and Y721F c-KIT and results were standardised to the internal MO7e control and then expressed as a ratio of the level of c-KIT in the untreated samples to correct for differences in expression levels (Figure 4.13C). Little difference in the level of c-KIT was observed throughout the time course, therefore it was not possible to determine if the mutation of Y721F in c-KIT affected degradation of c-KIT. The kinetics observed here for degradation of c-KIT were as expected since it was on the GNNK+ background of c-KIT (see section 3.4.2). It can be concluded that a lack of PI 3-K did not upregulate degradation however it remains unknown from this study if it was required.

4.7. INTERNALISATION OF C-KIT AFTER STIMULATION BY HUSCF

Previous experiments in the DA-1 murine lymphoma cell line have shown that PI 3-K is involved in SCF mediated internalisation of c-KIT (Gommerman *et al.*, 1997). It is not solely required though since the lack of direct PI 3-K recruitment must be coupled with a lack of calcium flux to prevent endocytosis (Gommerman *et al.*, 1997). To analyse the role of PI 3-K in c-KIT internalisation in early myeloid cells, FDC-P1 cells were starved of serum and factor for 2 hours and stimulated with either huSCF or muGM-CSF at 37°C. Reactions were terminated by the addition of an equal volume of ice cold PBS/BSA with 0.2% Az and incubation on ice. Samples were labelled for c-KIT using indirect immunofluorescence and analysed by flow cytometry. Antibodies used were 1DC3, an antibody to c-KIT, and the isotype matched negative control, 1B5.

The inhibition of antibody binding (1DC3) due to the presence of huSCF, was determined as described in section 3.5. Mutation of the PI 3-K binding site did not affect the

Figure 4.13: Degradation of c-KIT in response to huSCF stimulation.

FDC-P1 clones were treated as described for Figure 4.5. Membranes were probed using an antibody against the carboxy terminal tail of c-KIT and detected with sheep anti-rabbit alkaline phosphatase conjugate. Alkaline phosphatase activity was visualised using ECF and FluorImager analysis. **A:** Data from a representative WT clone, WT4. **B:** Data from a representative Y721F clone, Y721F3. **C:** Quantitation of c-KIT in FDC-P1 clones. Results for each of the clones were quantitated using ImageQuantTM software. These were standardised against the MO7e control loaded onto the gel and further standardised to the level of c-KIT in the absence of huSCF. Results are expressed as an average of three clones for each isoform, shown as mean ± SEM.

A

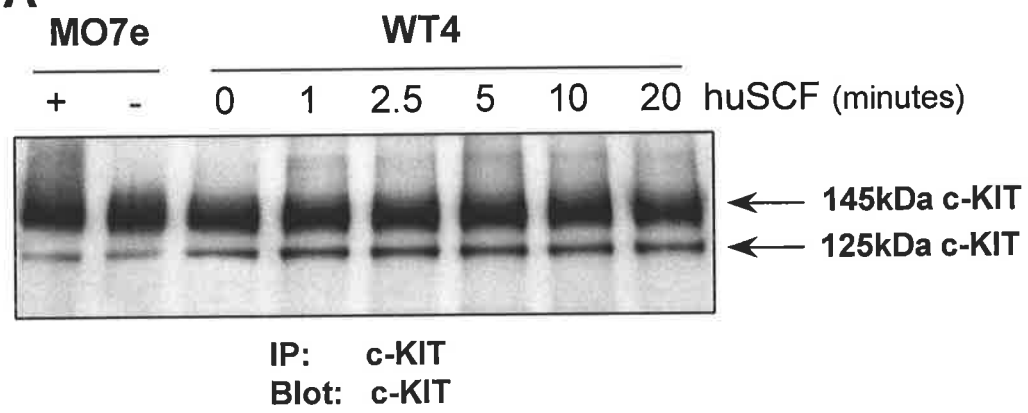
MO7e
WT4
+
-
0
1
2.5
5
10
20
huSCF (minutes)
145kDa c-KIT
125kDa c-KIT
IP: c-KIT
Blot: c-KIT

B

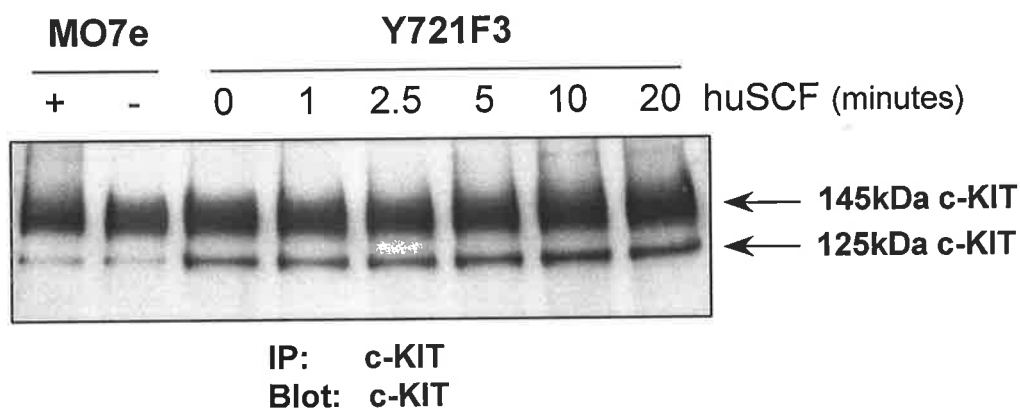
MO7e
Y721F3
+
-
0
1
2.5
5
10
20
huSCF (minutes)
145kDa c-KIT
125kDa c-KIT
IP: c-KIT
Blot: c-KIT

C

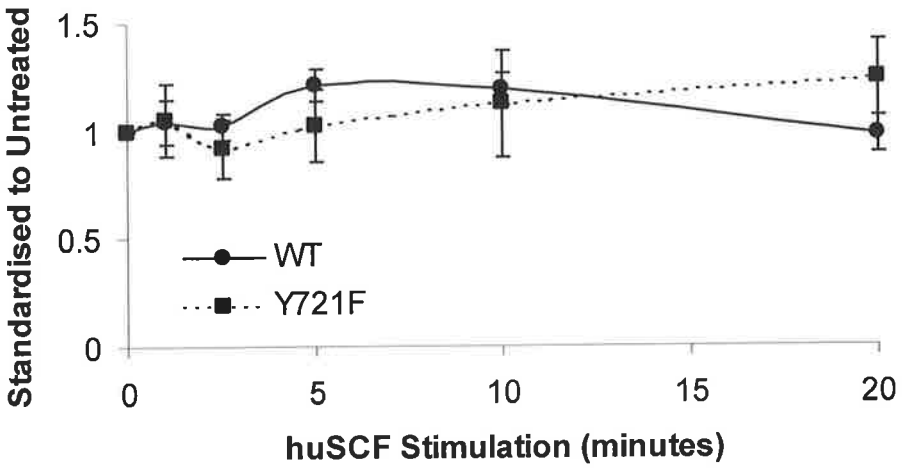
Standardised to Untreated
1.5
1
0.5
0
WT
Y721F
0
5
10
15
20
huSCF Stimulation (minutes)

inhibition due to the presence of huSCF with values for WT and Y721F c-KIT expressing cells being 80 ± 4.4% and 85 ± 0.7% of the control respectively.

With increasing huSCF stimulation, a decrease in surface expression of c-KIT was observed (Figure 4.14A and B). This was due to internalisation of c-KIT and not degradation since degradation was not observed over the time course studied (Figure 4.13C). Cells expressing both WT and Y721F c-KIT constructs internalised with similar kinetics with no significant decrease in internalisation being observed after 20 and 30 minutes of huSCF treatment ($p > 0.05$). Incubation with muGM-CSF did not result in c-KIT internalisation (Figure 4.14) confirming that the internalisation was due to an effect of huSCF on c-KIT.

In chapter 3, it was shown that the GNNK- isoform internalised more rapidly as compared to the GNNK+ isoform (Figure 3.12). Therefore it was possible that any reduction in ligand dependent internalisation as a result of the Y721F mutation in c-KIT was masked through the use of the GNNK+ isoform. To examine this further, a construct of GNNK- c-KIT with a Y721F mutation was created. The region of c-KIT containing the Y721F mutation was excised with restriction enzymes *Acc*III and *Apa*I and ligated into pRUFMC1*neo* containing GNNK- c-KIT that had been similarly treated. Psi2 cells were transfected with the GNNK-Y721F construct and factor dependent FDC-P1 cells were infected with the retrovirus. Cells were sorted based on c-KIT expression and the amount of c-KIT internalised was analysed on a pooled population of cells expressing GNNK- or GNNK-Y721F c-KIT. Results were analysed after 10 minutes huSCF stimulation since this was the minimal time required for maximal internalisation of the GNNK- isoform. Again, huSCF induced internalisation of the wild type (GNNK-) c-KIT and the isoform matched Y721F mutant to similar extents with no statistical significance being observed ($p = 0.13$) (Figure 4.15). This suggested that internalisation of both c-KIT isoforms is substantially independent of direct PI 3-K recruitment.

Figure 4.14: Internalisation of c-KIT in response to huSCF.

Cells starved of serum and factor for 2 hours were stimulated with huSCF at 37°C. Reactions were terminated at various time points by incubation on ice and the addition of an equal volume of ice cold PBS/BSA with 0.2% Az. Samples were labelled for c-KIT using indirect immunofluorescence and analysed by flow cytometry. **A:** Primary data from a representative WT clone, WT2, showing the amount of surface c-KIT after huSCF stimulation. **B:** Primary data from a representative Y721F clone, Y721F2, showing amount of surface c-KIT after huSCF stimulation. **C:** Changes in surface expression in the presence of huSCF or muGM-CSF. Average ± SEM of three clones after correction for decreased antibody binding in the presence of huSCF. Results are expressed as a percentage of c-KIT remaining on the surface after various times of huSCF and muGM-CSF stimulation.

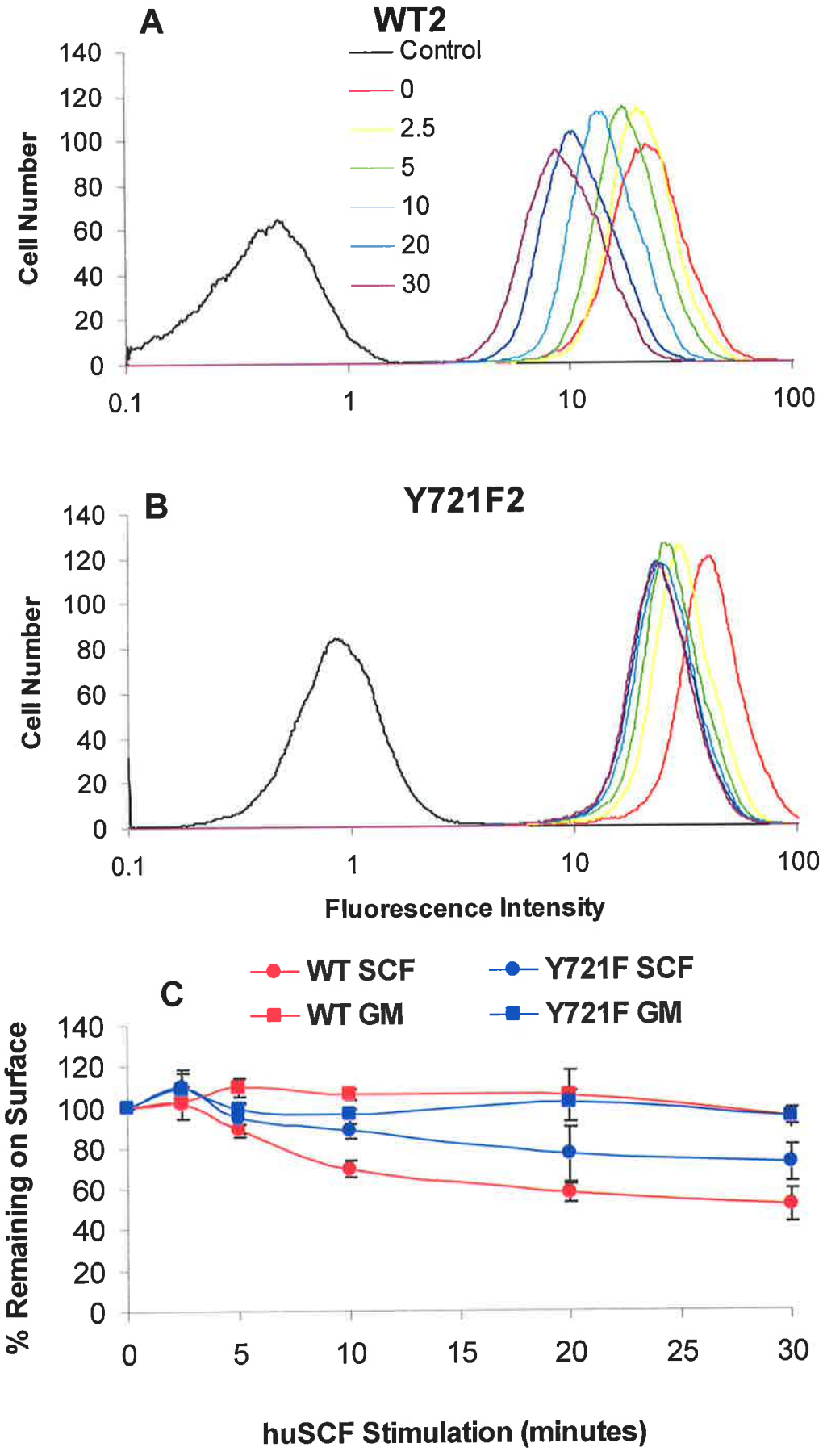
A
WT2
Control
0
2.5
5
10
20
30
Cell Number
140
120
100
80
60
40
20
0
0.1
1
10
100
B
Y721F2
Cell Number
Fluorescence Intensity
C
WT SCF
WT GM
Y721F SCF
Y721F GM
% Remaining on Surface
0
5
10
15
20
25
30
huSCF Stimulation (minutes)

Figure 4.15: Role of Y721F in the internalisation of GNNK- isoform of c-KIT.

Pooled populations of FDC-P1 cells expressing GNNK-S+ isoform of c-KIT with (GNNK-) or without (GNNK-Y721F) the PI 3-K binding site were starved of serum and factor for 2 hours and stimulated with huSCF or muGM-CSF for 10 minutes at 37°C. Reactions were terminated by the addition of an equal volume of PBS/BSA with 0.2%Az and incubation on ice and labelled for c-KIT by indirect immunofluorescence using 1DC3. The percent of c-KIT remaining on the surface is shown as mean ± SD from a duplicate experiment after correction for background fluorescence (1B5) and inhibition of antibody binding due to the presence of huSCF.

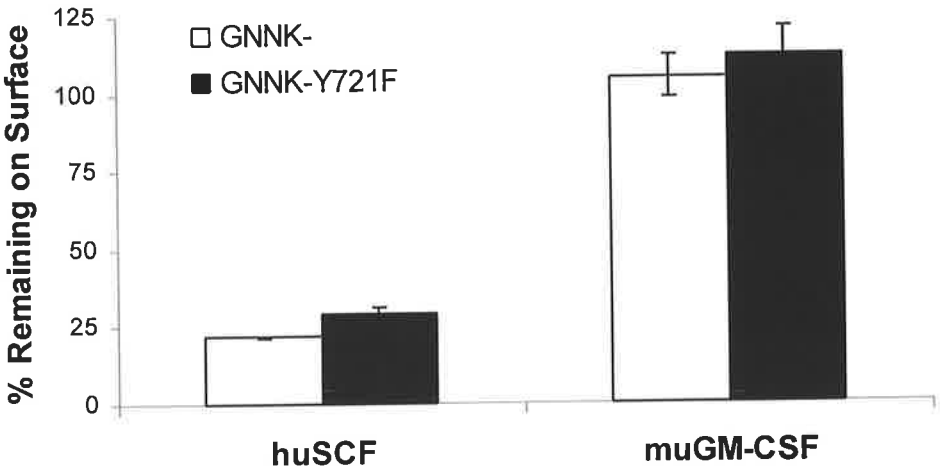
% Remaining on Surface
125
100
75
50
25
0
GNNK-
GNNK-Y721F
huSCF
muGM-CSF

4.8. Signal Transduction Pathways Activated Downstream of c-KIT

The activity of several protein kinases downstream of RTKs can be detected based on their phosphorylation, which is required for their activation. To assess the activation state of Akt and ERK1 and ERK2, antibodies raised against phosphorylated peptides were used as described in section 3.6.2 and 3.6.3. Briefly, whole cell lysates prepared in parallel to immunoprecipitates described in section 4.6 were resolved by SDS-PAGE, transferred to membrane and immunoblotted with phospho-specific antibody as well as an antibody detecting the total levels of the protein present. As with the immunoprecipitates, standard lysates from the human megakaryocytic cell line MO7e, stimulated with and without huSCF, were electrophoresed in parallel to the FDC-P1 lysates to control for transfer and immunoblotting differences to enable comparison between blots.

4.8.1. HuSCF Mediated Activation of Akt

Akt is a major downstream effector of PI 3-K which becomes phosphorylated and activated in response to c-KIT stimulation (Caruana *et al.*, 1999). To investigate the requirement of the PI 3-K binding site for the activation of Akt in FDC-P1 cells, the phosphorylation of S473 was assessed with phospho-specific antibodies. It was expected that the lack of direct PI 3-K recruitment to c-KIT would impair Akt activation. Results from representative clones showed that even though Y721F c-KIT was incapable of recruiting PI 3-K, it could still lead to huSCF dependent phosphorylation of Akt (Figure 4.16A and B). Similar amounts of total Akt were present in each track (Figure 4.16C and D). Quantitation of the results from three clones revealed that the amount of Akt activated by Y721F c-KIT was reduced by about 50% as compared to WT c-KIT but this difference was not statistically significant ($p = 0.14$). After 20 minutes huSCF stimulation, the levels of Akt phosphorylation

Figure 4.16: Activation of Akt in response to huSCF.

FDC-P1 clones expressing WT and Y721F c-KIT were starved of serum and factor for 2 hours, stimulated with 100 ng/ml huSCF at a density of $1x10^7$/ml and then lysed. Clarified lysates (15 μl) were loaded onto 10% gels, transferred to membranes and probed for either phosphorylated Akt **(A, B)** or total Akt **(C, D)**. Primary antibody was detected with a secondary antibody conjugated to alkaline phosphatase activity. Alkaline phosphatase activity was visualised using ECF and FluorImager analysis. Included on the gels was an aliquot of MO7e clarified lysate treated with or without 100 ng/ml huSCF for 2.5 minutes. **A, C:** Data from representative WT clone, WT4. **B, D:** Data from a representative Y721F clone, Y721F3. **E:** Quantitation of Akt phosphorylation. Results from three clones for each construct were quantitated using ImageQuant and standardised against the MO7e loading control. Phosphorylated Akt was expressed as a ratio of the total amount of Akt present and plotted as mean ± SEM.

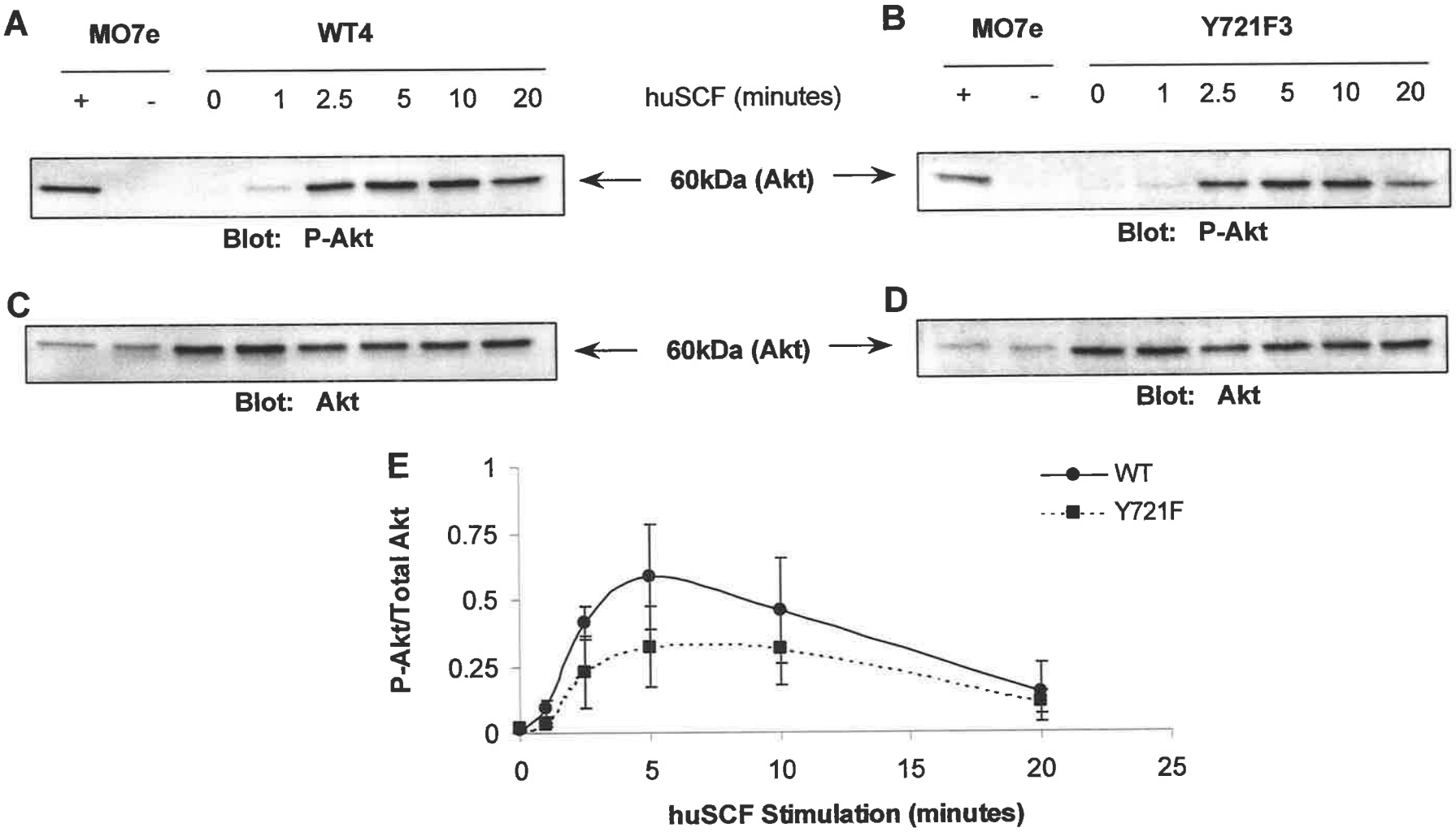
A
MO7e
WT4
+
-
0
1
2.5
5
10
20
huSCF (minutes)
60kDa (Akt)
Blot: P-Akt
B
MO7e
Y721F3
+
-
0
1
2.5
5
10
20
Blot: P-Akt
C
60kDa (Akt)
Blot: Akt
D
Blot: Akt
E
P-Akt/Total Akt
1
0.75
0.5
0.25
0
WT
Y721F
0
5
10
15
20
25
huSCF Stimulation (minutes)

were similar. Thus, alternative mechanisms were capable of mediating huSCF dependent Akt activation in the absence of direct PI 3-K recruitment to the Y721 site of c-KIT.

4.8.2. HuSCF Mediated Activation of ERK

Both ERK1 and ERK2 are known to be activated by c-KIT (Funasaka *et al.*, 1992; Miyazawa *et al.*, 1991). To determine if mutation of the PI 3-K binding site altered the activation of ERK1 and ERK2, the phosphorylation status of both isoforms was assessed. Phosphorylation of ERK1 and ERK2 was detected with a phospho-specific antibody raised against a peptide phosphorylated on T202 and Y204 with results from a representative Western blot presented in Figure 4.17A and B. Blots shown in Figure 4.17C and D show the total amount of ERK1 and ERK2 detected in representative WT and Y721F c-KIT expressing clones. Three clones for each construct were analysed by Western blotting and results were standardised against the MO7e control and then phosphorylated ERK was expressed as a ratio to the total amount of ERK present (Figure 4.17E). Results showed that mutation of the PI 3-K binding site did not alter the kinetics of ERK phosphorylation since both peaked approximately five minutes post huSCF stimulation. Levels of ERK phosphorylation were 1.7 fold lower in Y721F c-KIT expressing cells as compared to WT however this was not statistically significant ($p = 0.1$). After 20 minutes huSCF stimulation the amount of phosphorylated ERK had returned to near basal levels in all cases. Therefore direct recruitment of PI 3-K to c-KIT may have had some role in the initial activation of ERK isoforms.

4.9. Derivation of c-KIT Expressing MIHC

Proliferation and survival responses due to huSCF stimulation were analysed in FDC-P1 cells, however other parameters of biological response, such as differentiation could not be studied. It was anticipated that the MIHC model, capable of differentiating into

Figure 4.17: Activation of ERK1 and ERK2 in response to huSCF.

FDC-P1 clones expressing c-KIT constructs were starved of serum and factor for 2 hours, stimulated with 100 ng/ml huSCF at a density of $1x10^7$/ml and then lysed. Clarified lysates were loaded onto 10% gels, transferred to membranes and probed with antibodies to phosphorylated ERK1 and ERK2 **(A, B)** or ERK1 and ERK2 **(C, D)**. Primary antibody was detected with a secondary antibody conjugated to alkaline phosphatase activity. Alkaline phosphatase activity was visualised using ECF and FluorImager analysis. Included on the gels was an aliquot of MO7e clarified lysate treated with or without 100 ng/ml huSCF for 2.5 minutes. **A, C:** Data from a representative WT c-KIT expressing clone, WT4. **B, D:** Data from a representative Y721F c-KIT expressing clone, Y721F3. **E:** Quantitation of ERK phosphorylation. Results from three clones for each construct were quantitated using ImageQuant and standardised against the MO7e loading control. Phosphorylated ERK was expressed as a ratio of the total amount of ERK present and plotted as mean ± SEM.

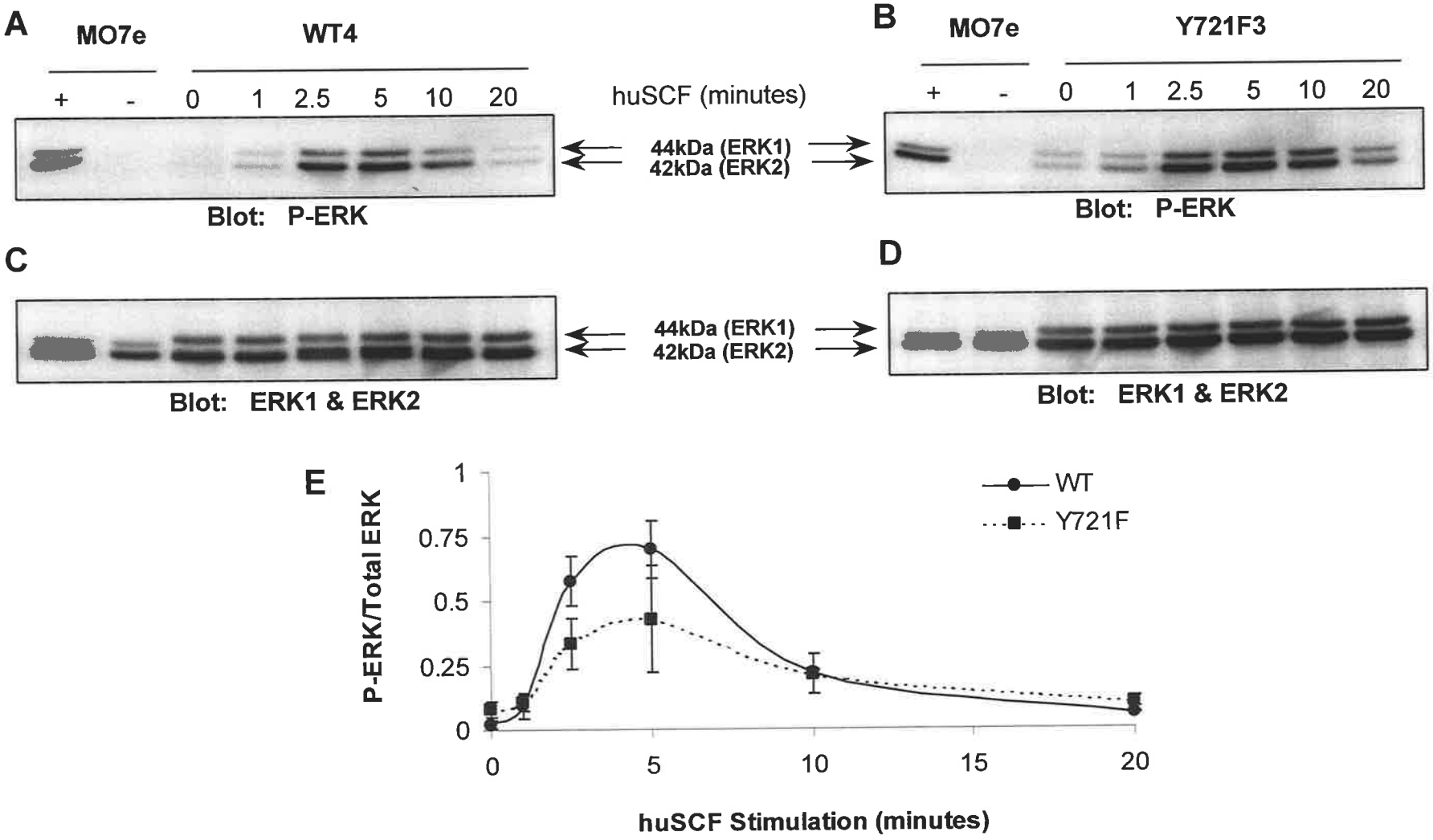
A
MO7e
WT4
+
-
0
1
2.5
5
10
20
huSCF (minutes)
44kDa (ERK1)
42kDa (ERK2)
Blot: P-ERK
B
MO7e
Y721F3
+
-
0
1
2.5
5
10
20
Blot: P-ERK
C
44kDa (ERK1)
42kDa (ERK2)
Blot: ERK1 & ERK2
D
Blot: ERK1 & ERK2
E
P-ERK/Total ERK
1
0.75
0.5
0.25
0
0
5
10
15
20
WT
Y721F
huSCF Stimulation (minutes)

granulocytes and monocytes (Ferrao *et al.*, 1997) could be used to analyse the effect PI 3-K recruitment had on differentiation. Based on data presented in chapter 3 concerning the background differentiation of the parental MIHC and clones expressing c-KIT the model was shown to be unsuitable. Therefore, the MIHC model was used instead to confirm proliferation and survival responses observed in FDC-P1.

MIHC derived from day 14 murine foetal livers infected with a truncated version of myb were selected for long term growth in muGM-CSF. Cells were superinfected with GNNK+ *c-KIT* constructs with or without the PI 3-K binding site by co-cultivation with transfected virus packaging psi2 cells. Infected cells expressing surface c-KIT were sorted into populations based on the binding of monoclonal antibody 1DC3 and fluorescence activated cell sorting. Clonal populations were obtained using the automated cell deposition facility of the fluorescence activated cell sorter. Clones were amplified and compared in regard to their surface expression of c-KIT. A narrow range of c-KIT was present in all clonal isolates, as opposed to FDC-P1 clones, which expressed a broad range of c-KIT. Five clones each of WT c-KIT and Y721F c-KIT expressing MIHC were chosen for further analysis. Surface expression of these clones was analysed in duplicate and is shown in Figure 4.18A. Expression of c-KIT on MIHC was also examined by immunohistochemistry (APAAP), a staining technique that allows detection of both surface and intracellular c-KIT. Cytocentrifuge smears of cells were fixed and incubated with an antibody to c-KIT (1DC3) or an isotype matched negative control, 1B5. The presence of c-KIT was denoted by red staining, while the nucleus was stained purple by haematoxylin counterstain (Figure 4.18B and D). Parental MIHC remained unstained with antibody to c-KIT (Figure 4.18B). Similarly no staining was observed with the negative control antibody for any of the clones (data not shown). Faint red staining was observed in all clones treated with antibody to c-KIT indicating a low level of c-KIT expression (Figure 4.18C and D). A representative clone for each construct is shown is Figure 4.18C and D. Selected clones were maintained in

Figure 4.18: Expression of c-KIT in MIHC clones.

MIHC infected with WT and Y721F c-KIT and maintained in muGM-CSF and muIL-3 were sorted into clones based on the surface expression of c-KIT. **A:** Surface expression of c-KIT in MIHC clones. After expansion, surface expression of c-KIT was determined for each clone by indirect immunofluorescence using monoclonal antibody 1DC3 (anti-c-KIT) and an isotype matched negative control 1B5 (anti-*giardia*). The histogram shows the relative surface expression of WT and Y721F c-KIT in MIHC clones after correction for background levels (where ΔMFI represents the change in mean fluorescence intensity). Results are mean ± SD from a duplicate experiment. In the figure, par represents parental MIHC. **B-D:** Expression of c-KIT as determined by immunohistochemistry. Cells cytocentrifuged onto glass slides were fixed and incubated with anti-c-KIT antibody (1DC3) or an isotype matched negative control (1B5). Detection of 1DC3 or 1B5 was performed using a bridging rabbit anti-mouse antibody, followed by APAAP complex. Cells were incubated with substrate causing c-KIT positive cells to be stained red. A haematoxylin counterstain stained the nucleus purple. Cells were visualised on an Olympus microscope and photographed with a 20x objective lens. **B**: Parental cells stained with 1DC3, **C**: MIHC WT2 clones stained with 1DC3, **D**: MIHC Y721F3 clone stained with 1DC3.

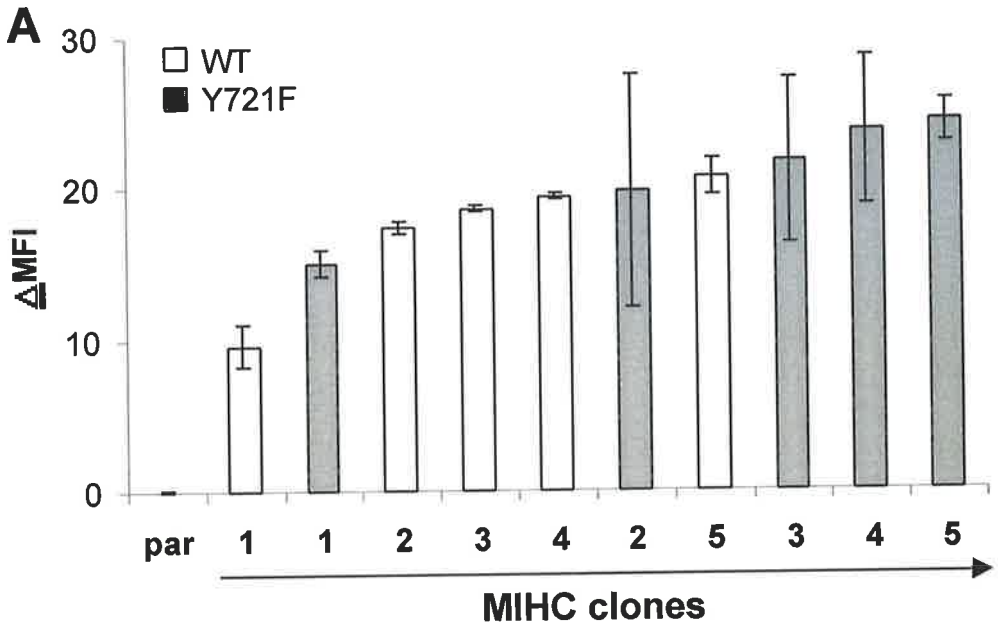
A
30
20
10
0
ΔMFI
WT
Y721F
par
1
1
2
3
4
2
5
3
4
5
MIHC clones

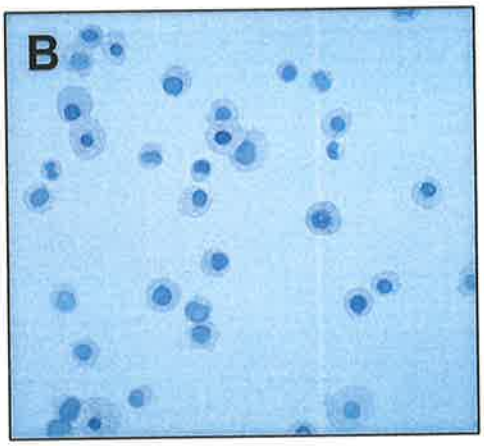
B

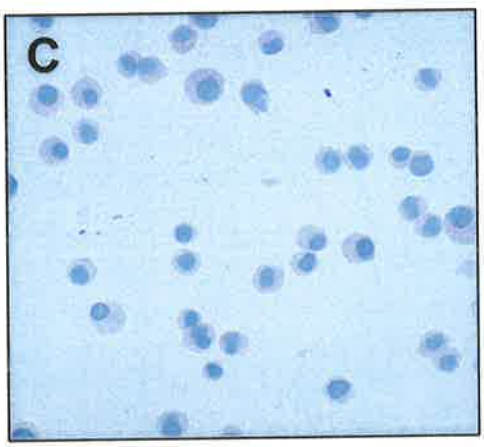
C

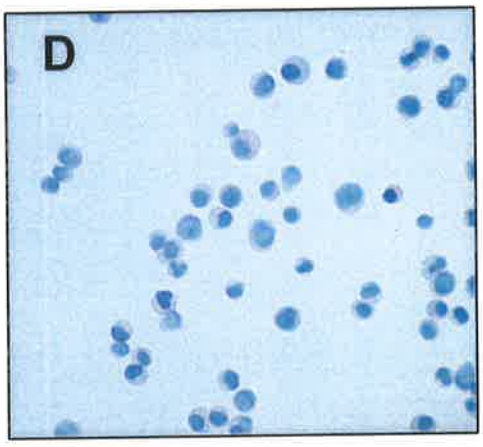
D

muGM-CSF and muIL-3 for about three weeks after which fresh cells were thawed from cryopreserved stocks.

4.10. Role of PI 3-K in c-KIT Mediated Biological Responses in MIHC

4.10.1. Growth in the Presence of huSCF

To investigate whether the expression of c-KIT lacking the PI 3-K binding site could promote huSCF dependent growth, a MTT assay was performed (see section 2.5.2). Cells were cultured in no factor, saturating huSCF or muGM-CSF and muIL-3 for up to 6 days. In the absence of factor, growth was not observed, confirming that these cells were factor dependent (Figure 4.19A and B). Growth was observed for both WT and Y721F c-KIT expressing cells in huSCF confirming that the c-KIT expressed was functional (Figure 4.19C and D). There was no statistical significance between the growth observed in huSCF for WT or Y721F c-KIT expressing cells after culture for either 4 or 6 days ($p > 0.07$ and 0.14 respectively) suggesting that lack of direct PI 3-K recruitment did not affect growth in this case. Similarly, there was no statistical difference in muGM-CSF and muIL-3 mediated growth of WT and Y721F c-KIT expressing clones ($p > 0.44$ after 4 days culture) (Figure 4.19E and F). The range of growth observed in muGM-CSF and muIL-3 possibly reflected the intrinsic ability of each clone to differentiate. This differing ability to grow and differentiate would affect results in huSCF. To examine this, the growth in huSCF after 4 days was expressed as a ratio of that in muGM-CSF and muIL-3. Results confirmed the above showing no significant difference between the growth of Y721F and WT c-KIT expressing cells in huSCF ($p = 0.06$).

Figure 4.19: Cellular growth in the absence or in the presence of huSCF or muGM-CSF and muIL-3.

Uninfected MIHC or MIHC clones expressing c-KIT with or without the PI 3-K binding site were seeded at a density of $2.5x10^4$/ml and assessed for total number of cells by absorbance after 0, 2, 4 and 6 days culture in the absence of factor **(A, B)**, in the presence of 100 ng/ml huSCF **(C, D)** or in the presence of muGM-CSF and muIL-3 **(E, F)**. Growth was analysed by absorbance at 490 nm. Data is presented as mean ± SEM of triplicate determinations. Due to overgrowth, time points for cultures in muGM-CSF at day 6 have been omitted.

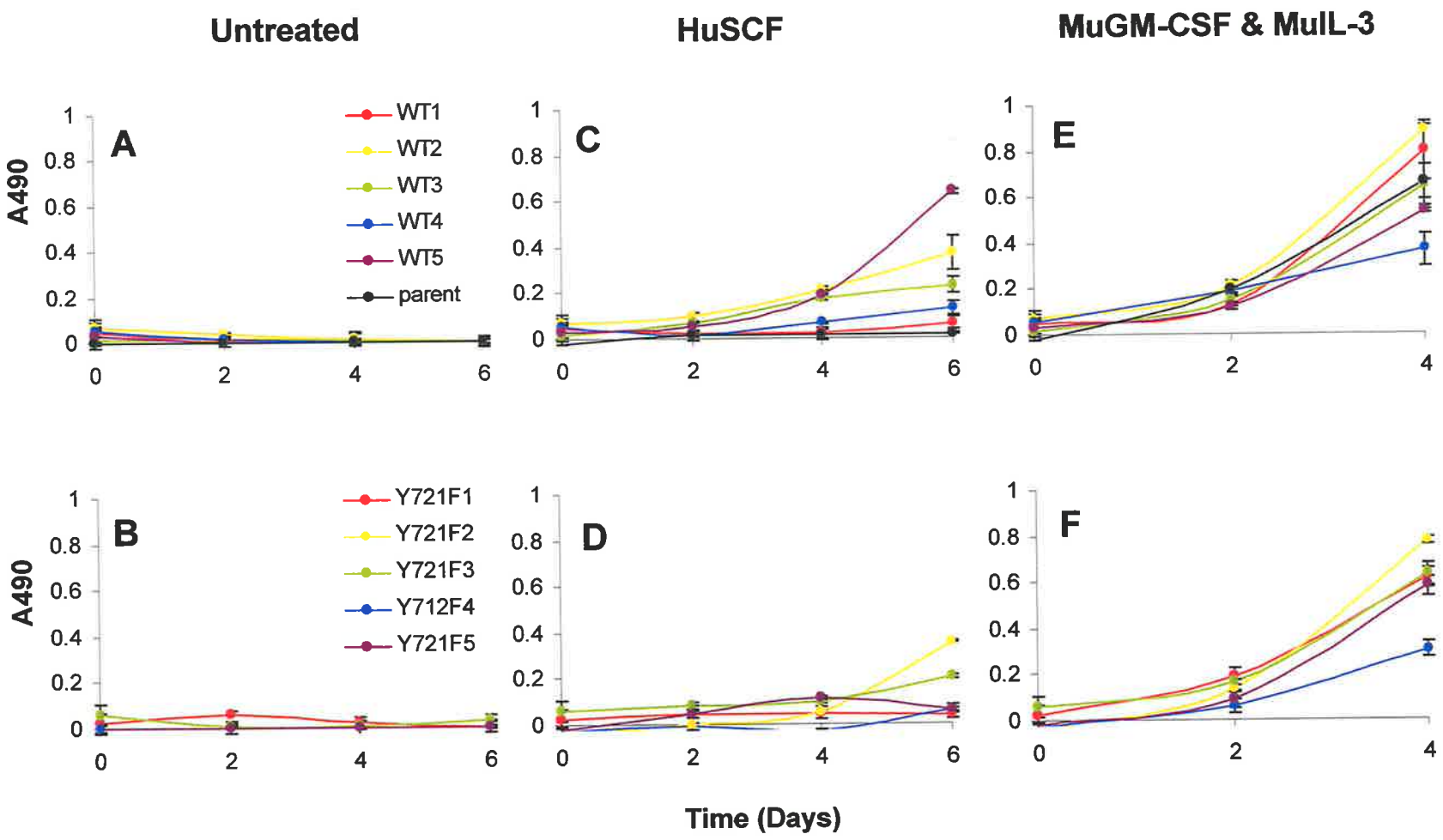
Untreated
HuSCF
MuGM-CSF & MuIL-3
A
B
C
D
E
F
A490
WT1
WT2
WT3
WT4
WT5
parent
Y721F1
Y721F2
Y721F3
Y712F4
Y721F5
Time (Days)

4.10.2. The Effect of Limiting huSCF on Proliferation and Survival

An alternate technique used to look at the effect huSCF had on cellular growth was by PKH assay. As performed in section 4.5.1, huSCF was titrated to determine if proliferation and survival for WT and Y721F c-KIT was concentration dependent. Cells for this experiment stained with PKH-26 were washed three times in serum free DMEM and seeded at $2x10^4$/ml in wells containing various concentrations of huSCF, muGM-CSF and muIL-3 or no factor. After 24 hours incubation, a half-medium change was performed to maintain limiting concentrations of huSCF and cells were harvested after 48 hours. Harvested cells were analysed by flow cytometry with only viable cells gated. Three clones were analysed for each construct (GNNK+2, 4, and 5 and Y721F1, 2 and 3) and since they all expressed similar levels of c-KIT, results were averaged (Figure 4.20). No difference was observed in the concentration required for half-maximal cell yield, which was approximately 7.5 ng/ml and 5 ng/ml for WT and Y721F c-KIT expressing cells respectively. Titration of huSCF affected survival but had little effect on the number of divisions undergone by surviving cells. That is, for these cells, as for FDC-P1 cells, the requirement of huSCF for survival appeared to be limiting.

Comparisons between clones expressing Y721F and WT c-KIT in saturating huSCF revealed a statistically significant decrease in the total cell yield ($p = 0.046$) and survival ($p = 0.017$) when the PI 3-K binding site was mutated, however the proliferation rate remained unaffected ($p > 0.3$). The statistically significant difference in cell yield was in contrast to the results from the MTT assay. To investigate this further, results in huSCF were standardised to those in muGM-CSF and muIL-3, which were performed in parallel. Results confirmed the above showing that there was a statistically significant decrease in survival ($p = 0.047$) with mutation of the PI 3-K recruitment site, while proliferation remained unaffected ($p > 0.4$).

Figure 4.20: Effect of huSCF titration on proliferation, survival and total cell yield.

MIHC clones expressing c-KIT with (WT) or without (Y721F) the PI 3-K binding site were seeded at a density of $2x10^4$/ml and assessed for proliferation, survival and total cells in sub-optimal levels of huSCF. Cells were harvested after 48 hours culture with a medium change performed after 24 hours to ensure the maintenance of the sub-optimal huSCF concentrations. Data from a triplicate experiment is expressed as mean ± SEM of results obtained from three clones for each c-KIT construct. Data points for the number of divisions where less than 1000 viable cells remained were considered unrealistic and have been omitted. **A:** The total number of viable cells present. **B:** The average number of cell divisions of the viable population. **C:** The percent fluorescence yield in the viable population (survival). Statistical significance ($\alpha < 0.05$) is represented by a *.

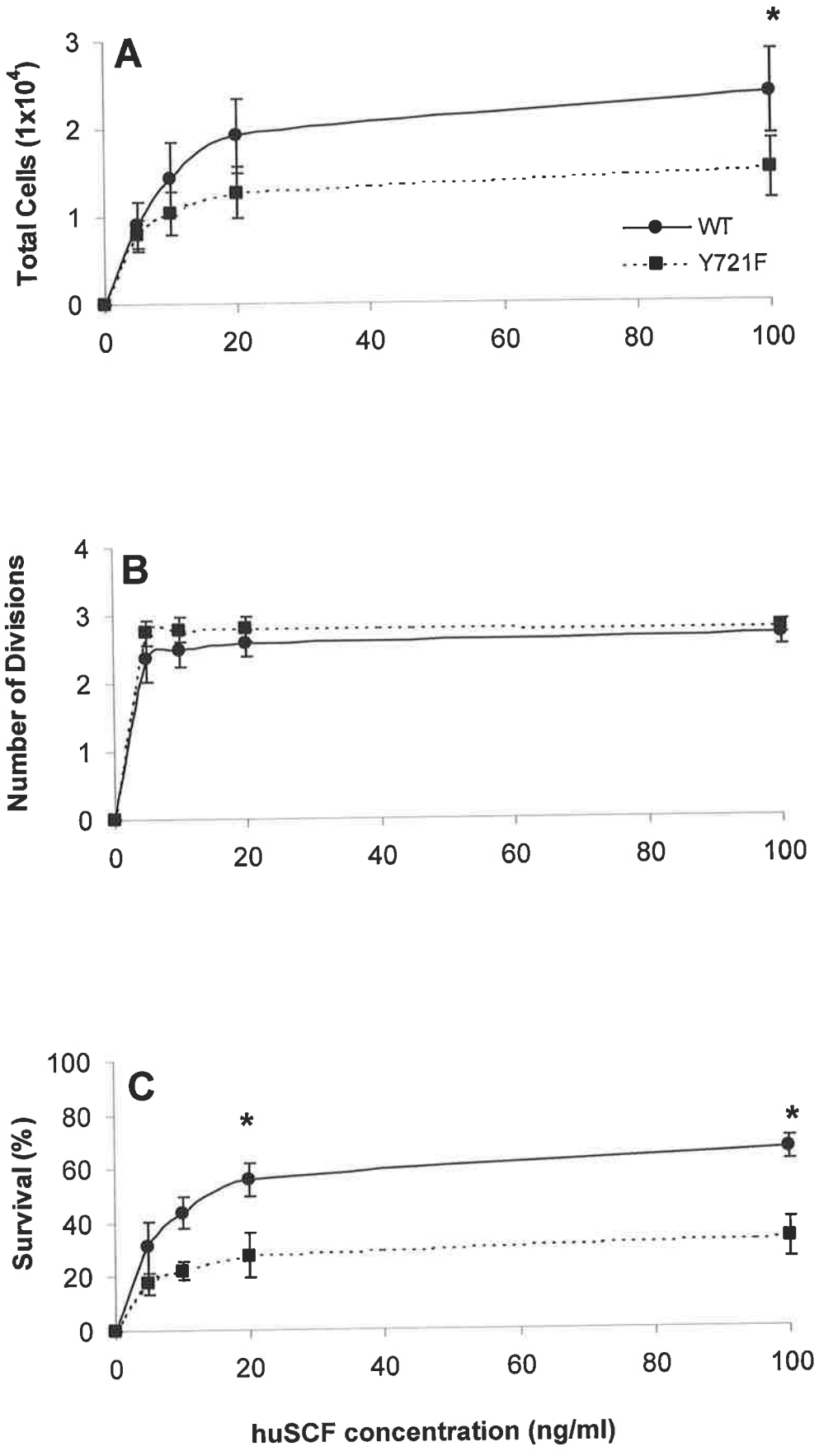
A
Total Cells (1x10^4)
3
2
1
0
0
20
40
60
80
100
*
WT
Y721F
B
Number of Divisions
4
3
2
1
0
0
20
40
60
80
100
C
Survival (%)
100
80
60
40
20
0
0
20
40
60
80
100
*
*
huSCF concentration (ng/ml)

At limiting concentrations of huSCF (10ng/ml) the clones appeared to behave similarly as compared to in saturating huSCF. Again, a statistically significant decrease in survival was observed for cells expressing Y721F c-KIT ($p = 0.017$), while proliferation was unaffected ($p > 0.15$). Therefore mutation of the PI 3-K binding site results in decreased survival without affecting proliferation.

4.10.3. Effect of a PI 3-K Inhibitor on Proliferation and Survival in the Presence of huSCF

A role of direct recruitment for PI 3-K in survival and total cell yield was observed in section 4.10.2. To further determine the role of PI 3-K in huSCF mediated survival and growth, an inhibitor, LY294002 was used in a PKH assay as used in section 4.5.2. Cells were stained with PKH a day prior to seeding in LY294002 and either huSCF (100ng/ml) or saturating muGM-CSF and muIL-3. Cells were harvested after 2 days and analysed by flow cytometry. Total cell yield, proliferation and survival were calculated and results were standardised to observations in the absence of LY294002. Since all MIHC clones expressed similar levels of surface c-KIT, results of the three clones were averaged and are presented in Figure 4.21. In huSCF, total cells obtained for WT and Y721F c-KIT expressing cells were inhibited to a similar extent by the addition of LY294002. This inhibition was partly due to reduced proliferation but more dependent on survival. Effects of LY294002 were also seen for cells grown in muGM-CSF and muIL-3 suggesting that this was dependent on PI 3-K activity to a certain extent. The growth of MIHC clones in huSCF did not appear to be as sensitive to LY294002 as compared to FDC-P1 since even at 10 μM approximately 30% survival was observed whereas there was no survival of FDC-P1 cells at 5 μM LY294002. Both cell lines were equally susceptible to LY294002 when maintained in muGM-CSF (and muIL-3 for MIHC). This suggested that LY294002 was active to the same extent in both

Figure 4.21: Effect of LY294002 on huSCF mediated cell yield, proliferation and survival in MIHC.

MIHC clones stained with PKH were seeded at a density of $1x10^5$/ml and assessed for total cell yield **(A, D)**, number of cell divisions of the viable populations **(B, E)** and survival **(C, F)** in huSCF **(A, B, C)** and muGM-CSF and muIL-3 **(D, E, F)** with varying concentrations of LY294002. Cells were harvested after 48 hours and analysed by flow cytometry. Data (mean ± SEM) from triplicate determinations is expressed as a ratio of values in LY294002 compared to controls without LY294002.

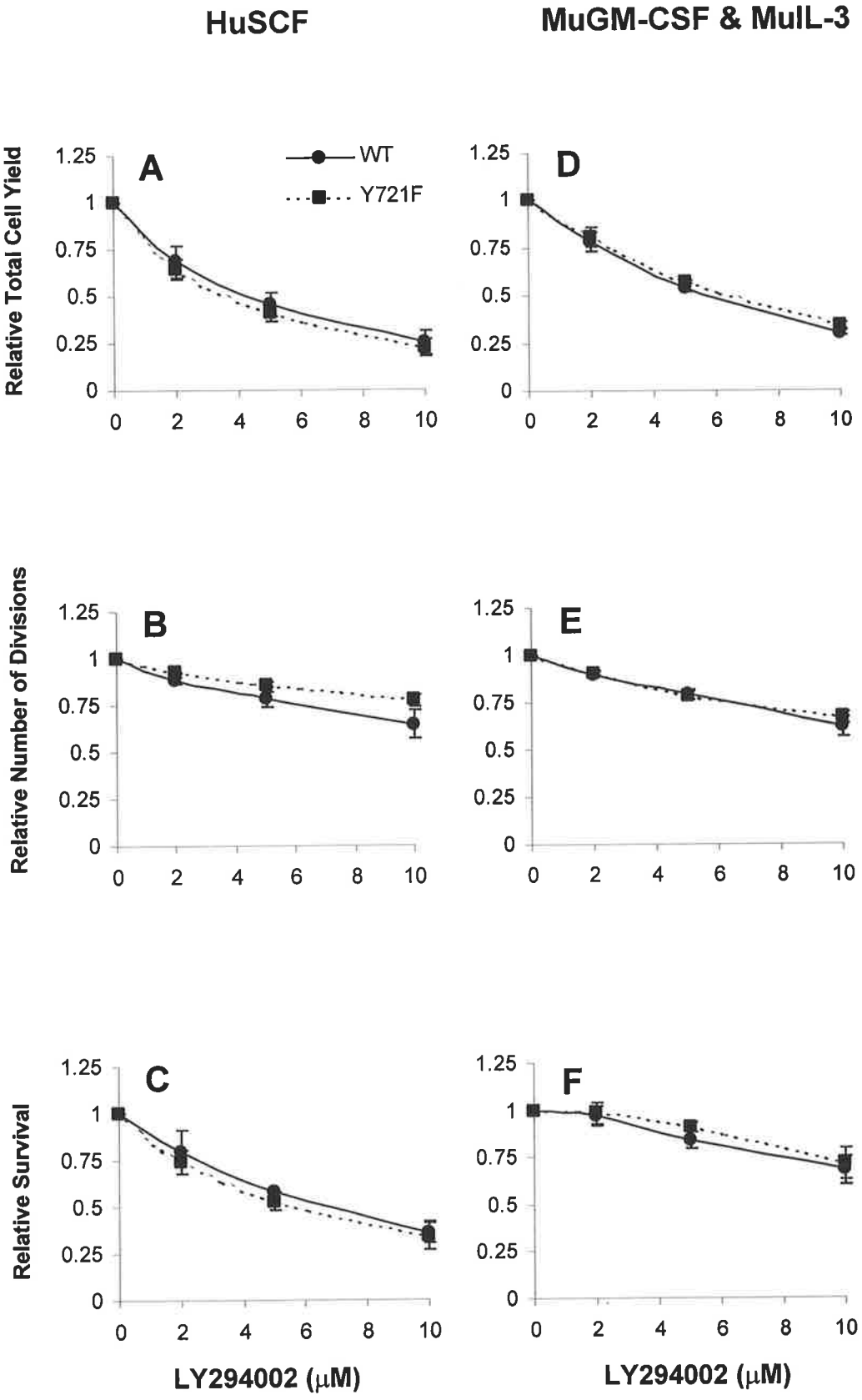
HuSCF
MuGM-CSF & MuIL-3
Relative Total Cell Yield
Relative Number of Divisions
Relative Survival
A
B
C
D
E
F
WT
Y721F
1.25
1
0.75
0.5
0.25
0
0
2
4
6
8
10
LY294002 (μM)

experiments and possibly indicated that huSCF mediated growth of FDC-P1 was more dependent on the activation of PI 3-K.

4.11. DISCUSSION

Activation of PI 3-K by c-KIT in bone marrow derived mast cells has been shown to be involved in degranulation, adhesion, membrane ruffling, cytoskeletal rearrangement and actin assembly with partial effects on cellular growth (Serve *et al.*, 1995; Vosseller *et al.*, 1997). Based on these results, it was of interest to evaluate the role of PI 3-K in eliciting biological responses in haemopoietic progenitor cells, another cell population containing endogenous c-KIT. A further interest was to address the signal transduction mechanisms requiring functional PI 3-K. Results indicated that direct recruitment of PI 3-K is involved in c-KIT mediated growth and survival in factor dependent haemopoietic cells.

To investigate the function of PI 3-K in biological responses, a construct of c-KIT containing a mutation at the PI 3-K binding site was created and expressed in two factor dependent haemopoietic progenitor cell lines. In response to huSCF, cells expressing Y721F c-KIT were unable to recruit or activate PI 3-K (Figures 4.5, 4.6). Stimulation of Y721F c-KIT in comparison to WT c-KIT with huSCF resulted in reduced growth, in both FDC-P1 (Figure 4.8) and MIHC (Figure 4.20). This supported observations in bone marrow derived mast cells and haemopoietic 32D cells (Gommerman *et al.*, 2000; Kissel *et al.*, 2000; Serve *et al.*, 1995; Timokhina *et al.*, 1998). It contradicts results obtained in a subline of murine myelomonocytic FDC-P1 cells which unlike FDC-P1 cells used here, can differentiate (Kubota *et al.*, 1998). This contradiction was surprising since cells of similar background were used and the difference may therefore be due to the level of receptor expressed since differences between WT and Y721F c-KIT were only seen at higher c-KIT surface expression levels. Kubota *et al.* (1998) instead reported that ligand mediated differentiation was

abolished when Y721 was mutated in c-KIT (Kubota *et al.*, 1998), however this was unable to be addressed here (see chapter 3).

Most of the studies to date have measured cellular growth by investigating DNA synthesis through tritiated thymidine and bromodeoxyuridine incorporation (Feng *et al.*, 2000; Gommerman *et al.*, 2000; Kissel *et al.*, 2000; Serve *et al.*, 1995; Timokhina *et al.*, 1998). These techniques are incapable of distinguishing between effects on survival or proliferation. By staining the cells with a fluorescent lipophilic dye and calculating the number of divisions undergone by surviving cells and determination of the yield of dye in the viable population, it was possible to separate the two variables. Results in FDC-P1 and MIHC showed that mutation of the Y721F binding site reduced survival in response to huSCF while having minimal effects on proliferation (Figures 4.10 and 4.20). Interestingly, two naturally occurring isoforms of ErbB4 exist, one with and the other without the PI 3-K binding domain (Kainulainen *et al.*, 2000). Stimulation of both isoforms with ligand enabled proliferation to an equivalent extent as measured by cell counts in the absence of death, while only the isoform activating PI 3-K was capable of rescuing cells from starvation-induced cell death in the presence of ligand (Kainulainen *et al.*, 2000). Therefore the direct recruitment of PI 3-K was similarly involved in survival but had little effect on proliferation. The mechanism by which PI 3-K activation mediates survival by RTKs is possibly through activation of Akt and phosphorylation of Bad at S136 resulting in its inactivation (Blume-Jensen *et al.*, 1998). Alternatively, Akt could be involved in the phosphorylation and inactivation of Caspase-9 (Kelley *et al.*, 1999) or an upstream effector of p38, a stress activated member of MAPK family of proteins (Gratton *et al.*, 2001).

PI 3-K appears to have a role in proliferation in spermatogonia since it upregulates cyclin D3 expression and Retinoblastoma protein phosphorylation (Feng *et al.*, 2000). A role of PI 3-K in proliferation may have been masked in this study due to the survival response being rate limiting. In the IL-3 receptor system, activation of PI 3-K was required more for

proliferation than survival (Craddock *et al.*, 1999). This was also observed for MIHC clones maintained in muGM-CSF and muIL-3 in the presence of LY294002 (Figure 4.21). Therefore the function of PI 3-K may vary depending on the growth factor stimulation.

Stimulation of Y721F c-KIT with huSCF, resulted in phosphorylation although this was weaker than in WT, supporting previous data (Kissel *et al.*, 2000; Timokhina *et al.*, 1998). A decrease in the peak level of c-KIT phosphorylation was observed, however by about 20 minutes, similar phosphorylation levels were observed (Figure 4.12). This, in conjunction with the association of p85 peaking prior to c-KIT phosphorylation suggested that Y721 was one of the initial sites to become phosphorylated. Indeed observations using site specific phospho-antibodies indicated that this was the case (Voytyuk *et al.*, 2003).

Akt was phosphorylated in the absence of direct PI 3-K recruitment to activated c-KIT. Some other studies have also observed phosphorylation of Akt when c-KIT lacks direct PI 3-K binding capabilities (Blume-Jensen *et al.*, 1998; Kissel *et al.*, 2000). This activation of Akt was either independent of PI 3-K (Kruszynska *et al.*, 2002; Moule *et al.*, 1997; Yano *et al.*, 1998) or due to alternative activation of PI 3-K. This could be resolved by investigating the effect LY294002 had on Akt phosphorylation.

In this study, no effect on internalisation or degradation due to the lack of direct recruitment of PI 3-K was observed (Figures 4.13 and 4.14). The internalisation result is in support of other experiments with c-KIT (Gommerman *et al.*, 1997; Jahn *et al.*, 2002a; Yee *et al.*, 1994), PDGF receptor (Joly *et al.*, 1995) and flt3/flk2 (Beslu *et al.*, 1996). In conjunction with other pathways such as those involving calcium flux, PI 3-K recruitment was found to be required (Gommerman *et al.*, 1997). Activation of PI 3-K is involved in the degradation of RTKs because the vesicles containing the internalised receptor remain near the surface and are unable to proceed along the endocytic pathway (Joly *et al.*, 1995; Murray *et al.*, 2000). This role in degradation is potentially due to PI 3-K mediated activation of Rab5, a GTPase involved in early endosome fusion (Li *et al.*, 1995). In this study, an effect of Y721F

substitution on c-KIT degradation was not seen possibly because the time course examined was not long enough.

In conclusion, mutation of the PI 3-K binding site of c-KIT in factor dependent haemopoietic progenitor cells resulted in decreased growth in response to huSCF. This was primarily due to an effect on cellular survival rather than proliferation. The residual growth in huSCF was due to indirect activation of PI 3-K in FDC-P1, while in MIHC, other mechanisms were also required.

CHAPTER 5:

ROLE OF PI 3-K IN ONCOGENIC c-KIT SIGNALLING

5. ROLE OF PI 3-K IN ONCOGENIC C-KIT SIGNALLING

5.1. INTRODUCTION

Oncogenic forms of c-KIT arising from deletions and point mutations have been identified in certain leukaemias and solid tumours. Substitution of **valine for aspartate** 816 (D816V) in the phosphotransferase domain of c-KIT was identified in HMC-1, a human mast cell line derived from a patient with mast cell leukaemia (Furitsu *et al.*, 1993; Kanakura *et al.*, 1994). Subsequent research has revealed an involvement of this mutation in systemic mastocytosis (Worobec *et al.*, 1998) and occasional cases of AML (Ashman *et al.*, 2000; Beghini *et al.*, 1998).

The mutation of D816 in c-KIT has biological implications since its expression induces factor independent growth of mast cells and early myeloid cells *in vitro* and tumour formation in mice (Ferrao *et al.*, 1997; Hashimoto *et al.*, 1996; Kitayama *et al.*, 1995; Tsujimura *et al.*, 1994). Associated with this is the constitutive phosphorylation of c-KIT (Furitsu *et al.*, 1993; Kanakura *et al.*, 1994). Little is known about the mechanism inducing this constitutive activation. It is believed that the mutation mediates its constitutive activity through a ligand independent dimerisation mechanism involving intracellular interactions (Lam *et al.*, 1999; Longley *et al.*, 2001). Further, a phosphatase, SHP-1, important in dephosphorylating c-KIT is degraded in the presence of D816V c-KIT (Piao *et al.*, 1996). Another possibility is the involvement of PI 3-K since D816V c-KIT constitutively associates with the p85 subunit (Furitsu *et al.*, 1993; Kanakura *et al.*, 1994). The role of PI 3-K in the oncogenic potential of D816V c-KIT was unknown. To address this, a construct lacking the PI 3-K binding site, Y721F along with the D816V c-KIT mutant was created and expressed in MIHC. Expression of D816V c-KIT in this cellular model has previously conferred factor independent growth and tumour formation in mice (Ferrao *et al.*, 1997).

5.2. GENERATION OF CONSTRUCTS AND ANALYSIS OF EXPRESSION

All constructs were created on the background of the GNNK+S+ isoform of human c-KIT. Human WT GNNK+S+ *c-KIT* cDNA in pRUFMC1*neo* vector was created as described in chapter 3. cDNA encoding human WT c-KIT containing a substitution of valine for aspartate at 816 (D816V) in the tyrosine kinase domain had been previously subcloned into pRUFMC1*neo* (Ferrao *et al.*, 1997). Briefly, RNA from HMC-1 cells was obtained and reverse transcribed for PCR. The PCR product was digested with *Esp*I (*Cel*II) to generate a 360 base pair fragment (residues 2330 - 2690) and the fragment cloned into WT *c-KIT* in pRUFMC1*neo* that had also been digested with *Esp*I. The mutation was selected by screening for the loss of a *Bsm*AI site due to the A to T mutation at 2468.

The pRUFMC1*neo* construct encoding Y721F c-KIT was generated as indicated in chapter 4. The Y721F/D816V *c-KIT* double mutant cDNA was created by inserting a sequence encoding the D816V mutation into Y721F *c-KIT* cDNA in pRUFMC1*neo*. pRUFMC1*neo* D816V *c-KIT* was digested with *Esp*I to generate a 360 base pair fragment (residues 2330 - 2690) which was gel purified. WT *c-KIT* cDNA containing the mutation encoding Y721F in pRUFMC1*neo* was also digested with *Esp*I and the 8.2 kb fragment gel purified and dephosphorylated. The 360 base pair insert was ligated into this dephosphorylated vector. Orientation of the insert was determined by PCR using primers 447 and SRC-10 (see Table 2.5 for PCR conditions). The primer 447 (1506 - 1524) annealed outside the inserted sequence while SRC-10 (2642 - 2660) annealed within the insert (Figure 5.1A). Therefore, PCR products were only present if the insert was correctly orientated allowing SRC-10 to prime in the correct direction. The presence of the D816V mutation was confirmed by the lack of a *Bsm*AI endonuclease site caused by the A to T substitution at 2468. DNA preparations from bacterial clones were screened by PCR amplification (primers SRC-09 and SRC-10) and digestion with *Bsm*AI. The newly created Y721F/D816V construct was

Figure 5.1: Insertion of D816V into Y721F *c-KIT* in pRUFMC1*neo*.

A: Schematic diagram of Y721F/D816V *c-KIT* in pRUFMC1*neo*. A fragment of D816V *c-KIT* in pRUFMC1*neo* digested with *Esp*I was inserted into the complementary site in Y721F *c-KIT* in pRUFMC1*neo*. To determine orientation of the fragment, the construct was PCR amplified with primers 447 (1506-1524) and SRC-10 (2642-2660). No product was obtained when the fragment was in the incorrect orientation. **B**: Sequence from the sense primer SRC-09 (2400-2418) corresponding to 2456 to 2480 base pairs in *c-KIT*. The point mutation of A to T at residue 2468 resulted in a codon change at 816 of GAC encoding aspartic acid to GTC encoding valine.

A

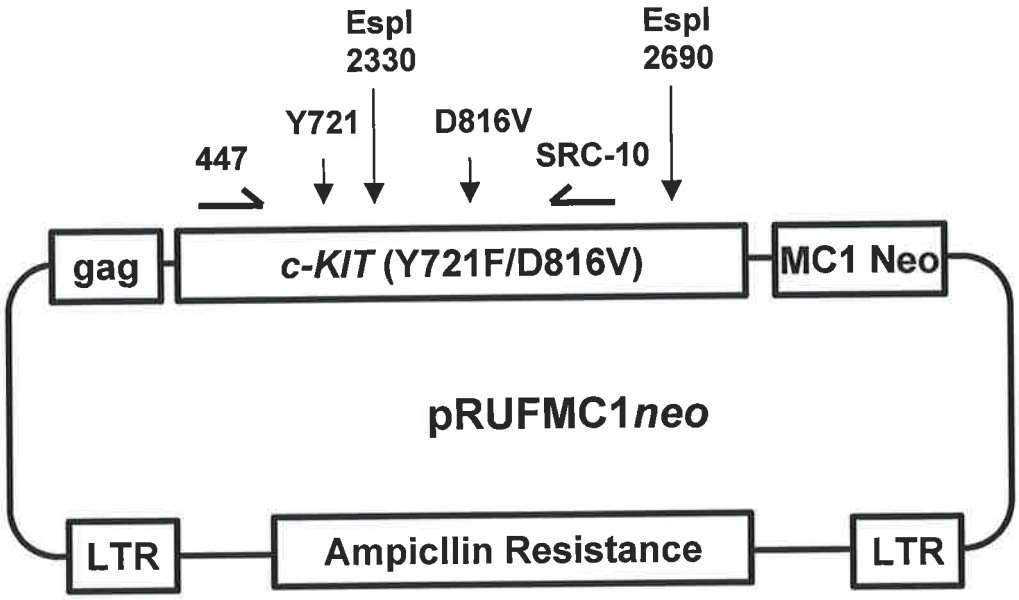
EspI
2330
EspI
2690
Y721
D816V
447
SRC-10
gag
c-KIT (Y721F/D816V)
MC1 Neo
pRUFMC1neo
LTR
Ampicllin Resistance
LTR

B

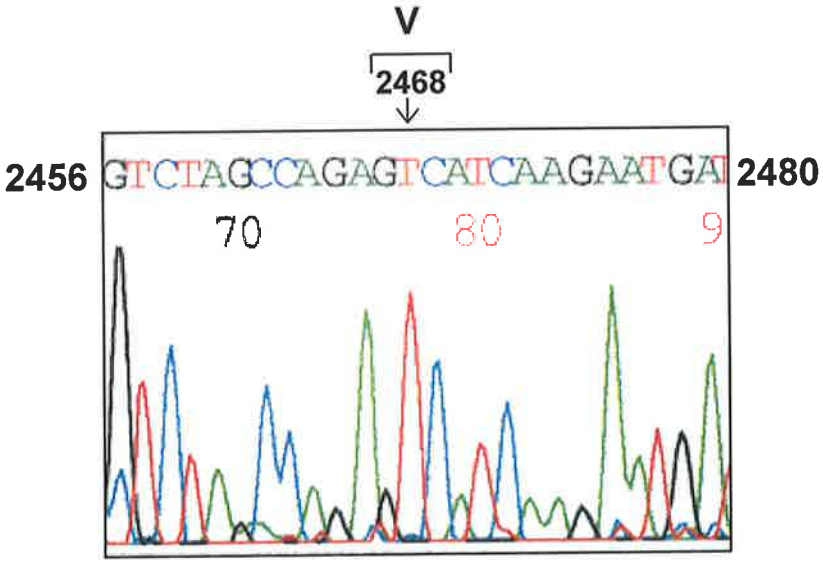
V
2468
2456
GTCTAGCCAGAGTCATCAAGAATGA
2480
70
80
9

sequenced across the insert region using primers 1002, SRC-05, SRC-09 and SRC-10 to confirm the presence of the A2468T mutation encoding the D816V substitution and the absence of any further mutations (Figure 5.1B).

All plasmids used for transfection were expanded and purified as outlined in sections 2.9.9. The ecotropic retrovirus packaging cell line, psi2, was transfected using the calcium phosphate technique (see section 2.10.2 for details) with pRUFMC1*neo* constructs encoding WT, Y721F, D816V or Y721F/D816V all on the GNNK+S+ isoform of c-KIT. Transfectants were selected with 400 μg/ml geneticin until untransfected cells died. Drug-resistant cells were further selected for c-KIT expression by fluorescence activated cell sorting using a c-KIT specific monoclonal antibody, 1DC3.

5.3. EXPRESSION OF C-KIT

MIHC were infected with c-KIT expression constructs by co-cultivation with irradiated psi2 transfectants (see section 2.10.3). Infected cells were selected with 1 mg/ml geneticin until uninfected control cells died. Once selected, cells were amplified in standard medium supplemented with muGM-CSF and stocks cryopreserved. Cells were cultured for a maximum of three weeks before thawing a fresh ampoule in order to minimise genetic drift. In order to determine the role of PI 3-K in D816V factor independent growth, D816V and Y721F/D816V c-KIT expressing cells were maintained in muGM-CSF and were not selected for factor independent growth as other studies have done (Ferrao *et al.*, 1997). To serve as a control, cells expressing D816V c-KIT that had been selected and maintained in the absence of factor (Ferrao *et al.*, 1997) were used.

The surface expression of c-KIT on each of the infectants was determined by indirect immunofluorescence using monoclonal IgG1 antibody, 1DC3 or an isotype matched negative control, 1B5. No fluorescence above background was observed for parental MIHC, whereas

infection with retrovirus encoding either WT or Y721F c-KIT resulted in heterogeneous levels of expression (Figure 5.2A).

Based on the constitutive activity of D816V c-KIT (Moriyama *et al.*, 1996) and previous results in MIHC (Ferrao *et al.*, 1997), it was expected to be present on the cell surface at low levels compared to WT c-KIT, as was observed (Figure 5.1B). Expression of D816V c-KIT containing a mutation at the PI 3-K binding site (Y721F/D816V) resulted in similar low level surface expression (Figure 5.1B). In Y721F/D816V c-KIT expressing cells, it was possible to see subtly higher expression compared to D816V c-KIT suggesting that the lack of direct PI 3-K recruitment may have affected the internalisation or degradation of c-KIT. Factor independent selection of D816V transduced cells slightly increased c-KIT surface expression relative to those maintained in muGM-CSF. These factor independent D816V c-KIT cells were used as a positive control for subsequent studies.

Protein expression of D816V c-KIT on cells is low due to its continual activation and degradation (Moriyama *et al.*, 1996). To compare the level of *c-KIT* RNA present, Northern blot analysis was performed (refer to section 2.11 for details). Total RNA was extracted from cells and the levels of *c-KIT* and a control marker (GAPDH) were investigated using ^{32}P labelled probes (refer to section 2.11 for details). Human *c-KIT* was absent in the uninfected parental population of MIHC, however it was detected in all infected lines (Figure 5.3A). The membrane was stripped and reprobed for GAPDH (Figure 5.3B). The Northern blots were analysed on a phosphorimager and quantitated using ImageQuantTM software. The amount of *c-KIT* present was standardised to the GAPDH loading control (Figure 5.3C). Similar levels of RNA expression were obtained for WT and D816V *c-KIT* both with and without the Y721F mutation. Cells expressing D816V c-KIT that had been maintained in the absence of factor expressed higher levels of *c-KIT* mRNA. In conclusion, despite low surface levels of D816V c-KIT, the expression of RNA was equivalent to non-oncogenic versions of *c-KIT*. Further, factor independent selection resulted in an increase in *c-KIT* RNA expression.

Figure 5.2: Surface expression of c-KIT constructs by indirect immunofluorescence assay.

Surface expression of c-KIT was determined by indirect immunofluorescence using monoclonal antibody 1DC3 (anti-c-KIT) and an isotype matched negative control 1B5 (anti-*giardia*). The histograms show the relative surface expression profiles of the negative control, parent, WT, Y721F c-KIT expressing MIHC **(A)** and parent, Y721F/D816V, D816V and factor independent D816V (D816V(FI)) c-KIT expressing MIHC **(B)**.

A

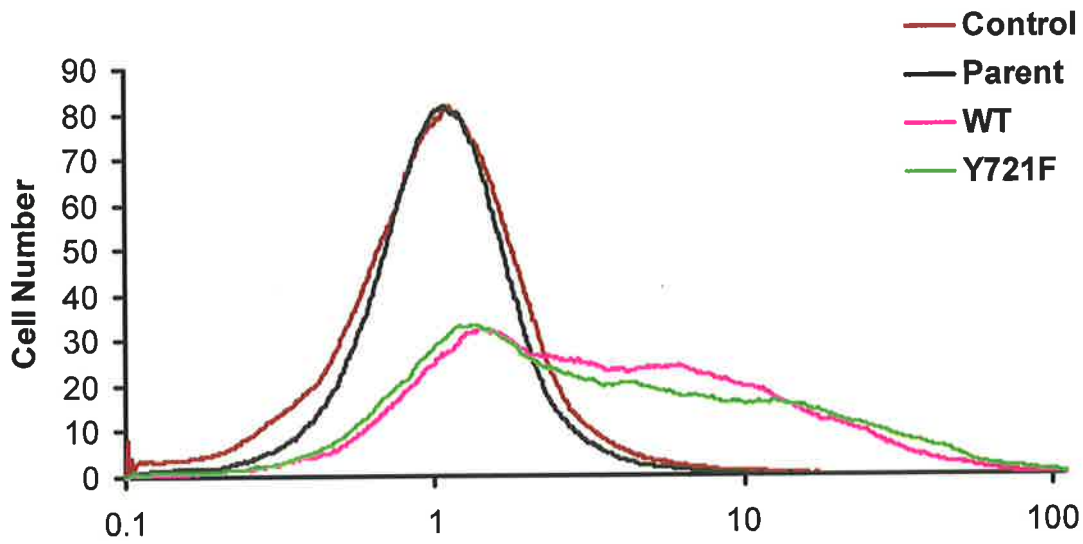
Control
Parent
WT
Y721F
Cell Number
90
80
70
60
50
40
30
20
10
0
0.1
1
10
100

B

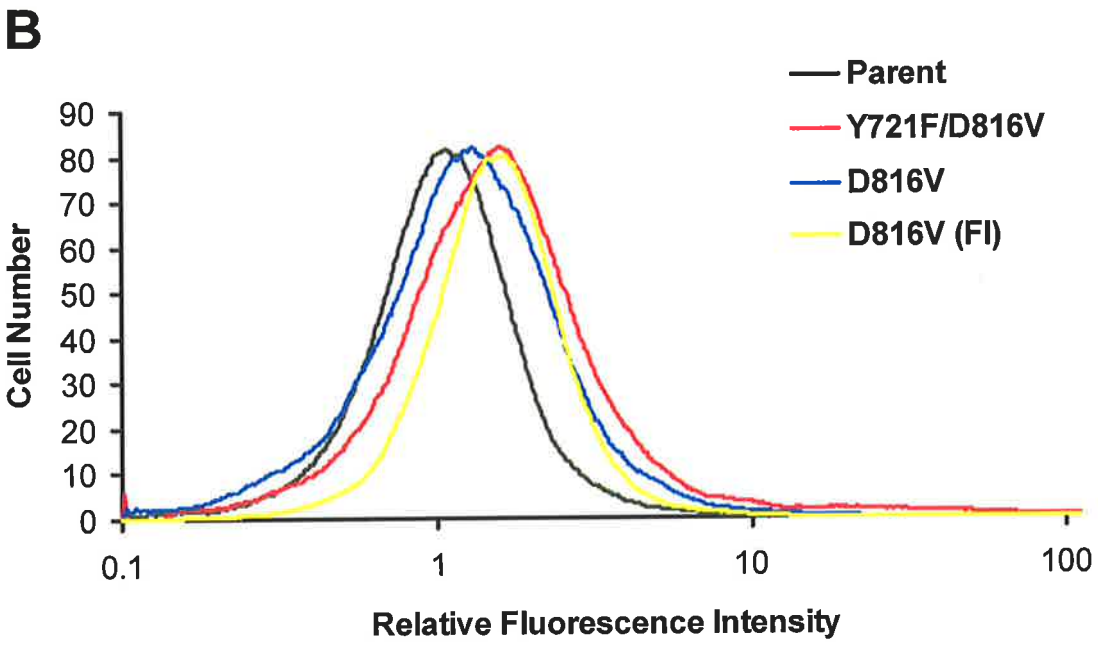
Parent
Y721F/D816V
D816V
D816V (FI)
Cell Number
90
80
70
60
50
40
30
20
10
0
0.1
1
10
100
Relative Fluorescence Intensity

Figure 5.3: Expression of *c-KIT* mRNA by Northern analysis.

Total RNA (10μg) was harvested from MIHC parent (1), and MIHC infected with WT *c-KIT* (2), Y721F *c-KIT* (3), Y721F/D816V *c-KIT* (4), D816V *c-KIT* (5) and D816V *c-KIT* selected for factor independent growth (6) and was analysed by agarose gel electrophoresis and Northern blot hybridisation. The membrane was initially probed with a 700 base pair fragment of *c-KIT* DNA **(A)** and then stripped and reprobed with a 780 base pair GAPDH fragment (see section 2.11.3) **(B)**. Signal was detected using Molecular Dynamics PhosphorImager. Hybridisation signals were quantitated with ImageQuantTM software and the ratios of *c-KIT* signal to the assay loading control (GAPDH) are shown in **(C)** where Par represents MIHC parent, and D816V(FI) represents D816V *c-KIT* cells selected for factor independent growth.

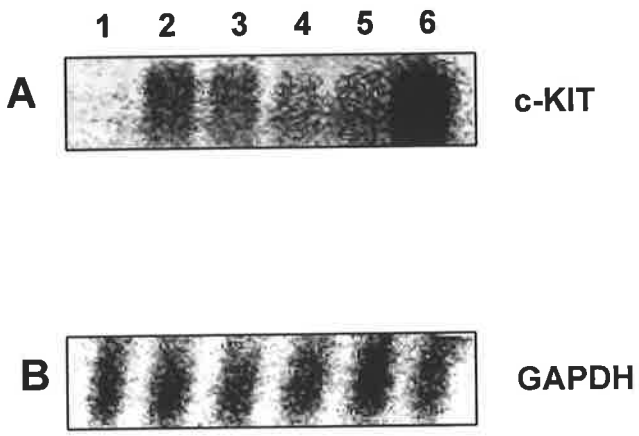
1 2 3 4 5 6
A
c-KIT
B
GAPDH

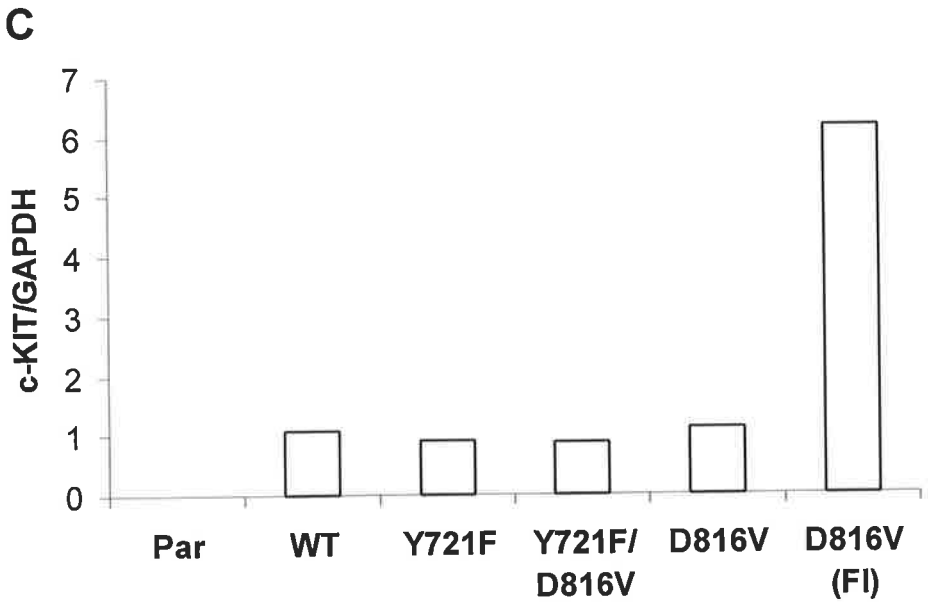
C
c-KIT/GAPDH
0
1
2
3
4
5
6
7
Par
WT
Y721F
Y721F/ D816V
D816V
D816V (Fl)

5.4. ACTIVATION OF ONCOGENIC C-KIT AND ASSOCIATION TO PI 3-K

An alternate method to detect c-KIT was by Western blot analysis. Cells were lysed in 1% Triton x100 with protease and phosphatase inhibitors and c-KIT was immunoprecipitated. Immunoprecipitates from $4x10^7$ cells were electrophoresed under reducing conditions by SDS-PAGE, transferred to membrane and probed for c-KIT using a rabbit polyclonal antibody against the carboxy terminus (see section 2.7). This was developed with sheep anti-rabbit antibody conjugated to alkaline phosphatase followed by ECF substrate. To serve as a control for immunoprecipitation, an isotype matched antibody (1D4.5) was used. High levels of 145 kDa c-KIT was detected in WT c-KIT expressing cells that had been maintained in 100 ng/ml huSCF (Figure 5.4A). Also detected was the 125 kDa immature form of c-KIT. A low level of D816V c-KIT was detected in factor independent MIHC appearing as an "upward smear" (Figure 5.4A) suggesting that it was constitutively active and ubiquitinated. A low level of c-KIT above that seen in the control immunoprecipitate was detected in Y721F/D816V c-KIT expressing cells. The immature form of c-KIT was also detected in Y721F/D816V c-KIT cells as a band at 125 kDa. Unlike Y721F/D816V c-KIT expressing cells, D816V c-KIT was not detected in cells after multiple attempts. The absence of detection is likely due to the low protein expression as shown by indirect immunofluorescence since it was below that for Y721F/D816V c-KIT expressing MIHC maintained in muGM-CSF and D816V c-KIT maintained in the absence of factor.

To investigate the activation of the c-KIT mutants, their phosphorylation status was assessed. c-KIT immunoprecipitates from cells starved of growth factors and FCS for 2 hours prior to lysis were electrophoresed under reducing conditions and transferred to membrane. Membranes were probed with a cocktail of phosphotyrosine specific antibodies (see Table 2.2). Considerable huSCF specific phosphorylation was observed for WT c-KIT expressing MIHC (Figure 5.4B). D816V c-KIT immunoprecipitated from cells selected for factor

Figure 5.4: Expression and activation of c-KIT and its association to PI 3-K.

MIHC WT, Y721F/D816V (FV), D816V (V) or factor independent D816V (V(FI)) c-KIT expressing cells were starved of serum and factor for 2 hours, stimulated with huSCF for 5 minutes (+) or unstimulated (-) and then lysed at $2x10^7$ cells/ml. Clarified lysates were immunoprecipitated with 5 μg KIT4.G12 antibody (K) or 5 μg of an isotype matched negative control antibody, 1D4.5 (C) and Protein A Sepharose for 2 hours. Pooled immunoprecipitates from $4x10^7$ cells were electrophoresed on 8% gels, transferred to membrane and immunoblotted for c-KIT **(A)**, phosphotyrosine **(B)**, and the p85 subunit of PI 3-K **(C)**. Bound antibody was detected with alkaline phosphatase conjugated secondary antibody and alkaline phosphatase activity was visualised using ECF and FluorImager analysis.

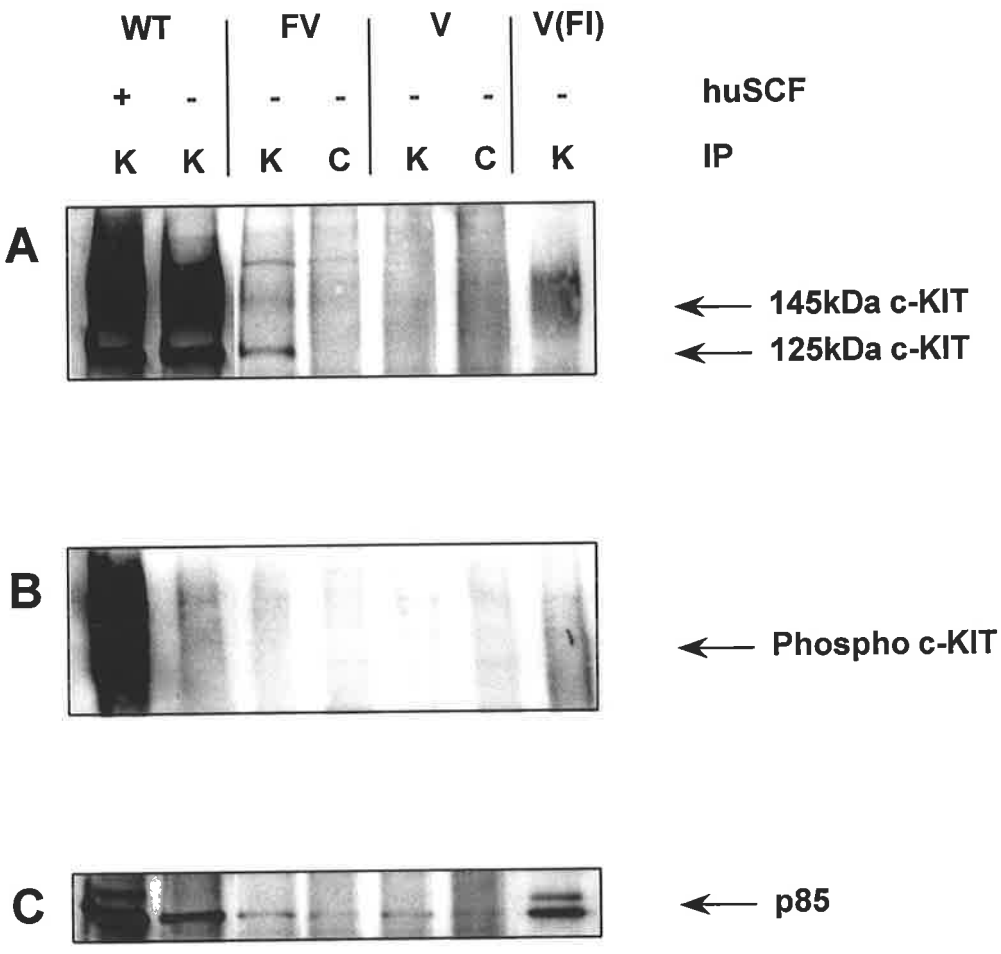
WT
FV
V
V(FI)
+ - - - - - -
huSCF
K K K C K C K
IP
A
145kDa c-KIT
125kDa c-KIT
B
Phospho c-KIT
C
p85

independent growth was phosphorylated in the absence of huSCF (Figure 5.4B). The intensity of phosphorylation was substantially decreased relative to WT c-KIT stimulated with huSCF. No phosphotyrosine bands corresponding to Y721F/D816V or D816V c-KIT were detected in multiple attempts (Figure 5.4B) probably due to the low levels of protein expression.

The association of p85 with c-KIT is induced by huSCF (chapter 4) and is constitutive in D816V c-KIT expressing cells (Furitsu *et al.*, 1993; Kanakura *et al.*, 1994). Analysis of this association in WT c-KIT immunoprecipitates by immunoblot with antibody to p85 confirmed that it was induced by the presence of huSCF (Figure 5.4C). As predicted, in the absence of factor, p85 co-precipitated with D816V c-KIT from cells selected for factor independent growth (Figure 5.4C). It was difficult to quantitate the level of association in Y721F/D816V and D816V c-KIT expressing cells, due to a non-specific band in the 1D4.5 immunoprecipitates. Multiple attempts were made to investigate p85 association with D816V and Y721F/D816V c-KIT mutants but the levels of expression were too low to enable definitive results to be obtained.

To investigate the role of PI 3-K further, its activity in c-KIT immunoprecipitates was assessed. Cellular lysates immunoprecipitated with antibody to c-KIT or a control antibody were used in an *in vitro* kinase assay with PtdIns as a substrate (see section 2.8.4). Inducible activation of PI 3-K was observed in WT c-KIT immunoprecipitates after stimulation with huSCF as shown by the formation of PtdIns-3-P (Figure 5.5A and B). c-KIT immunoprecipitates from D816V c-KIT expressing cells selected for factor independent growth contained PI 3-K activity which was absent in the presence of 70 nM wortmannin or a control immunoprecipitate (Figure 5.5A and B). Only background levels of PI 3-K activity were observed in immunoprecipitates from Y721F/D816V and D816V c-KIT expressing cells (Figure 5.5A and B). As a further control, the activity in p85 immunoprecipitates was assessed. All p85 immunoprecipitated samples exhibited PI 3-K activity, which was inhibited by 70 nM wortmannin (Figure 5.5C). Thus, cells expressing WT c-KIT stimulated with

Figure 5.5: Activation of PI 3-K by D816V c-KIT.

An *in vitro* kinase assay detecting PI 3-K activity was performed as described in the materials and methods (section 2.8) and the signal was detected and visualised using the Molecular Dynamics PhosphorImager. WT represents WT c-KIT, FV represents Y721F/D816V c-KIT, V represents D816V c-KIT, and V(FI) represents D816V c-KIT selected for factor independent growth. Wm indicates the addition of 70 nM Wortmannin to the kinase reaction. **A:** PI 3-K activity detected in c-KIT (K) and control (C) immunoprecipitates in the presence (+) or absence (-) of huSCF or Wortmannin (Wm). **B:** Signals observed in A were quantitated using ImageQuantTM software and expressed in relative units. **C:** PI 3-K activity detected in p85 immunoprecipitates in the presence (+) or absence (-) of huSCF and Wortmannin (Wm).

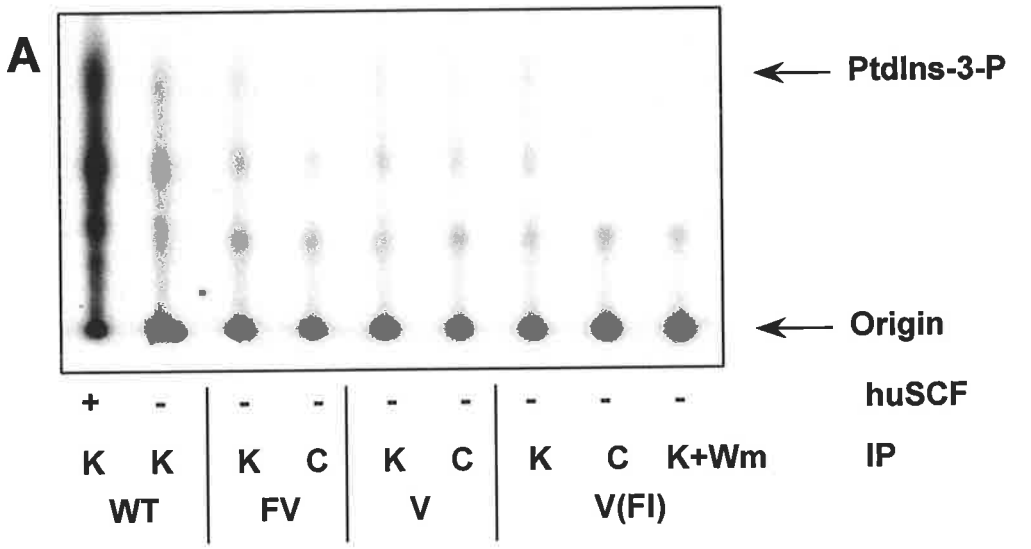
A
PtdIns-3-P
Origin
huSCF
+ - - - - - - - -
K K K C K C K C K+Wm
IP
WT
FV
V
V(FI)

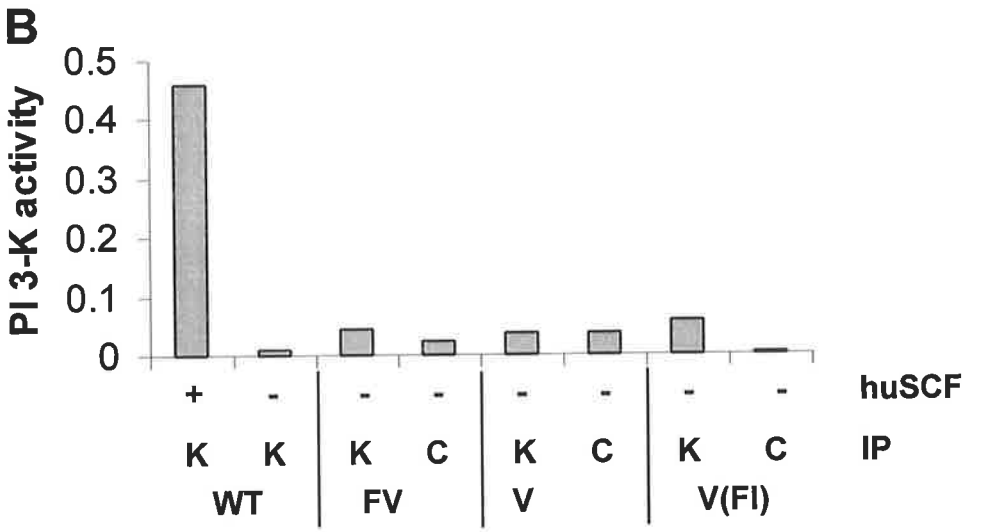
B
PI 3-K activity
0.5
0.4
0.3
0.2
0.1
0
huSCF
+ - - - - - - -
K K K C K C K C
IP
WT
FV
V
V(FI)

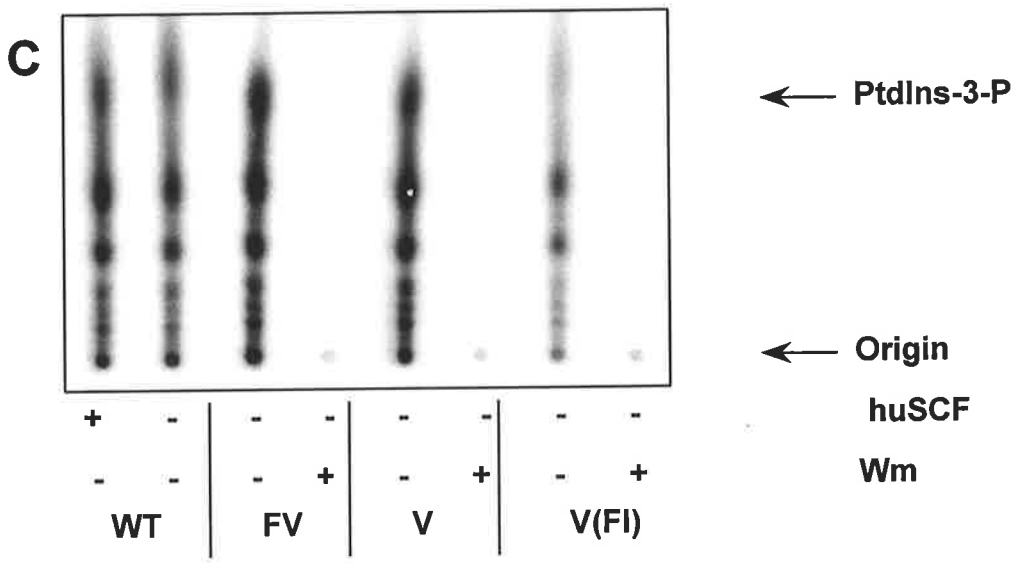
C
PtdIns-3-P
Origin
huSCF
Wm
+ - - - - - - -
- - - + - + - +
WT
FV
V
V(FI)

huSCF or expressing D816V c-KIT and selected for factor independent growth exhibited c-KIT associated PI 3-K activity. Consistent with the low amount of c-KIT protein present in D816V c-KIT and Y721F/D816V c-KIT expressing cells (Figure 5.4A) no PI 3-K activity could be co-immunoprecipitated with c-KIT.

5.5. Factor Independent Growth of D816V c-KIT Expressing Cells

The D816V mutation in c-KIT confers an ability to grow in the absence of factor in various cells, including the factor dependent MIHC model (Ferrao *et al.*, 1997; Hashimoto *et al.*, 1996; Kitayama *et al.*, 1995; Tsujimura *et al.*, 1994). The mechanism by which this occurred was largely unknown. Since, PI 3-K was found to be constitutively associated with and activated by D816V c-KIT, it was thought that this was responsible for the factor independent growth. To determine if this was the case, MIHC expressing c-KIT constructs including D816V c-KIT and D816V lacking the core PI 3-K binding residue, Y721, were assessed for factor-independent growth in semi-solid medium (clonogenic potential) and in liquid culture.

In semi-solid medium, the numbers of colonies formed from $5x10^3$ cells were scored at one week. Results show that expression of various constructs of c-KIT in MIHC did not alter the number of colonies formed in muGM-CSF (Figure 5.6). As expected, MIHC expressing D816V c-KIT were capable of forming colonies in the absence of factor, unlike parental MIHC or those infected with WT or Y721F c-KIT. Mutation of the PI 3-K binding site, Y721 in D816V c-KIT, still allowed colony formation in the absence of factor. The number of colonies was significantly reduced when compared to cells expressing D816V c-KIT ($p < 0.00001$), even though there was no difference in the ability to form colonies in muGM-CSF ($p > 0.1$). This indicated that mutation of the PI 3-K binding site in D816V c-KIT reduced but did not abolish colony formation in the absence of factor, suggesting that additional mechanisms are involved in factor independent growth induced by D816V c-KIT.

Figure 5.6: Colony formation in the presence or absence of muGM-CSF.

MIHC ($5x10^3$) transduced with c-KIT constructs as indicated were seeded in triplicate in methylcellulose with or without muGM-CSF. After one week, the numbers of colonies containing greater than 50 cells were scored, with the data shown as mean ± SEM.

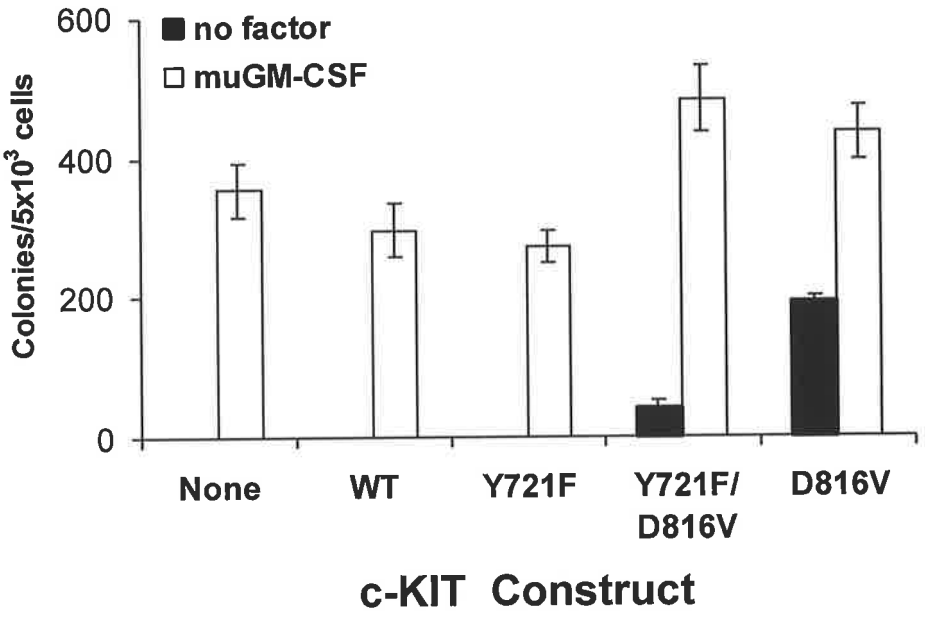
600
400
200
0
Colonies/5x10^3 cells
no factor
muGM-CSF
None
WT
Y721F
Y721F/ D816V
D816V
c-KIT Construct

Growth in liquid culture of MIHC expressing the various c-KIT constructs was determined in the presence or absence of muGM-CSF by MTT assay for total cells (see methods section 2.5.2). In the presence of muGM-CSF, similar growth rates were observed for each of the cell lines (Figure 5.7A). Cells expressing D816V c-KIT were capable of growth in the absence of factor (Figure 5.7B), which was decreased but not abolished with loss of the PI 3-K binding site (Y721F/D816V c-KIT), thus supporting the colony assay observations.

Previous observations have shown that D816V c-KIT when expressed in the MIHC model, confers a growth advantage over the parental line or cells expressing WT c-KIT (Ferrao *et al.*, 1997). Expression of D816V c-KIT does not affect the proliferative capacity of MIHC, but instead promotes survival close to 100%, which is significantly higher than MIHC expressing WT c-KIT grown in huSCF, or parental MIHC in muGM-CSF (Ferrao *et al.*, 1997). Since PI 3-K has been implicated in survival responses (Kennedy *et al.*, 1997; Philpott *et al.*, 1997; Ueno *et al.*, 1997), it was hypothesised that the constitutive association of p85 with D816V c-KIT was mediating this effect. To determine if this was the case, proliferation and survival of cells expressing D816V c-KIT and Y721F/D816V c-KIT was compared using the PKH assay (see section 2.5.3). Growth in the absence of factor was observed for D816V c-KIT maintained in the presence or absence of muGM-CSF (Figure 5.8A, B and C). D816V c-KIT lacking the PI 3-K binding site was also capable of growth in the absence of factor however this was at a much reduced rate (Figure 5.8A, B and C). The decreased number of cells obtained in Y721F/D816V c-KIT cells was totally attributable to reduced survival as the proliferation rate was equivalent for Y721F/D816V and D816V c-KIT cells (Figure 5.8A to C). Confirming previous observations (Ferrao *et al.*, 1997), D816V c-KIT expressing cells that had been selected for factor independent growth exhibited minimal cellular attrition over the time course studied (Figure 5.8C). In the absence of factor, some cellular attrition was seen for D816V c-KIT expressing cells that had not been selected for factor independence,

Figure 5.7: Growth in liquid culture in the presence or absence of muGM-CSF.

MIHC uninfected or infected with c-KIT constructs were seeded in triplicate at a density of $5x10^4$/ml and were assessed for total number of cells at days 0, 2, 4 and 6 in the presence (**A**) and absence (**B**) of muGM-CSF by absorbance at 570 nm (MTT assay). Data are represented as mean ± SEM. Due to overgrowth, several points at day 6 in **A** and **B** have been omitted.

A

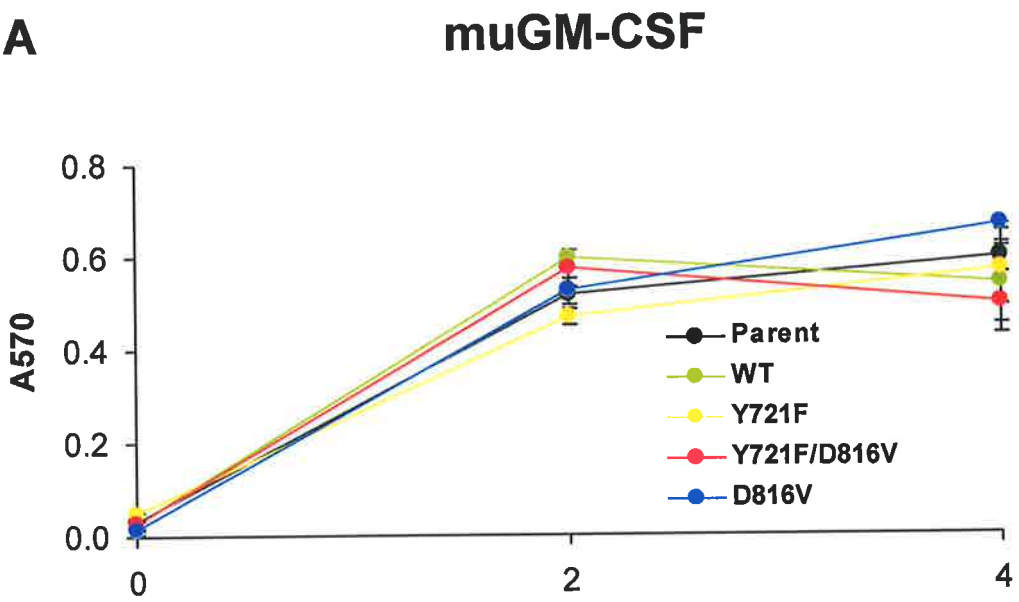
muGM-CSF
0.8
0.6
0.4
0.2
0.0
A570
0
2
4
Parent
WT
Y721F
Y721F/D816V
D816V

B

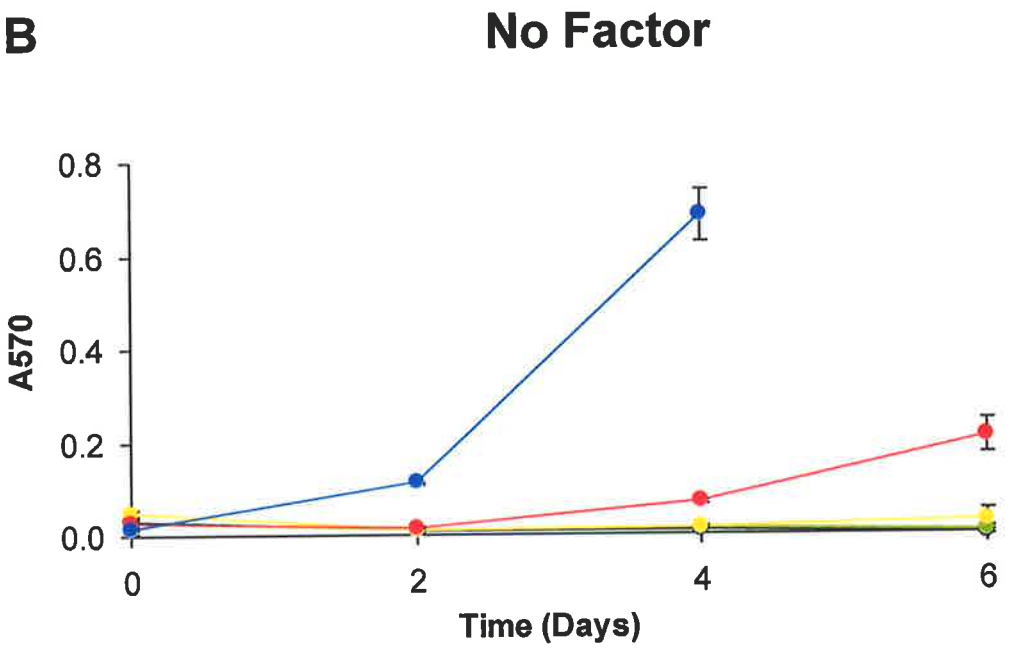
No Factor
0.8
0.6
0.4
0.2
0.0
A570
0
2
4
6
Time (Days)

Figure 5.8: Survival and proliferation of MIHC in liquid culture.

MIHC uninfected or infected with c-KIT constructs seeded in triplicate at a density of $5x10^4$ cells/ml were assessed for proliferation, survival and total cell yield as described in section 2.5.3 in the absence **(A, B, C)** or the presence **(D, E, F)** of muGM-CSF. Data shown are mean ± SEM. **A** and **D** show the total number of viable cells present, **B** and **E** show the average number of divisions undergone by viable cells while **C** and **F** show the percent of fluorescence yield in the viable population (survival). Data points for number of divisions where less than 1000 viable cells remained were considered unrealistic and have been omitted.

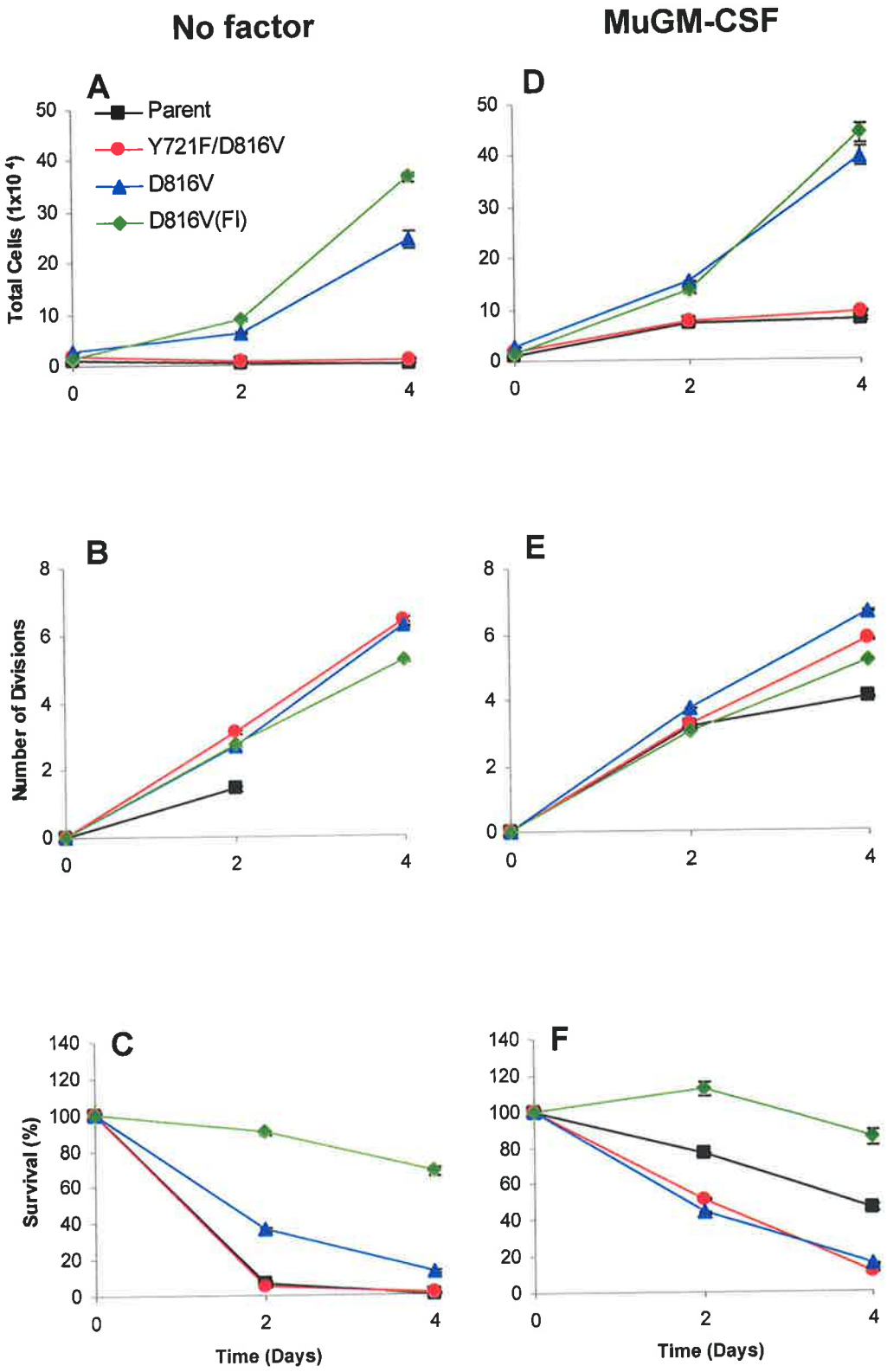
No factor
MuGM-CSF
A
D
Parent
Y721F/D816V
D816V
D816V(FI)
Total Cells (1x10 4)
B
E
Number of Divisions
C
F
Survival (%)
Time (Days)
Time (Days)

and this was responsible for the decreased total yield of cells (Figure 5.8A and C). In muGM-CSF, equivalent numbers of cells were obtained with D816V c-KIT expressing cells irrespective of whether or not they had been selected for factor independence (Figure 5.8F). The yield of cells was much higher than the parental population or cells expressing the double mutant, again due to an effect on cellular attrition rather than the rate of proliferation (Figure 5.8D, E and F). This suggests that the activation of PI 3-K by oncogenic c-KIT may be involved in synergy with muGM-CSF. Therefore mutation of the PI 3-K binding site had an effect on survival but not on proliferation.

5.6. Effect of the PI 3-K Inhibitor, LY294002 on Proliferation and Survival of D816V c-KIT Expressing Cells

The results above indicated that direct recruitment of PI 3-K was involved in the increased survival exhibited by D816V c-KIT, however other mechanisms were also employed. To confirm this result and to determine if alternate activation of PI 3-K had a role, growth in the presence of a PI 3-K inhibitor, LY294002 was examined. Cells were seeded at $5x10^4$/ml in various concentrations of LY294002 in either the presence or absence of muGM-CSF and proliferation, survival and cell number were determined after two days incubation (see section 2.5.3). Data standardised to the values in the absence of LY294002 are shown in Figure 5.9. In muGM-CSF, growth of each cell line (total cell yield) was affected similarly by titrated levels of LY294002 (Figure 5.9D). This appeared to be predominantly due to an effect on proliferation (Figure 5.9E), therefore, PI 3-K activity enhanced muGM-CSF induced proliferation. In the absence of factor, the predominant effect of LY294002 was on survival (Figure 5.9A, B and C). Cells expressing the D816V c-KIT mutant lacking direct PI 3-K recruitment were more sensitive to LY294002 possibly because the survival response was more reliant on the alternate activation of PI 3-K which rapidly became limiting. At 10 μM LY294002, no survival was observed in Y721F/D816V c-KIT

Figure 5.9 Cellular growth in the presence of LY294002.

MIHC uninfected or infected with c-KIT constructs seeded in triplicate at a density of $5x10^4$/ml were assessed for proliferation, survival and total cell yield as described in section 2.5.3 in the presence of the PI 3-K inhibitor LY294002, with **(D, E, F)** or without **(A, B, C)** muGM-CSF. Data are represented as mean ± SEM and have been standardised to the parameters in the absence of LY294002. **A** and **D** show the relative viable cell yield, **B** and **E** show the relative number of divisions undergone by viable cells and **C** and **F** indicate the percent of fluorescence yield in the viable population (survival). Data points for number of divisions where less than 1000 viable cells remained were considered unrealistic and have been omitted.

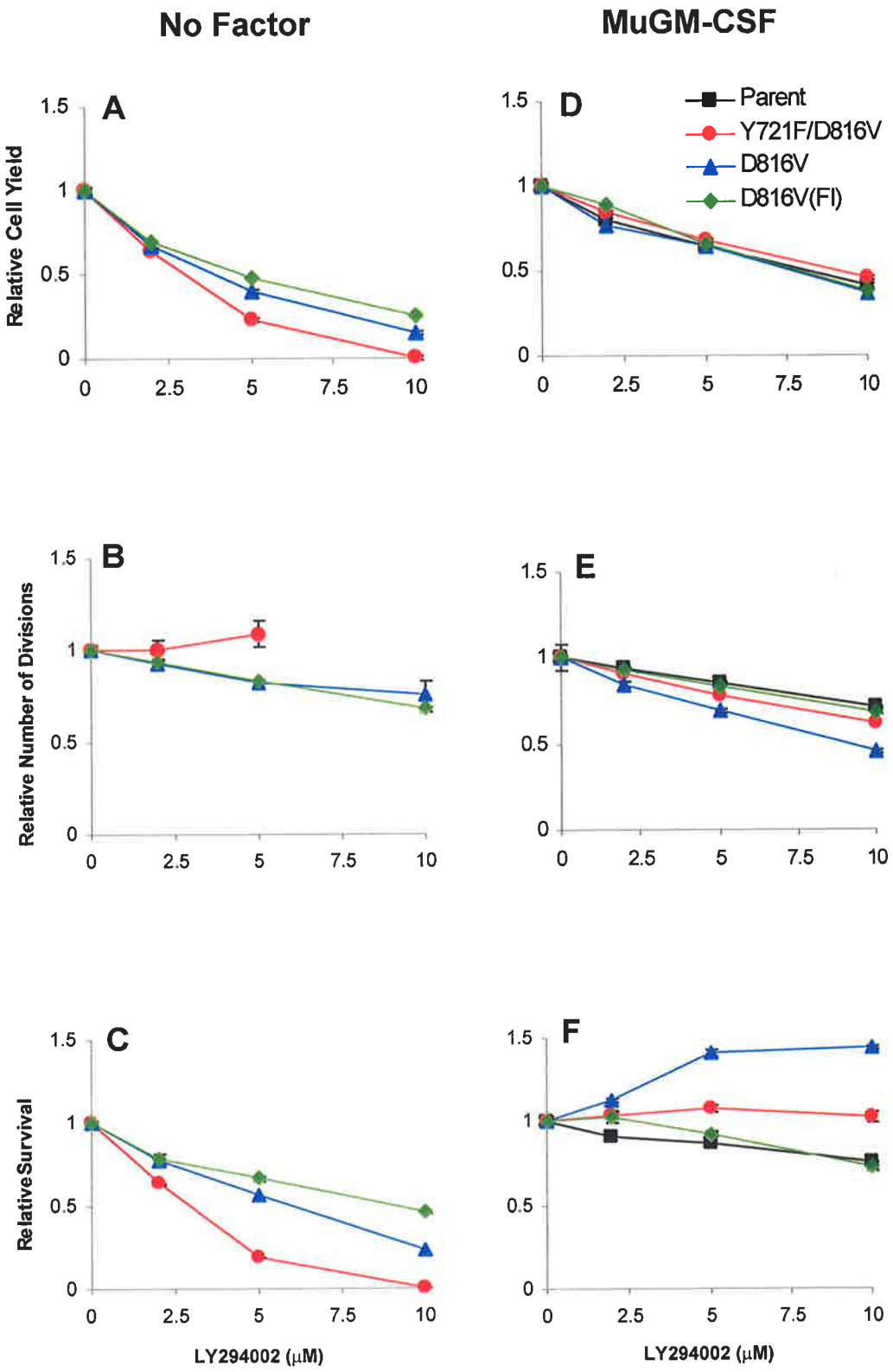
No Factor
MuGM-CSF
A
B
C
D
E
F
Parent
Y721F/D816V
D816V
D816V(FI)
Relative Cell Yield
Relative Number of Divisions
RelativeSurvival
LY294002 (μM)
LY294002 (μM)
1.5
1
0.5
0
0
2.5
5
7.5
10

expressing cells in the absence of factor. Overall, factor independent growth was more sensitive to LY294002 than growth in muGM-CSF. These results suggest that PI 3-K activity is necessary for factor independent growth of cells expressing mutant c-KIT.

5.7. TUMOURIGENIC POTENTIAL OF D816V C-KIT

Subcutaneous injection of MIHC expressing D816V c-KIT into syngeneic mice induces tumour formation (Ferrao *et al.*, 1997). These tumours exhibit characteristics of malignant histiocytes with many of the cells undergoing mitosis. To determine the involvement of direct PI 3-K recruitment in D816V c-KIT mediated tumourigenicity, the capacity of cells expressing Y721F/D816V c-KIT to form tumours in mice was assessed. Aliquots of $2x10^6$ cells of either parental MIHC or those infected with either WT, Y721F, Y721F/D816V or D816V c-KIT were injected subcutaneously into syngeneic (CBA) mice. As a positive control, factor independent D816V c-KIT expressing cells as studied previously (Ferrao *et al.*, 1997) were also injected. Mice were monitored for the development of tumours for up to 24 weeks. Injection of mice with factor independent D816V c-KIT cells resulted in tumour formation after 2 weeks (Figure 5.10A), confirming results from a previous study (Ferrao *et al.*, 1997). Mice injected with MIHC expressing D816V c-KIT that had been maintained in muGM-CSF developed tumours after 5 to 7 weeks. Thus an increased latency period was observed for non-factor independent selected cells (Figure 5.10A). Cells derived from these tumours were capable of factor independent growth *in vitro* (data not shown). After 21 weeks, a tumour arising from cells expressing WT c-KIT was identified. No tumours were identified in mice injected with Y721F/D816V c-KIT expressing cells over the duration of the experiment (Figure 5.10A). Mice injected with Y721F/D816V c-KIT expressing cells sacrificed at 24 weeks did not differ in weight from those injected with parental or WT c-KIT cells. Upon dissection, no tumours at the site of injection were visible. Dissection of the fat deposits above and at the injection site were also found to be normal in each case. These

Figure 5.10: Tumour formation by MIHC expressing c-KIT constructs.

Female syngeneic (CBA) mice were injected subcutaneously in the hind flank with $2x10^6$ MIHC expressing WT c-KIT (n=6), D816V c-KIT (n=7), Y721F/D816V c-KIT (n=7) and D816V c-KIT selected for factor independence (D816V(FI)) (n=2). Parental MIHC (n=6) and Y721F c-KIT expressing MIHC (n=6) were also included in the experiment but no tumours were observed (data not shown). Mice were monitored for tumour formation over 24 weeks, with the proportion remaining tumour free plotted in **A**. Formalin fixed paraffin embedded tumour sections were stained with haematoxylin and eosin to identify tumour morphology. A representative section of a tumour from D816V c-KIT cells that had been maintained in muGM-CSF prior to injection (40x initial magnification) **(B)**. Tumour invading surrounding fat **(C)**, blood and lymph **(D)** and muscle tissue **(E)** is shown at 20x magnification.

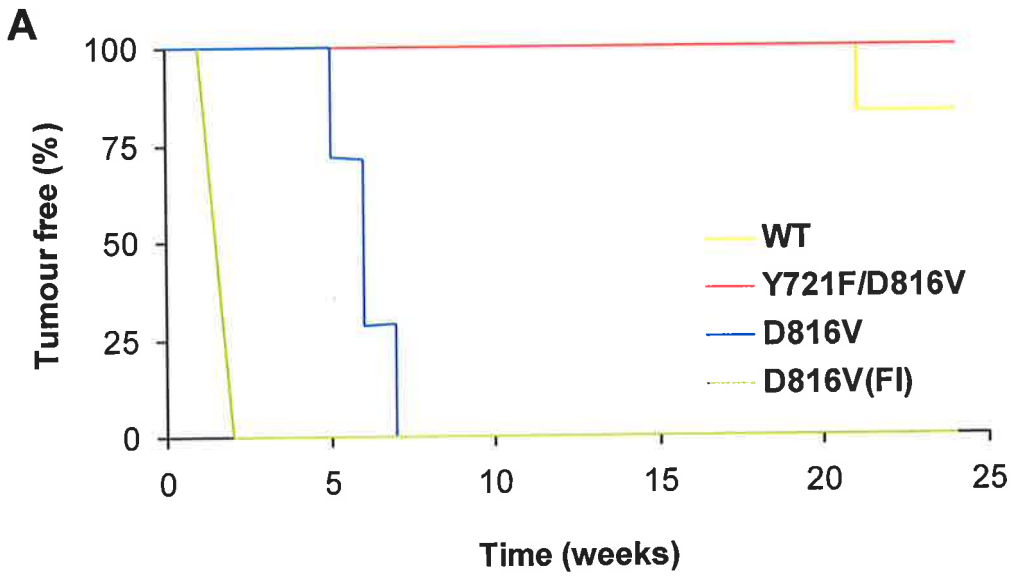
A
100
75
50
25
0
Tumour free (%)
0
5
10
15
20
25
Time (weeks)
WT
Y721F/D816V
D816V
D816V(Fl)

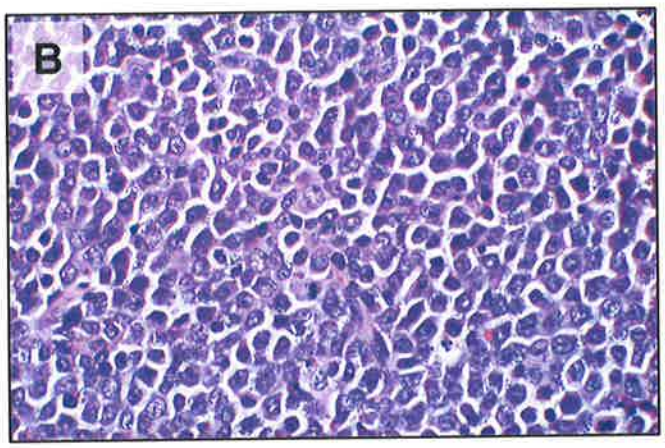
B

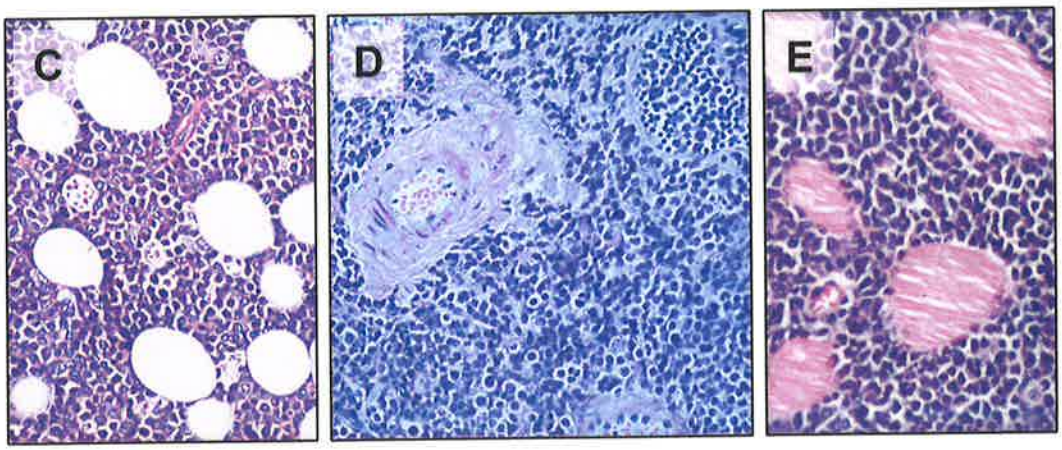
C
D
E

results demonstrated that although Y721F/D816V c-KIT conferred some factor independent growth *in vitro*, MIHCs expressing this mutant were not able to form tumours *in vivo*.

All tumours obtained from mice were morphologically examined to determine the types of cells within the tumour. Formalin fixed, paraffin embedded tumour sections stained with haematoxylin and eosin (see section 2.2.1) showed that the cells from all tumours were malignant histiocytes with many in various stages of mitosis (Figure 5.10B). All tumours showed vascularisation and invasion of fat and muscle tissue with some exhibiting lymphocyte infiltration (Figure 5.10C, D and E). The differentiation status of the tumours was assessed on fresh frozen sections by esterase staining. Tumours derived from D816V c-KIT expressing cells showed patchy staining for macrophage and neutrophil esterases (Figure 5.11A and B), while tumour cells from the mouse injected with WT c-KIT expressing cells had more general macrophage and neutrophil staining (Figure 5.11C).

5.8. Signal Transduction Activated by D816V c-KIT

To begin to address the mechanism for the factor independent growth of D816V c-KIT expressing cells and to determine the role direct PI 3-K recruitment had in this response, the activation of downstream signal transduction pathways involving the protein kinases Akt, MAPK and JNK were investigated. Cells starved of growth factor and FCS for 2 hours were lysed at $2x10^7$/ml (see section 2.7) and whole cell lysates were electrophoresed and transferred to membrane. Activated kinases were detected with antibodies specific for the phosphorylated versions of the proteins. Duplicate blots were probed for total Akt, MAPK and JNK.

It was of interest to investigate the phosphorylation status of Akt as it is activated downstream of PI 3-K. Since D816V c-KIT constitutively associates with and activates PI 3-K, it may be expected that Akt would be phosphorylated in the absence of factor and this would decrease with the Y721F mutation. Stimulation of WT c-KIT expressing cells with

Figure 5.11: Esterase staining of MIHC derived from tumours.

Fresh frozen sections from tumours were stained for the presence of lineage specific esterases (see section 2.2.2). Brown staining indicates the expression of α-naphthyl acetate esterase (macrophage specific) while the presence of naphthol-AS-D-chloroacetate esterase (neutrophil specific) is shown by blue staining with methyl green used as a counterstain. Representative sections were photographed from a tumour derived from D816V c-KIT MIHC selected for factor independent growth **(A)**, D816V c-KIT MIHC that had been maintained in muGM-CSF **(B)** and WT c-KIT MIHC **(C)**. All are at 20x magnification.

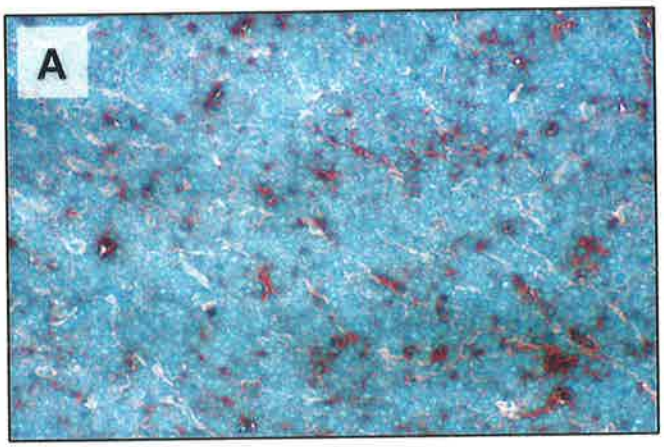
A

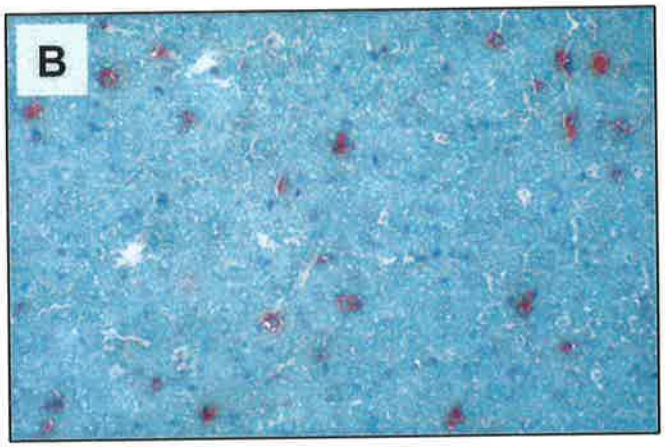
B

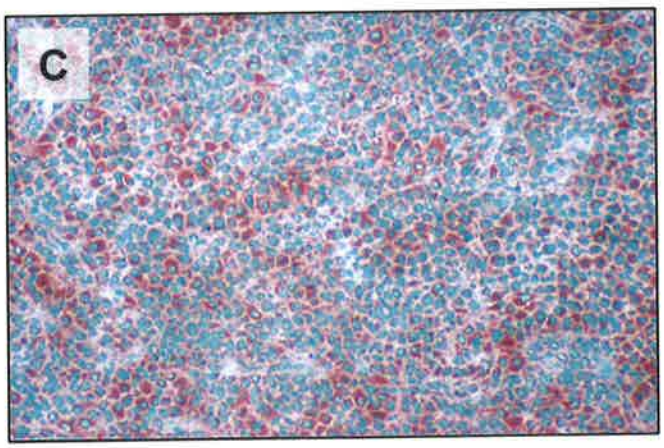
C

huSCF for 5 minutes resulted in inducible phosphorylation of Akt (Figure 5.12A). Surprisingly, D816V c-KIT cells maintained in the absence of factor did not show constitutive phosphorylation of Akt, even though total Akt was detected in the lysate (Figure 5.12A and B). Y721F/D816V and D816V c-KIT expressing cells that had been maintained in muGM-CSF prior to the 2 hour starve showed phosphorylation of Akt to similar levels as WT c-KIT expressing cells stimulated with huSCF (Figure 5.12A). This was unexpected considering results from the factor independent D816V c-KIT expressing cells and was deduced to be due to the parental background of the line. Y721F/D816V and D816V c-KIT expressing cells were created on a different MIHC pedigree and maintained in baculovirus derived muGM-CSF in comparison to WT c-KIT maintained in huSCF and factor independent D816V c-KIT. Therefore, even though D816V c-KIT activated PI 3-K in the absence of factor, it did not induce detectable phosphorylation of Akt.

A downstream protein activated strongly by WT c-KIT is ERK. Results showed that WT c-KIT stimulated the phosphorylation of both p42 and p44 isoforms of ERK in response to huSCF (Figure 5.12C). Surprisingly, factor independent D816V c-KIT expressing cells did not constitutively activate ERK even though similar levels of total protein were present on the Western blots (Figure 5.12C and D). In the absence of stimulation, parental MIHC as well as Y721F/D816V and D816V c-KIT expressing cells had low basal phosphorylation of ERK isoforms. This suggested that neither Y721F/D816V nor D816V c-KIT constitutively activated ERK since levels were equivalent to background.

A protein belonging to the MAPK family known to be involved in stress responses is JNK (Cohen, 1997) and can be activated by RTKs (Foltz and Schrader, 1997). In response to stimulation, this protein is phosphorylated on T183 and Y185, resulting in its activation. Phosphorylation of this protein could not be detected by Western blotting in response to huSCF stimulation of WT c-KIT or D816V c-KIT expressing cells (data not shown). Two different antibodies were used to detect phosphorylated JNK (see Table 2.2) and both were

Figure 5.12: Activation of downstream signal transduction proteins by WT and oncogenic c-KIT.

WT, Y721F/D816V (FV), D816V (V), D816V c-KIT expressing cells selected for factor independence (V(FI)) or parental MIHC (par) were starved of serum and factor for 2 hours, stimulated without (-) or with huSCF for 5 minutes (+) and then lysed at $2x10^7$/ml. Clarified lysates (15 μl) were resolved by SDS-PAGE, transferred to membrane and immunoblotted with antisera specific for phosphorylated Akt **(A)**, total Akt **(B)**, phosphorylated ERK1 and ERK2 **(C)** and total ERK1 and ERK2 **(D)**. Alkaline phosphatase activity was visualised using an ECF substrate and FluorImager analysis.

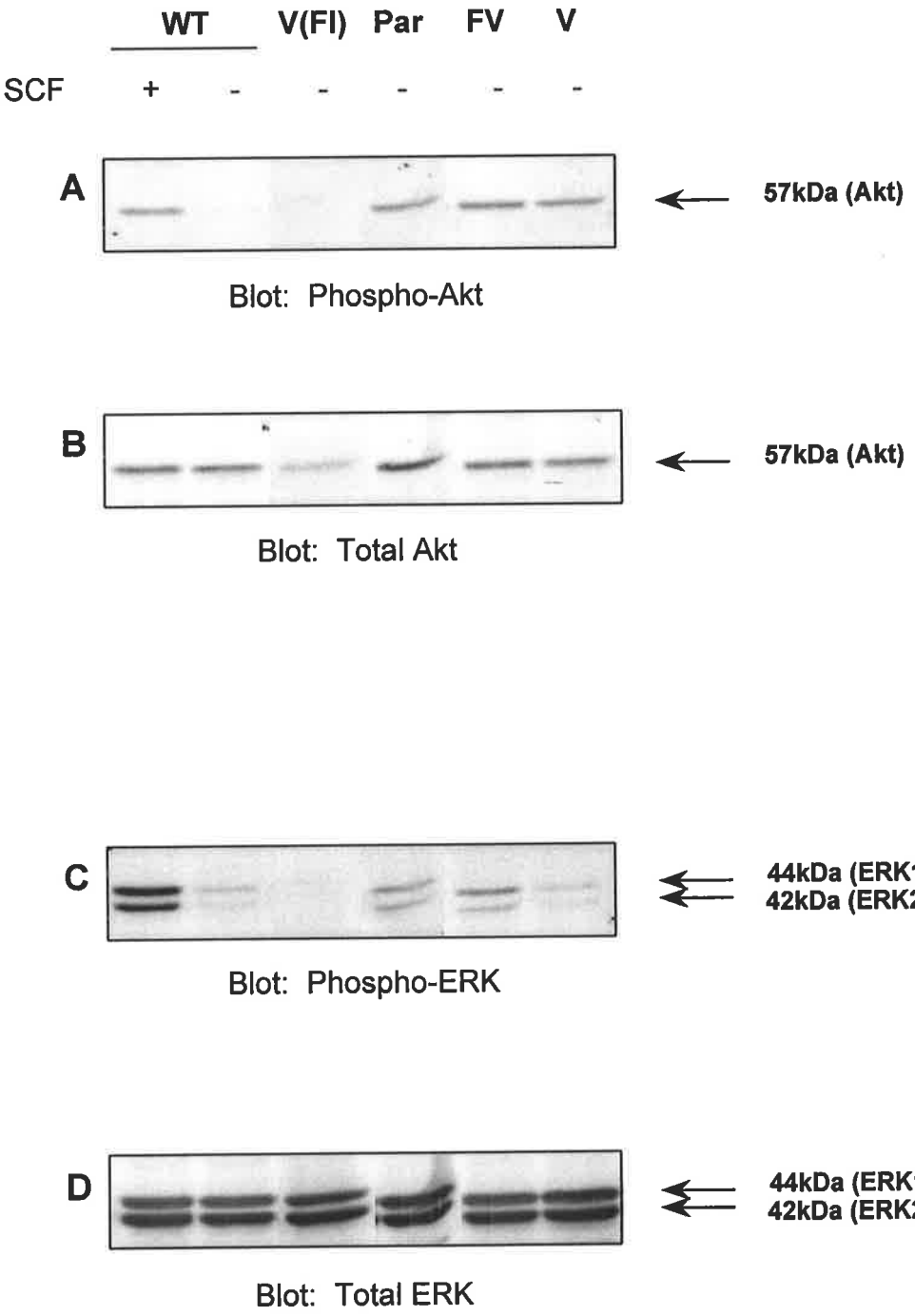
WT
V(FI)
Par
FV
V
SCF
+
-
-
-
-
-
A
57kDa (Akt)
Blot: Phospho-Akt
B
57kDa (Akt)
Blot: Total Akt
C
44kDa (ERK1)
42kDa (ERK2)
Blot: Phospho-ERK
D
44kDa (ERK1)
42kDa (ERK2)
Blot: Total ERK

active based on the positive control supplied with the sample (293 cell extracts treated with or without ultraviolet light; Cell Signalling, Beverly, MA, Cat. No. 9253). These results appear to rule out the involvement of JNK in D816V c-KIT signal transduction, however our collaborators have detected constitutive JNK phosphorylation in factor independent D816V c-KIT expressing MIHC (Chian *et al.*, 2001).

5.9. DISCUSSION

The D816V c-KIT mutation has been proposed to have a role in various malignancies including mastocytosis and AML (Ashman *et al.*, 2000; Buchdunger *et al.*, 2000; Ching *et al.*, 2001; Longley *et al.*, 1999; Worobec *et al.*, 1998). *In vitro* studies have shown that D816V c-KIT confers the ability of cells to grow in the absence of factor and produce tumours in mice (Ferrao *et al.*, 1997). The mechanism inducing this response was largely undefined. This study has shown that the constitutive recruitment of PI 3-K to D816V c-KIT is involved in factor independent growth and tumour formation.

To investigate the role of PI 3-K in mediating factor independent growth and tumour formation, the PI 3-K binding site was mutated (Y721F). This mutation has been shown to remove recruitment of PI 3-K to c-KIT (Figure 4.5). This could not be directly examined in the D816V c-KIT mutant as the protein expression levels were too low (Figures 5.2 and 5.4). Mutation of the PI 3-K binding site decreased but did not abolish the ability of cells to grow in the absence of factor (Figures 5.6, 5.7, and 5.8). Another study using the murine version of the double mutant, Y719F/D814V reported that the expression of this construct in Ba/F3 cells abolished factor independent growth (Jahn *et al.*, 2002b). This group used a MTT assay to monitor factor independent growth of Y719F/D814V c-KIT expressing cells which was the least sensitive of the three techniques performed here.

Even though Y721F/D816V c-KIT expressing MIHC were capable of some factor independent growth *in vitro* (Figures 5.6, 5.7 and 5.8), the cells were incapable of producing

tumours *in vivo* (Figure 5.10). Similarly, expression of D816V c-KIT with dominant negative STAT3 resulted in reduced factor independent growth *in vitro* and abolished tumour formation *in vivo* (Ning *et al.*, 2001a; Ning *et al.*, 2001b). This may suggest that less activity is required by oncogenic receptors for factor independent growth and survival as compared to tumour formation. Therefore, simply analysing the effect of oncogenes by factor independent growth may not be adequate in assessing tumourigenicity and an *in vivo* model is also required.

In the presence of muGM-CSF, substantial cellular attrition was observed for parental MIHC. This was absent for D816V c-KIT expressing cells maintained in the absence of factor (Ferrao *et al.*, 1997). These results were confirmed in this study (Figure 5.8), suggesting that D816V c-KIT delivers a survival advantage to cells. Direct recruitment of PI 3-K was important in cellular survival, yet it had no detectable role in the proliferation of cells in the absence of factor (Figure 5.8). This is similar to results obtained with the Y721F mutation in WT c-KIT presented in chapter 4, where proliferation was minimally affected (Figure 4.20). The survival response would be presumably due to PI 3-K mediated inhibition of proteins involved in apoptosis (Blume-Jensen *et al.*, 1998; Datta *et al.*, 1997; Kimura *et al.*, 1994; Martin *et al.*, 2001). Besides the effect on survival observed here, the D816V c-KIT substitution has also been demonstrated to enhance chemotaxis to huSCF (Taylor *et al.*, 2001).

To try and dissect the signalling requirements of D816V c-KIT further, activation of several downstream components was investigated. Akt, a protein implicated in PI 3-K mediated survival (Kelley *et al.*, 1999; Kulik and Webber, 1998) was surprisingly not activated by D816V c-KIT (Figure 5.12A and B). The antibody used in this study only detected Akt phosphorylated on S473, however phosphorylation at both S473 and T308 is required for its activation (Vanhaesebroeck *et al.*, 1997). This result is in contrast to other studies where Akt was constitutively active in D816V c-KIT expressing cells (Jahn *et al.*,

2002b; Ning *et al.*, 2001a). In one of these studies c-KIT containing a mutation at D816 was expressed in MO7e, a human megakaryoblastic cell line, already expressing high levels of WT c-KIT, and interaction between these two forms of c-KIT may have induced Akt phosphorylation (Ning *et al.*, 2001a). In the other study, Akt was overexpressed which may augment the response and/or aid in identification of its phosphorylation status (Jahn *et al.*, 2002b). Our results suggest that PI 3-K activates alternate pathways to lead to a survival response as has previously been observed (Craddock *et al.*, 1999). Alternatively, D816V c-KIT, which is continually active may only result in a low level of phosphorylation of Akt which is sufficient for the response because it is of a constitutive nature and not transient as in stimulation of WT c-KIT with huSCF.

The MAPK family members were not constitutively active in D816V MIHC (Figure 5.12C and D). This is consistent with other studies (Ning *et al.*, 2001a) and suggests that the Ras-MAPK pathway is not important in oncogenesis by D816V c-KIT. Interestingly, investigation of the oncogenic potential of two other receptors capable of activating PI 3-K, namely TGFα and heregulin/NDF, revealed only weak activation of ERK (Amundadottir and Leder, 1998). This is in contrast to *neu,* which caused strong phosphorylation of ERK but only weak induction of PI 3-K activity (Amundadottir and Leder, 1998). Therefore, receptors activate a different subset of specific signal transduction pathways required for their oncogenicity. Other proteins potentially involved in signal transduction downstream of D816V c-KIT include STAT1 and STAT3 (Ning *et al.*, 2001a; Ning *et al.*, 2001b).

Expression levels of Y721F/D816V and D816V c-KIT in MIHC, when maintained in muGM-CSF, were barely detectable by flow cytometry (Figure 5.2) or Western blot analysis (Figure 5.4A) even though the cells expressed equivalent amounts of *c-KIT* transcripts as compared to WT (Figure 5.3). Detection of D816V c-KIT was possible in cells maintained in the absence of factor, which showed high levels of *c-KIT* mRNA. In this case, D816V c-KIT appeared as an upward smear on SDS-PAGE suggesting that it was continually ubiquitinated

and turned over as has also been shown by Moriyama *et al.* (1996). Constitutive turnover of the pre-T cell receptor is dependent on Cbl mediated ubiquitination as activated by Src (Panigada *et al.*, 2002). This process may also be involved in the regulation of D816V c-KIT levels.

In conclusion, D816V c-KIT mediates factor independent growth *in vitro* predominantly through a survival response, which is partially dependent on the direct recruitment of PI 3-K. Furthermore, direct PI 3-K recruitment was essential for D816V c-KIT mediated tumour formation *in vivo*. The mechanism responsible for the residual factor independent growth of Y721F/D816V c-KIT is unknown, however it is possible that either the involvement of indirect PI 3-K activation or the activation of other signalling intermediates such as STAT3 are responsible.

CHAPTER 6:

GENERAL DISCUSSION

6. GENERAL DISCUSSION

To understand cancer and to develop new, targeted therapies, it is necessary to investigate the activation and function of signal transduction pathways. The research presented here analysed the biological responses and activation of signal transduction pathways by c-KIT; a RTK involved in normal and malignant haemopoiesis. The objectives of this study were fulfilled in three ways. Firstly, the function of two naturally occurring isoforms of c-KIT were compared. The remaining two sections were involved in elucidating the role of an important downstream effector of c-KIT, PI 3-K, in both normal and oncogenic c-KIT signalling.

To analyse the role of c-KIT in huSCF mediated growth in factor dependent early myeloid cells, murine FDC-P1 cells were retrovirally transduced with *c-KIT* cDNA and clones expressing physiological levels of c-KIT protein were selected. Interestingly, a positive relationship was observed between the level of cell surface c-KIT and huSCF mediated growth. A positive correlation has previously been shown between huSCF mediated anchorage independent colony formation and c-KIT protein and mRNA expression levels in NIH-3T3 fibroblasts (Caruana *et al.*, 1998). Caruana *et al.,* (1998) showed that maximal growth was observed at about $5x10^4$ receptors per cell which was approximately the highest level observed in this study. Surprisingly, NIH-3T3 fibroblasts expressing higher levels of c-KIT displayed poor colony formation in huSCF (Caruana *et al.*, 1998). This was possibly due to a G1 specific cell cycle growth arrest mediated by strong Raf activation leading to the induction of $p21^{CIP1}$ expression, an inhibitor of cyclin dependent kinases (Sewing *et al.*, 1997; Woods *et al.*, 1997). FDC-P1 clones expressing c-KIT at levels greater than $5x10^4$ receptors per cell were not generated, suggesting that expression of c-KIT at high levels had a detrimental effect on cell growth even in the absence of huSCF.

The growth of a cell population, defined as the total cell yield, is dependent on the rate of cell death as well as the number of divisions undergone by viable cells. To examine each parameter, a PKH assay (section 2.5.3), measuring the number of divisions and total fluorescence yield of the viable population was performed. Titration of huSCF in both c-KIT expressing FDC-P1 and MIHC cultures highlighted that maximal proliferation required less huSCF than survival. Similarly, the varied growth rate exhibited by FDC-P1 clones was predominantly due to the rate of cellular attrition rather than proliferation. Higher expression of Bcr-Abl is required for protection of myeloid and lymphoid cell lines from apoptotic stimuli as compared to factor independent growth (Cambier *et al.*, 1998). Therefore, survival appears to be the rate limiting process, indicating that if little stimulation is received, these factor dependent early haemopoietic cells are not maintained for an extended period of time in G0, instead they die, possibly through apoptosis. In this regard, immortalised cell lines differ from normal haemopoietic progenitor cells, in that the latter can undergo prolonged periods of quiescence.

The activation kinetics of two naturally occurring isoforms of c-KIT expressed in FDC-P1 cells differed greatly in their responses to huSCF. The rate of turnover for the GNNK- isoform was more rapid as compared to the GNNK+ isoform of c-KIT as previously demonstrated using NIH-3T3 fibroblasts (Caruana *et al.*, 1999; Voytyuk *et al.*, 2003). As shown here, and in previous studies in a murine lymphoma cell line and bone marrow derived mast cells, lack of PI 3-K activation did not affect internalisation of c-KIT (Gommerman *et al.*, 1997; Yee *et al.*, 1994). However, PI 3-K has been shown to have a role in internalisation if calcium flux is also inhibited (Gommerman *et al.*, 1997). The interaction of Src family kinases with c-KIT at Y568 and Y570 is also necessary for internalisation (Broudy *et al.*, 1999). Src was shown to be involved through the use of PP1, a Src inhibitor, however PP1 also inhibits c-KIT function (Tatton *et al.*, 2002). Subsequent studies have confirmed a role of Src in internalisation through mutation of the tyrosine recruitment sites (Jahn *et al.*, 2002a)

or by the use of another Src inhibitor, SU6656 (Voytyuk *et al.*, 2003). Src may mediate its effects on receptor internalisation through the phosphorylation of dynamin (Ahn *et al.*, 2002; Miller *et al.*, 2000), a GTPase involved in cleavage of endocytic vesicles from the plasma membrane. Additionally, Src has been shown to phosphorylate clathrin (Wilde *et al.*, 1999), a protein also involved in endocytosis. Interestingly, differential recruitment and activation of Src by the c-KIT isoforms is capable of explaining the difference in phosphorylation and internalisation in NIH-3T3 fibroblasts (Voytyuk *et al.*, 2003). The GNNK- isoform of c-KIT associates strongly with Src while only associating weakly to the GNNK+ isoform (Voytyuk *et al.*, 2003). Inhibition of Src with SU6656 decreased the rate of internalisation for the GNNK- c-KIT isoform causing it to exhibit similar kinetics to the GNNK+ isoform (Voytyuk *et al.*, 2003). These observations are potentially due to differences in the phosphorylation of the Src recruitment site since this was rapid and transient for the GNNK- isoform while the GNNK+ isoform exhibited a constant low level of phosphorylation (Voytyuk *et al.*, 2003). In NIH-3T3 fibroblasts, the intensity of ERK activation was higher in cells expressing the GNNK- isoform and this was dependent on Src activity (Voytyuk *et al.*, 2003). This result on ERK activity is in contrast to results reported here with FDC-P1 cells, which exhibited minimal difference between the isoforms. Therefore, it would be interesting to address the role of Src in huSCF mediated activation kinetics in FDC-P1 cells. Antibodies directed against specific phospho-tyrosine residues could be used, as done in the NIH-3T3 study, to determine if similar mechanisms operate. Additionally, the expression of kinase inactive forms of Src such as a dominant negative form of Lyn could be used to elucidate its role in these responses and to determine downstream components.

Degradation of c-KIT isoforms expressed in FDC-P1 cells differed with GNNK- being degraded at a more rapid rate as compared to GNNK+. This was also observed in NIH-3T3 cells (Caruana *et al.*, 1999; Voytyuk *et al.*, 2003) and may be due to the differential activation of c-Cbl, a ubiquitin protein ligase (Voytyuk *et al.*, 2003). A similar process involving Src

activation may also be involved for D816V c-KIT degradation since constitutive turnover of another receptor, the pre-T cell receptor is dependent on c-Cbl mediated ubiquitination activated by Src (Panigada *et al.*, 2002). The role of c-Cbl in huSCF mediated degradation of c-KIT could be addressed by the use of c-Cbl containing a mutation in the RING finger domain, which abolishes its ability to promote receptor ubiquitination (Thien *et al.*, 2001).

It is surprising that the insertion or deletion of 12 base pairs in the extracellular juxtamembrane region can lead to profound effects on the behaviour of the isoforms and hence regulate the biological outcome. Interestingly, ligand activation of two isoforms of the insulin receptor differing by 12 amino acids in the extracellular α subunit (Leibiger *et al.*, 2001) resulted in the activation of different classes of PI 3-K and different downstream effectors (Leibiger *et al.*, 2001). Similarly, the activation of different signal transduction pathways is associated with two isoforms of the RTK, Ret (Alberti *et al.*, 1998). Therefore, alternate splicing to create different isoforms may be a general mechanism cells utilise to increase the repertoire of functional receptors, each with slightly different capacities in activating signal transduction pathways. In contrast to results in NIH-3T3 cells (Caruana *et al.*, 1999; Voytyuk *et al.*, 2003), the activation of the downstream signalling protein ERK in FDC-P1 did not differ between the two isoforms of c-KIT even though the intensity of c-KIT phosphorylation was significantly different. The activation of other potentially important pathways, notably Src kinases, were not investigated, therefore, downstream differences in the function of the c-KIT isoforms may have been missed in this study.

Recent studies have highlighted the importance of the juxtamembrane and transmembrane regions in the kinase activity and signal transduction by receptor kinases (Bell *et al.*, 2000; Leibiger *et al.*, 2001; Moriki *et al.*, 2001; Remy *et al.*, 1999; Zhu and Sizeland, 1999). In the case of c-KIT, mutations in the intracellular juxtamembrane region leading to constitutive kinase activity result in gastrointestinal stromal tumours (Moskaluk *et al.*, 1999; Taniguchi *et al.*, 1999) suggesting that this region must have important functions in regulating

activity. The study by Bell and co-workers (2000) investigated the function of the α-helical transmembrane region by inserting a dimerisation motif obtained from an oncogenic version of neu into WT neu and PDGF receptor. Movement of this motif across the transmembrane domain rotated the kinase domain 103° per amino acid. Measurement of receptor phosphorylation and transformation showed that peak activity occurred when the two kinase domains were specifically orientated with respect to each other (Bell *et al.*, 2000). Similar observations were made with the receptor for TGFβ and EGF receptor when the juxtamembrane and transmembrane regions were manipulated (Moriki *et al.*, 2001; Zhu and Sizeland, 1999). Therefore, juxtamembrane and transmembrane regions are important in regulating kinase activity by structurally orientating the kinase domain so it is accessible in the dimer configuration. The insertion or deletion of GNNK in the extracellular juxtamembrane region of c-KIT would be expected to alter the relative orientation of the extracellular domain and the transmembrane domain, in the SCF cross linked active dimer. This could be translated to the intracellular region, where it would affect the orientation of monomers in the dimer and hence kinase activity. Based on preliminary studies, using the structural prediction program of Rost and Sander (1993), it was found that the GNNK stretch of amino acids in the juxtamembrane region was located between two β-sheets (Rowan Koina and Sonia Young; data not shown). Deletion of these four amino acids in the GNNK- isoform altered the predicted location of the second β-sheet and also affected the positioning of the transmembrane domain (Rowan Koina and Sonia Young; data not shown). It would be interesting to investigate this further with modelling studies since alteration of kinase activity by changes in the juxtamembrane and transmembrane domains appears to be a common mechanism employed by receptor kinases.

Phosphorylation of the GNNK- isoform of c-KIT decreased substantially following peak phosphorylation at 2.5 minutes and this preceded degradation. Dephosphorylation occurred after half-maximal internalisation suggesting that a large proportion of

dephosphorylation occurs in the endosome. This may potentially be performed by PTP1B, a prototypical non-transmembrane phosphatase anchored to the cytoplasmic surface of the endoplasmic reticulum via a hydrophobic carboxy terminal anchor sequence (Haj *et al.*, 2002). This phosphatase has been shown to be involved in the dephosphorylation of EGF and PDGF receptors by fluorescent resonance energy transfer (FRET) (Haj *et al.*, 2002). Supporting this, little or no dephosphorylation of GNNK+ c-KIT, which is internalised at a slower rate was observed. This does not rule out the function of other phosphatases, since it is known that SHP1 is important in c-KIT downregulation (Paulson *et al.*, 1996), however it does suggest an additional mechanism.

Analysis of the role of PI 3-K in the activation of signal transduction pathways by huSCF stimulated c-KIT was performed on the GNNK+ isoform of c-KIT. Although this isoform is generally expressed in lower abundance than GNNK- (Crosier *et al.*, 1993; Giebel *et al.*, 1992; Piao *et al.*, 1994), it corresponds to the original published sequence (Yarden *et al.*, 1987) and has been used in most studies of human c-KIT. Phosphorylation of Akt, a well-known downstream effector of PI 3-K reached peak levels after 5 minutes of huSCF stimulation and was substantially reduced by 20 minutes even though the level of PI 3-K associated with the receptor remained constant. This decrease in Akt phosphorylation could be through the activation of PTEN, a phosphatase hydrolysing the 3' phosphoinositide products of PI 3-K (Maehama and Dixon, 1998) resulting in the loss of membrane recruitment of Akt. It could also be due to the translocation of phosphorylated Akt to the nucleus (Meier *et al.*, 1997) from where it maybe poorly extracted by the solubilisation process. In addition, endocytosis results in the termination of further Akt activation since endocytic vesicles do not contain lipid substrates or products of PI 3-K (Haugh and Meyer, 2002). Thus, even though PI 3-K is shown to enter the endocytic pathway associated to RTKs (Kapeller *et al.*, 1993), this may have little relevance to Akt activation and suggests that the location of the enzyme

dictates its function. Interestingly, this may explain why Akt is poorly activated by an oncogenic form of c-KIT, D816V c-KIT, which is continually internalised and degraded.

Internalisation of c-KIT appeared to be a key process regulating receptor function. This was shown by the dephosphorylation of c-KIT and Akt after internalisation as mentioned above. Modification of receptor location, for example through endocytosis, appears to alter the activation of signal transduction pathways and biological responses. This has also been shown for activation of TrkA by NGF where internalisation-competent cells underwent neuronal differentiation, while cells expressing mutant dynamin exhibited increased survival responses (Zhang *et al.*, 2000a). This result was explained by the activation of different signal transduction pathways after internalisation (Zhang *et al.*, 2000a). Similar results have also been obtained with the EGF receptor using mutant dynamin (Vieira *et al.*, 1996), however results performed later by Johannessen and co-workers contradicted this (Johannessen *et al.*, 2000). Investigation of the difference in signalling between EGF and insulin receptors suggested that the differential activation of signal transduction pathways was due to the rates of receptor endocytosis (Di Guglielmo *et al.*, 1994). Compartmentalisation of active receptors to patches of cellular membrane termed 'lipid rafts' also appears important since inhibition of their formation by cholesterol depletion with methyl-β-cyclodextrin results in altered receptor phosphorylation and activation of downstream pathways (Pike and Casey, 2002). Therefore, receptor trafficking to the endocytic pathways appears to be important in attenuating the activation of signal transduction pathways and ensuing biological responses.

Mutation of the PI 3-K recruitment site, Y721 on GNNK+ and D816V c-KIT allowed growth of early myeloid cells in the presence of huSCF or no factor respectively, albeit at a reduced rate. Knock-in mice expressing Y719F, exhibited no haemopoietic defects as judged by haematocrit, red blood cell, white blood cell, granulocyte and platelet numbers (Kissel *et al.*, 2000), instead the phenotype was restricted mainly to reproductive lineages (Blume-Jensen *et al.*, 2000; Kissel *et al.*, 2000). Together with results presented here this suggests

that PI 3-K is involved in haemopoiesis however, compensatory mechanisms absent in gametogenesis must exist, since the defect is not observed in steady state haemopoiesis. The residual response obtained may be due to the cooperation of other pathways with PI 3-K to exert the full mitogenic response. Lack of Src recruitment through mutation of Y567, the murine equivalent of Y568 in humans to phenylalanine, in conjunction with Y719F (site required for PI 3-K recruitment in murine c-Kit), resulted in an abrogation of DNA synthesis in mast cells (Timokhina *et al.*, 1998). Each mutation on its own only had a slight effect (Timokhina *et al.*, 1998). PI 3-K also cooperates with PLCγ in 32D myelomonocytic cells to mediate huSCF dependent mitogenesis (Gommerman *et al.*, 2000).

Alternative PI 3-K activation mechanisms may be important in the residual growth response since the Y721F mutation only removed direct recruitment of PI 3-K to that site. Other recruitment mechanisms appeared to have a role as shown through the inhibition observed with the use of the reversible ATP competitive PI 3-K inhibitor, LY294002. Further, the activation of Akt by Y721F c-KIT suggested that other mechanisms were employed to activate PI 3-K. Localisation of PI 3-K at the membrane in close proximity to its substrates could be by indirect activation of PI 3-K or the use of additional recruitment sites on c-KIT. Indirect activation of PI 3-K could occur through Ras since it is involved in Ras mediated transformation (Rodriguez-Viciana *et al.*, 1997). Other mechanisms to activate PI 3-K include c-Cbl which binds the p85 subunit (Kassenbrock *et al.*, 2002) and is dependent on the activation of Src. Otherwise, Shc maybe involved since it mediates PI 3-K activation by the oncogenic form of the RTK, Ret (Segouffin-Cariou and Billaud, 2000). In response to IL-3, Gab2 was shown to activate PI 3-K via its association to Shc and Grb2 (Gu *et al.*, 2000). Similarly, Gab1 activated PI 3-K in response to EGF or FGF stimulation (Ong *et al.*, 2001; Zhang *et al.*, 2002). Therefore, indirect activation could potentially occur through various intermediates, however alternate recruitment of PI 3-K to c-KIT may also be involved. The consensus sequence for the p85 SH2 domain binding phosphorylated tyrosines has been

identified as pY-X-X-M where a methionine or valine at the first X site increases the p85 binding affinity (Fruman *et al.*, 1998). The sequence surrounding the tyrosine at 721 is pY-M-D-M, corresponding to a high affinity site for p85. In the intracellular domain of c-KIT, two other sites, Y870 and Y900 also have the critical methionine as the third amino acid which may make them candidates for PI 3-K recruitment. It is unknown whether these sites are phosphorylated in response to ligand stimulation. Undoubtedly, Y721 is the major recruitment site for PI 3-K, however the use of one or both of the alternate sites can not be excluded and may potentially explain the trace association of p85 with Y721F c-KIT in response to huSCF.

In summary, studies with c-KIT isoforms indicate that internalisation and degradation are important factors governing biological responses and the attenuation of signal transduction by c-KIT. Although activation of PI 3-K was important for cellular growth, in particular survival, mediated by both GNNK+ and oncogenic c-KIT, it was not absolutely essential indicating that other mechanisms can to some extent compensate for the absence of direct recruitment of this enzyme. Nevertheless, direct PI 3-K recruitment was shown to be important in transformation of early myeloid cells by oncogenic D816V c-KIT and was essential for tumourigenicity.

CHAPTER 7:

REFERENCES

7. REFERENCES

Adachi, S., Ebi, Y., Nishikawa, S., Hayashi, S., Yamazaki, M., Kasugai, T., Yamamura, T., Nomura, S. and Kitamura, Y. (1992). Necessity of extracellular domain of *W* (*c-kit*) receptors for attachment of murine cultured mast cells to fibroblasts. *Blood* **79**: 650-656.

Adams, J. M. and Cory, S. (2001). Life-or-death decisions by the Bcl-2 protein family. *Trends Biochem. Sci.* **26**: 61-66.

Ahn, S., Kim, J., Lucaveche, C. L., Reedy, M. C., Luttrell, L. M., Lefkowitz, R. J. and Daaka, Y. (2002). Src-dependent tyrosine phosphorylation regulates dynamin self-assembly and ligand-induced endocytosis of the epidermal growth factor receptor. *J. Biol. Chem.* **277**: 26642-26651.

Alberti, L., Borrello, M. G., Ghizzoni, S., Torriti, F., Rizzetti, M. G. and Pierotti, M. A. (1998). Grb2 binding to the different isoforms of Ret tyrosine kinase. *Oncogene* **17**: 1079-1087.

Alexander, W. S., Lyman, S. D. and Wagner, E. F. (1991). Expression of functional c-kit receptors rescues the genetic defect of W mutant mast cells. *EMBO J.* **10**: 3683-3691.

Amundadottir, L. T. and Leder, P. (1998). Signal transduction pathways activated and required for mammary carcinogenesis in response to specific oncogenes. *Oncogene* **16**: 737-746.

Anderson, D. M., Lyman, S. D., Baird, A., Wignall, J. M., Eisenman, J., Rauch, C., March, C. J., Boswell, H. S., Gimpel, S. D., Cosman, D. and Williams, D. E. (1990). Molecular cloning of mast cell growth factor, a hematopoietin that is active in both membrane bound and soluble forms. *Cell* **63**: 235-243.

Anderson, K. E., Coadwell, J., Stephens, L. R. and Hawkins, P. T. (1998). Translocation of PDK-1 to the plasma membrane is important in allowing PDK-1 to activate protein kinase B. *Curr. Biol.* **8**: 684-691.

Andjelkovic, M., Alessi, D. R., Meier, R., Fernandez, A., Lamb, N. J. C., Frech, M., Cron, P., Cohen, P., Lucocq, J. M. and Hemmings, B. A. (1997). Role of translocation in the activation and function of protein kinase B. *J. Biol. Chem.* **272**: 31515-31524.

Andre, C., Martin, E., Cornu, F., Hu, W. X., Wang, X. P. and Galibert, F. (1992). Genomic organization of the human *c-kit* gene: evolution of the receptor tyrosine kinase subclass III. *Oncogene* **7**: 685-691.

Aoki, M., Schetter, C., Himly, M., Bastista, O., Chang, H. W. and Vogt, P. K. (2000). The catalytic subunit of phosphoinositide 3-kinase: Requirements for oncogenicity. *J. Biol. Chem.* **275**: 6267-6275.

Arudchandran, R., Brown, M. J., Peirce, M. J., Song, J. S., Zhang, J., Siraganian, R. P., Blank, U. and Rivera, J. (2000). The src homology 2 domain of Vav is required for its compartmentation to the plasma membrane and activation of c-Jun NH_2-terminal kinase 1. *J. Exp. Med.* **191**: 47-59.

Ashley, D. M., Bol, S. J. and Kannourakis, G. (1994). Measurement of the growth parameters of precursor B-acute lymphoblastic leukaemic cells in co-culture with bone marrow stromal cells; detection of two cd10 positive populations with different proliferative capacities and survival. *Leuk. Res.* **18**: 37-48.

Ashman, L. K., Roberts, M. M., Gadd, S. J., Cooper, S. J. and Juttner, C. A. (1988). Expression of a 150-kD cell surface antigen identified by monoclonal antibody YB5.B8 is associated with poor prognosis in acute non-lymphoblastic leukaemia. *Leuk. Res.* **12**: 923-928.

Ashman, L. K., Cambareri, A. C., To, L. B., Levinsky, R. J. and Juttner, C. A. (1991). Expression of the YB5.B8 antigen (c-kit proto-oncogene product) in normal human bone marrow. *Blood* **78**: 30-37.

Ashman, L. K., Ferrao, P., Cole, S. R. and Cambareri, A. C. (2000). Effects of mutant c-Kit in early myeloid cells. *Leuk. Lymphoma* **37**: 233-243.

Auger, K. R., Serunian, L. A., Soltoff, S. P., Libby, P. and Cantley, L. C. (1989). PDGF-dependent tyrosine phosphorylation stimulates production of novel polyphosphoinositides in intact cells. *Cell* **57**: 167-175.

Austyn, J. M. and Gordon, S. (1981). F4/80, a monoclonal antibody directed specifically against the mouse macrophage. *Eur. J. Immunol.* **11**: 805-815.

Avanzi, G. C., Lista, P., Giovinazzo, B., Miniero, R., Saglio, G., Benetton, G., Coda, R., Cattoretti, G. and Pegoraro, L. (1988). Selective growth response to IL-3 of a human leukaemic cell line with megakaryoblastic features. *Br. J. Haematol.* **69**: 359-366.

Avraham, S., Jiang, S., Ota, S., Fu, Y., Deng, B., Dowler, L. L., White, R. A. and Avraham, H. (1995). Structural and functional studies of the intracellular tyrosine kinase MATK gene and its translated product. *J. Biol. Chem.* **270**: 1833-1842.

Avruch, J., Zhang, X.-F. and Kyriakis, J. M. (1994). Raf meets Ras: completing the framework of a signal transduction pathway. *Tibs.* **19**: 279-283.

Aylett, G., Cole, S. R., Caruana, G. and Ashman, L. K. (1995). Specificity and functional effects of mAb to c-Kit protein (SCF receptor). In *Leucocyte Typing V -White Cell Differentiation Antigens*, vol. 2 (ed. Schlossman, S. F., Boumsell, L., Gilks, W., Harlan, J. M., Kishimoto, T., Morimoto, C., Ritz, J., Shaw, S., Silverstein, R., Springer, T. A., Tedder, T. F. and Todd, R. F.), pp. 1917. Oxford: Oxford University Press.

Backer, J. M., Myers, M. G., Jr., Shoelson, S. E., Chin, D. J., Sun, X. J., Miralpeix, M., Hu, P., Margolis, B., Skolnik, E. Y., Schlessinger, J. and et al. (1992). Phosphatidylinositol 3'-kinase is activated by association with IRS-1 during insulin stimulation. *EMBO J.* **11**: 3469-3479.

Backer, J. M. (2000). Phosphoinositide 3-kinases and the regulation of vesicular trafficking. *Mol. Cell Biol. Res. Commun.* **3**: 193-204.

Bazan, J. F. (1991). Genetic and structural homology of stem cell factor and macrophage colony-stimulating factor. *Cell* **65**: 9-10.

Beghini, A., Cairoli, R., Morra, E. and Larizza, L. (1998). In vivo differentiation of mast cells from acute myeloid leukemia blasts carrying a novel activating ligand-independent C-kit mutation. *Blood Cells Mol. Dis.* **24**: 262-270.

Bell, C. A., Tynan, J. A., Hart, K. C., Meyer, A. N., Robertson, S. C. and Donoghue, D. J. (2000). Rotational coupling of the transmembrane and kinase domains of the Neu receptor tyrosine kinase. *Mol. Biol. Cell* **11**: 3589-3599.

Bellacosa, A., Testa, J. R., Staal, S. P. and Tsichlis, P. N. (1991). A retroviral oncogene, Akt, encoding a serine-threonine kinase containing an SH2-like region. *Science* **254**: 274-277.

Bellacosa, A., de Feo, D., Godwin, A. K., Bell, D. W., Cheng, J. Q., Altomare, D. A., Wan, M., Dubeau, L., Scambia, G., Masciullo, V. and et al. (1995). Molecular alterations of the AKT2 oncogene in ovarian and breast carcinomas. *Int. J. Cancer* **64**: 280-285.

Bendall, L. J., Makrynikola, V., Hutchinson, A., Bianchi, A. C., Bradstock, K. F. and Gottlieb, D. J. (1998). Stem cell factor enhances the adhesion of AML cells to fibronectin and augments fibronectin-mediated anti-apoptotic and proliferative signals. *Leukemia* **12**: 1375-1382.

Bernstein, A., Forrester, L., Reith, A. D., Dubreuil, P. and Rottapel, R. (1991). The murine *W/c-kit* and *Steel* loci and the control of hematopoiesis. *Seminars in Hematology* **28 (2)**: 138-142.

Berridge, M. J. (1993). Inositol trisphosphate and calcium signalling. *Nature* **361**: 315-325.

Berrozpe, G., Timokhina, I., Yukl, S., Tajima, Y., Ono, M., Zelenetz, A. D. and Besmer, P. (1999). The W^{sh}, W^{57} and *Ph Kit* expression mutations define tissue-specific control elements located between -23 and -154kb upstream of *Kit*. *Blood* **94**: 2658-2666.

Beslu, N., LaRose, J., Casteran, N., Birnbaum, D., Lecocq, E., Dubreuil, P. and Rottapel, R. (1996). Phosphatidylinositol-3' kinase is not required for mitogenesis or internalization of the Flt3/Flk2 receptor tyrosine kinase. *J. Biol. Chem.* **271**: 20075-20081.

Besmer, P., Murphy, J. E., George, P. C., Qui, F., Bergold, P. J., Lederman, L., Snyder, H. W., Brodeur, D., Zuckerman, E. E. and Hardy, W. D. (1986). A new acute transforming feline retrovirus and relationship of its oncogene *v-kit* with the protein kinase gene family. *Nature* **320**: 415-421.

Bishop, J. M. (1982). Oncogenes. *Scientific American* **246**: 69-78.

Bishop, J. M. (1987). The Molecular Genetics of Cancer. *Science* **235**: 305-311.

Bishop, J. M. (1991). Molecular Themes in Oncogenesis. *Cell* **64**: 235-248.

Blechman, J. M., Lev, S., Brizzi, M. F., Leitner, O., Pegoraro, L., Givol, D. and Yarden, Y. (1993a). Soluble c-Kit proteins and antireceptor monoclonal antibodies confine the binding site of the stem cell factor. *J. Biol. Chem.* **268**: 4399-4406.

Blechman, J. M., Lev, S., Givol, D. and Yarden, Y. (1993b). Structure-function analyses of the kit receptor for the steel factor. *Stem Cells* **11**: 12-21.

Blechman, J. M., Lev, S., Barg, J., Eisenstein, M., Vaks, B., Vogel, Z., Givol, D. and Yarden, Y. (1995). The fourth immunoglobulin domain of the stem cell factor receptor couples ligand binding to signal transduction. *Cell* **80**: 103-113.

Blume-Jensen, P., Claesson-Welsh, L., Siegbahn, A., Zsebo, K. M., Westermark, B. and Heldin, C. H. (1991). Activation of the human *c-kit* product by ligand-induced dimerization mediates circular actin reorganization and chemotaxis. *EMBO J.* **10**: 4121-4128.

Blume-Jensen, P., Siegbahn, A., Stabel, S., Heldin, C. H. and Ronnstrand, L. (1993). Increased Kit/SCF receptor induced mitogenicity but abolished cell motility after inhibition of protein kinase C. *EMBO J.* **12**: 4199-4209.

Blume-Jensen, P., Ronnstrand, L., Gout, I., Waterfield, M. D. and Heldin, C. H. (1994). Modulation of Kit/stem cell factor receptor-induced signaling by protein kinase C. *J. Biol. Chem.* **269**: 21793-21802.

Blume-Jensen, P., Wernstedt, C., Heldin, C.-H. and Roennstrand, L. (1995). Identification of the major phosphorylation sites for protein kinase C in Kit/stem cell factor receptor *in vitro* and in intact cells. *J. Biol. Chem.* **270**: 14192-14200.

Blume-Jensen, P., Janknecht, R. and Hunter, T. (1998). The Kit receptor promotes cell survival via activation of PI 3-kinase and subsequent Akt-mediated phosphorylation of Bad on Ser136. *Curr. Biol.* **8**: 779-782.

Blume-Jensen, P., Jiang, G., Hyman, R., Lee, K.-F., O'Gorman, S. and Hunter, T. (2000). Kit/stem cell factor receptor-induced activation of phosphatidylinositol 3'-kinase is essential for male fertility. *Nature Genet.* **24**: 157-162.

Blume-Jensen, P. and Hunter, T. (2001). Oncogenic kinase signalling. *Nature* **411**: 355-365.

Boswell, H. S., Mochizuki, D. Y., Burgess, G. S., Gillis, S., Walker, E. B., Anderson, D. and Williams, D. E. (1990). A novel mast cell growth factor (MCGF-3) produced by marrow-adherent cells that synergizes with Interleukin 3 and 4. *Exp. Hematol.* **18**: 794-800.

Brizzi, M. F., Dentelli, P., Lanfrancone, L., Rosso, A., Pelicci, P. G. and Pegoraro, L. (1996). Discrete protein interactions with Grb2/c-Cbl complex in SCF- and TPO-mediated myeloid cell proliferation. *Oncogene* **13**: 2067-2076.

Brizzi, M. F., Dentelli, P., Rosso, A., Yarden, Y. and Pegoraro, L. (1999). STAT protein recruitment and activation in c-Kit deletion mutants. *J. Biol. Chem.* **274**: 16965-16972.

Brondello, J.-M., Brunet, A., Pouyssegur, J. and McKenzie, F. R. (1997). The dual specificity mitogen-activated protein kinase phosphatase-1 and -2 are induced by the p42/p44(MAPK) cascade. *J. Biol. Chem.* **272**: 1368-1376.

Broudy, V. C., Lin, N. L., Liles, W. C., Corey, S. J., O'Laughlin, B., Mou, S. and Linnekin, D. (1999). Signaling via src family kinases is required for normal internalization of the receptor c-Kit. *Blood* **94**: 1979-1986.

Brown, G. C., Hoek, J. B. and Kholodenko, B. N. (1997). Why do protein kinase cascades have more than one level? *Tibs.* **22**: 288.

Buchdunger, E., Zimmermann, J., Mett, H., Meyer, T., Muller, M., Druker, B. J. and Lydon, N. B. (1996). Inhibition of the Abl protein-tyrosine kinase in vitro and in vivo by a 2-phenylaminopyrimidine derivative. *Cancer Res.* **56**: 100-104.

Buchdunger, E., Cioffi, C. L., Law, N., Stover, D., Ohno-Jones, S., Druker, B. J. and Lydon, N. B. (2000). Abl protein-tyrosine kinase inhibitor STI571 inhibits in vitro signal transduction mediated by c-kit and platelet-derived growth factor receptors. *J. Pharmacol. Exp. Ther.* **295**: 139-145.

Buday, L., Warne, P. H. and Downward, J. (1995). Downregulation of the Ras pathway by MAP Kinase phosphorylation of Sos. *Oncogene* **11**: 1327-1331.

Bühring, H. J., Herbst, R., Kostka, G., Bossenmaier, B., Bartke, I., Kropshofer, H., Kalbacher, H., Busch, F. W., Muller, C. A., Schlessinger, J. and et al. (1993). Modulation of p145c-kit function in cells of patients with acute myeloblastic leukemia. *Cancer Res* **53**: 4424-4431.

Cambier, N., Chopra, R., Strasser, A., Metcalf, D. and Elefanty, A. G. (1998). BCR-ABL activates pathways mediating cytokine independence and protection against apoptosis in murine hematopoietic cells in a dose-dependent manner. *Oncogene* **16**: 335-348.

Cantley, L. C., Auger, K. R., Carpenter, C., Duckworth, B., Graziani, A., Kapeller, R. and Soltoff, S. (1991). Oncogenes and Signal Transduction. *Cell* **64**: 281-302.

Cantley, L. C. and Neel, B. G. (1999). New insights into tumor suppression: PTEN suppresses tumor formation by restraining the phosphoinositide 3-kinase/AKT pathway. *Proc. Natl. Acad. Sci. U.S.A.* **96**: 4240-4245.

Carlberg, K., Tapley, P., Haystead, C. and Rohrschneider, L. (1991). The role of kinase activity and the kinase insert region in ligand-induced internalization and degradation of the c-fms protein. *EMBO J.* **10**: 877-883.

Carpenter, C. L., Duckworth, B. C., Auger, K. R., Cohen, B., Schaffhausen, B. S. and Cantley, L. C. (1990). Purification and characterization of phosphoinositide 3-kinase from rat liver. *J. Biol. Chem.* **265**: 19704-19711.

Caruana, G., Cambareri, A. C., Gonda, T. J. and Ashman, L. K. (1998). Transformation of NIH3T3 fibroblasts by the c-Kit receptor tyrosine kinase: effect of receptor density and ligand-requirement. *Oncogene* **16**: 179-190.

Caruana, G., Cambareri, A. C. and Ashman, L. K. (1999). Isoforms of c-KIT differ in activation of signalling pathways and transformation of NIH3T3 fibroblasts. *Oncogene* **18**: 5573-5581.

Chabot, B., Stephenson, D. A., Chapman, V. M., Besmer, P. and Bernstein, A. (1988). The proto-oncogene *c-kit* encoding a transmembrane tyrosine kinase receptor maps to the mouse *W* locus. *Nature* **335**: 88-89.

Chang, H. W., Aoki, M., Fruman, D., Auger, K. R., Bellacosa, A., Tsichlis, P. N., Cantley, L. C., Roberts, T. M. and Vogt, P. K. (1997). Transformation of chicken cells by the gene encoding the catalytic subunit of PI 3-kinase. *Science* **276**: 1848-1850.

Chen, R., Kim, O., Yang, J., Sato, K., Eisenmann, K. M., McCarthy, J., Chen, H. and Qiu, Y. (2001). Regulation of Akt/PKB activation by tyrosine phosphorylation. *J. Biol. Chem.* **276**: 31858-31862.

Cheng, J. Q., Godwin, A. K., Bellacosa, A., Taguchi, T., Franke, T. F., Hamilton, T. C., Tsichlis, P. N. and Testa, J. R. (1992). AKT2, a putative oncogene encoding a member of a subfamily of protein-serine/threonine kinases, is amplified in human ovarian carcinomas. *Proc. Natl. Acad. Sci. U.S.A.* **89**: 9267-9271.

Cheng, J. Q., Ruggeri, B., Klein, W. M., Sonoda, G., Altomare, D. A., Watson, D. K. and Testa, J. R. (1996). Amplification of AKT2 in human pancreatic cells and inhibition of AKT2 expression and tumorigenicity by antisense RNA. *Proc. Natl. Acad. Sci. U.S.A.* **93**: 3636-3641.

Chian, R., Young, S., Danilkovitch-Miagkova, A., Ronnstrand, L., Leonard, E., Ferrao, P., Ashman, L. and Linnekin, D. (2001). Phosphatidylinositol 3 kinase contributes to the transformation of hematopoietic cells by the D816V c-Kit mutant. *Blood* **98**: 1365-1373.

Ching, T. T., Lin, H. P., Yang, C. C., Oliveira, M., Lu, P. J. and Chen, C. S. (2001). Specific binding of the C-terminal Src homology 2 domain of the p85alpha subunit of phosphoinositide 3-kinase to phosphatidylinositol 3,4,5-trisphosphate. Localization and engineering of the phosphoinositide-binding motif. *J. Biol. Chem.* **276**: 43932-43938.

Claesson-Welsh, L. (1994). Platelet-derived growth factor receptor signals. *J. Biol. Chem.* **51**: 32023-32026.

Coffer, P. J. and Woodgett, J. R. (1991). Molecular cloning and characterisation of a novel putative protein-serine kinase related to the cAMP-dependent and protein kinase C families. *Eur. J. Biochem.* **201**: 475-481.

Cohen, P. (1997). The search for physiological substrates of MAP and SAP kinases in mammalian cells. *Trends in Cell Biology* **7**: 353-361.

Cole, S. R., Ashman, L. K. and Ey, P. L. (1987). Biotinylation: an alternative to radioiodination for the identification of cell surface antigens in immunoprecipitates. *Mol. Immunol.* **24**: 699-705.

Cole, S. R., Aylett, G. W., Casey, G., Harvey, N. L., Cambareri, A. C. and Ashman, L. K. (1996). Increased expression of c-Kit or its ligand Steel Factor is not a common feature of adult acute myeloid leukaemia. *Leukemia* **10**: 288-296.

Colucci, F. and Di Santo, J. P. (2000). The receptor tyrosine kinase c-kit provides a critical signal for survival, expansion, and maturation of mouse natural killer cells. *Blood* **95**: 984-991.

Copeland, N. G., Gilbert, D. J., Cho, B. C., Donovan, P. J., Jenkins, N. A., Cosman, D., Anderson, D., Lyman, S. D. and Williams, D. E. (1990). Mast cell growth factor maps near

the steel locus on mouse chromosome 10 and is deleted in a number of steel alleles. *Cell* **63**: 175-183.

Craddock, B. L., Orchiston, E. A., Hinton, H. J. and Welham, M. J. (1999). Dissociation of apoptosis from proliferation, protein kinase B activation, and BAD phosphorylation in interleukin-3-mediated phosphoinositide 3-kinase signaling. *J. Biol. Chem.* **274**: 10633-10640.

Crosier, P. S., Ricciardi, S. T., Hall, L. R., Vitas, M. R., Clark, S. C. and Crosier, K. E. (1993). Expression of isoforms of the human receptor tyrosine kinase c-kit in leukemic cell lines and acute myeloid leukemia. *Blood* **82**: 1151-1158.

Damen, J. E., Ware, M. D., Kalesnikoff, J., Hughes, M. R. and Krystal, G. (2001). SHIP's C-terminus is essential for its hydrolysis of PIP3 and inhibition of mast cell degranulation. *Blood* **97**: 1343-1351.

Dastych, J., Taub, D., Hardison, M. C. and Metcalfe, D. D. (1998). Tyrosine kinase-deficient W^v c-kit induces mast cell adhesion and chemotaxis. *Am. J. Physiol.*. **275**: C1291-C1299.

Datta, S. R., Dudek, H., Tao, X., Masters, S., Fu, H., Gotoh, Y. and Greenberg, M. E. (1997). Akt phosphorylation of BAD couples survival signals to the cell-intrinsic death machinery. *Cell* **91**: 231-241.

Davis, R. J. (1993). The mitogen-activated protein kinase signal transduction pathway. *J. Biol. Chem.* **268**: 14553-14556.

De Sepulveda, P., Okkenhaug, K., La Rose, J., Hawley, R. G., Dubreuil, P. and Rottapel, R. (1999). Socs1 binds to multiple signalling proteins and suppresses Steel factor-dependent proliferation. *EMBO J.* **18**: 904-915.

Dent, P., Jarvis, W. D., Birrer, M. J., Fisher, P. B., Schmidt-Ullrich, R. K. and Grant, S. (1998). The roles of signaling by the p42/p44 mitogen-activated protein (MAP) kinase pathway; a potential route to radio-and chemo-sensitization of tumor cells resulting in the induction of apoptosis and loss of clonogenicity. *Leukemia* **12**: 1843-1850.

Dexter, T. M., Garland, J., Scott, D., Scolnick, E. and Metcalf, D. (1980). Growth of factor-dependent hemopoietic precursor cell lines. *J Exp Med* **152**: 1036-1047.

Di Guglielmo, G. M., Baass, P. C., Ou, W.-J., Posner, B. I. and Bergeron, J. J. M. (1994). Compartmentalization of SHC, GRB2 and mSOS, and hyperphosphorylation of Raf-1 by EGF but not insulin in liver parenchyma. *EMBO J.* **13**: 4269-4277.

Dikic, I., Schlessinger, J. and Lax, I. (1994). PC12 cells overexpressing the insulin receptor undergo insulin- dependent neuronal differentiation. *Curr. Biol.* **4**: 702-708.

Downing, J. R., Roussel, M. F. and Sherr, C. J. (1989). Ligand and protein kinase C downmodulate the colony-stimulating factor 1 receptor by independent mechanisms. *Mol. Cell. Biol.* **9**: 2890-2896.

Druker, B. J., Tamura, S., Buchdunger, E., Ohno, S., Segal, G. M., Fanning, S., Zimmermann, J. and Lydon, N. B. (1996). Effects of a selective inhibitor of the Abl tyrosine kinase on the growth of Bcr-Abl positive cells. *Nat. Med.* **2**: 561-566.

Duronio, V., Welham, M. J., Abraham, S., Dryden, P. and Schrader, J. W. (1992). p21ras activation via hemopoietin receptors and c-kit requires tyrosine kinase activity but not tyrosine phosphorylation of p21ras GTPase-activating protein. *Proc. Natl. Acad. Sci. U.S.A.* **89**: 1587-1591.

Duronio, V., Scheid, M. P. and Ettinger, S. (1998). Downstream signalling events regulated by phosphatidylinositol 3- kinase activity. *Cellular Signalling* **10**: 233-239.

Erber, W. N., Pinching, A. J. and Mason, D. Y. (1984). Immunocytochemical detection of T and B cell populations in routine blood smears. *Lancet* **1**: 1042-1046.

Ettenberg, S. A., Magnifico, A., Cuello, M., Nau, M. M., Rubinstein, Y. R., Yarden, Y., Weissman, A. M. and Lipkowitz, S. (2001). Cbl-b-dependent coordinated degradation of the epidermal growth factor receptor signaling complex. *J. Biol. Chem.* **276**: 27677-27684.

Eves, E. M., Xiong, W., Bellacosa, A., Kennedy, S. G., Tsichlis, P. N., Rosner, M. R. and Hay, N. (1998). Akt, a target of phosphatidylinositol 3-kinase, inhibits apoptosis in a differentiating neuronal cell line. *Mol. Cell. Biol.* **18**: 2143-2152.

Fantl, W. J., Johnson, D. E. and Williams, L. T. (1993). Signalling by receptor tyrosine kinases. *Annu. Rev. Biochem.* **62**: 453-481.

Feng, L.-X., Ravindranath, N. and Dym, M. (2000). Stem cell factor/c-kit up-regulates cyclin D3 and promotes cell cycle progression via the phosphoinositide 3-kinase/p70 S6 kinase pathway in spermatogonia. *J. Biol. Chem.* **275**: 25572-25576.

Ferrao, P., Gonda, T. J. and Ashman, L. K. (1997). Expression of constitutively activated human c-Kit in Myb transformed early myeloid cells leads to factor independence, histiocytic differentiation, and tumorigenicity. *Blood* **90**: 4539-4552.

Ferrell, J. E. J. (1996). Tripping the switch fantastic: how a protein kinase cascade can covert graded inputs into switch-like outputs. *Tibs.* **21**: 460-466.

Ferrell, J. E. J. (1997). How responses get more switch-like as you move down a protein kinase cascade. *Tibs.* **22**: 288-289.

Flanagan, J. G. and Leder, P. (1990). The kit ligand: a cell surface molecule altered in steel mutant fibroblasts. *Cell* **63**: 185-194.

Flanagan, J. G., Chan, D. C. and Leder, P. (1991). Transmembrane form of the kit ligand growth factor is determined by alternative splicing and is missing in the Sl^d mutant. *Cell* **64**: 1025-1035.

Fleischman, R. A., Saltman, D. L., Stastny, V. and Zneimer, S. (1991). Deletion of the *c-kit* protooncogene in the human developmental defect piebald trait. *Proc. Natl. Acad. Sci. U.S.A.* **88**: 10885-10889.

Foltz, I. N. and Schrader, J. W. (1997). Activation of the stress-activated protein kinases by multiple hematopoietic growth factors with the exception of interleukin-4. *Blood* **89**: 3092-3096.

Franke, T. F., Yang, S. I., Chan, T. O., Datta, K., Kazlauskas, A., Morrison, D. K., Kaplan, D. R. and Tsichlis, P. N. (1995). The protein kinase encoded by the Akt proto-oncogene is a target of the PDGF-activated phosphatidylinositol 3-kinase. *Cell* **81**: 727-736.

Frost, M. J., Ferrao, P. T., Hughes, T. P. and Ashman, L. K. (2002). Juxtamembrane mutant V560GKit is more sensitive to Imatinib (STI571) compared with wild-type c-kit whereas the kinase domain mutant D816VKit is resistant. *Mol. Cancer. Ther.* **1**: 1115-1124.

Fruman, D. A., Meyers, R. E. and Cantley, L. C. (1998). Phosphoinositide kinases. *Annu. Rev. Biochem.* **67**: 481-507.

Funasaka, Y., Boulton, T., Cobb, M., Yarden, Y., Fan, B., Lyman, S. D., Williams, D. E., Anderson, D. M., Zakut, R., Mishima, Y. and Halaban, R. (1992). c-kit-kinase induces a cascade of protein tyrosine phosphorylation in normal human melanocytes in response to mast cell growth factor and stimulates mitogen-activated protein kinase but is down-regulated in melanomas. *Mol. Biol. Cell* **3**: 197-209.

Furitsu, T., Tsujimura, T., Tono, T., Ikeda, H., Kitayama, H., Koshimizu, U., Sugahara, H., Butterfield, J. H., Ashman, L. K., Kanayama, Y., Matsuzawa, Y., Kitamura, Y. and Kanakura, Y. (1993). Identification of mutations in the coding sequence of the proto- oncogene c-kit in a human mast cell leukemia cell line causing ligand-independent activation of c-kit product. *J. Clin. Invest.* **92**: 1736-1744.

Gadd, S. J. and Ashman, L. K. (1985). A murine monoclonal antibody specific for a cell-surface antigen expressed by a subgroup of human myeloid leukaemias. *Leuk. Res.* **9**: 1329-1336.

Galetic, I., Andjelkovic, M., Meier, R., Brodbeck, D., Park, J. and Hemmings, B. A. (1999). Mechanism of protein kinase B activation by insulin/insulin-like growth factor-1 revealed by

specific inhibitors of phosphoinositide 3-kinase - Significance for diabetes and cancer. *Pharmacol. Ther.* **82**: 409-425.

Gari, M., Goodeve, A., Wilson, G., Winship, P., Langabeer, S., Linch, D., Vandenberghe, E., Peake, I. and Reilly, J. (1999). c-kit proto-oncogene exon 8 in-frame deletion plus insertion mutations in acute myeloid leukaemia. *Br. J. Haematol.* **105**: 894-900.

Garrington, T. P. and Johnson, G. L. (1999). Organization and regulation of mitogen-activated protein kinase signaling pathways. *Curr. Opin. Cell Biol.* **11**: 2011-2218.

Giebel, L. B. and Spritz, R. A. (1991). Mutation of the *Kit* (mast/stem cell growth factor receptor) protooncogene in human piebaldism. *Proc. Natl. Acad. Sci. U.S.A.* **88**: 8696-8699.

Giebel, L. B., Strunk, K. M., Holmes, S. A. and Spritz, R. A. (1992). Organization and nucleotide sequence of the human KIT (mast/stem cell growth factor receptor) proto-oncogene. *Oncogene* **7**: 2207-2217.

Gillham, H., Golding, M. C. H. M., Pepperkok, R. and Gullick, W. J. (1999). Intracellular movement of green fluorescent protein-tagged phosphatidylinositol 3-kinase in response to growth factor receptor signaling. *J. Cell Biol.* **146**: 869-880.

Gokkel, E., Grossman, Z., Ramot, B., Yarden, Y., Rechavi, G. and Givol, D. (1992). Structural organization of the murine *c-kit* proto-oncogene. *Oncogene* **7**: 1423-1429.

Gommerman, J. L., Rottapel, R. and Berger, S. A. (1997). Phosphatidylinositol 3-kinase and Ca^{2+} influx dependence for ligand-stimulated internalization of the c-Kit receptor. *J. Biol. Chem.* **272**: 30519-30525.

Gommerman, J. L., Sittaro, D., Klebasz, N. Z., Williams, D. A. and Berger, S. A. (2000). Differential stimulation of c-Kit mutants by membrane-bound and soluble Steel Factor correlates with leukemic potential. *Blood* **96**: 3734-3742.

Grammer, T. C., Cheatham, L., Chou, M. M. and Blenis, J. (1996). The p70S6K signalling pathway: a novel signalling system involved in growth regulation. *Cancer Surv.* **27**: 271-292.

Gratton, J. P., Morales-Ruiz, M., Kureishi, Y., Fulton, D., Walsh, K. and Sessa, W. C. (2001). Akt down regulation of p38 signaling provides a novel mechanism of VEGF mediated cytoprotection in endothelial cells. *J. Biol. Chem.* **276**: 30359-30365.

Gu, H., Maeda, H., Moon, J. J., Lord, J. D., Yoakim, M., Nelson, B. H. and Neel, B. G. (2000). New role for Shc in activation of the phosphatidylinositol 3-kinase/Akt pathway. *Mol. Cell. Biol.* **20**: 7109-7120.

Hahn, W. C., Counter, C. M., Lundberg, A. S., Beijersbergen, R. L., Brooks, M. W. and Weinberg, R. A. (1999). Creation of human tumour cells with defined genetic elements. *Nature* **400**: 464-468.

Haj, F. G., Verveer, P. J., Squire, A., Neel, B. G. and Bastiaens, P. I. (2002). Imaging sites of receptor dephosphorylation by PTP1B on the surface of the endoplasmic reticulum. *Science* **295**: 1708-1711.

Hallek, M., Druker, B., Lepisto, E. M., Wood, K. W., Ernst, T. J. and Griffin, J. D. (1992). Granulocyte-macrophage colony-stimulating factor and steel factor induce phosphorylation of both unique and overlapping signal transduction intermediates in a human factor-dependent hematopoietic cell line. *J. Cell. Physiol.* **153**: 176-186.

Hashimoto, K., Tsujimura, T., Moriyama, Y., Yamatodani, A., Kimura, M., Tohya, K., Morimoto, M., Kitayama, H., Kanakura, Y. and Kitamura, Y. (1996). Transforming and differentiation-inducing potential of constitutively activated c-kit mutant genes in the IC-2 murine interleukin-3-dependent mast cell line. *Am. J. Path.* **148**: 189-200.

Haugh, J. M. and Meyer, T. (2002). Active EGF receptors have limited access to PtdIns(4,5)P(2) in endosomes: implications for phospholipase C and PI 3-kinase signaling. *J. Cell Sci.* **115**: 303-310.

Hayashi, S.-I., Kunisada, T., Ogawa, M., Yamaguchi, K. and Nishikawa, S.-I. (1991). Exon skipping by mutation of an authentic splice site of *c-kit* gene in *W/W* mouse. *Nucleic Acids Research* **19 (6)**: 1267-1271.

Heldin, C.-H. (1995). Dimerization of cell surface receptors in signal transduction. *Cell* **80**: 213-223.

Herbst, R., Lammers, R., Schlessinger, J. and Ullrich, A. (1991). Substrate phosphorylation specificity of the human c-kit receptor tyrosine kinase. *J. Biol. Chem.* **266**: 19908-19916.

Herbst, R., Shearman, M. S., Obermeier, A., Schlessinger, J. and Ullrich, A. (1992). Differential effects of *W* mutations on $p145^{c\text{-}kit}$ tyrosine kinase activity and substrate interaction. *J. Biol. Chem.* **267**: 13210-13216.

Herbst, R., Munemitsu, S. and Ullrich, A. (1995a). Oncogenic activation of *v-kit* involves deletion of a putative tyrosine-substrate interaction site. *Oncogene* **10**: 369-379.

Herbst, R., Shearman, M. S., Jallal, B., Schlessinger, J. and Ullrich, A. (1995b). Formation of signal transfer complexes between stem cell and platelet-derived growth factor receptors and SH2 domain proteins in vitro. *Biochemistry* **34**: 5971-5979.

Hicke, L. (1999). Gettin' down with ubiquitin: turning off cell-surface receptors, transporters and channels. *Trends in Cell Biology* **9**: 107-112.

Hirota, S., Isozaki, K., Moriyama, Y., Hashimoto, K., Nishida, T., Ishiguro, S., Kawano, K., Hanada, M., Kurata, A., Takeda, M., Muhammad Tunio, G., Matsuzawa, Y., Kanakura, Y., Shinomura, Y. and Kitamura, Y. (1998). Gain-of-function mutations of c-kit in human gastrointestinal stromal tumors. *Science* **279**: 577-580.

Hirota, S., Nishida, T., Isozaki, K., Taniguchi, M., Nakamura, J., Okazaki, T. and Kitamura, Y. (2001). Gain-of-function mutation at the extracellular domain of KIT in gastrointestinal stromal tumours. *J. Pathol.* **193**: 505-510.

Holmes, K. L., Langdon, W. Y., Fredrickson, T. N., Coffman, R. L., Hoffman, P. M., Hartley, J. W. and Morse, H. C., 3rd. (1986). Analysis of neoplasms induced by Cas-Br-M MuLV tumor extracts. *J. Immunol.* **137**: 679-688.

Hsu, Y. R., Wu, G. M., Mendiaz, E. A., Syed, R., Wypych, J., Toso, R., Mann, M. B., Boone, T. C., Narhi, L. O., Lu, H. S. and Langley, K. E. (1997). The majority of stem cell factor exists as monomer under physiological conditions. *J. Biol. Chem.* **272**: 6406-6415.

Hu, P., Mondino, A., Skolnik, E. Y. and Schlessinger, J. (1993). Cloning of a novel, ubiquitously expressed human phosphatidylinositol 3-kinase and identification of its binding site on p85. *Mol. Cell. Biol.* **13**: 7677-7688.

Huang, E., Nocka, K., Beier, D. R., Chu, T. Y., Buck, J., Lahm, H. W., Wellner, D., Leder, P. and Besmer, P. (1990). The hematopoietic growth factor KL is encoded by the Sl locus and is the ligand of the c-kit receptor, the gene product of the W locus. *Cell* **63**: 225-233.

Hubbard, S. R., Mohammadi, M. and Schlessinger, J. (1998). Autoregulatory mechanisms in protein-tyrosine kinases. *J. Biol. Chem.* **273**: 11987-11990.

Hubbard, S. R. and Till, J. H. (2000). Protein tyrosine kinase structure and function. *Annu. Rev. Biochem.* **69**: 373-398.

Hughes, P. E., Renshaw, M. W., Pfaff, M., Forsyth, J., Keivens, V. M., Schwartz, M. A. and Ginsberg, M. H. (1997). Suppression of integrin activation: a novel function of a Ras/Raf-initiated MAP kinase pathway. *Cell* **88**: 521-530.

Hunter, T. (1995). Protein kinases and phosphatases: The yin and yang of protein phosphorylation and signaling. *Cell* **80**: 225-236.

Hunter, T. (2000). Signaling - 2000 and beyond. *Cell* **100**: 113-127.

Ikeda, H., Kanakura, Y., Tamaki, T., Kuriu, A., Kitayama, H., Ishikawa, J., Kanayama, Y., Yonezawa, T., Tarui, S. and Griffin, J. D. (1991). Expression and functional role of the proto-oncogene *c-kit* in acute myeloblastic leukemia cells. *Blood* **78**: 2962-2968.

Ikeda, H., Kanakura, Y., Furitsu, T., Kitayama, H., Sugahara, H., Nishiura, T., Karasuno, T., Tomiyama, Y., Yamatodani, A., Kanayama, Y. and Matsuzawa, Y. (1993). Changes in

phenotype and proliferative potential of human acute myeloblastic leukemia cells in culture with stem cell factor. *Exp. Hematol.* **21**: 1686-1694.

Ilic, D., Furuta, Y., Kanazawa, S., Takeda, N., Sobue, K., Nakatsuji, N., Nomura, S., Fujimoto, J., Okada, M. and Yamamoto, T. (1995). Reduced cell motility and enhanced focal adhesion contact formation in cells from FAK-deficient mice. *Nature* **377**: 539-544.

Jahn, T., Seipel, P., Coutinho, S., Urschel, S., Schwarz, K., Miething, C., Serve, H., Peschel, C. and Duyster, J. (2002a). Analysing c-kit internalization using a functional c-kit-EGFP chimera containing the fluorochrome within the extracellular domain. *Oncogene* **21**: 4508-4520.

Jahn, T., Seipel, P., Urschel, S., Peschel, C. and Duyster, J. (2002b). Role for the adaptor protein Grb10 in the activation of Akt. *Mol. Cell. Biol.* **22**: 979-991.

Jhun, B. H., Rivnay, B., Price, D. and Avraham, H. (1995). The MATK tyrosine kinase interacts in a specific and SH2- dependent manner with c-Kit. *J. Biol. Chem.* **270**: 9661-9666.

Jiang, X., Gurel, O., Mendiaz, E. A., Stearns, G. W., Clogston, C. L., Lu, H. S., Osslund, T. D., Syed, R. S., Langley, K. E. and Hendrickson, W. A. (2000). Structure of the active core of human stem cell factor and analysis of binding to its receptor KIT. *EMBO J.* **19**: 3192-3203.

Jimenez, C., Jones, D. R., Rodríguez-Viciana, P., Gonzalez-García, A., Leonardo, E., Wennström, S., Von Kobbe, C., Toran, J. L., Borlado, L. R., Calvo, V., Copin, S. G., Albar, J. P., Gaspar, M. L., Diez, E., Marcos, M. A. R., Downward, J., Martinez, C., Mérida, I. and Carrera, A. C. (1998). Identification and characterization of a new oncogene derived from the regulatory subunit of phosphoinositide 3-kinase. *EMBO J.* **17**: 743-753.

Johannessen, L. E., Ringerike, T., Molnes, J. and Madshus, I. H. (2000). Epidermal growth factor receptor efficiently activates mitogen- activated protein kinase in HeLa cells and Hep2 cells conditionally defective in clathrin-dependent endocytosis. *Exp. Cell Res.* **260**: 136-145.

Joly, M., Kazlauskas, A. and Corvera, S. (1995). Phosphatidylinositol 3-kinase activity is required at a postendocytic step in platelet-derived growth factor receptor trafficking. *J. Biol. Chem.* **270**: 13225-13230.

Jones, P. F., Jakubowicz, T., Pitossi, F. J., Maurer, F. and Hemmings, B. A. (1991). Molecular cloning and identification of a serine/threonine protein kinase of the second-messenger subfamily. *Proc. Natl. Acad. Sci. U.S.A.* **88**: 4171-4175.

Kainulainen, V., Sundvall, M., Maatta, J. A., Santiestevan, E., Klagsbrun, M. and Elenius, K. (2000). A natural ErbB4 isoform that does not activate phosphoinositide 3- kinase mediates proliferation but not survival or chemotaxis. *J. Biol. Chem.* **275**: 8641-8649.

Kanagasundaram, V., Jaworowski, A. and Hamilton, J. A. (1996). Association between phosphatidylinositol-3 kinase, Cbl and other tyrosine phosphorylated proteins in colony-stimulating factor-1- stimulated macrophages. *Biochem. J.* **320**: 69-77.

Kanakura, Y., Furitsu, T., Tsujimura, T., Butterfield, J. H., Ashman, L. K., Ikeda, H., Kitayama, H., Kanayama, Y., Matsuzawa, Y. and Kitamura, Y. (1994). Activating mutations of the c-kit proto-oncogene in a human mast cell leukemia cell line. *Leukemia* **8 Suppl 1**: S18-S22.

Kantarjian, H. M., Cortes, J., O'Brien, S., Giles, F. J., Albitar, M., Rios, M. B., Shan, J., Faderl, S., Garcia-Manero, G., Thomas, D. A., Resta, D. and Talpaz, M. (2002). Imatinib mesylate (STI571) therapy for Philadelphia chromosome-positive chronic myelogenous leukemia in blast phase. *Blood* **99**: 3547-3553.

Kapeller, R., Chakrabarti, R., Cantley, L., Fay, F. and Corvera, S. (1993). Internalization of activated platelet-derived growth factor receptor-phosphatidylinositol-3' kinase complexes: Potential interactions with microtubule cytoskeleton. *Mol. Cell. Biol.* **13**: 6052-6063.

Kassenbrock, C. K., Hunter, S., Garl, P., Johnson, G. L. and Anderson, S. M. (2002). Inhibition of Src family kinases blocks epidermal growth factor (EGF)- induced activation of Akt, phosphorylation of c-Cbl, and ubiquitination of the EGF receptor. *J. Biol. Chem.* **277**: 24967-24975.

Kavanaugh, W. M., Klippel, A., Escobedo, J. A. and Williams, L. T. (1992). Modification of the 85-kilodalton subunit of phosphatidylinositol-3 kinase in platelet-derived growth factor-stimulated cells. *Mol. Cell. Biol.* **12**: 3415-3424.

Kelley, T. W., Graham, M. M., Doseff, A. I., Pomerantz, R. W., Lau, S. M., Ostrowski, M. C., Franke, T. F. and Marsh, C. B. (1999). Macrophage colony-stimulating factor promotes cell survival through Akt/protein kinase B. *J. Biol. Chem.* **274**: 26393-26398.

Kennedy, S. G., Wagner, A. J., Conzen, S. D., Jordan, J., Bellacosa, A., Tsichlis, P. N. and Hay, N. (1997). The PI 3-kinase/Akt signaling pathway delivers an anti-apoptotic signal. *Genes & Development* **11**: 701-713.

Keshet, E., Lyman, S. D., Williams, D. E., Anderson, D. M., Jenkins, N. A., Copeland, N. G. and Parada, L. F. (1991). Embryonic RNA expression patterns of the *c-kit* receptor and its cognate ligand suggest multiple functional roles in mouse development. *EMBO J.* **10**: 2425-2435.

Kharitonenkov, A., Chen, Z., Sures, I., Wang, H., Schilling, J. and Ullrich, A. (1997). A family of proteins that inhibit signalling through tyrosine kinase receptors. *Nature* **386**: 181-186.

Kimura, A., Nakata, Y., Katoh, O. and Hyodo, H. (1997). c-Kit point mutation in patients with myeloproliferative disorders. *Leuk. Lymphoma* **25**: 281-287.

Kimura, K., Hattori, S., Kabuyama, Y., Shizawa, Y., Takayanagi, J., Nakamura, S., Toki, S., Matsuda, Y., Onodera, K. and Fukui, Y. (1994). Neurite outgrowth of PC12 cells is suppressed by wortmannin, a specific inhibitor of phosphatidylinositol 3-kinase. *J. Biol. Chem.* **269**: 18961-18967.

Kinashi, T. and Springer, T. A. (1994). Steel factor and c-kit regulate cell-matrix adhesion. *Blood* **83**: 1033-1038.

Kissel, H., Timokhina, I., Hardy, M. P., Rothschild, G., Tajima, Y., Soares, V., Angeles, M., Whitlow, S. R., Manova, K. and Besmer, P. (2000). Point mutation in Kit receptor tyrosine kinase reveals essential roles for Kit signaling in spermatogenesis and oogensis without affecting other Kit responses. *EMBO J.* **19**: 1312-1326.

Kitamura, Y. and Go, S. (1978). Decreased production of mast cells in Sl/Sl*d* anemic mice. *Blood* **53**: 492-497.

Kitamura, Y., Go, S. and Hatanaka, K. (1978). Decrease of mast cells in *W/Wv* mice and their increase by bone marrow transplantation. *Blood* **52**: 447-452.

Kitayama, H., Kanakura, Y., Furitsu, T., Tsujimura, T., Oritani, K., Ikeda, H., Sugahara, H., Mitsui, H., Kanayama, Y., Kitamura, Y. and et al. (1995). Constitutively activating mutations of c-kit receptor tyrosine kinase confer factor-independent growth and tumorigenicity of factor-dependent hematopoietic cell lines. *Blood* **85**: 790-798.

Klippel, A., Kavanaugh, W. M., Pot, D. and Williams, L. T. (1997). A specific product of phosphatidylinositol 3-kinase directly activates the protein kinase Akt through its pleckstrin homology domain. *Mol. Cell. Biol.* **17**: 338-344.

Koike, T., Hirai, K., Morita, Y. and Nozawa, Y. (1993). Stem cell factor-induced signal transduction in rat mast cells. Activation of phospholipase D but not phosphoinositide-specific phospholipase C in c-kit receptor stimulation. *J. Immunol.* **151**: 359-366.

Kon-Kozlowski, M., Pani, G., Pawson, T. and Siminovich, K. A. (1996). The tyrosine phosphatase PTP1C associates with Vav, Grb2, and mSOS1 in hematopoietic cells. *J. Biol. Chem.* **271**: 3856-3862.

Koshimizu, U., Tsujimura, T., Isozaki, K., Nomura, S., Furitsu, T., Kanakura, Y., Kitamura, Y. and Nishimune, Y. (1994). W^n mutation of *c-kit* receptor affects its post-translational processing and extracellular expression. *Oncogene* **9**: 157-162.

Kozawa, O., Blume-Jensen, P., Heldin, C. H. and Rönnstrand, L. (1997). Involvement of phosphatidylinositol 3'-kinase in stem-cell- factor-induced phospholipase D activation and arachidonic acid release. *Eur. J. Biochem.* **248**: 149-155.

Kozlowski, M., Larose, L., Lee, F., Le, D. M., Rottapel, R. and Siminovitch, K. A. (1998). SHP-1 binds and negatively modulates the c-Kit receptor by interaction with tyrosine 569 in the c-Kit juxtamembrane domain. *Mol. Cell. Biol.* **18**: 2089-2099.

Kruszynska, Y. T., Worrall, D. S., Ofrecio, J., Frias, J. P., Macaraeg, G. and Olefsky, J. M. (2002). Fatty acid-induced insulin resistance: decreased muscle PI3K activation but unchanged Akt phosphorylation. *J. Clin. Endocrinol. Metab.* **87**: 226-234.

Kubota, Y., Angelotti, T., Niederfellner, G., Herbst, R. and Ullrich, A. (1998). Activation of phosphatidylinositol 3-kinase is necessary for differentiation of FDC-P1 cells following stimulation of type III receptor tyrosine kinases. *Cell Growth and Differentiation* **9**: 247-256.

Kulik, G. and Webber, M. J. (1998). Akt-dependent and -independent survival signaling pathways utilized by insulin-like growth factor 1. *Mol. Cell. Biol.* **18**: 6711-6718.

Kuriu, A., Ikeda, H., Kanakura, Y., Griffin, J. D., Druker, B., Yagura, H., Kitayama, H., Ishikawa, J., Nishiura, T., Kanayama, Y. and al., e. (1991). Proliferation of human myeloid leukemia cell line associated with the tyrosine-phosphorylation and activation of the proto-oncogene c-kit product. *Blood* **78**: 2834-2840.

Lam, L. P. Y., Chow, R. Y. K. and Berger, S. A. (1999). A transforming mutation enhances the activity of the c-Kit soluble tyrosine kinase domain. *Biochem. J.* **338**: 131-138.

Lammie, A., Drobnjak, M., Gerald, W., Saad, A., Cote, R. and Cordon-Cardo, C. (1994). Expression of c-kit and kit ligand proteins in normal human tissues. *Journal of Histochemistry and Cytochemistry* **42**: 1417-1425.

Lang, R. A., Metcalf, D., Gough, N. M., Dunn, A. R. and Gonda, T. J. (1985). Expression of a hemopoietic growth factor cDNA in a factor-dependent cell line results in autonomous growth and tumorigenicity. *Cell* **43**: 531-542.

Langlois, W. J., Sasaoka, T., Saltiel, A. R. and Olefsky, J. M. (1995). Negative feedback regulation and desensitization of insulin- and epidermal growth factor-stimulated p21ras activation. *J. Biol. Chem.* **270**: 25320-25323.

Ledbetter, J. A. and Herzenberg, L. A. (1979). Xenogeneic monoclonal antibodies to mouse lymphoid differentiation antigens. *Immunol. Rev.* **47**: 63-90.

Leevers, S. J., Vanhaesebroeck, B. and Waterfield, M. D. (1999). Signalling through phosphoinositide 3-kinases: the lipids take centre stage. *Curr. Opin. Cell Biol.* **11**: 219-225.

Leibiger, B., Leibiger, I. B., Moede, T., Kemper, S., Kulkarni, R. N., Kahn, C. R., de Vargas, L. M. and Berggren, P. O. (2001). Selective insulin signaling through A and B insulin receptors regulates transcription of insulin and glucokinase genes in pancreatic beta cells. *Mol. Cell.* **7**: 559-570.

Lemmon, M. A., Pinchasi, D., Zhou, M., Lax, I. and Schlessinger, J. (1997). Kit receptor dimerization is driven by bivalent binding of stem cell factor. *J. Biol. Chem* **272**: 6311-6317.

Lemmon, M. A. and Ferguson, K. M. (1998). Pleckstrin homology domains. In *Protein modules in signal transduction*, vol. 228 (ed. Pawson, A. J.), pp. 39-74. Berlin Heidelberg: Springer -Verlag.

Lennartsson, J., Blume-Jensen, P., Hermanson, M., Ponten, E., Carlberg, M. and Ronnstrand, L. (1999). Phosphorylation of Shc by Src family kinases is necessary for stem cell factor receptor/c-kit mediated activation of the Ras/MAP kinase pathway and c-fos induction. *Oncogene* **18**: 5546-5553.

Lerner, N. B., Nocka, K. H., Cole, S. R., Qiu, F. H., Strife, A., Ashman, L. K. and Besmer, P. (1991). Monoclonal antibody YB5.B8 identifies the human c-kit protein product. *Blood* **77**: 1876-1883.

Lev, S., Givol, D. and Yarden, Y. (1991). A specific combination of substrates is involved in signal transduction by the kit-encoded receptor. *EMBO J.* **10 (3)**: 647-654.

Lev, S., Givol, D. and Yarden, Y. (1992a). Interkinase domain of kit contains the binding site for phosphatidylinositol 3' kinase. *Proc. Natl.Acad Sci. U.S.A.* **89**: 678-682.

Lev, S., Yarden, Y. and Givol, D. (1992b). A recombinant ectodomain of the receptor for the stem cell factor (SCF) retains ligand-induced receptor dimerization and antagonizes SCF-stimulated cellular responses. *J. Biol. Chem.* **267**: 10866-10873.

Lev, S., Yarden, Y. and Givol, D. (1992c). Dimerization and activation of the kit receptor by monovalent and bivalent binding of the stem cell factor. *J. Biol. Chem.* **267**: 15970-15977.

Lev, S., Blechman, J., Nishikawa, S.-I., Givol, D. and Yarden, Y. (1993). Interspecies molecular chimeras of kit help define the binding site of the stem cell factor. *Mol. Cell. Biol.* **13**: 2224-2234.

Levesque, J.-P., Leavesley, D. I., Niutta, S., Vadas, M. and Simmons, P. J. (1995). Cytokines increase human hemopoietic cell adhesiveness by activation of very late antigen (VLA)-4 and VLA-5 integrins. *J. Exp. Med.* **181**: 1805-1815.

Levesque, J.-P., Haylock, D. N. and Simmons, P. J. (1996). Cytokine regulation of proliferation and cell adhesion are correlated events in human $CD34^+$ hemopoietic progenitors. *Blood* **88**: 1168-1176.

Li, G., D'Souza-Schorey, C., Barbieri, M. A., Roberts, R. L., Klippel, A., Williams, L. T. and Stahl, P. D. (1995). Evidence for phosphatidylinositol 3-kinase as a regulator of endocytosis via activation of Rab5. *Proc. Natl. Acad. Sci. U.S.A.* **92**: 10207-10211.

Li, J., Yen, C., Liaw, D., Podsypanina, K., Bose, S., Wang, S. I., Puc, J., Miliaresis, C., Rodgers, L., McCombie, R., Bigner, S. H., Giovanella, B. C., Ittmann, M., Tycko, B., Hibshoosh, H., Wigler, M. H. and Parsons, R. (1997). PTEN, a putative protein tyrosine phosphatase gene mutated in human brain, breast, and prostate cancer. *Science* **275**: 1943-1947.

Liao, A. T., Chien, M. B., Shenoy, N., Mendel, D. B., McMahon, G., Cherrington, J. M. and London, C. A. (2002). Inhibition of constitutively active forms of mutant kit by multitargeted indolinone tyrosine kinase inhibitors. *Blood* **100**: 585-593.

Liaw, D., Marsh, D. J., Li, J., Dahia, P. L., Wang, S. I., Zheng, Z., Bose, S., Call, K. M., Tsou, H. C., Peacocke, M., Eng, C. and Parsons, R. (1997). Germline mutations of the PTEN gene in Cowden disease, an inherited breast and thyroid cancer syndrome. *Nat. Genet.* **16**: 64-67.

Linnekin, D., Weiler, S. R., Mou, S., DeBerry, C. S., Keller, J. R., Ruscetti, F. W., Ferris, D. K. and Longo, D. L. (1996). JAK2 is constitutively associated with c-kit and is phosphorylated in response to stem cell factor. *Acta Haematologica* **95**: 224-228.

Linnekin, D., DeBerry, C. S. and Mou, S. (1997). Lyn associates with the juxtamembrane region of c-Kit and is activated by stem cell factor in hematopoietic cell lines and normal progenitor cells. *J. Biol. Chem.* **272**: 27450-27455.

Logan, S. K., Falasca, M., Hu, P. and Schlessinger, J. (1997). Phosphatidylinositol 3-kinase mediates epidermal growth factor- induced activation of the c-Jun N-terminal kinase signaling pathway. *Mol. Cell. Biol.* **17**: 5784-5790.

Longley, B. J., Tyrrell, L., Ma, Y. S., Williams, D. A., Halaban, R., Langley, K., Lu, H. S. and Schechter, N. M. (1997). Chymase cleavage of stem cell factor yields a bioactive, soluble product. *Proc. Natl. Acad. Sci. U.S.A.* **94**: 9017-9021.

Longley, B. J., Metcalfe, D. D., Tharp, M., Wang, X., Tyrrell, L., Lu, S.-H., Heitjan, D. and Ma, Y. (1999). Activating and dominant inactivating c-KIT catalytic domain mutations in distinct clinical forms of human mastocytosis. *Proc. Natl. Acad. Sci. U.S.A.* **96**: 1609-1614.

Longley, B. J., Reguera, M. J. and Ma, Y. (2001). Classes of c-KIT activating mutations: proposed mechanisms of action and implications for disease classification and therapy. *Leuk. Res.* **25**: 571-576.

Lux, M. L., Rubin, B. P., Biase, T. L., Chen, C.-J., Maclure, T., Demetri, G., Xiao, S., Singer, S., Fletcher, C. D. M. and Fletcher, J. A. (2000). KIT extracellular and kinase domain mutations in gastrointestinal stromal tumors. *Am. J. Path.* **156**: 791-795.

Ma, Y., Zeng, S., Metcalfe, D. D., Akin, C., Dimitrijevic, S., Butterfield, J. H., McMahon, G. and Longley, B. J. (2002). The c-KIT mutation causing human mastocytosis is resistant to STI571 and other KIT kinase inhibitors; kinases with enzymatic site mutations show different inhibitor sensitivity profiles than wild-type kinases and those with regulatory-type mutations. *Blood* **99**: 1741-1744.

Maehama, T. and Dixon, J. E. (1998). The tumor suppressor, PTEN/MMAC1, dephosphorylates the lipid second messenger, phosphatidylinositol 3,4,5-trisphosphate. *J. Biol. Chem.* **273**: 13375-13378.

Mainiero, F., Murgia, C., Wary, K. K., Curatola, A. M., Pepe, A., Blumemberg, M., Westwick, J. K., Der, C. J. and Giancotti, F. G. (1997). The coupling of $\alpha_6\beta_4$ integrin to Ras-MAP kinase pathways mediated by Shc controls keratinocyte proliferation. *EMBO J.* **16**: 2365-2375.

Majumdar, M. K., Feng, L., Medlock, E., Toksoz, D. and Williams, D. A. (1994). Identification and mutation of primary and secondary proteolytic cleavage sites in murine stem cell factor cDNA yields biologically active, cell-associated protein. *J. Biol. Chem.* **269**: 1237-1242.

Mann, R., Mulligan, R. C. and Baltimore, D. (1983). Construction of a retrovirus packaging mutant and its use to produce helper-free defective retrovirus. *Cell* **33**: 153-159.

Manova, K. and Bachvarova, R. F. (1991). Expression of *c-kit* encoded at the *W* locus of mice in developing embryonic germ cells and presumptive melanoblasts. *Developmental Biology* **146**: 312-324.

Marshall, C. J. (1995). Specificity of receptor tyrosine kinase signaling: transient versus sustained extracellular signal-regulated kinase activation. *Cell* **80**: 179-185.

Marte, B. M. and Downward, J. (1997). PKB/Akt: connecting phosphoinositide 3-kinase to cell survival and beyond. *Tibs.* **22**: 355-358.

Martin, F. H., Suggs, S. V., Langley, K. E., Lu, H. S., Ting, J., Okino, K. H., Morris, C. F., McNiece, I. K., Jacobsen, F. W., Mendiaz, E. A., Birkett, N. C., Smith, K. A., Johnson, M., Parker, V. P., Flores, J. C., Patel, A. C., Fisher, E. F., Erjavec, H. O., Herrera, C. J., Wypych, J., Sachdev, R. K., Pope, J. A., Leslie, I., Wen, D., Lin, C.-H., Cupples, R. L. and Zsebo, K. M. (1990). Primary structure and functional expression of rat and human stem cell factor DNAs. *Cell* **63**: 203-211.

Martin, K. A., Schalm, S. S., Richardson, C., Romanelli, A., Keon, K. L. and Blenis, J. (2001). Regulation of ribosomal S6 kinase 2 by effectors of the phosphoinositide 3-kinase pathway. *J. Biol. Chem.* **276**: 7884-7891.

Martin, T. F. J. (1998). Phosphoinositide lipids as signaling molecules: Common themes for signal transduction, cytoskeletal regulation, and membrane trafficking. *Ann. Rev. Cell Dev. Biol.* **14**: 231-264.

Massague, J. (1990). Transforming growth factor-alpha. A model for membrane-anchored growth factors. *J. Biol. Chem.* **265**: 21393-21396.

Matous, J. V., Langley, K. and Kaushansky, K. (1996). Structure-function relationships of stem cell factor: an analysis based on a series of human-murine stem cell factor chimera and the mapping of a neutralizing monoclonal antibody. *Blood* **88**: 437-444.

Mayrhofer, G., Gadd, S. J., Spargo, L. D. and Ashman, L. K. (1987). Specificity of a mouse monoclonal antibody raised against acute myeloid leukaemia cells for mast cells in human mucosal and connective tissues. *Immunol. Cell Biol.* **65**: 241-250.

McNeil, H. P., Frenkel, D. P., Austen, K. F., Friend, D. S. and Stevens, R. L. (1992). Translation and granule localization of mouse mast cell protease-5. Immunodetection with specific antipeptide Ig. *J. Immunol.* **149**: 2466-2472.

Meier, R., Alessi, D. R., Cron, P., Andjelkovic, M. and Hemmings, B. A. (1997). Mitogenic activation, phosphorylation, and nuclear translocation of protein kinase Bβ. *J. Biol. Chem.* **272**: 30491-30497.

Meininger, C. J., Yano, H., Rottapel, R., Bernstein, A., Zsebo, K. and Zetter, B. R. (1992). The c-kit receptor ligand functions as a mast cell chemoattractant. *Blood* **79**: 958-963.

Miller, W. E., Maudsley, S., Ahn, S., Khan, K. D., Luttrell, L. M. and Lefkowitz, R. J. (2000). beta-arrestin1 interacts with the catalytic domain of the tyrosine kinase c-SRC. Role of beta-arrestin1-dependent targeting of c-SRC in receptor endocytosis. *J. Biol. Chem.* **275**: 11312-11319.

Miyamoto, S., Teramoto, H., Gutkind, J. S. and Yamada, K. M. (1996). Integrins can collaborate with growth factors for phosphorylation of receptor tyrosine kinases and MAP kinase activation: Roles of integrin aggregation and occupancy of receptors. *J. Cell Biol.* **135**: 1633-1642.

Miyazawa, K., Hendrie, P. C., Mantel, C., Wood, K., Ashman, L. K. and Broxmeyer, H. E. (1991). Comparative analysis of signaling pathways between Mast Cell Growth Factor (c-kit Ligand) and granulocyte-macrophage colony- stimulating factor in a human factor-dependent myeloid cell line involves phosphorylation of Raf-1, GTPase-activating protein and mitogen-activated protein kinase. *Exp. Hematol.***19**: 1110-1123.

Miyazawa, K., Toyama, K., Gotoh, A., Hendrie, P. C., Mantel, C. and Broxmeyer, H. E. (1994). Ligand-dependent polyubiquitination of c-kit gene product: a possible mechanism of receptor down modulation in MO7e cells. *Blood* **83**: 137-145.

Moriki, T., Maruyama, H. and Maruyama, I. N. (2001). Activation of preformed EGF receptor dimers by ligand-induced rotation of the transmembrane domain. *J. Mol. Biol.* **311**: 1011-1026.

Moriyama, Y., Tsujimura, T., Hashimoto, K., Morimoto, M., Kitayama, H., Matsuzawa, Y., Kitamura, Y. and Kanakura, Y. (1996). Role of aspartic acid 814 in the function and expression of c- kit receptor tyrosine kinase. *J. Biol. Chem.* **271**: 3347-3350.

Moskaluk, C. A., Tian, Q., Marshall, C. R., Rumpel, C. A., Franquemont, D. W. and Frierson, H. F. J. (1999). Mutations of c-kit JM domain are found in a minority of human gastrointestinal stromal tumors. *Oncogene* **18**: 1897-1902.

Moule, S. K., Welsh, G. I., Edgell, N. J., Foulstone, E. J., Proud, C. G. and Denton, R. M. (1997). Regulation of protein kinase B and glycogen synthase kinase-3 by insulin and beta-adrenergic agonists in rat epididymal fat cells. Activation of protein kinase B by wortmannin-sensitive and -insensitive mechanisms. *J. Biol. Chem.* **272**: 7713-7719.

Murray, J., Wilson, L. and Kellie, S. (2000). Phosphatidylinositol-3' kinase-dependent vesicle formation in macrophages in response to macrophage colony stimulating factor. *J. Cell Sci.* **113 Pt 2**: 337-348.

Myers, M. P., Pass, I., Batty, I. H., Van der Kaay, J., Stolarov, J. P., Hemmings, B. A., Wigler, M. H., Downes, C. P. and Tonks, N. K. (1998). The lipid phosphatase activity of PTEN is critical for its tumor supressor function. *Proc. Natl. Acad. Sci. U.S.A.* **95**: 13513-13518.

Nagata, H., Worobec, A. S., Oh, C. K., Chowdhury, B. A., Tannenbaum, S., Suzuki, Y. and Metcalfe, D. D. (1995). Identification of a point mutation in the catalytic domain of the protooncogene c-kit in peripheral blood mononuclear cells of patients who have mastocytosis with an associated hematologic disorder. *Proc. Natl. Acad. Sci. U.S.A.* **92**: 10560-10564.

Nagata, H., Worobec, A. S., Semere, T. and Metcalfe, D. D. (1998). Elevated expression of the proto-oncogene c-kit in patients with mastocytosis. *Leukemia* **12**: 175-181.

Nakata, Y., Kimura, A., Katoh, O., Kawaishi, K., Hyodo, H., Abe, K., Kuramoto, A. and Satow, Y. (1995). *c-kit* point mutation of extracellular domain in patients with myeloproliferative disorders. *Br. J. Haematol.* **91**: 661-663.

Narhi, L. O., Wypych, J., Li, T., Langley, K. E. and Arakawa, T. (1998). Changes in conformation and stability upon SCF sKit complex formation. *Journal of Protein Chemistry* **17**: 387-396.

Nilsson, I. and Hoffmann, I. (2000). Cell cycle regulation by the Cdc25 phosphatase family. *Prog. Cell Cycle Res.* **4**: 107-114.

Ning, Z. Q., Li, J. and Arceci, R. J. (2001a). Signal transducer and activator of transcription 3 activation is required for Asp(816) mutant c-Kit-mediated cytokine-independent survival and proliferation in human leukemia cells. *Blood* **97**: 3559-3567.

Ning, Z. Q., Li, J., McGuinness, M. and Arceci, R. J. (2001b). STAT3 activation is required for Asp(816) mutant c-Kit induced tumorigenicity. *Oncogene* **20**: 4528-4536.

Nishizuka, Y. (1986). Studies and perspectives of protein kinase C. *Science* **233**: 305-312.

Nocka, K., Majumder, S., Chabot, B., Ray, P., Cervone, M., Bernstein, A. and Besmer, P. (1989). Expression of *c-kit* gene products in known cellular targets of *W* mutations in normal and *W* mutant mice - evidence for an impaired *c-kit* kinase in mutant mice. *Genes & Development* **3**: 816-826.

Nocka, K., Buck, J., Levi, E. and Besmer, P. (1990a). Candidate ligand for the c-kit transmembrane kinase receptor: KL, a fibroblast derived growth factor stimulates mast cells and erythroid progenitors. *EMBO J.* **9**: 3287-3294.

Nocka, K., Tan, J. C., Chiu, E., Chu, T. Y., Ray, P., Traktman, P. and Besmer, P. (1990b). Molecular bases of dominant negative and loss of function mutations at the murine *c-kit*/white spotting locus: W^{37}, W^{v}, W^{41} and *W*. *EMBO J.* **9**: 1805-1813.

O'Connor, C. G. and Ashman, L. K. (1982). Application of the nitrocellulose transfer technique and alkaline phosphatase conjugated anti-immunoglobulin for determination of the specificity of monoclonal antibodies to protein mixtures. *J. Immunol. Methods* **54**: 267-271.

Ogawa, M., Matsuzaki, Y., Nishikawa, S., Hayashi, S., Kunisada, T., Sudo, T., Kina, T. and Nakauchi, H. (1991a). Expression and function of c-kit in hemopoietic progenitor cells. *J. Exp. Med.* **174**: 63-71.

Ogawa, M., Matsuzaki, Y., Nishikawa, S., Hayashi, S., Kunisada, T., Sudo, T., Kina, T., Nakauchi, H. and Nishikawa, S. (1991b). Expression and function of c-kit in hemopoietic progenitor cells. *J. Exp. Med.* **174**: 63-71.

Ohtsuka, M., Roussel, M. F., Sherr, C. J. and Downing, J. R. (1990). Ligand-induced phosphorylation of the colony-stimulating factor 1 receptor can occur through an intermolecular reaction that triggers receptor down modulation. *Mol. Cell. Biol.* **10**: 1664-1671.

Ong, S. H., Hadari, Y. R., Gotoh, N., Guy, G. R., Schlessinger, J. and Lax, I. (2001). Stimulation of phosphatidylinositol 3-kinase by fibroblast growth factor receptors is mediated by coordinated recruitment of multiple docking proteins. *Proc. Natl. Acad. Sci. U.S.A.* **98**: 6074-6079.

Panigada, M., Porcellini, S., Barbier, E., Hoeflinger, S., Cazenave, P. A., Gu, H., Band, H., von Boehmer, H. and Grassi, F. (2002). Constitutive endocytosis and degradation of the pre-T cell receptor. *J. Exp. Med.* **195**: 1585-1597.

Parsons, R. (1998). Phosphatases and tumorigenesis. *Curr. Opin. Oncol.* **10**: 88-91.

Paulson, R. F., Vesely, S., Siminovitch, K. A. and Bernstein, A. (1996). Signalling by the W/Kit receptor tyrosine kinase is negatively regulated in vivo by the protein tyrosine phosphatase Shp1. *Nature Genet.* **13**: 309-315.

Pawson, T. and Schlessinger, J. (1993). SH2 and SH3 domains. *Curr. Biol.* **3**: 434-442.

Pawson, T. (1995). Protein modules and signalling networks. *Nature* **373**: 573-580.

Pawson, T. and Nash, P. (2000). Protein-protein interactions define specificity in signal transduction. *Genes & Development* **14**: 1027-1047.

Persad, S., Attwell, S., Gray, V., Mawji, N., Deng, J. T., Leung, D., Yan, J., Sanghera, J., Walsh, M. P. and Dedhar, S. (2001). Regulation of protein kinase B/Akt-serine 473

phosphorylation by integrin-linked kinase: critical roles for kinase activity and amino acids arginine 211 and serine 343. *J. Biol. Chem.* **276**: 27462-27469.

Phillips, W. A., Clair, F. S., Munday, A. D., Thomas, R. J. S. and Mitchell, C. A. (1998). Increased levels of phosphatidylinositol 3-kinase activity in colorectal tumors. *Cancer* **83**: 41-47.

Philo, J. S., Wen, J., Wypych, J., Schwartz, M. G., Mendiaz, E. A. and Langley, K. E. (1996). Human stem cell factor dimer forms a complex with two molecules of the extracellular domain of its receptor, Kit. *J. Biol. Chem.* **271**: 6895-6902.

Philpott, K. L., McCarthy, M. J., Klippel, A. and Rubin, L. L. (1997). Activated phosphatidylinositol 3-kinase and Akt kinase promote survival of superior cervical neurons. *J. Cell Biol.***139**: 809-815.

Piao, X., Curtis, J. E., Minkin, S., Minden, M. D. and Bernstein, A. (1994). Expression of the *Kit* and *KitA* receptor isoforms in human acute myelogenous leukemia. *Blood* **83**: 476-481.

Piao, X., Paulson, R., Van, d. G. P., Pawson, T. and Bernstein, A. (1996). Oncogenic mutation in the Kit receptor tyrosine kinase alters substrate specificity and induces degradation of the protein tyrosine phosphatase SHP-1. *Proc. Natl. Acad Sci. U.S.A.* **93**: 14665-14669.

Pike, L. J. and Casey, L. (2002). Cholesterol levels modulate EGF receptor-mediated signaling by altering receptor function and trafficking. *Biochemistry* **41**: 10315-10322.

Plopper, G. E., McNamee, H. P., Dike, L. E., Bojanowski, K. and Ingber, D. E. (1995). Convergence of integrin and growth factor receptor signaling pathways within the focal adhesion complex. *Mol. Biol. Cell* **6**: 1349-1365.

Podsypanina, K., Ellenson, L. H., Nemes, A., Gu, J., Tamura, M., Yamada, K. M., Cordon-Cardo, C., Catoretti, G., Fisher, P. E. and Parsons, R. (1999). Mutation of Pten/Mmac1 in mice causes neoplasia in multiple organ systems. *Proc. Natl. Acad. Sci. U.S.A.* **96**: 1563-1568.

Prediction of Protein Secondary Structure: http://cubic.bioc.columbia.edu/predictprotein (Accessed Nov 2002)

Qiu, F., Ray, P., Brown, K., Barker, P. E., Jhanwar, S., Ruddle, F. H. and Besmer, P. (1988). Primary structure of *c-kit*: relationship with the CSF-1/PDGF receptor kinase family-oncogenic activation of *v-kit* involves deletion of extracellular domain and C terminus. *EMBO J.* **7**: 1003-1011.

Qu, C. K., Shi, Z. Q., Shen, R., Tsai, F. Y., Orkin, S. H. and Feng, G. S. (1997). A deletion mutation in the SH2-N domain of Shp-2 severely suppresses hematopoietic cell development. *Mol. Cell. Biol.* **17**: 5499-5507.

Qui, M.-S. and Green, S. H. (1992). PC12 cell neuronal differentiation is associated with prolonged $p21^{ras}$ activity and consequent prolonged ERK activity. *Neuron* **9**: 705-717.

Rameh, L. E., Chen, C.-S. and Cantley, L. C. (1995). Phosphatidylinositol (3,4,5)P3 interacts with SH2 domains and modulates PI 3-kinase association with tyrosine-phosphorylated proteins. *Cell* **83**: 821-830.

Rameh, L. E. and Cantley, L. C. (1999). The role of phosphoinositide 3-kinase lipid products in cell function. *J. Biol. Chem.* **274**: 8347-8350.

Rasheed, B. K., Stenzel, T. T., McLendon, R. E., Parsons, R., Friedman, A. H., Friedman, H. S., Bigner, D. D. and Bigner, S. H. (1997). PTEN gene mutations are seen in high-grade but not in low-grade gliomas. *Cancer Res.* **57**: 4187-4190.

Ratajczak, M. Z., Luger, S. M., DeRiel, K., Abraham, J., Calabretta, B. and Gewirtz, A. M. (1992). Role of the Kit protooncogene in normal and malignant human hematopoiesis. *Proc. Natl. Acad. Sci. U.S.A.* **89**: 1710-1714.

Rayner, J. R. and Gonda, T. J. (1994). A simple and efficient procedure for generating stable expression libraries by cDNA cloning in a retroviral vector. *Mol. Cell. Biol.* **14**: 880-887.

Rebollo, A. and Martinez, C. (1999). Ras proteins: Recent advances and new functions. *Blood* **94**: 2971-2980.

Reith, A. D., Rottapel, R., Giddens, E., Brady, C., Forrester, L. and Bernstein, A. (1990). *W* mutant mice with mild or severe developmental defects contain distinct point mutations in the kinase domain of the *c- kit* receptor. *Genes & Development* **4**: 390-400.

Reith, A. D., Ellis, C., Lyman, S. D., Anderson, D. M., Williams, D. E., Bernstein, A. and Pawson, T. (1991). Signal transduction by normal isoforms and W mutant variants of the Kit receptor tyrosine kinase. *EMBO J.* **10**: 2451-2459.

Remy, I., Wilson, I. A. and Michnick, S. W. (1999). Erythropoietin receptor activation by a ligand-induced conformation change. *Science* **283**: 990-993.

Ricotti, E., Fagioli, F., Garelli, E., Linari, C., Crescenzio, N., Horenstein, A. L., Pistamiglio, P., Vai, S., Berger, M., Di Montezemolo, L. C., Madon, E. and Basso, G. (1998). c-*kit* is expressed in soft tissue sarcoma of neuroectodermic origin and its ligand prevents apoptosis of neoplastic cells. *Blood* **91**: 2397-2405.

Rodriguez-Viciana, P., Warne, P. H., Dhand, R., Vanhaesebroeck, B., Gout, I., Fry, M. J., Waterfield, M. D. and Downward, J. (1994). Phosphatidylinositol-3-OH kinase as a direct target of Ras. *Nature* **370**: 527-532.

Rodriguez-Viciana, P., Warne, P. H., Khwaja, A., Marte, B. M., Pappin, D., Das, P., Waterfield, M. D., Ridley, A. and Downward, J. (1997). Role of phosphoinositide 3-OH kinase in cell transformation and control of the actin cytoskeleton by Ras. *Cell* **89**: 457-467.

Rost, B. and Sander, C. (1993). Prediction of protein secondary structure at better than 70% accuracy. *J. Mol. Biol.* **232**: 584-599.

Rottapel, R., Reedijk, M., Williams, D. E., Lyman, S. D., Anderson, D. M., Pawson, T. and Bernstein, A. (1991). The Steel/W transduction pathway: Kit autophosphorylation and its association with a unique subset of cytoplasmic signaling proteins is induced by the Steel Factor. *Mol. Cell. Biol.* **11**: 3043-3051.

Sattler, M., Salgia, R., Shrikhande, G., Verma, S., Pisick, E., Prasad, K. V. S. and Griffin, J. D. (1997). Steel factor induces tyrosine phosphorylation of CRKL and binding of CRKL to a complex containing c-Kit, phosphatidylinositol 3-kinase, and $p120^{CBL}$. *J. Biol. Chem.* **272**: 10248-10253.

Sawyers, C. L. (1999). Chronic myeloid leukemia. *N. Engl. J. Med.* **340**: 1330-1340.

Sawyers, C. L., Hochhaus, A., Feldman, E., Goldman, J. M., Miller, C. B., Ottmann, O. G., Schiffer, C. A., Talpaz, M., Guilhot, F., Deininger, M. W., Fischer, T., O'Brien, S. G., Stone, R. M., Gambacorti-Passerini, C. B., Russell, N. H., Reiffers, J. J., Shea, T. C., Chapuis, B., Coutre, S., Tura, S., Morra, E., Larson, R. A., Saven, A., Peschel, C., Gratwohl, A., Mandelli, F., Ben-Am, M., Gathmann, I., Capdeville, R., Paquette, R. L. and Druker, B. J. (2002). Imatinib induces hematologic and cytogenetic responses in patients with chronic myelogenous leukemia in myeloid blast crisis: results of a phase II study. *Blood* **99**: 3530-3539.

Schlessinger, J. (1986). Allosteric regulation of the epidermal growth factor receptor kinase. *J. Cell Biol.* **103**: 2067-2072.

Schlessinger, J. and Ullrich, A. (1992). Growth factor signaling by receptor tyrosine kinases. *Neuron* **9**: 383-391.

Schlessinger, J. (1994). SH2/SH3 signaling proteins. *Curr. Opin. Genet. Dev.* **4**: 25-30.

Schlessinger, J. (1995). Cellular signalling by receptor tyrosine kinases. *The Harvey Lectures* **89**: 105-123.

Schlessinger, J. and Bar-Sagi, D. (1997). Activation of ras and other signaling pathways by receptor tyrosine kinases. *Cold Spring Harbor Symposia on Quantitative Biology* **LIX**: 173-179.

Schlessinger, J. (2000). Cell signaling by receptor tyrosine kinases. *Cell* **103**: 211-225.

Schneller, M., Vuori, K. and Ruoslahti, E. (1997). αvβ3 integrin associates with activated insulin and PDGFβ receptors and potentiates the biological activity of PDGF. *EMBO J.* **16**: 5600-5607.

Segouffin-Cariou, C. and Billaud, M. (2000). Transforming ability of MEN2A-RET requires activation of the phosphatidylinositol 3-kinase/AKT signaling pathway. *J. Biol. Chem.* **275**: 3568-3576.

Serve, H., Hsu, Y. C. and Besmer, P. (1994). Tyrosine residue 719 of the c-kit receptor is essential for binding of the P85 subunit of phosphatidylinositol (PI) 3-kinase and for c-kit-associated PI 3-kinase activity in COS-1 cells. *J. Biol. Chem.* **269**: 6026-6030.

Serve, H., Yee, N. S., Stella, G., Sepp-Lorenzino, L., Tan, J. C. and Besmer, P. (1995). Differential roles of PI3-kinase and Kit tyrosine 821 in Kit receptor-mediated proliferation, survival and cell adhesion in mast cell. *EMBO J.* **14(3)**: 473-483.

Sewing, A., Wiseman, B., Lloyd, A. C. and Land, H. (1997). High-intensity Raf signal causes cell cycle arrest mediated by $p21^{Cip1}$. *Mol. Cell. Biol.* **17**: 5588-5597.

Shah, N., Nicoll, J., Nagar, B., Gorre, M., Paquette, R., Kuriyan, J. and Sawyers, C. (2002). Multiple BCR-ABL kinase domain mutations confer polyclonal resistance to the tyrosine kinase inhibitor imatinib (STI571) in chronic phase and blast crisis chronic myeloid leukemia. *Cancer Cell* **2**: 117-125.

Shayesteh, L., Lu, Y., Kuo, W. L., Baldocchi, R., Godfrey, T., Collins, C., Pinkel, D., Powell, B., Mills, G. B. and Gray, J. W. (1999). PIK3CA is implicated as an oncogene in ovarian cancer. *Nat. Genet.* **21**: 99-102.

Shearman, M. S., Herbst, R., Schlessinger, J. and Ullrich, A. (1993). Phosphatidylinositol 3'-kinase with p145 c-kit as part of a cell type characteristic multimeric signalling complex. *EMBO J.* **12**: 3817-3826.

Smith, A. and Ashworth, A. (1998). Cancer predisposition: where's the phosphate? *Curr. Biol.* **8**: R241-243.

Smithgall, T. E. (1995). SH2 and SH3 domains: Potential targets for anti-cancer drug design. *Journal of Pharmacological and Toxicological Methods* **34**: 125-132.

Springer, T., Galfre, G., Secher, D. S. and Milstein, C. (1979). Mac-1: a macrophage differentiation antigen identified by monoclonal antibody. *Eur. J. Immunol.* **9**: 301-306.

Stambolic, V., Mak, T. W. and Woodgett, J. R. (1999). Modulation of cellular apoptotic potential: contributions to oncogenesis. *Oncogene* **18**: 6094-6103.

Stokoe, D., Stephens, L. R., Copeland, T., Gaffney, P. R. J., Reese, C. B., Painter, G. F., Holmes, A. B., McCormick, F. and Hawkins, P. T. (1997). Dual role of phosphatidylinositol-3,4,5-trisphosphate in the activation of protein kinase B. *Science* **277**: 567-570.

Suzuki, A., de la Pompa, J. L., Stambolic, V., Elia, A. J., Sasaki, T., del Barco Barrantes, I., Ho, A., Wakeham, A., Itie, A., Khoo, W., Fukumoto, M. and Mak, T. W. (1998). High cancer susceptibility and embryonic lethality associated with mutation of the PTEN tumor suppressor gene in mice. *Curr. Biol.* **8**: 1169-1178.

Tajima, Y., Huang, E. J., Vosseller, K., Ono, M., Moore, M. A. S. and Besmer, P. (1998). Role of dimerization of the membrane-associated growth factor Kit ligand in juxtacrine signaling: The Sl^{17H} mutation affects dimerization and stability-phenotypes in hematopoiesis. *J. Exp. Med.* **187**: 1451-1461.

Tamura, M., Gu, J., Matsumoto, K., Aota, S., Parsons, R. and Yamada, K. M. (1998). Inhibition of cell migration, spreading, and focal adhesions by tumor suppressor PTEN. *Science* **280**: 1614-1617.

Tan, J. C., Nocka, K., Ray, P., Trakman, P. and Besmer, P. (1990). The dominant W^{42} spotting phenotype results form a missense mutation in the *c-kit* receptor kinase. *Science* **247**: 209-212.

Tang, B., Mano, H., Yi, T. and Ihle, J. N. (1994). Tec kinase associates with c-kit and is tyrosine phosphorylated and activated following stem cell factor binding. *Mol. Cell. Biol.* **14**: 8432-8437.

Taniguchi, M., Nishida, T., Hirota, S., Isozaki, K., Ito, T., Nomura, T., Matsuda, H. and Kitamura, Y. (1999). Effect of *c-kit* mutation on prognosis of gastrointestinal stromal tumors. *Cancer Res.* **59**: 4297-4300.

Tatton, L., Morley, G. M., Chopra, R. and Khwaja, A. (2003). The Src-selective kinase inhibitor PP1 also inhibits kit and Bcr-Abl tyrosine kinases. *J. Biol. Chem.* **278**: 4847-4853.

Tauchi, T., Feng, G. S., Marshall, M. S., Shen, R., Mantel, C., Pawson, T. and Broxmeyer, H. E. (1994). The ubiquitously expressed Syp phosphatase interacts with c-kit and Grb2 in hematopoietic cells. *J. Biol. Chem.* **269**: 25206-25211.

Taylor, M. L., Dastych, J., Sehgal, D., Sundstrom, M., Nilsson, G., Akin, C., Mage, R. G. and Metcalfe, D. D. (2001). The Kit-activating mutation D816V enhances stem cell factor--dependent chemotaxis. *Blood* **98**: 1195-1199.

Thien, C. B. F., Walker, F. and Langdon, W. Y. (2001) RING finger mutations that abolish c-Cbl directed polyubiquitination and downregulation of the EGF receptor are insufficient for cell transformation. *Mol. Cell* **7**: 355-365

Thommes, K., Lennartsson, J., Carlberg, M. and Ronnstrand, L. (1999). Identification of Tyr-703 and Tyr-936 as the primary association sites for Grb2 and Grb7 in the c-Kit/stem cell factor receptor. *Biochem. J.* **341**: 211-216.

Timokhina, I., Kissel, H., Stella, G. and Besmer, P. (1998). Kit signaling through PI 3-kinase and Src kinase pathways: an essential role for Rac1 and JNK activation in mast cell proliferation. *EMBO J.* **17**: 6250-6262.

Toker, A. and Cantley, L. C. (1997). Signalling through the lipid products of phosphoinositide-3-OH kinase. *Nature* **387**: 673-676.

Traverse, S., Gomez, N., Paterson, H., Marshall, C. and Cohen, P. (1992). Sustained activation of the mitogen-activated protein (MAP) kinase cascade may be required for differentiation of PC12 cells. *Biochem. J.* **288**: 351-355.

Traverse, S., Seedorf, K., Paterson, H., Marshall, C. J., Cohen, P. and Ullrich, A. (1994). EGF triggers neuronal differentiation of PC12 cells that overexpress the EGF receptor. *Curr. Biol.* **4**: 694-701.

Tsai, M., Takeishi, T., Thompson, H., Langley, K. E., Zsebo, K. M., Metcalfe, D. D., Geissler, E. N. and Galli, S. J. (1991). Induction of mast cell proliferation, maturation, and heparin synthesis by the rat c-kit ligand, stem cell factor. *Proc. Natl. Acad. Sci. U.S.A.* **88**: 6382-6386.

Tsujimura, T., Furitsu, T., Morimoto, M., Isozaki, K., Nomura, S., Matsuzawa, Y., Kitamura, Y. and Kanakura, Y. (1994). Ligand-independent activation of c-kit receptor tyrosine kinase in a murine mastocytoma cell line P-815 generated by a point mutation. *Blood* **83**: 2619-2626.

Tsujimura, T., Morimoto, M., Hashimoto, K., Moriyama, Y., Kitayama, H., Matsuzawa, Y., Kitamura, V. and Kanakura, Y. (1996). Constitutive activation of c-kit in FMA3 murine mastocytoma cells caused by deletion of seven amino acids at the juxtamembrane domain. *Blood* **87**: 273-283.

Tsujimura, T., Hashimoto, K., Kitayama, H., Ikeda, H., Sugahara, H., Matsumura, I., Kaisho, T., Terada, N., Kitamura, Y. and Kanakura, Y. (1999). Activating mutation in the catalytic domain of c-kit elicits hematopoietic transformation by receptor self-association not at the ligand-induced dimerization site. *Blood* **93**: 1319-1329.

Tuveson, D. A., Willis, N. A., Jacks, T., Griffin, J. D., Singer, S., Fletcher, C. D., Fletcher, J. A. and Demetri, G. D. (2001). STI571 inactivation of the gastrointestinal stromal tumor c-KIT oncoprotein: biological and clinical implications. *Oncogene* **20**: 5054-5058.

Ueno, H., Honda, H., Nakamoto, T., Yamagata, T., Sasaki, K., Miyagawa, K., Mitani, K., Yazaki, Y. and Hirai, H. (1997). The phosphatidylinositol 3' kinase pathway is required for the survival signal of leukocyte tyrosine kinase. *Oncogene* **14**: 3067-3072.

Ullrich, A. and Schlessinger, J. (1990). Signal transduction by receptors with tyrosine kinase activity. *Cell* **61**: 203-212.

van Dijk, T. B., van Den Akker, E., Amelsvoort, M. P., Mano, H., Lowenberg, B. and von Lindern, M. (2000). Stem cell factor induces phosphatidylinositol 3'-kinase-dependent Lyn/Tec/Dok-1 complex formation in hematopoietic cells. *Blood* **96**: 3406-3413.

van Oosterom, A. T., Judson, I., Verweij, J., Stroobants, S., Donato di Paola, E., Dimitrijevic, S., Martens, M., Webb, A., Sciot, R., Van Glabbeke, M., Silberman, S. and Nielsen, O. S. (2001). Safety and efficacy of imatinib (STI571) in metastatic gastrointestinal stromal tumours: a phase I study. *Lancet* **358**: 1421-1423.

Vandenbark, G. R., de Castro, C. M., Taylor, H., Dew-Knight, S. and Kaufman, R. E. (1992). Cloning and structural analysis of the human *c-kit* gene. *Oncogene* **7**: 1259-1266.

Vanhaesebroeck, B., Stein, R. C. and Waterfield, M. D. (1996). The study of phosphoinositide 3-kinase function. *Cancer Surveys* **27**: 249-270.

Vanhaesebroeck, B., Leevers, S. J., Panayotou, G. and Waterfield, M. D. (1997). Phosphoinositide 3-kinases: a conserved family of signal transducers. *Tibs.* **22**: 267-272.

Vanhaesebroeck, B. and Alessi, D. R. (2000). The PI3K-PDK1 connection: more than just a road to PKB. *Biochem. J.* **346 Pt 3**: 561-576.

Varmus, H. (1989). An Historical Overview of Oncogenes. In *Oncogenes and the Molecular Origins of Cancer*, (ed. Weinberg, R. A.), pp. 4-39. New York: Cold Spring Harbor Laboratory Press.

Vieira, A. V., Lamaze, C. and Schmid, S. L. (1996). Control of EGF receptor signaling by clathrin-mediated endocytosis. *Science* **274**: 2086-2089.

Vlahos, C. J., Matter, W. F., Hui, K. Y. and Brown, R. F. (1994). A specific inhibitor of phosphatidylinositol 3-kinase, 2-(4-morpholinyl)-8-phenyl-4H-1-benzopyran-4-one (LY294002). *J. Biol. Chem.* **269**: 5241-5248.

Vliagoftis, H., Worobec, A. S. and Metcalfe, D. D. (1997). The protooncogene c-*kit* and c-*kit* ligand in human disease. *Journal of Allergy and Clinical Immunology* **100**: 435-440.

Vojtek, A. B. and Der, C. J. (1998). Increasing complexity of the ras signaling pathway. *J. Biol. Chem.* **273**: 19925-19928.

Vosseller, K., Stella, G., Yee, N. S. and Besmer, P. (1997). c-Kit receptor signaling through its phosphatidylinositide- 3'- kinase-binding site and protein kinase C: Role in mast cell enhancement of degranulation, adhesion, and membrane ruffling. *Mol. Biol. Cell.* **8**: 909-922.

Voytyuk, O., Lennartsson, J., Mogi, A., Caruana, G., Courtneidge, S., Ashman, L. K. and Ronnstrand, L. (2003). Src family kinases are involved in the differential signaling from two splice-forms of c-Kit. *J. Biol. Chem.* **278**: 9159-9166.

Walker, E. H., Perisic, O., Ried, C., Stephens, L. and Williams, L. R. (1999). Structural insights into phosphoinositide 3-kinase catalysis and signalling. *Nature* **402**: 313-319.

Wartmann, M., Hofer, P., Turowski, P., Saltiel, A. R. and Hynes, N. E. (1997). Negative modulation of membrane localisation of the Raf-1 protein kinase by hyperphosphorylation. *J. Biol. Chem.* **272**: 3915-3923.

Weiler, S. R., Mou, S., DeBerry, C. S., Keller, J. R., Ruscetti, F. W., Ferris, D. K., Longo, D. L. and Linnekin, D. (1996). JAK2 is associated with the c-kit proto-oncogene product and is phosphorylated in response to stem cell factor. *Blood* **87**: 3688-3693.

Weng, G., Bhalla, U. S. and Iyengar, R. (1999). Complexity in biological signaling systems. *Science* **284**: 92-96.

Whitman, M., Kaplan, D. R., Schaffhausen, B., Cantley, L. and Roberts, T. M. (1985). Association of phosphatidylinositol kinase activity with polyoma middle- T competent for transformation. *Nature* **315**: 239-242.

Wilde, A., Beattie, E. C., Lem, L., Riethof, D. A., Liu, S. H., Mobley, W. C., Soriano, P. and Brodsky, F. M. (1999). EGF receptor signaling stimulates SRC kinase phosphorylation of clathrin, influencing clathrin redistribution and EGF uptake. *Cell* **96**: 677-687.

Williams, D. E., Eisenman, J., Baird, A., Rauch, C., Van Ness, K., March, C. J., Park, L. S., Martin, U., Mochizuki, D. Y., Boswell, H. S., Burgess, G. S., Cosman, D. and Lyman, S. D. (1990). Identification of a ligand for the c-kit proto-oncogene. *Cell* **63**: 167-174.

Williams, D. E., de Vries, P., Namen, A. E., Widmer, M. B. and Lyman, S. D. (1992). The Steel factor. *Dev. Biol.* **151**: 368-376.

Woods, D., Parry, D., Cherwinski, H., Bosch, E., Lees, E. and McMahon, M. (1997). Raf-induced proliferation or cell cycle arrest is determined by the level of Raf activity with arrest mediated by $p21^{Cip1}$. *Mol. Cell. Biol.* **17**: 5598-5611.

Worobec, A. S., Semere, T., Nagata, H. and Metcalfe, D. D. (1998). Clinical correlates of the presence of the Asp816Val c-kit mutation in the peripheral blood mononuclear cells of patients with mastocytosis. *Cancer* **83**: 2120-2129.

Xia, P., Gamble, J. R., Wang, L., Pitson, S. M., Moretti, P. A., Wattenberg, B. W., D'Andrea, R. J. and Vadas, M. A. (2000). An oncogenic role of sphingosine kinase. *Curr. Biol.* **10**: 1527-1530.

Yam, L. T., Li, C. Y. and Crosby, W. H. (1971). Cytochemical identification of monocytes and granulocytes. *Am. J. Clin. Pathol.* **55**: 283-290.

Yano, S., Tokumitsu, H. and Soderling, T. R. (1998). Calcium promotes cell survival through CaM-K kinase activation of the protein-kinase-B pathway. *Nature* **396**: 584-587.

Yarden, Y., Escobedo, J. A., Kuang, W.-J., Yang-Feng, T. L., Daniel, T. O., Tremble, P. M., Chen, E. Y., Ando, M. E., Harkins, R. N., Francke, U., Fried, V. A., Ullrich, A. and Williams, L. T. (1986). Structure of the receptor for platelet-derived growth factor helps define a family of closely related growth factor receptors. *Nature* **323**: 226-232.

Yarden, Y., Kuang, W.-J., Yang-Feng, T., Coussens, L., Munemitsu, S., Dull, T. J., Chen, E., Schlessinger, J., Francke, U. and Ullrich, A. (1987). Human proto-oncogene *c-kit*: a new cell surface receptor tyrosine kinase for an unidentified ligand. *EMBO J.* **6**: 3341-3351.

Yarden, Y. and Ullrich, A. (1988). Growth factor receptor tyrosine kinases. *Ann. Rev. Biochem.* **57**: 443-478.

Yee, N. S., Langen, H. and Besmer, P. (1993). Mechanism of kit ligand, phorbol ester, and calcium-induced down- regulation of c-kit receptors in mast cells. *J. Biol. Chem.* **268**: 14189-14201.

Yee, N. S., Hsiau, C.-W. M., Serve, H., Vosseller, K. and Besmer, P. (1994). Mechanism of down-regulation of c-kit receptor. Roles of receptor tyrosine kinase, phosphatidylinositol 3'-kinase, and protein kinase C. *J. Biol. Chem.* **269**: 31991-31998.

Yi, T. and Ihle, J. N. (1993). Association of hematopoietic cell phosphatase with c-Kit after stimulation with c-Kit ligand. *Mol. Cell. Biol.* **13**: 3350-3358.

Yi, T., Mui, A. L.-F., Krystal, G. and Ihle, J. N. (1993). Hematopoietic cell phosphatase associates with the interleukin-3 (IL-3) receptor beta chain and down-regulates IL-3-induced tyrosine phosphorylation and mitogenesis. *Mol. Cell. Biol.* **13**: 7577-7586.

Yu, J., Zhang, Y., McIlroy, J., Rordorf-Nikolic, T., Orr, G. A. and Backer, J. M. (1998). Regulation of the p85/p110 phosphatidylinositol 3'-kinase: Stabilization and inhibition of the p110α catalytic subunit by the p85 regulatory subunit. *Mol. Cell. Biol.* **18**: 1379-1387.

Yuan, Q., Austen, K. F., Friend, D. S., Heidtman, M. and Boyce, J. A. (1997). Human peripheral blood eosinophils express a functional c-*kit* receptor for stem cell factor that stimulates very late antigen 4 (VLA-4)-mediated cell adhesion to fibronectin and vascular cell adhesion molecule 1 (VCAM-1). *J. Exp. Med.* **186**: 313-323.

Zha, J., Harada, H., Yang, E., Jockel, J. and Korsmeyer, S. J. (1996). Serine phosphorylation of death agonist BAD in response to survival factor results in binding to 14-3-3 not BCL-X_L. *Cell* **87**: 619-628.

Zhang, S. Q., Tsiaras, W. G., Araki, T., Wen, G., Minichiello, L., Klein, R. and Neel, B. G. (2002). Receptor-specific regulation of phosphatidylinositol 3'-kinase activation by the protein tyrosine phosphatase Shp2. *Mol. Cell. Biol.* **22**: 4062-4072.

Zhang, Y., Moheban, D. B., Conway, B. R., Bhattacharyya, A. and Segal, R. A. (2000a). Cell surface Trk receptors mediate NGF-induced survival while internalized receptors regulate NGF-induced differentiation. *J. Neurosci.* **20**: 5671-5678.

Zhang, Z., Zhang, R., Joachimiak, A., Schlessinger, J. and Kong, X.-P. (2000b). Crystal structure of human stem cell factor: Implication for stem cell factor receptor dimerisation and activation. *Proc. Natl. Acad. Sci. U.S.A.* **97**: 7732-7737.

Zhu, H. J. and Sizeland, A. M. (1999). A pivotal role for the transmembrane domain in transforming growth factor-beta receptor activation. *J. Biol. Chem.* **274**: 11773-11781.

Zsebo, K. M., Williams, D. A., Geissler, E. N., Broudy, V. C., Martin, F. H., Atkins, H. L., Hau, R.-Y., Birkett, N. C., Okino, K. H., Murdock, D. C., Jacobsen, F. W., Langley, K. E., Smith, K. A., Takeishi, T., Cattanach, B. M., Galli, S. J. and Suggs, S. V. (1990a). Stem cell factor is encoded at the Sl locus of the mouse and is the ligand for the c-kit tyrosine kinase receptor. *Cell* **63**: 213-224.

Zsebo, K. M., Wypych, J., McNiece, I. K., Lu, H. S., Smith, K. A., Karkare, S. B., Sachdev, R. K., Yuschenkoff, V. N., Birkett, N. C., Williams, L. R., Satyagal, V. N., Tung, W., Bosselman, R. A., Mendiaz, E. A. and Langley, K. E. (1990b). Identification, purification, and biological characterization of hematopoietic stem cell factor from buffalo rat liver-conditioned medium. *Cell* **63**: 195-201.

CHAPTER 8:

REAGENTS

8. REAGENTS

All reagents in individual categories are listed in alphabetical order.

8.1. IMMUNOCYTOCHEMISTRY, IMMUNOHISTOCHEMISTRY AND IMMUNOFLUORESCENCE REAGENTS

0.066 M Phosphate Buffer, pH 6.3: 3.5 g KH_2PO_4 and 1.1 g Na_2HPO_4 was added to 500 ml of distilled water gradually while stirring. The solution was stored at 4°C.

0.066 M Phosphate Buffer, pH 7.4: 0.087 g KH_2PO_4 and 3.84 g Na_2HPO_4 was added to 500 ml of distilled water gradually while stirring. The solution was stored at 4°C.

APAAP Substrate: Prepared immediately before use. For 100ml (which is sufficient for 3 Coplin jars): 20mg napthol AS-MX phosphate free acid (Sigma, St Louis, MO, Cat. No. N4875) was dissolved in 2 ml of dimethyl formamide. This solution along with 100 µl 1 M levamisole (Sigma, St Louis, MO, Cat. No. L-9756) diluted in water was added to 100ml 0.1 M Tris (pH8.2). 100mg of Fast Red TR salt (Sigma, St Louis, MO, Cat. No. F-1500) was added to the solution and filtered with Whatman paper directly into Coplin jars.

'Chloroacetate' Esterase Substrate Solution: 5 mg naphthol-AS-D-chloroacetate (Sigma, St Louis, MO, Cat. No. N-0758) was dissolved in 2.5 ml N-N dimethylformamide and then added to a fresh solution of 38 ml 0.066 M phosphate buffer pH 7.4 containing 20 mg Fast Blue (Sigma, St Louis, MO, Cat. No. F-0250). The solution was immediately filtered with Whatman paper.

Esterase Fixative: 100 mg Na_2HPO_4, 500 mg KH_2PO_4, 225 ml acetone and 125 ml formalin (40% formaldehyde in water) were added to 150 ml distilled water. The solution was stored at 4°C.

FacsFix: 2% w/v D-glucose, 1% v/v 37 - 40% formaldehyde and 0.02% Az dissolved in PBS and stored at 4°C.

Glycerol-glycine Mountant: 1.4 g glycine was dissolved in 100 ml water and pH adjusted to 8.6 with NaOH. To 30 ml glycine buffer, 70 ml glycerol was added and stored at room temperature.

'Non-specific' Esterase Substrate Solution: 0.3 ml of pararosanaline solution was mixed with 0.3 ml of 4% sodium nitrite solution and allowed to stand for 1 minute. This was added to a freshly made solution of 30 ml 0.066 M phosphate buffer pH 6.3 containing 1 ml of 10 mg/ml α-naphthyl acetate (Sigma, St Louis, MO Cat. No. N-8505) in acetone. The final pH was adjusted to 6.1 with 5 M NaOH.

Pararosanaline: 0.2 g pararosanaline hydrochloride (Sigma, St Louis, MO, P-3750) was added to 10 ml of 20% v/v HCl in water and incubated at 56° for 30 minutes in the dark. The solution was filtered (0.45 μm) and stored in the dark at room temperature for no greater than 1 month.

Standard Fixative: Acetone: methanol: formaldehyde (47.5:47.5:5 v/v). Solution was stored at 4°C.

Scott's Gentle Alkaline Solution: 3.5 g $NaHCO_3$ and 20 g $MgSO_4.7H_2O$ was dissolved in 1 L water. Solution was stored at room temperature.

TBS (for APAAP): 50 mM Tris (pH 7.6), 120 mM NaCl in water.

8.2. Reagents for Protein Analysis

0.5 M Activated Sodium Orthovanadate: This solution was activated by altering the pH and temperature as follows. 0.5 M solution made in Milli-Q water. The pH of the solution adjusted to 11 with 0.5 M HCl, which was then heated, cooled to room temperature and adjusted to the original volume with Milli-Q water. This step was repeated three times The pH of the solution was then adjusted to 10, filtered (0.45 μm) and stored in aliquots at -20°C.

1% Nonidet P 40 (NP40) in Tris-Sodium chloride-EDTA (TSE): 50 mM Tris, 150 mM NaCl, 1 mM EDTA was dissolved in water and the solution adjusted to a pH of 8. NP40 was added (1% v/v final) and solution filtered (0.45 μm) and stored at 4°C.

1% Triton x100 in TSE: 10 mM Tris, 50 mM NaCl, 5 mM EDTA was dissolved in water and the solution adjusted to a pH of 7.6. Triton x100 was added (1% v/v final) and solution filtered (0.45 μm) and stored at 4°C.

10x TBS (for Western Blots): 0.2 M Tris, 1.5 M NaCl dissolved in water, pH adjusted to 7.5 with 10 M HCl. For use, this stock was diluted to 1x in Milli-Q water.

Double Strength Reduced Loading Buffer: 125 mM Tris (pH6.8), 20% glycerol, 4% SDS, 10% β-mercaptoethanol, 0.0025% bromophenol blue. Aliquots were stored at -20°C.

Electrophoresis Buffer: 25 mM Tris, 192 mM glycine, 0.1% SDS, should be pH 8.3 without further adjustment.

Lysis Buffer: Either 1% NP40 or 1% Triton in TSE with 5 mM sodium fluoride, 5 mM tetrasodium pyrophosphate, 5mM sodium vanadate, 1 mg/ml leupeptin, 1 mg/ml aprotinin, 1 mM PMSF and Complete Protease Inhibitor Cocktail (Roche Diagnostics, Mannheim, Germany, Cat. No. 1836145)

Resolving Gel:

% gel	**8%**	**10%**
Acrylamide-bis (37.5:1)	8% final	10% final
1.5 M Tris (pH 8.8)	25%	25%
SDS	0.1% w/v	0.1% w/v
Ammonium persulphate	0.1% w/v	0.1% w/v
TEMED	0.0006% v/v	0.0004% v/v
Made in water		

Stacking Gel:

Acrylamide-bis (37.5:1)	5% final
0.5 M Tris (pH 6.8)	25% v/v
SDS	0.1% w/v
Ammonium persulphate	0.1% w/v
TEMED	0.001% v/v
Made in water	

Transfer Buffer: 25 mM Tris, 192 mM glycine with 20% v/v or 10% v/v methanol in water for PVDF or nitrocellulose respectively.

8.3. PI 3-K Assay Reagents

1x Kinase Buffer: 20 mM Hepes (pH 7.5), 5 mM $MgCl_2$, 1 mM EGTA in water

Lipid Resuspension Buffer: 29 mM Hepes (pH 7.5), 1 mM $MgCl_2$, 1 mM EGTA in water

Potassium Oxalate Solution: 50% v/v ethanol, 2 mM EDTA, 1% w/v potassium oxalate in water.

Tris Saline: 20 mM Tris (pH 7.4), 150 mM NaCl in water

8.4. DNA Manipulation Reagents

2x YT: 2% Bacto-tryptone, 1% Bacto-yeast extract, 1% NaCl in water and autoclaved.

1x TAE: 0.04 M Tris-Acetate, 0.001 M EDTA, pH 8.

100x TE: 1 M Tris (pH 7.5), 100 mM EDTA.

Ψa Agar Plates: 5 g/L Bacto-yeast extract (Difco, Sparks, MD, Cat. No. 012-01-7), 20 g/L Bacto-tryptone (Difco, Sparks, MD, Cat. No. 0127-01-7), 5 g/L $MgSO_4$ in water and the pH adjusted to 7.6 with KOH. Prior to autoclaving, added 14 g/L Bacto-agar (Difco, Sparks, MD, Cat. No. 0140-01).

Gel Loading Buffer: 0.25% bromophenol blue, 0.25% xylene cyanol FF, 30% glycerol in water. Solution was stored in aliquots at -20°C.

Luria Agar Plates: 1.5% w/v Bacto-agar in Luria broth was autoclaved. Agar was cooled to ~ 55°C prior to the addition of 100 μg/ml ampicillin and then poured onto Petri dishes. Plates were allowed to set and stored at 4°C.

Luria Broth: 1% Bacto-tryptone, 0.5% Bacto-yeast extract, 1% NaCl in water and pH adjusted to 7 - 7.2 and autoclaved.

Lysis Buffer (for Bacteria): 50mM Tris HCl, pH 7.5; 62.5mM EDTA, pH 8; 0.4% Triton X100; 2.5M LiCl

SOC Medium: 2% Bacto-tryptone, 0.5% Bacto-yeast extract, 10 mM NaCl and 2.5 mM KCl in water were autoclaved. When cool, 10mM $MgCl_2$, Mg SO_4 and 20 mM glucose were added and the medium filter sterilised through a 0.22 μm filter unit.

Super Broth: 3.2% Bacto-tryptone, 2% Bacto-yeast extract, 0.5% NaCl in water and autoclaved.

8.5. RNA Reagents

1% RNA agarose gel: 1 g molecular biology grade RNase-free agarose was dissolved by heating in 72ml DEPC treated Milli-Q water and 10 ml 10x running buffer. The solution was cooled to less than 60°C and 18 ml 37 - 40% formaldehyde (2.2 M final) was added.

10x Running Buffer: 200 mM 3-[N-Morpholino]propane-sulfonic acid (MOPS), 10 mM EDTA (pH8), 50 mM sodium acetate, pH to 7 in DEPC and stored at room temperature in the dark.

10x SSC: 43.8 g NaCl and 22.1 g sodium citrate dissolved in DEPC and made to a final volume of 500 ml.

Formaldehyde Running Buffer: 100 ml 10x running buffer, 180 ml 40% formaldehyde to a final volume of 1 L with DEPC treated Milli-Q water. Solution stored at room temperature.

Loading Buffer: 0.25% bromophenol blue, 0.25% xylene cyanol FF, 20% Ficoll (Type 400) in DEPC treated water.

Sample Buffer: 1x running buffer, 50% formamide, 2.2 M formaldehyde in DEPC water. Aliquots were stored at -20°C.

Chian, R., Young, S., Danilkovitch-Miagkova, A., Rönnstrand, L., (et al.) (2001)
Phosphatidylinositol 3 kinase contributes to the transformation of hematopoietic cells by the D816V c-Kit mutant.
Blood, v. 98 (5), pp. 1365-1373.

Chapter 9: Amendments to Thesis

1. Insert sentences at the end of the fifth paragraph in section 3.11 (page 114).

In order to investigate the role of the different c-KIT isoforms in regulating haemopoietic cellular differentiation, MIHC generated and maintained in yeast derived muGM-CSF should be used. Subsequent attempts using yeast derived muGM-CSF to derive and maintain MIHC has resulted in a substantial decrease in the background differentiation status of parental MIHC and those infected with c-KIT isoforms (S. Young; data not shown).

2. Question: In Chapter 3, estimates of receptor content by indirect immunofluorescence and IP/Western blot disagree. Are the IPs quantitative (ie is it possible that the IPing Ab is limiting)? Are similar results obtained in straight western blots of cell lysates?

The results for immunoprecipitation and Western blot disagree. This does not appear to be due to a limiting amount of immunoprecipitating antibody since greater than five times the amount of c-KIT was immunoprecipitated from MO7e immunoprecipitates that had been loaded onto the blot to serve as a control. To answer the second question, c-KIT can not be detected on Western blots from whole cell lysates since the expression is too low and therefore was not investigated.

3. Insert sentences at the end of the second paragraph in section 5.9 (page 149).

The biological responses observed when the tyrosine at 721 had been mutated appear likely to be due to a lack of PI 3-K association and activation. It is possible however that other proteins are also recruited to that site and are partially responsible for the biological responses elicited. For example, the tyrosine at 751 of the PDGF receptor is responsible for recruiting p85 also associates to Nck (Nishimura *et al.,* 1993).

Nishimura, R., Li, W., Kashishian, A., Mondino, A., Zhou, M., Cooper, J. and Schlessinger, J. (1993). Two signaling molecules share a phosphotryosine-containing binding site in the platelet-derived growth factor receptor. *Mol. Cell. Biol.* **13**: 6889-6896.

4. Question: In relation to the biological properties of D816V c-KIT are there PI 3-K-dependent survival pathways that do not involve Akt activation?

So far as I know, Akt is required for PI 3-K dependent survival pathways activated by RTKs. It does appear however that HIV-1 Nef associates and activates PI 3-K, resulting in Akt-independent phosphorylation of Bad and survival through p21 activated kinase (PAK) (Wolf *et al.,* 2001).

Wolf, D., Witte, V., Laffert, B., Blume, K., Stromer, E., Trapp, S., d'Aloja, P., Schürmann, A., Baur, A. S. (2001). HIV-1 Nef associated PAK and PI3-Kinase stimulate Akt-independent Bad-phosphorylation to induce anti-apoptotic signals. *Nature Med.* **7**: 1217-1224.

- Comment: (Page 34) Bcl-2 and Bcl-X_L are not pro-apoptotic proteins.

Change sentence on page 34 beginning with 'Phosphorylation of BAD at two sites ...' to:

Phosphorylation of BAD at two sites is important to induce an association with 14-3-3 which leads to its sequestration in the cytosol, preventing its association to anti-apoptotic proteins such as Bcl-X_L and Bcl-2 (Datta et al., 1997; Stambolic et al., 1999; Zha et al., 1996).

- Question: Figure 5.8 legend - In this figure, survival of D816V and D816V/Y721F cells in muGM-CSF is similar. Is this correct?

Yes.

- Comment: (Page 151) - TGFα and heregulin/NDF are the ligands, not the receptors.

Change sentence to:

Interestingly, investigation of the oncogenic potential of two other receptors capable of activating PI 3-K, namely **the receptors for** TGFα and heregulin/NDF, revealed only weak activation of ERK (Amundadottir and Leder, 1998).

- Suggestion: Change the wording of sentence on page 155 line 7 beginning with 'The GNNK- isoform ...' to:

Src strongly associates to the GNNK- isoform while it only associates weakly to the GNNK+ isoform (Voytyuk *et al.*, 2003).

- Remaining amendments have been made throughout the thesis.